FITNESS OF MARINE CALCIFIERS IN THE FUTURE ACIDIFYING OCEAN

EDITED BY: Jonathan Y. S. Leung, Ben P. Harvey and Bayden D. Russell
PUBLISHED IN: Frontiers in Marine Science

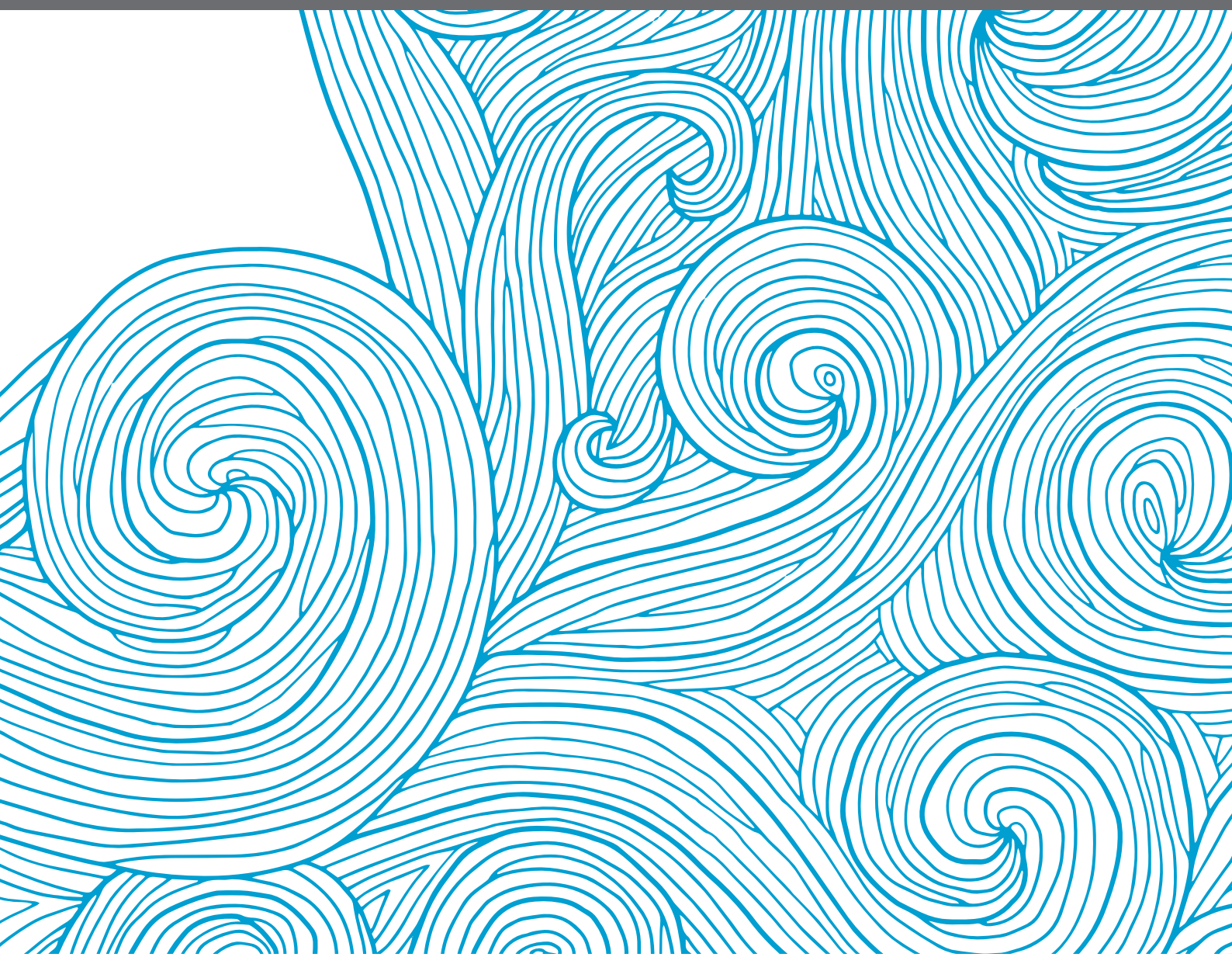

frontiers Research Topics

frontiers

ISSN 1664-8714
ISBN 978-2-88971-616-6
DOI 10.3389/978-2-88971-616-6

About Frontiers

Frontiers is more than just an open-access publisher of scholarly articles: it is a pioneering approach to the world of academia, radically improving the way scholarly research is managed. The grand vision of Frontiers is a world where all people have an equal opportunity to seek, share and generate knowledge. Frontiers provides immediate and permanent online open access to all its publications, but this alone is not enough to realize our grand goals.

Frontiers Journal Series

The Frontiers Journal Series is a multi-tier and interdisciplinary set of open-access, online journals, promising a paradigm shift from the current review, selection and dissemination processes in academic publishing. All Frontiers journals are driven by researchers for researchers; therefore, they constitute a service to the scholarly community. At the same time, the Frontiers Journal Series operates on a revolutionary invention, the tiered publishing system, initially addressing specific communities of scholars, and gradually climbing up to broader public understanding, thus serving the interests of the lay society, too.

Dedication to Quality

Each Frontiers article is a landmark of the highest quality, thanks to genuinely collaborative interactions between authors and review editors, who include some of the world's best academicians. Research must be certified by peers before entering a stream of knowledge that may eventually reach the public - and shape society; therefore, Frontiers only applies the most rigorous and unbiased reviews.
Frontiers revolutionizes research publishing by freely delivering the most outstanding research, evaluated with no bias from both the academic and social point of view. By applying the most advanced information technologies, Frontiers is catapulting scholarly publishing into a new generation.

What are Frontiers Research Topics?

Frontiers Research Topics are very popular trademarks of the Frontiers Journals Series: they are collections of at least ten articles, all centered on a particular subject. With their unique mix of varied contributions from Original Research to Review Articles, Frontiers Research Topics unify the most influential researchers, the latest key findings and historical advances in a hot research area! Find out more on how to host your own Frontiers Research Topic or contribute to one as an author by contacting the Frontiers Editorial Office: frontiersin.org/about/contact

FITNESS OF MARINE CALCIFIERS IN THE FUTURE ACIDIFYING OCEAN

Topic Editors:
Jonathan Y. S. Leung, University of Adelaide, Australia
Ben P. Harvey, University of Tsukuba, Japan
Bayden D. Russell, University of Hong Kong, Hong Kong, SAR China

Citation: Leung, J. Y. S., Harvey, B. P., Russell, B. D., eds. (2021). Fitness of Marine Calcifiers in the Future Acidifying Ocean. Lausanne: Frontiers Media SA.
doi: 10.3389/978-2-88971-616-6

Table of Contents

frontiers in Marine Science

EDITORIAL
published: 23 September 2021
doi: 10.3389/fmars.2021.752635

Editorial: Fitness of Marine Calcifiers in the Future Acidifying Ocean

Jonathan Y. S. Leung[1,2]*, *Ben P. Harvey*[3] and *Bayden D. Russell*[4]

[1] Faculty of Materials and Energy, Southwest University, Chongqing, China, [2] Southern Seas Ecology Laboratories, School of Biological Sciences, The Environment Institute, The University of Adelaide, Adelaide, SA, Australia, [3] Shimoda Marine Research Center, University of Tsukuba, Shimoda, Japan, [4] The Swire Institute of Marine Science and School of Biological Sciences, The University of Hong Kong, Hong Kong, SAR China

Keywords: adaptation, biomineralization, calcification, climate change, fitness and survival, marine organism, ocean acidification

Editorial on the Research Topic

Fitness of Marine Calcifiers in the Future Acidifying Ocean

INTRODUCTION

Over the last century, anthropogenic CO_2 emissions *via* combustion of fossil fuels have caused drastic changes in oceans with sea surface temperatures increasing steadily due to global warming. In addition to ocean warming, seawater has become more acidic as more CO_2 is dissolved into the world's oceans (IPCC, 2019). As CO_2 emissions are forecast to accelerate in the future (Caldeira and Wickett, 2005), understanding how marine organisms are influenced by ocean acidification (OA) and warming has received substantial attention (Doney et al., 2009). Organisms which build calcareous structures for growth and protection (e.g., coccolithophores, corals, gastropods, bivalves, and sea urchins) are of particular concern because OA is expected to make calcification more energy-demanding and increase dissolution of calcareous structures (Harvey et al., 2018; Byrne and Fitzer, 2019). Consequently, the fitness and survival of marine calcifiers could be reduced, possibly affecting the integrity of marine ecosystems in view of their abundance, diversity, and ecological functions in oceans.

There is now a large body of literature which demonstrates that calcifiers can indeed be impaired by OA in various aspects, such as physiology, calcification, growth, and survival (Harvey et al., 2013). Nevertheless, growing evidence reveals that some calcifiers can prevail in the CO_2-acidified environment and produce durable calcareous structures (e.g., Leung et al., 2019, 2020a; Di Giglio et al., 2020), implying their resistance and adaptability to OA. Thus, more comprehensive studies are needed to decipher how calcifiers adjust or succumb to OA and how warming modulates the impacts of OA on calcifiers. We brought together this Research Topic to address these issues and provide better insights into the fate of calcifiers in future marine ecosystems.

SUMMARY OF THE STUDIES IN THIS SPECIAL ISSUE

Ocean acidification is expected to undermine calcification (or shell building) due to the decreased carbonate saturation state and increased acidity of seawater (Byrne and Fitzer, 2019). Yet, calcification is a physiological process and thus can be affected by temperature (Clark et al., 2020), possibly leading to unexpected outcomes when warming interacts with OA. For example, crystallographic disorientation during calcification can be caused by warming in the mussel *Mytilus edulis*, but OA can mitigate this adverse effect (Knights et al.). Using 3D micro-computed tomography, Chatzinikolaou et al. observed that the gastropod *Nassarius nitidus* formed thinner and more porous shells under OA, but these negative effects disappeared when exposed to combined OA and warming. In contrast, the gastropod *Columbella rustica*

OPEN ACCESS

Edited by:
Carlos M. Duarte, King Abdullah University of Science and Technology, Saudi Arabia

Reviewed by:
Nelson A. Lagos, Universidad Santo Tomás, Chile

***Correspondence:**
Jonathan Y. S. Leung
jonathan.leung@adelaide.edu.au

Specialty section:
This article was submitted to Global Change and the Future Ocean, a section of the journal Frontiers in Marine Science

Received: *03 August 2021*
Accepted: *30 August 2021*
Published: *23 September 2021*

Citation:
Leung JYS, Harvey BP and Russell BD (2021) Editorial: Fitness of Marine Calcifiers in the Future Acidifying Ocean. Front. Mar. Sci. 8:752635. doi: 10.3389/fmars.2021.752635

produced thicker and denser shells under warming; however, when combined with OA, the shells became thinner and more porous (Chatzinikolaou et al.). These findings clearly indicate the species-specific nature of responses to OA and warming, probably driven by the differences in physiology among calcifiers. Identifying the mechanisms underlying the mixed responses of calcifiers to OA and warming is important to shed light on their fitness and survival in future oceans. For example, since energy is required for calcification, altering the energy allocated for calcification may underlie the response of calcifiers to future seawater conditions (Leung et al., 2020b). By studying resistant corals that can survive in the CO_2-acidified environment, Agostini et al. found that they had a higher potential for energy production and inherent capacity to allocate more energy for calcification than the sensitive corals. This finding not only helps explain the inconsistent responses of calcifiers to OA, but also implies that OA-sensitive species would be replaced by OA-resistant species in future oceans.

It is noteworthy that short-term experiments (typically <3 months) using organisms within a single generation have been predominantly used for OA research due to the inherent logistical constraints of longer experiments. Despite the scientific merits, these studies could underestimate the capacity of calcifiers to accommodate future seawater conditions *via* long-term and multi-generational exposure (Zhao et al., 2019; Cornwall et al., 2020; Leung et al., 2021). Thus, research on transgenerational plasticity (i.e., phenotypic change in offspring in response to the environmental stress experienced by parents) is of particular interest. In this Special Issue, Harianto et al. revealed that parental exposure of the urchin *Heliocidaris erythrogramma* to warming for 3 months can elevate the metabolic rate of offspring as juveniles, which may facilitate their persistence to warming. By conducting transplant experiments, Kurihara et al. showed that adult coral *Pocillopora acuta* inhibiting the CO_2-acidified habitat not only had higher calcification and net photosynthetic rates than those under control conditions, but also their larvae had higher lipid and chlorophyll contents (c.f. control larvae reared under high-CO_2 conditions) that indicate greater energy availability and tolerance to OA. These results suggest that transgenerational acclimatization can be a critical mechanism allowing calcifiers to survive under future seawater conditions, which cannot be unraveled by short-term experiments.

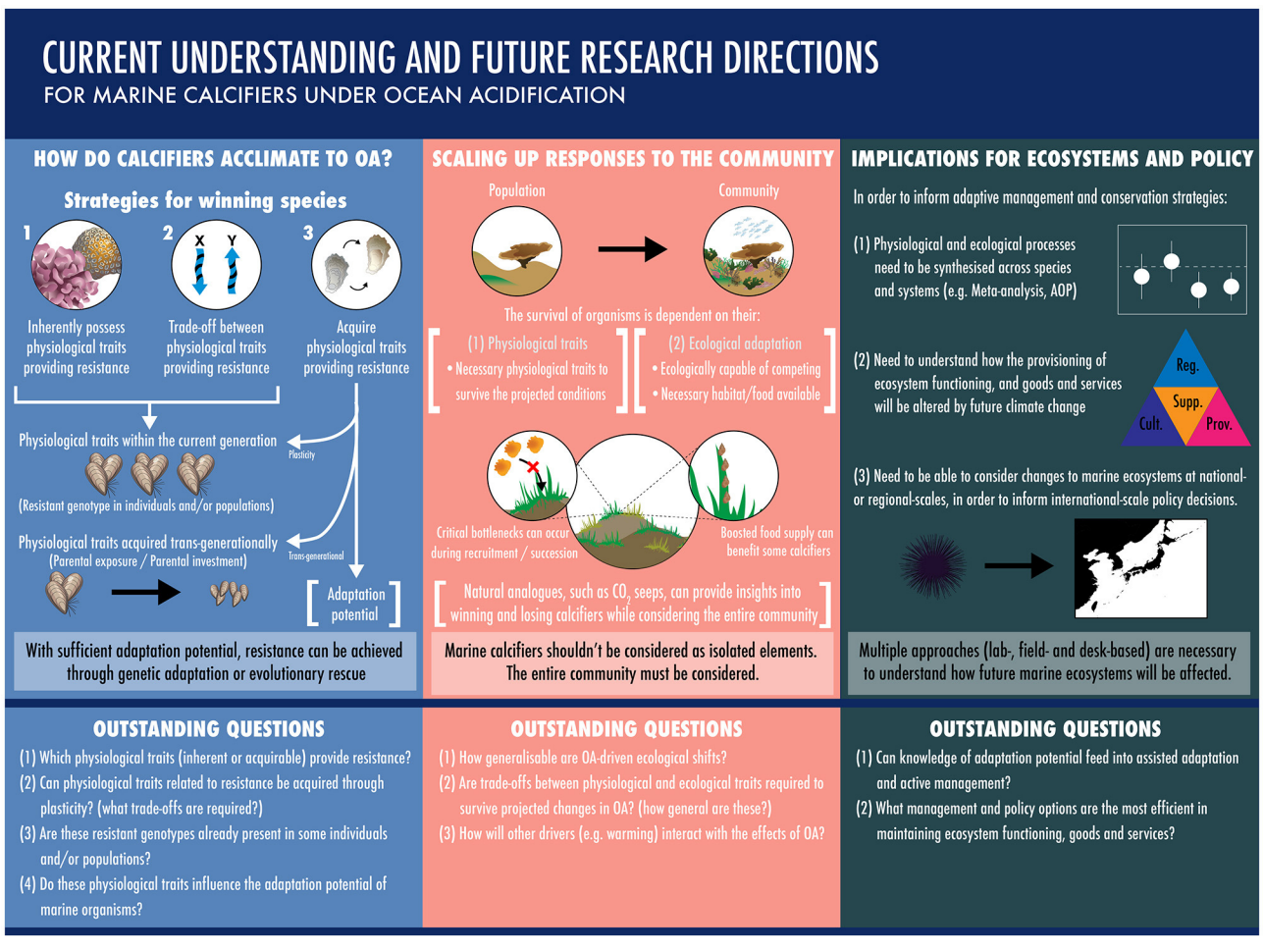

FIGURE 1 | Suggested future research directions to understand how ocean acidification affects the fitness and survival of marine calcifiers by considering adaptation potential and species interaction in the community, with implications for management of ecosystems.

Although calcifiers can exhibit compensatory responses (e.g., phenotypic plasticity) to counter the impacts of climate change (Leung et al., 2017; Peck et al., 2018; Glazier et al., 2020; Wang et al., 2020), trade-offs against other biological processes are often incurred. For instance, the coral *Galaxea fascicularis* can accommodate OA by sustaining photosynthetic performance, but the nitrogen fixation machinery is compromised as a trade-off, possibly affecting coral resilience to OA (Zheng et al.). In addition, plastic responses to climate change may not always be exhibited, depending on phenotypes. Minuti et al. showed metabolic acclimation of the gastropod *Trochus maculatus* to OA and warming by boosting the temperature of maximum metabolic rate; however, the upper lethal temperature decreased, implying that this gastropod is still vulnerable to warming.

CONCLUSION AND PERSPECTIVES

The studies in this Special Issue not only illustrate the impacts of OA and warming on calcifiers (e.g., physiology, calcification, and survival), but also reveal potential mechanisms driving these impacts. Importantly, the adaptive response shown by some calcifiers, such as transgenerational plasticity, indicates their potential capacity to persist in future oceans. Yet, some of them (e.g., coralline algae) are predicted to be vulnerable to future seawater conditions and therefore conservation policy should be amended to protect their populations (Simon-Nutbrown et al.). More long-term, mechanistic studies using more realistic experimental design (e.g., species interactions and habitat complexity considered) are still needed to decipher the potential fate of calcifiers in future oceans (see **Figure 1** for the recommended future research directions). This would allow the use of integrative analyses (e.g., Adverse Outcome Pathway framework, Ducker and Falkenberg) to provide insights into generalities in responses and underlying mechanisms, and to give directions for management and mitigation efforts.

AUTHOR CONTRIBUTIONS

All authors listed have made a substantial, direct and intellectual contribution to the work, and approved it for publication.

ACKNOWLEDGMENTS

We thank all authors and reviewers for their contributions to this Research Topic. We thank the Frontiers in Marine Science Editorial staff for their invitation and support in producing this Special Issue. Some of the images used in **Figure 1** are courtesy of the Integration and Application Network, University of Maryland Center for Environmental Science (ian.umces.edu/symbols/).

REFERENCES

Byrne, M., and Fitzer, S. (2019). The impact of environmental acidification on the microstructure and mechanical integrity of marine invertebrate skeletons. *Conserv. Physiol.* 7:coz062. doi: 10.1093/conphys/coz062

Caldeira, K., and Wickett, M. E. (2005). Ocean model predictions of chemistry changes from carbon dioxide emissions to the atmosphere and ocean. *J. Geophys. Res. Oceans* 110:C09S4. doi: 10.1029/2004JC002671

Clark, M. S., Peck, L. S., Arivalagan, J., Backeljau, T., Berland, S., Cardoso, J. C. R., et al. (2020). Deciphering mollusc shell production: the roles of genetic mechanisms through to ecology, aquaculture and biomimetics. *Biol. Rev.* 95, 1812–1837. doi: 10.1111/brv.12640

Cornwall, C. E., Comeau, S., DeCarlo, T. M., Larcombe, E., Moore, B., Giltrow, K., et al. (2020). A coralline alga gains tolerance to ocean acidification over multiple generations of exposure. *Nat. Clim. Change* 10, 143–146. doi: 10.1038/s41558-019-0681-8

Di Giglio, S., Spatafora, D., Milazzo, M., M'Zoudi, S., Zito, D., Dubois, P., et al. (2020). Are control of extracellular acid-base balance and regulation of skeleton genes linked to resistance to ocean acidification in adult sea urchins? *Sci. Total Environ.* 720:137443. doi: 10.1016/j.scitotenv.2020.137443

Doney, S. C., Fabry, V. J., Feely, R. A., and Kleypas, J. A. (2009). Ocean acidification: the other CO_2 problem. *Annu. Rev. Mar. Sci.* 1, 169–192. doi: 10.1146/annurev.marine.010908.163834

Glazier, A., Herrera, S., Weinnig, A., Kurman, M., Gómez, C. E., and Cordes, E. (2020). Regulation of ion transport and energy metabolism enables certain coral genotypes to maintain calcification under experimental ocean acidification. *Mol. Ecol.* 29, 1657–1673. doi: 10.1111/mec.15439

Harvey, B. P., Agostini, S., Wada, S., Inaba, K., and Hall-Spencer, J. M. (2018). Dissolution: The Achilles' heel of the triton shell in an acidifying ocean. *Front. Mar. Sci.* 5:371. doi: 10.3389/fmars.2018.00371

Harvey, B. P., Gwynn-Jones, D., and Moore, P. J. (2013). Meta-analysis reveals complex marine biological responses to the interactive effects of ocean acidification and warming. *Ecol. Evol.* 3, 1016–1030. doi: 10.1002/ece3.516

IPCC (2019). "Summary for policymakers," in *IPCC Special Report on the Ocean and Cryosphere in a Changing Climate*, eds H.-O. Pörtner, D. C. Roberts, V. Masson-Delmotte, P. Zhai, M. Tignor, E. Poloczanska, et al. Available online at: https://www.ipcc.ch/site/assets/uploads/sites/3/2019/11/03_SROCC_SPM_FINAL.pdf

Leung, J. Y. S., Chen, Y., Nagelkerken, I., Zhang, S., Xie, Z., and Connell, S. D. (2020a). Calcifiers can adjust shell building at the nanoscale to resist ocean acidification. *Small* 16:2003186. doi: 10.1002/smll.202003186

Leung, J. Y. S., Doubleday, Z. A., Nagelkerken, I., Chen, Y., Xie, Z., and Connell, S. D. (2019). How calorie-rich food could help marine calcifiers in a CO_2-rich future. *Proc. R. Soc. B* 286:20190757. doi: 10.1098/rspb.2019.0757

Leung, J. Y. S., Russell, B. D., Coleman, M. A., Kelaher, B. P., and Connell, S. D. (2021). Long-term thermal acclimation drives adaptive physiological adjustments of a marine gastropod to reduce sensitivity to climate change. *Sci. Total Environ.* 771:145208. doi: 10.1016/j.scitotenv.2021.145208

Leung, J. Y. S., Russell, B. D., and Connell, S. D. (2017). Mineralogical plasticity acts as a compensatory mechanism to the impacts of ocean acidification. *Environ. Sci. Technol.* 51, 2652–2659. doi: 10.1021/acs.est.6b04709

Leung, J. Y. S., Russell, B. D., and Connell, S. D. (2020b). Linking energy budget to physiological adaptation: how a calcifying gastropod adjusts or succumbs to ocean acidification and warming. *Sci. Total Environ.* 715:136939. doi: 10.1016/j.scitotenv.2020.136939

Peck, V. L., Oakes, R. L., Harper, E. M., Manno, C., and Tarling, G. A. (2018). Pteropods counter mechanical damage and dissolution through extensive shell repair. *Nat. Commun.* 9:264. doi: 10.1038/s41467-017-02692-w

Wang, X., Wang, M., Wang, W., Liu, Z., Xu, J., Jia, Z., et al. (2020). Transcriptional changes of Pacific oyster *Crassostrea gigas* reveal essential role of calcium signal pathway in response to CO_2-driven acidification. *Sci. Total Environ.* 741:140177. doi: 10.1016/j.scitotenv.2020.140177

Zhao, L., Liu, B., An, W., Deng, Y., Lu, Y., Liu, B., et al. (2019). Assessing the impact of elevated pCO_2 within and across generations in a highly invasive fouling mussel (Musculista senhousia). *Sci. Total Environ.* 689, 322–331. doi: 10.1016/j.scitotenv.2019.06.466

Conflict of Interest: The authors declare that the research was conducted in the absence of any commercial or financial relationships that could be construed as a potential conflict of interest.

Publisher's Note: All claims expressed in this article are solely those of the authors and do not necessarily represent those of their affiliated organizations, or those of the publisher, the editors and the reviewers. Any product that may be evaluated in this article, or claim that may be made by its manufacturer, is not guaranteed or endorsed by the publisher.

frontiers in Marine Science

ORIGINAL RESEARCH
published: 14 September 2020
doi: 10.3389/fmars.2020.575825

Species Distribution Modeling Predicts Significant Declines in Coralline Algae Populations Under Projected Climate Change With Implications for Conservation Policy

Cornelia Simon-Nutbrown[1,2], Peter M. Hollingsworth[2], Teresa F. Fernandes[3], Lisa Kamphausen[4], John M. Baxter[3,5] and Heidi L. Burdett[1]*

[1] The Lyell Centre for Earth and Marine Science and Technology, Heriot-Watt University, Edinburgh, United Kingdom, [2] Royal Botanic Garden Edinburgh, Edinburgh, United Kingdom, [3] Institute of Life and Earth Sciences, Heriot-Watt University, Edinburgh, United Kingdom, [4] Scottish Natural Heritage, Great Glen House, Inverness, United Kingdom, [5] School of Biology, Faculty of Science, University of St Andrews, St Andrews, United Kingdom

OPEN ACCESS

Edited by:
Jonathan Y. S. Leung, University of Adelaide, Australia

Reviewed by:
Cristina Pardo Carabias, University of A Coruña, Spain
Chiara Lombardi, Italian National Agency for New Technologies, Energy and Sustainable Economic Development (ENEA), Italy

***Correspondence:**
Cornelia Simon-Nutbrown
ccs3@hw.ac.uk

Specialty section:
This article was submitted to Global Change and the Future Ocean, a section of the journal Frontiers in Marine Science

Received: *24 June 2020*
Accepted: *21 August 2020*
Published: *14 September 2020*

Citation:
Simon-Nutbrown C, Hollingsworth PM, Fernandes TF, Kamphausen L, Baxter JM and Burdett HL (2020) Species Distribution Modeling Predicts Significant Declines in Coralline Algae Populations Under Projected Climate Change With Implications for Conservation Policy. Front. Mar. Sci. 7:575825. doi: 10.3389/fmars.2020.575825

Anthropogenic climate change presents a major challenge to coastal ecosystems. Mass population declines or geographic shifts in species ranges are expected to occur, potentially leading to wide-scale ecosystem disruption or collapse. This is particularly important for habitat-forming species such as free-living non-geniculate coralline algae that aggregate to form large, structurally complex reef-life ecosystems with high associated biodiversity and carbon sequestration capability. Coralline algal beds have a worldwide distribution, but have recently experienced global declines due to anthropogenic pressures and changing environmental conditions. However, the environmental factors controlling coralline algal bed distribution remain poorly understood, limiting our ability to make adequate assessments of how populations may change in the future. We constructed the first species distribution model for non-geniculate coralline algae (focusing on maerl-forming species but including crustose coralline algae associated with coralline algal beds) and showed that bathymetry, temperature at the seabed and light availability are the primary environmental drivers of present-day non-geniculate coralline algae distribution. Our model also identifies suitable areas for species presence that currently lack records of occurrence. Large-scale spatial declines in coralline algal distribution were observed under all IPCC Representative Concentration Pathways (ranging from 38% decline under RCP 2.6 up to 84% decline under RCP 8.5), with the most rapid rate of decline up to 2050. Refuge populations that may persist under projected climate change were also identified – informing priority areas for future conservation efforts to maximize the long-term survival of this globally important ecosystem.

Keywords: biodiversity, biogeography, climate change, Scotland, ecology, marine conservation, maerl, rhodolith

INTRODUCTION

Rising anthropogenic carbon dioxide (CO_2) emissions are causing rapid environmental change and under some scenarios, the mean ocean surface temperature is projected to rise by up to 4.3°C by 2100 (IPCC, 2014). Geographic shifts or declines in the distribution of species and ecosystems in response to this rapid environmental change have already been observed (e.g., Bellard et al., 2012; Gallon et al., 2014; Martínez et al., 2018). This can result in significant ecosystem disruption (Hoegh-Guldberg et al., 2007; Noisette et al., 2013a; Teagle and Smale, 2018), threatening the long-term survival of key ecosystem components and the associated biodiversity and ecosystem services they provide.

Free-living non-geniculate red coralline algae are globally distributed ecosystem engineers (Foster, 2001). They give rise to three-dimensional marine habitats, and these so-called "maerl" or "rhodolith" beds have high associated biodiversity (Barbera et al., 2003; Peña et al., 2014) – supporting many rare, endemic or commercially important species (Grall and Hall-Spencer, 2003; Wilson et al., 2004; Nelson, 2009; Riosmena-Rodriguez et al., 2016) – and globally significant roles in biogeochemical cycling, particularly long-term carbon burial (Burdett et al., 2015; van der Heijden and Kamenos, 2015; Mao et al., 2020). Aggregations of free-living, non-geniculate coralline algae (maerl-beds), although found globally, are particularly abundant in the North-East Atlantic (from the Arctic Ocean to the wider North Atlantic and the Canary Islands) (Pardo et al., 2014a), with Galicia, Brittany, Norway, Ireland, and Scotland being particular strongholds (Hall-Spencer et al., 2010). In this North-East Atlantic region, beds most abundant up to a depth of ∼50 m (Pardo et al., 2014a). There are thought to be around 24 maerl-forming species found throughout the North-East Atlantic but the most common are *Phymatolithon calcareum*, *Lithothamnion coralloides*, *Lithothamnion glaciale*, and *Lithothamnion tophiforme* (Pardo et al., 2014a). These species appear to follow a thermal cline, with *L. tophiforme* being limited to Arctic waters, *L. glaciale* occurring in Arctic and sub-Arctic areas, *P. calcareum* stretching from the sub-Arctic to tropical waters and *L. coralloides* occurring from the Southern British Isles to the Canary Islands and throughout the Mediterranean (Hall-Spencer et al., 2010; Pardo et al., 2014a). However, there are uncertainties regarding species identification and hence species' ranges, as morphological identification is difficult and few widespread molecular studies have been carried out to-date. Poor species identification additionally makes identifying species-specific environmental requirements challenging. Current evidence suggests that *L. glaciale* mostly occurs between 6–50 m (Perry et al., 2017a; Schoenrock et al., 2018) while *L. coralloides* appears to be more restricted to shallower depths, rarely being recorded below 30 m (Perry et al., 2017a). *P. calcareum* is also more frequently recorded in shallower waters (above 30 m) (Perry et al., 2017a), but sporadic deep-water observations are known [e.g., 80 m in the Pontian Archipelago, Mediterranean (Basso, 1998)].

Currently, all coralline algae beds are listed as "Vulnerable" or "Endangered" on the IUCN Red List (Gubbay et al., 2016). In Europe they are protected under the EU Habitats Directive and the OSPAR Commission in the North Atlantic (under "*OSPAR list of Threatened and/or Declining habitats*") (Hall-Spencer et al., 2008; European Commission, 2018), supported by local implementation such as designation as Priority Marine Features in Scotland (Scottish Government, 2018). Seven marine features were included in the EU Species and Habitats Directive some of which encompassed habitats where coralline algal beds occur (e.g., "*Large shallow inlets and bays*" and "*Sandbanks which are slightly covered by seawater at all times*") which are listed under Annex I. Two maerl-forming species (*L. coralloides* and *P. calcareum*) are additionally listed under Annex V (The Council of the European Communities, 1992; European Commission, 2016; Riosmena-Rodriguez et al., 2016; Perry et al., 2017b). Although the Habitats Directive has since been superseded into national law, it is the starting point from which most non-geniculate coralline algal bed conservation and later European legislation [e.g., the United Kingdom Biodiversity Action Plan (JNCC, 2016)] has evolved.

Habitat-forming ecosystem engineers, such as free-living non-geniculate coralline algae, modify their environment in such a way that benefits other species, for example, through the provision of shelter and food, or by the reduction of environmental stress (Hastings et al., 2007; Peña et al., 2014; Sheehan et al., 2015; Martínez et al., 2018). These ecosystems, therefore, are of high conservation concern and understanding how they may react to changing environmental conditions is important as their loss or geographic shift could pose threats to whole systems (Martínez et al., 2018; Teagle and Smale, 2018; Cornwall et al., 2019). Projected changes in marine environmental conditions, particularly ocean warming (Martin and Gattuso, 2009; Noisette et al., 2013a; Qui-Minet et al., 2019) and acidification (Porzio et al., 2011; Noisette et al., 2013b; Legrand et al., 2017; Martin and Hall-Spencer, 2017), are expected to have significant impacts on non-geniculate coralline algal distribution (Brodie et al., 2014). This is due to the consequential negative impacts on species-specific thermal niches, reduced calcification (Burdett et al., 2012a, 2018; Kamenos et al., 2013; Qui-Minet et al., 2019) and potential overgrowth by opportunistic non-calcifying algae, as has been observed during coral reef degradation (Hughes et al., 2007).

Non-geniculate coralline algal beds form biogenic reefs, which provide a myriad of ecosystem services globally that are often overlooked and their potential underestimated (Bindoff et al., 2019). These bed systems are biodiversity hotspots forming a living layer over sediments that provides habitat and supports high numbers of species including many invertebrate phyla (crustaceans, echinoderms, polychaetes, and mollusks), fleshy macroalgae, and various species which burrow either into individual free-living algae or the sediments below the bed (Jackson et al., 2004; Hall-Spencer et al., 2008, 2010; Foster et al., 2013). When compared to adjacent habitat types it was found that coralline algal beds had nearly twice the species richness (Steller et al., 2003). Similarly, non-geniculate coralline algal beds support numerous commercial fish species, often forming nursery habitats for economically important species such as cod (*Gadus morhua*) and hake (*Melanogrammus aeglefinus*)

(Kamenos et al., 2004; Hall-Spencer et al., 2006; Riosmena-Rodriguez et al., 2016; Elliott et al., 2017). However, despite their importance there is still a paucity of knowledge surrounding these ecosystems and how a rapidly changing climate will affect them (Bindoff et al., 2019).

Species distribution models (SDMs) or environmental niche models (ENMs) are commonly used tools to estimate the relationships between species and environmental or spatial factors (Elith et al., 2011; Merow et al., 2013). SDMs represent an important addition to direct environmental change experiments on non-geniculate coralline algae and their associated habitats which are difficult to extrapolate to range-wide predictions (Wernberg et al., 2012), and do not take into account the spatial variability of projected changes in environmental conditions. SDMs are capable of modeling both small-scale local responses and range-wide changes, provided that datasets are available at a suitable scale.

Here, we constructed the first SDM for coralline algal beds, focusing on Scottish regional waters – a European stronghold for this habitat (Hall-Spencer et al., 2008) and of conservation priority at national and international scales (Hall-Spencer et al., 2008; JNCC, 2016; European Commission, 2018; Scottish Government, 2018). This enabled us to identify: (1) the primary environmental drivers of present-day coralline algal bed distribution, (2) previously unknown areas of occurrence, (3) regional-scale impacts of projected climate change on coralline algal bed distribution, and (4) refuge populations tolerant to projected climate change. Synthesizing this information allowed us to identify areas of priority conservation effort to maximize the likelihood of long-term survival of this globally important marine habitat.

MATERIALS AND METHODS

Study Area

Scotland is a European stronghold for non-geniculate coralline algae beds. Consequently, it was selected as the focus area for distribution modeling in this study. The study area runs from the Solway Firth in the southeast, to the northern coasts of the Shetland Isles, including the Outer Hebrides in the west (**Supplementary Figure S1**). Within this region "maerl beds" (i.e., aggregations of non-geniculate coralline algae) are Priority Marine Features and protected under Scottish legislation (Scottish Government, 2018), ten marine protected areas around the Scottish coastline are designated for the protection of coralline algal beds (referred to in legislation as "maerl beds"). Despite this, the true extent of these systems in Scottish waters remains unknown, and even less is known about the factors that govern their local distribution.

Species Distribution Model

Maximum entropy (MaxEnt) modeling was chosen to construct a species distribution model (SDM) for maerl-forming species (i.e., non-geniculate coralline algae) as it is effective with presence-only data, is well regarded in the literature and can be highly modified so all modeling decisions are based on biological justifications (Pearson, 2010; Elith et al., 2011; Merow et al., 2013). MaxEnt v3.4.1 (Phillips et al., 2006) was run through the R v 3.6.1 (R Core Team, 2019) package DISMO v1.4 (Hijmans, 2017) to model the species niche and construct a probabilistic distribution map of non-geniculate coralline algal beds around Scotland.

Non-geniculate Coralline Algae

Occurrence Records

Occurrence records for the study region were obtained from the Geodatabase of Marine Features in Scotland (GeMS) (Scottish Natural Heritage, 2019a) under the Open Government and Creative Commons License. Geographic locations and study area are provided in **Supplementary Figure S1**. The annually updated database includes observed, georeferenced occurrence records of Priority Marine Features in Scotland from 1970 to 2017 curated by Scottish Natural Heritage (SNH). "Maerl beds" are one of these features. For this study, cut-offs were imposed on occurrence data by removing entries from before 1990. This was done to increase reliability, as older records may have been subject to different environmental conditions than recent records – for example due to construction of causeways changing tidal patterns [known to have happened in several locations, for example the Vatersay causeway (1989) (Comhairle nan Eilean Siar, 2020b) or the Benbecula causeway (1983) (Comhairle nan Eilean Siar, 2020a)]. Similarly, where there was evidence of a bed no longer supporting live individuals the occurrence point was removed prior to analysis.

Keyword searches in the GeMS database for "maerl" yielded species-specific records of free-living coralline algae species (i.e., "*L. glaciale*" or "*P. calcareum*") and records with no species identification ("*maerl beds*"). All records pertaining to aggregations of free-living non-geniculate coralline algae are labeled as "maerl bed" in GeMS and therefore no other search terms were needed. Within the study region species ranges overlap and species identification in coralline algae without molecular analyses can be difficult and unreliable (Pardo et al., 2014a,b). In order to maintain the maximum number of results for the model, no attempt was therefore made to split these records up into species-specific groups, however; it is assumed that the model will target the two main species in this region *P. calcareum* and *L. glaciale*. The database searching yielded 1430 occurrence records.

Although all records in the GeMS database are of free-living, non-geniculate coralline algae, not enough is known about the differentiation between this and crustose coralline algae (CCA) to conclusively say the model will only predict the distribution of free-living non-geniculate coralline algae, especially when considering free-living specimens that are grown around a non-algal core.

Observed occurrence records within the database which were not the result of a targeted survey, e.g., SeaSearch data[1], have inherent amounts of observer and spatial bias (Veloz, 2009; Fithian et al., 2015). Similarly, some beds have multiple (but geographically close) location points, creating further

[1]http://www.seasearch.org.uk/

spatial bias (Veloz, 2009). To eliminate the subsequent spatial-autocorrelation a 2-dimensional kernel density estimation of the data was created in R (R Core Team, 2019) using the package "spatstat" v1.61-0 (Baddeley et al., 2019). This was then used in the Java application OccurenceThinner (Verbruggen et al., 2013) to reduce geographical sampling bias leaving 314 occurrence points in the model.

Environmental Variables

Environmental layers were accessed from bio-ORACLE v2 (Tyberghein et al., 2012). The datasets have a spatial resolution of five arc minutes (Tyberghein et al., 2012; Assis et al., 2018). Bathymetry data were accessed through Bio-ORACLE from MARSPEC (Assis et al., 2018) and masked to the same resolution as the Bio-ORACLE datasets (Assis et al., 2018).

Environmental variables were selected for their potential links to coralline algae distribution. Initially 21 datasets were considered (**Supplementary Table S1**). Variables were examined for collinearity which may interfere with the performance of the model (Júnior and Nóbrega, 2018). This was done by calculating the Pearson correlation coefficient (r) between the datasets; datasets were considered collinear when $-0.6 \leq r \geq 0.6$ (Assis et al., 2018; Júnior and Nóbrega, 2018). A high degree of collinearity was observed between the 16 available variables. Where inclusion of maximum and minimum datasets created collinearity with another dataset, the mean datasets were used instead. Following analysis for collinearity, the most ecologically significant datasets were selected, according to literature evidence (e.g., Dutertre et al., 2014). These were: bathymetry (m), pH, mean diffuse attenuation coefficient (DA) (m^{-1}), mean dissolved nitrate concentration ($\mu mol\ L^{-1}$), minimum benthic temperature (°C) (i.e., average minimum temperature recorded at average seabed depth across the coastal shelf ranging from 0 to 200 m depth), mean photo-active radiation (PAR) at seabed ($E\ m^{-2}\ year^{-1}$), mean seabed salinity (PSS), maximum current velocity at seabed ($m\ s^{-1}$) and minimum current velocity at seabed ($m\ s^{-1}$).

The modeled benthic datasets used here contain some inherent collinearity, however, this is negligible in the Bio-ORACLE datasets as *in situ* quality control has been carried out by the Global Ocean Data Analyses Project (Assis et al., 2018) and high agreement found between the interpolated benthic datasets and *in situ* data gathered (Assis et al., 2018). For pH and DA, benthic datasets were not available, so sea surface datasets were used. Since these may not accurately represent benthic conditions (where non-geniculate coralline algal beds are found), test models were run with and without these datasets and the probabilistic distribution maps produced compared against known occurrence data. The results of these test models showed that the overall models were more statistically robust with the inclusion of surface datasets. pH was consistently found to be the variable that contributed fourth highest to the model (10.8% of the observed distribution) and is known to be environmentally relevant to non-geniculate coralline algal survival (McCoy and Kamenos, 2015), and so warranted inclusion in the model. Additionally, when run without pH and DA, overfitting (Pearson et al., 2007; Muscarella et al., 2014) was observed [Area Under Curve (AUC) with pH and DA = 0.0757; without pH and DA = 0.108] (**Supplementary Table S3**). Average omission rates for the minimum training presence were higher for models without pH and DA compared to those with them (0.310 and 0.263, respectively) thus also suggesting models were more over fit without pH and DA (Pearson et al., 2007; Muscarella et al., 2014) (**Supplementary Table S3**). Model evaluation was conducted in the R package ENMeval v0.3.0 (Muscarella et al., 2018). Model performance was assessed based on standard statistical assessments including AUC, receiver operating characteristics (ROC) and Akaike Information Criterion (AIC) (Muscarella et al., 2014; Steen, 2019).

Spatial Distribution Model Settings

ENMeval was further used to select model parameters that enabled the most efficient model performance (**Supplementary Material**). The optimal settings were found to be a regularization multiplier of one, and all feature classes. Models were clamped to training conditions to avoid extrapolation uncertainty. Once these settings were established the model was run in the R package Dismo v1.4 (Hijmans, 2017). The contribution of each environmental variable was assessed by excluding it from the model and assessing the performance of the model without it (jack-knifing). Forty per cent of the occurrence data points were randomly held back for model calibration and the model was trained on the remaining 60% of the occurrence data. The resultant model performed well under cross validation and evaluation statistics (**Supplementary Table S3**). In the final model, the AUC value was 0.959 ± 0.008 (mean $\pm$ SD), indicating high predictive ability. Some areas of predicted distribution were not covered by presence records. Field validation of two positive prediction sites were found to be true (Daliburgh, South Uist [57.160913, −7.408005] and Kildonan [57.218810, −7.427824]) and one modeled "absence" site was confirmed to not have any free-living coralline algae or CCA present (Loch Eyenort, South Uist [around 57.230275, −7.3514]), providing further evidence of model reliability.

Threshold Selection

Implementation of thresholds was carried out in R to transform logarithmic model predictions of probability of presence of non-geniculate coralline algae to binary presences and absences (**Supplementary Material**).

Climate Projections

Climate projection datasets were sourced from Bio-ORACLE for Representative Concentration Pathway (RCP) scenarios 2.6, 4.5, 6.0, and 8.5 for the years 2050 and 2100 (Assis et al., 2018). These are all based on the IPCC Coupled Model Intercomparison Project (CMIP) 5 model for climate scenarios, ranging from a significant reduction in greenhouse gas emissions (RCP 2.6) to a continuation at the current level (RCP 8.5) (Assis et al., 2018). Where available, the environmental variables used to train the MaxEnt SDM were replaced with the projected future levels – this was possible for benthic temperature, salinity and current velocity (Assis et al., 2018) (**Supplementary Table S2**). Projection datasets for other environmental variables (pH,

diffuse attenuation, nitrate concentration, photoactive radiation at seabed and bathymetry), were not available, so present-day datasets were used.

RESULTS

Present Day Coralline Algal Distribution

The top three primary environmental drivers (total explanation = 85%) of non-geniculate coralline algal bed distribution were bathymetry (51.8%), minimum benthic temperature (17.4%) and PAR at the seabed (15.8%). Sea surface pH accounted for an additional 10.8% of the association between environmental variables and non-geniculate coralline algal distribution. Coralline algal beds were predicted from the intertidal, down to 40 m depth, within a minimum temperature range of 2–9°C, a PAR range of 0–25 (E m^{-2} yr^{-1}) and a pH range of 8.16–8.21. Predicted non-geniculate coralline algae habitat was spatially heterogeneous, characterized by a general east/west divide. The most suitable areas for non-geniculate coralline algal habitats were predominantly located in the coastal waters and sea lochs of the west coast of mainland Scotland, around Orkney, and Shetland (north of mainland Scotland) and around the southern islands of the Outer Hebrides (**Figure 1**). The east coast of Scotland is predominantly devoid of suitable areas for non-geniculate coralline algal habitats, except for the Moray Firth on the northeast mainland (**Figure 1**). The total area suitable for non-geniculate coralline algal bed presence during present-day conditions was predicted to be 7130 km^2.

Regional-Scale Distribution Under Projected Environmental Change

Under all RCPs, a large decrease in suitable habitat is predicted with at least a 38% decline by 2050 (**Table 1**). The most immediate losses in suitable habitat are in southern areas of mainland Scotland under all RCPs (**Figures 2**, **3**). At the most extreme, under RCP 8.5 a predicted 83.7% reduction in suitable habitat for non-geniculate coralline algae was found in 2100 compared to the present-day (**Figure 3E** and **Table 1**). The north-west mainland coast of Scotland, patches around the Northern Islands and the area around the inner Moray Firth remained strongholds for non-geniculate coralline algae under all future climate projections (**Figures 2**, **3**). No habitat that was previously unsuitable for non-geniculate coralline algal beds (present day) became suitable under any of the RCP scenarios.

Regional Variation in Distribution Under Projected Climate Change

Some areas were predicted to be more negatively affected, in terms of coralline algal distribution, by projected environmental change. This spatial variability in persistence was exacerbated under higher-emission scenarios. The Outer Hebrides – currently one of the most important regions for non-geniculate coralline algae – were predicted to experience a 29% decline in coralline algal distribution by 2050 under RCP 2.6, leaving only small patches remaining in the Sound of Barra, west of North Uist and the north of Lewis (**Figure 2A**). Apart from under RCP 2.6, suitable habitat in the Outer Hebrides was predicted to be restricted to small areas in the north of Lewis by 2100 and was completely lost under RCP 8.5 (**Figure 3**). By 2050, the Isle of Skye (Inner Hebrides) – was predicted to no longer support non-geniculate coralline algae under RCPs 6.0 and 8.5 (**Figures 2D,E**). Interestingly, the area east of Skye, which was deemed unsuitable for non-geniculate coralline algal beds under RCP 6.0 in 2050 was retained under RCP 6.0 in 2100, but then lost under RCP 8.5 (2100) (**Figures 3D,E**).

Some areas were predicted to maintain non-geniculate coralline algal populations throughout the coming decades. In the north of mainland Scotland (Loch Laxford and Ullapool/Loch Broom) and around Orkney and Shetland, high probabilities of coralline algae occurrence (>0.7) were maintained by 2100, even under RCP 8.5 (**Figure 3** and **Supplementary Figures S2**, **S3**). A relatively high probability (>0.7) of persistence in 2100 under all RCPs was also predicted for Loch Sunart (mainland Scotland) and north Bute (Inner Hebrides) (**Figure 3** and **Supplementary Figure S3**). Under RCP 2.6, 6.0, a refuge population remained on the west of Islay by 2100 (**Figures 3A–C**) but there was lower probability of it being maintained under RCP 8.5 (0.5–0.7) (**Figure 3** and **Supplementary Figure S3**). There is also a small patch of habitat near Carnigaan (south-west mainland) that retains a higher probability of occurrence even under RCP 8.5 in 2100 (>0.7) (**Figure 3E** and **Supplementary Figure S3**).

Similarly, under all RCPs the inner Moray Firth retains several areas of suitable habitat by 2100 (>0.7) (**Figure 3E** and **Supplementary Figure S3**).

DISCUSSION

Free-living non-geniculate coralline algal beds are a globally distributed, ecologically important ecosystem (Pardo et al., 2014a; Riosmena-Rodriguez, 2016). Using regional-scale modeling, bathymetry, water temperature and light availability were found to be the primary environmental drivers of non-geniculate coralline algal bed distribution. Projected environmental change is predicted to have a severe negative impact on overall regional-scale coralline algal distribution in Scotland, although spatial heterogeneity in the magnitude of environmental change with the current distributional range has allowed potential future refugia to be identified – areas we propose for priority conservation status.

This regional-scale model highlights the need to understand how small-scale environmental changes affect non-geniculate coralline algae and how beds may be adapted to very localized conditions. Further investigation and understanding of both are key to fully understanding the implications of climate change for non-geniculate coralline algae populations globally.

Spatial Distributions Driven by Environmental Heterogeneity

We have identified a regional-scale east/west division in coralline algal habitat. Coralline algae have not been extensively observed on the east coast, despite extensive surveys (both grab and

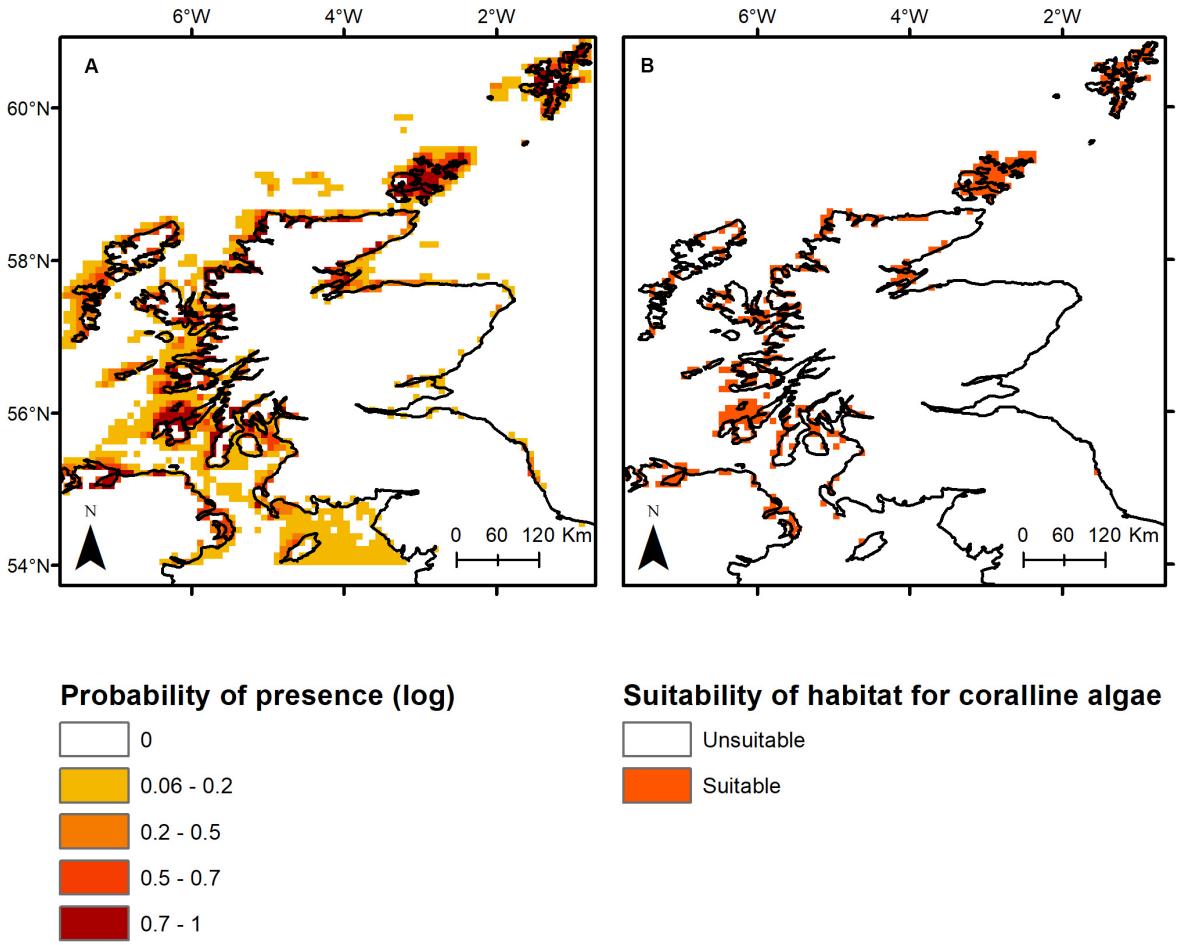

FIGURE 1 | Present-day modeled occurrence of coralline algae around Scotland as **(A)** probability of presence on a log likelihood scale ranging from 1 (dark red) to 0 (white), and **(B)** the probabilistic distribution with threshold of occurrence applied, where orange indicates presence while white (background) indicates absence.

TABLE 1 | Predicted coralline algal bed extent around Scotland in the present-day and under Representative Concentration Pathway (RCP) emission scenarios in the years 2050 and 2100.

RCP Scenario	Year	Total predicted area (km^2)	Percentage decline from present-day (%)
Present-day		7130	
2.6	2050	4446	38
	2100	2640	63
4.5	2050	4029	44
	2100	2223	69
6.0	2050	3380	53
	2100	2130	70
8.5	2050	2778	61
	2100	1158	84

SCUBA) in the area (e.g., Dargie, 2001), and as the model also identifies this area as predominantly unsuitable, with a low probability of presence, this is unlikely to purely be due to a lack of colonization opportunity in this area, but more to environmental conditions. Higher temperatures on the east coast, coupled with lower current velocities, are likely to be the reason the region is predominantly devoid of non-geniculate coralline algal bed populations. It is noteworthy that overall, the differences in environmental conditions between the east and west coasts of Scotland are relatively minor, indicating how sensitive these non-geniculate coralline algal populations are to their local conditions.

Fine sediments are known to be detrimental to coralline algal survival due to smothering (Fabricius and De'ath, 2001). This may explain why the only predicted east-coast population (inner Moral Firth) is not backed up by records of non-geniculate coralline algal presence – this area is comprised of patchy gravel and sand (British Geological Survey, 2020). Where this mixed sediment is present on the west coast, coralline algae are commonly only found in areas of gravel (e.g., Sound of Barra, Outer Hebrides). This may be further compounded by dredging and shipping activities – extensive in Scotland (Fox et al., 2015) – leading to a resuspension and subsequent smothering of suitable bottom-types for coralline algal colonization. Unfortunately, substrate-type could not be included in the model due to incompatibilities in the dataset resolution.

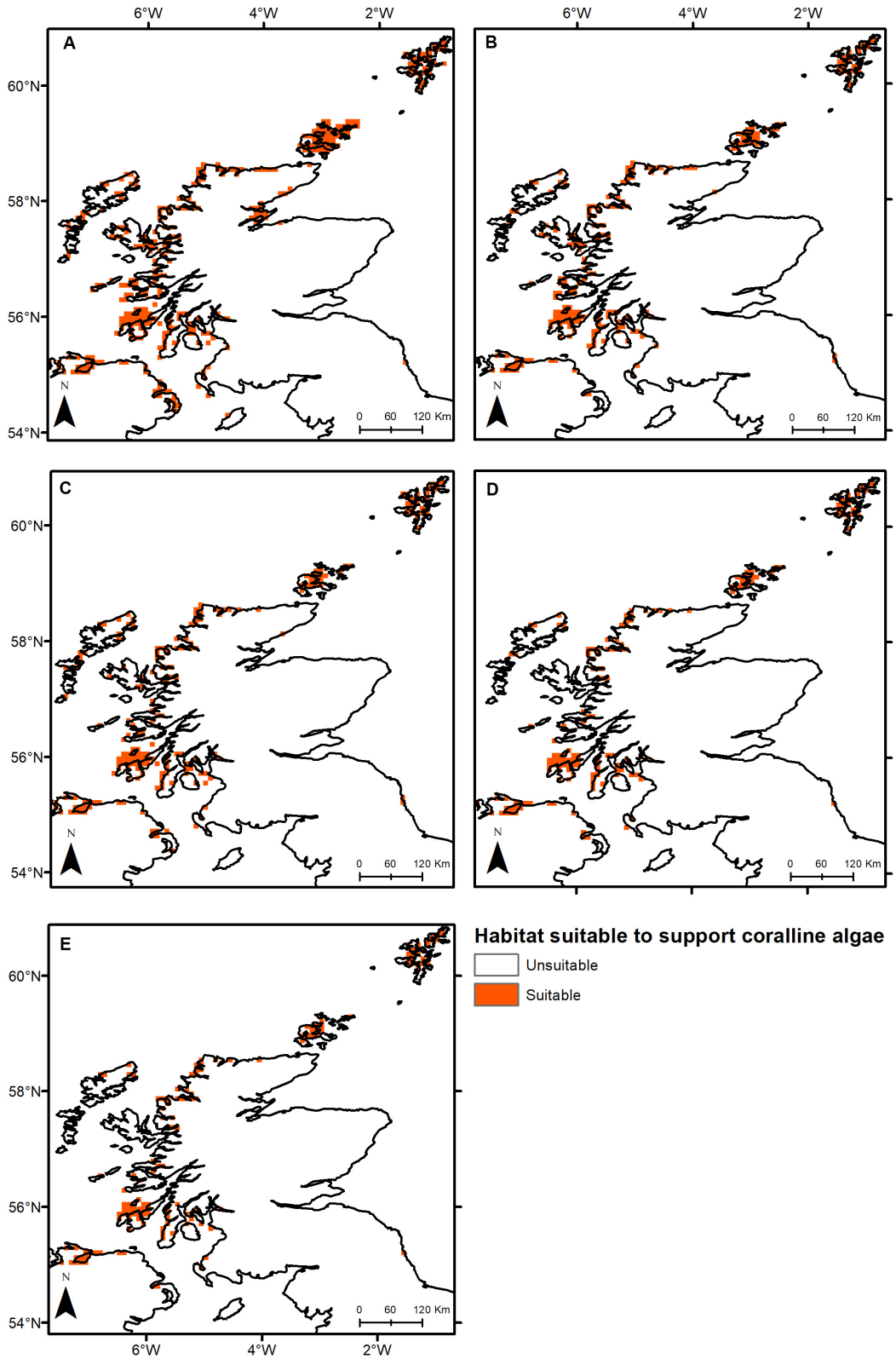

FIGURE 2 | Threshold maps of coralline algal bed distribution around Scotland in **(A)** the present-day and by 2050 under **(B)** RCP 2.6, **(C)** RCP 4.5, **(D)** RCP 6.0, and **(E)** RCP 8.5. Orange indicates predicted presence of coralline algal beds.

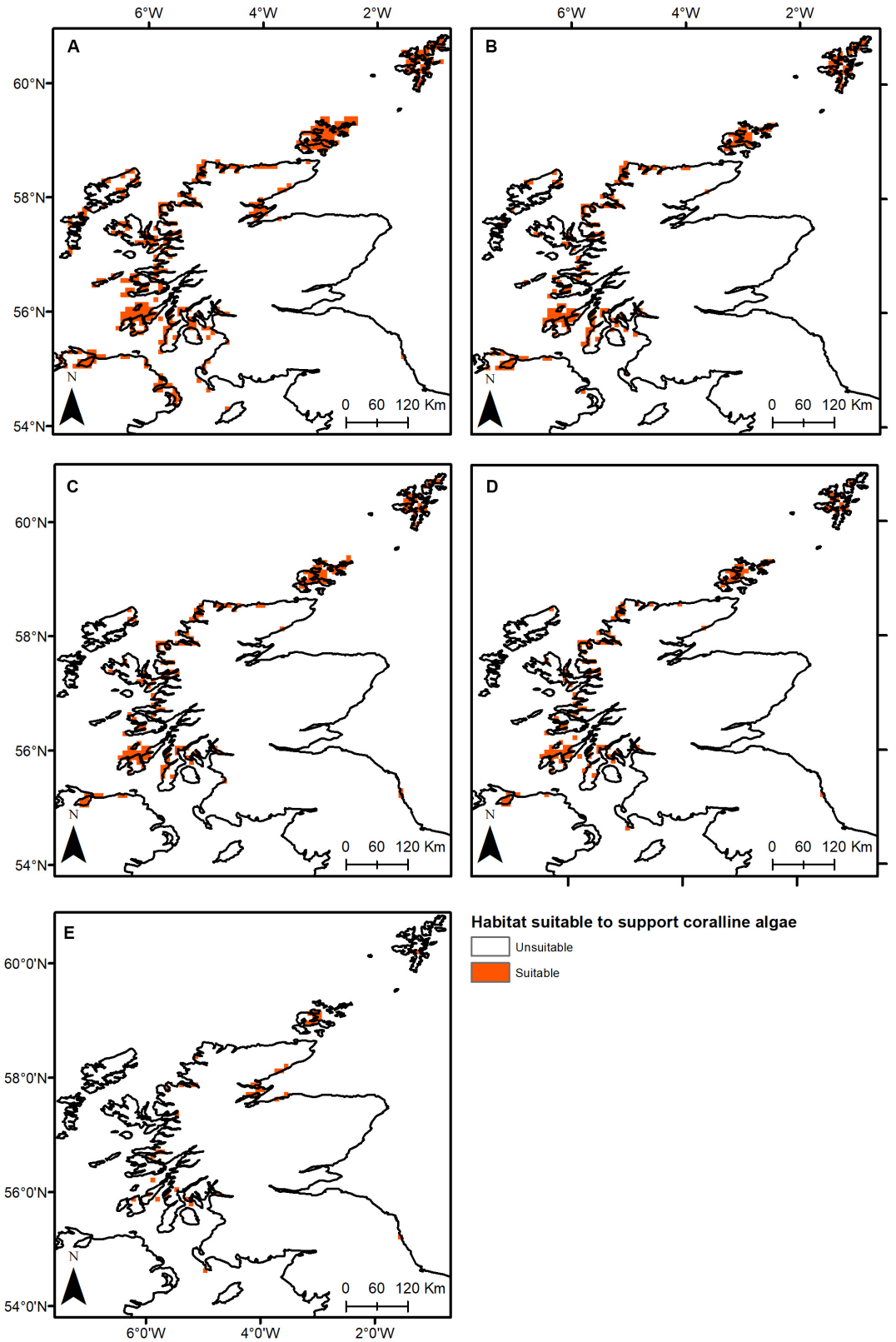

FIGURE 3 | Threshold maps of coralline algal bed distribution around Scotland in **(A)** the present-day and by 2100 under **(B)** RCP 2.6, **(C)** RCP 4.5, **(D)** RCP 6.0, and **(E)** RCP 8.5. Orange indicates predicted presence of coralline algal beds.

Looking forward, the ability to identify local areas within a regional space which have the potential to support non-geniculate coralline algae but where it is currently not present highlights a potential opportunity for the translocation of populations as climate change progresses (National Species Reintroduction Forum, 2014). This is particularly pertinent given that no new areas of suitable habitat were identified under climate change scenarios, in line with other previous distributional studies on other calcified marine organisms such as corals (Freeman et al., 2013). Reef restoration is of growing conservation interest, particularly on tropical coral reefs (Suggett et al., 2019), but this is likely to be even more challenging for maerl-forming species due to their slow growth rates (Adey and McKibbin, 1970; Blake and Maggs, 2003; Brodie et al., 2014; Pardo et al., 2019), even if environmentally suitable areas can be identified.

Bathymetry and Light Availability Limit Depth Distribution

Despite low-light adaption (Burdett et al., 2012b) and known worldwide deep-water occurrences (Peña and Barbara, 2009; Hall-Spencer et al., 2010; Friedlander et al., 2014; Pardo et al., 2014a), non-geniculate coralline algal survival was limited to <40 m depth in this region of the NE Atlantic, with the majority found between 5 and 20 m depth. Mitigation of some effects of climate change may be possible for marine organisms that can shift their habitats along a vertical gradient, i.e., moving into deeper cooler waters (Jorda et al., 2020). However, our results do not predict this kind of range shift to be available for non-geniculate coralline algae because of light limitation. Increased Arctic melt-water introduction (Pan et al., 2019), may enable a downward expansion or movement of non-geniculate coralline algae populations due to clearing of the water column. If this was to occur, there would also be knock-on implications for the biodiversity associated with this habitat, which may be depth limited or increased light penetration may lead to macroalgae overgrowth. This could result in major shifts in community structure and subsequent changes in ecosystems services, as have been seen and modeled in coastal fish and invertebrate communities of Australia (Cheung et al., 2012).

Temperature Exerts Control on Latitudinal Extent

The second most important environmental driver of distribution was minimum benthic temperature – known to be a key factor in determining non-geniculate coralline algal species extent globally (McCoy and Kamenos, 2015). Where regional-scale non-geniculate coralline algal communities consist of species with differing thermal envelopes, future distributional changes may become more complex. This is the case here: the two dominant free-living species – *P. calcareum* and *L. glaciale* – have different distributional ranges that overlap but show different thermal tolerances; this may affect their survival under projected climate change (especially warming). *P. calcareum*, one of the dominant free-living non-geniculate coralline algal species throughout Europe (Pardo et al., 2014a; Qui-Minet et al., 2019) is at its northerly limit in Scotland, suggesting a potential capacity to tolerate warming [although this has not been supported by laboratory experimentation (e.g., Qui-Minet et al., 2019)]. Conversely, *L. glaciale* is at its southerly limit in Scotland (Pardo et al., 2014a) and is known to be prevalent across the Atlantic Arctic (Schoenrock et al., 2018). Calcification and temperature in *L. glaciale* are known to be negatively related (Kamenos and Law, 2010), suggesting projected warming over the coming century will negatively impact *L. glaciale* populations, supporting the habitat declines seen here. Species-specific responses to projected environmental change will thus determine the magnitude of coralline algal ecosystem change but input data at the species level was not available for this study. However, it is clear from the results presented here that coralline algal beds at the edges of their range (be that geographically, or by depth) face severe threats over the coming century and should be the focus of immediate conservation management.

Future Drivers of Distributional Change

Under all RCPs, there was a significant decrease in the amount of suitable areas for non-geniculate coralline algal habitat, but this was accompanied by high spatial variability. Warming projections for our study region were characterized by latitudinal trends in the magnitude of projected warming (higher in the south, lower in the north; **Supplementary Figure S4**) combined with localized areas of little warming compared to the overall trend – this local-regional scale heterogeneity in warming has also been projected globally (IPCC, 2014). Importantly, variability in warming led to the persistence of refuge populations throughout the study region. However, this may increase habitat fragmentation, which can lead to inbreeding depression and decreasing population health (Pavlova et al., 2017; Pardo et al., 2019), ultimately weakening the likelihood of long-term survival throughout the coming century and beyond.

Clamping of the SDM to conditions only encountered in the training data mean that the results presented here perhaps represent a "worst-case scenario" for the effects of environmental change – it is assumed that environmental conditions beyond present-day variability will not be suitable for non-geniculate coralline algal habitat in the future. Present-day latitudinal distributions, especially for *P. calcareum*, suggest this may not be representative, but the capacity for coralline algae to shift poleward is expected to be minimal because of their slow growth rates and limited dispersal abilities (Brodie et al., 2014). This contrasts with other ecosystem engineers such as kelp, for which poleward shifts have already been recorded around the world (Smale, 2020). Likewise, there may be some opportunity for *in situ* adaptation to changing conditions, although there is little supporting evidence to suggest this is likely to occur within the short-time frame involved, and this is confounded by a general lack of knowledge of population dynamics and the extent of sexual reproduction in non-geniculate coralline algal populations (Pardo et al., 2019).

Future non-geniculate coralline algal bed distribution may also be affected by projected declines in ocean pH

(McCoy and Kamenos, 2015) – red coralline algae and their associated communities are generally considered to be highly sensitive to low pH (Martin and Gattuso, 2009; Burdett et al., 2012a, 2018; Kroeker et al., 2012; Kamenos et al., 2013, 2016; Qui-Minet et al., 2019). Thus, it would be expected that projected declines in ocean pH would further limit the distributional extent of non-geniculate coralline algae, perhaps counter-balancing the effects of clamping in the model. Unfortunately, a pH projection dataset at a suitable spatial resolution and extent was not available for inclusion in the projection modeling and so could not be tested here.

Wider Ecosystem Implications

Reduced coralline algal habitat as a result of environmental change will also have significant effects on associated species and biogeochemical cycling. This may result in large community shifts (Brodie et al., 2014), as has been previously observed e.g., during the Little Ice Age/Medieval Warm Period transition (Mao et al., 2020). Coralline algal beds are a globally important store of blue carbon (van der Heijden and Kamenos, 2015; Porter et al., 2020), with the potential to store the most carbon per unit area of all coastal ecosystems in the study area (Burrows et al., 2014, 2017). The magnitude of stored carbon in coralline algal beds is known to be positively related to water temperature (Mao et al., 2020), suggesting areas of future coralline algal persistence may also experience a proportional increase in carbon storage. However, in areas of coralline algal bed loss, disturbance to the system may release carbon that had been previously locked away for centuries if not millennia (Macreadie et al., 2019). Conversely, without disturbance, the persistence of a dead skeletal framework may enable the continued accumulation of incoming organic carbon and maintain sediment carbon stability, albeit without photosynthetic carbon sequestration.

The value of these non-geniculate coralline algal habitats, along with other biogenic reef habitats, has been broadly overlooked to-date (Sunday et al., 2017; Bindoff et al., 2019). Globally, the value of these habitats as ecosystem engineers, biodiversity hotspots and nursey habitats is still underestimated and under-protected despite the growing threat they face due to increasingly changing climates (Bindoff et al., 2019). Understanding, the environmental conditions needed to maintain these habitats and the degree to which they are locally adapted, emphasizes the need for better protection and further study of these fragile but globally important systems (Kamenos et al., 2008b; Sheehan et al., 2015; Sunday et al., 2017; Bindoff et al., 2019).

Policy Implications

Few marine protected areas (MPAs) or special areas of conservation (SACs) around the world are specifically designated for the protection of non-geniculate coralline algal beds (Barbera et al., 2003), but the results from our study suggest their long-term large-scale distribution is at risk. Although conservation management is not able to directly protect against changing environmental conditions, it does lessen the impact of other pressures, enhancing the potential for climate change-related mitigation and/or adaptation (Roberts et al., 2017).

In our study region, although the majority of known non-geniculate coralline algal beds are located within the Scottish MPA and SAC network (**Supplementary Figure S6**), only ten of 217 are designated for free-living coralline algae bed protection (as "maerl beds") (*Fetlar to Haroldswick, Wyre and Rousay Sounds, Loch Laxford, Wester Ross, Loch Carron, Loch nam Madadh, Sound of Barra, Loch Sween, South Arran and Luce Bay, and Sands)* (**Supplementary Figure S6**). Even in these areas some permitted activities (e.g., licensed fishing) may detrimentally affect this ecosystem, Scottish Natural Heritage (2019b). The placement of non-geniculate coralline algae-specific MPAs does not cover full present-day extent, and only 20% of the potential future refuge populations are currently covered (**Supplementary Figures S7**, **S8**).

Connectivity between refugia and neighboring habitats may strengthen the future persistence of non-geniculate coralline algal beds, similar to the "spill over" of ecosystem services seen in other MPA networks (Lynham et al., 2020). We therefore propose that the refuge areas (Loch Laxford, inner Moray Firth, north of Arran, north of Islay, Mainland Orkney and Mainland Shetland) should be of high conservation priority since they are expected to offer persistently suitable habitat for the coming decades – expected to be the period of most rapid distributional decline. In support of this, a current consultation by the Scottish Government and Marine Scotland, supported by Scottish Natural Heritage, aims to develop fisheries management measures to protect particularly sensitive benthic habitats and PMFs (including coralline algal beds) outside of MPAs (Marine Scotland, 2018; Scottish Government, 2019).

SUMMARY AND CONCLUSION

Non-geniculate coralline algal beds are a globally important ecosystem for biodiversity, socio-economic benefit and carbon storage. Scotland is a European regional stronghold for these coralline algal beds, but here we demonstrate their high sensitivity to projected climate change, and demonstrate the value of SDMs for understanding regional-scale environmental drivers of their distribution. Projected climate change over the coming century is predicted to leave fragmented refugia that may be more vulnerable to long-term survival and therefore should be a priority for conservation management for favorable conditions. Applications of this SDM approach to free-living, non-geniculate coralline algae in other regions around the world will enable a global network of distributional change to be determined, facilitating international-scale conservation decisions and an assessment of the knock-on implications for the future of coralline algal ecosystem service provision.

This paper highlights the need for a greater understanding of non-geniculate coralline algal bed habitats in order to prepare for various climate futures. Increased survey activity in order to better establish true presences and absences of beds, and high resolution data on environmental conditions would be appropriate places to start and allow for more detailed and in depth modeling to be carried out.

DATA AVAILABILITY STATEMENT

Publicly available datasets were analyzed in this study. This data can be found here: Geodatabase of Marine Features in Scotland (GeMS) (https://data.gov.uk/dataset/0e78afea-ac1e-4080-8758-980f2d5cff6d/gems-scottish-priority-marine-features-pmf). Bio-ORACLE (https://www.bio-oracle.org/).

AUTHOR CONTRIBUTIONS

HB, TF, JB, PH, and CS-N designed the experiment. LK and CS-N identified and accessed the data. CS-N carried out modeling and analysis, with help from HB, and wrote the manuscript. LK and JB provided information on conservation management in Scotland and provided links to policy organizations. All authors have confirmed and approved the submitted version of the manuscript, provided input on methods and provided detailed edits, and feedback on the manuscript.

FUNDING

This work was funded by a NERC iCASE studentship award to HB, PH, JB, and TF (NE/R007233/1). The Royal Botanic Garden Edinburgh acknowledges funding support from the Scottish Government Rural and Environment Sciences and Analytical Services Division (RESAS). This is a contribution to the Scottish Blue Carbon Forum.

SUPPLEMENTARY MATERIAL

The Supplementary Material for this article can be found online at: https://www.frontiersin.org/articles/10.3389/fmars.2020.575825/full#supplementary-material

REFERENCES

Adey, W. H., and McKibbin, D. L. (1970). Studies on the maerl species Phymatolithon calcareum (Pallas) nov. comb. and *Lithothamnium coralloides* Crouan in the Ria de Vigo. *Bot. Mar.* 13, 100–106.

Assis, J., Tyberghein, L., Bosch, S., Verbruggen, H., Serrão, E. A., and Clerck, O. D. (2018). Bio-ORACLE v2.0: extending marine data layers for bioclimatic modelling. *Glob. Ecol. Biogeogr.* 27, 277–284. doi: 10.1111/geb.12693

Baddeley, A., Turner, R., and Rubak, E. (2019). *CRAN - Package Spatstat*. Available online at: https://cran.r-project.org/web/packages/spatstat/index.html (accessed November 8, 2019).

Barbera, C., Bordehore, C., Borg, J. A., Glémarec, M., Grall, J., Hall-Spencer, J. M., et al. (2003). Conservation and management of northeast Atlantic and *Mediterranean maerl* beds. *Aquat. Conserv. Mar. Freshw. Ecosyst.* 13, S65–S76. doi: 10.1002/aqc.569

Basso, D. (1998). Deep rhodolith distribution in the Pontian Islands, Italy: a model for the paleoecology of a temperate sea. *Palaeogeogr. Palaeoclimatol. Palaeoecol.* 137, 173–187. doi: 10.1016/s0031-0182(97)00099-0

Bellard, C., Bertelsmeier, C., Leadley, P., Thuiller, W., and Courchamp, F. (2012). Impacts of climate change on the future of biodiversity. *Ecol. Lett.* 15, 365–377. doi: 10.1111/j.1461-0248.2011.01736.x

Bindoff, N., Cheung, W. W. L., Kairo, J. G., Arístegui, J., Guinder, V. A., Hallberg, R., et al. (2019). *Changing Ocean, Marine Ecosystems, and Dependent Communities.* . Available online at: https://www.ipcc.ch/srocc/chapter/chapter-5/ (accessed August 3, 2020).

Blake, C., and Maggs, C. (2003). Comparative growth rates and internal banding periodicity of maerl species (Corallinales, Rhodophyta) from northern Europe. *Phycologia* 42, 606–612. doi: 10.2216/i0031-8884-42-6-606.1

British Geological Survey (2020). *British Geological Survey (BGS) Offshore Marine Products*. Available online at: https://www.bgs.ac.uk/data/services/offprodwms.html (accessed January 23, 2020).

Brodie, J., Williamson, C. J., Smale, D. A., Kamenos, N. A., Mieszkowska, N., Santos, R., et al. (2014). The future of the northeast Atlantic benthic flora in a high CO2 world. *Ecol. Evol.* 4, 2787–2798. doi: 10.1002/ece3.1105

Burdett, H., Perna, G., McKay, L., Broomhead, G., and Kamenos, N. (2018). Community-level sensitivity of a calcifying ecosystem to acute in situ CO2 enrichment. *Mar. Ecol. Prog. Ser.* 587, 73–80. doi: 10.3354/meps12421

Burdett, H. L., Aloisio, E., Calosi, P., Findlay, H. S., Widdicombe, S., Hatton, A. D., et al. (2012a). The effect of chronic and acute low pH on the intracellular DMSP production and epithelial cell morphology of red coralline algae. *Mar. Biol. Res.* 8, 756–763. doi: 10.1080/17451000.2012.676189

Burdett, H. L., Hatton, A. D., and Kamenos, N. A. (2015). Coralline algae as a globally significant pool of marine dimethylated sulfur. *Glob. Biogeochem. Cycles* 29, 1845–1853. doi: 10.1002/2015GB005274

Burdett, H. L., Hennige, S. J., Francis, F. T.-Y., and Kamenos, N. A. (2012b). The photosynthetic characteristics of red coralline algae, determined using pulse amplitude modulation (PAM) fluorometry. *Bot. Mar.* 55, 499–509. doi: 10.1515/bot-2012-0135

Burrows, M. T., Hughes, D. J., Austin, W. E. N., Smeaton, C., Hicks, N., Howe, J. A., et al. (2017). Assessment of blue carbon resources in Scotland's inshore marine protected area network. *Scott. Nat. Herit. Comm. Rep.* 957:283.

Burrows, M. T., Kamenos, N. A., Hughes, D. J., Stahl, H., Howe, J. A., and Tett, P. (2014). Assessment of carbon budgets and potential blue carbon stores in Scotland's coastal and marine environment. *Scott. Nat. Herit. Comm. Rep.* 761:90.

Cheung, W. W. L., Meeuwig, J. J., Feng, M., Harvey, E., Lam, V. W. Y., Langlois, T., et al. (2012). Climate-change induced tropicalisation of marine communities in Western Australia. *Mar. Freshw. Res.* 63, 415. doi: 10.1071/MF11205

Comhairle nan Eilean Siar (2020a). *South Ford Causeway*. Available online at: https://www.cne-siar.gov.uk/roads-travel-and-parking/bridges-causeways-and-ferries/south-ford-causeway/ (accessed May 14, 2020).

Comhairle nan Eilean Siar (2020b). *Vatersay Causeway. Vatersay Causew*. Available online at: https://www.cne-siar.gov.uk/roads-travel-and-parking/bridges-causeways-and-ferries/vatersay-causeway/ (accessed May 14, 2020).

Cornwall, C. E., Diaz-Pulido, G., and Comeau, S. (2019). Impacts of ocean warming on coralline Algal calcification: meta-analysis, knowledge gaps, and key recommendations for future research. *Front. Mar. Sci.* 6:186. doi: 10.3389/fmars.2019.00186

Dargie, T. (2001). *Sand Dune Vegetation Survey of Scotland: East Coast. Volume 1: Main report*. Available online at: https://www.nature.scot/sites/default/files/2017-07/Publication%202001%20-%20SNH%20Research%2C%20Survey%20and%20Monitoring%20Report%20179%20-%20Sand%20dune%20vegetation%20survey%20of%20Scotland%20-%20East%20Coast%20-%20Volume%201%20-%20Main%20report.pdf (accessed August 9, 2019).

Dutertre, M., Grall, J., Ehrhold, A., and Hamon, D. (2014). Environmental factors affecting maerl bed structure in Brittany (France). *Eur. J. Phycol* 50, 371–383. doi: 10.1080/09670262.2015.1063698

Elith, J., Phillips, S. J., Hastie, T., Dudík, M., Chee, Y. E., and Yates, C. J. (2011). A statistical explanation of MaxEnt for ecologists: statistical explanation of MaxEnt. *Divers. Distrib.* 17, 43–57. doi: 10.1111/j.1472-4642.2010.00725.x

Elliott, S., Turrell, W., Heath, M., and Bailey, D. (2017). Juvenile gadoid habitat and ontogenetic shift observations using stereo-video baited cameras. *Mar. Ecol. Prog. Ser.* 568, 123–135. doi: 10.3354/meps12068

European Commission (2016). *The Habitats Directive - Environment - European Commission. EU Nat. Law*. Available online at: http://ec.europa.eu/environment/nature/legislation/habitatsdirective/index_en.htm (accessed November 10, 2018).

European Commission (2018). *Natura 2000*. Available online at: http://ec.europa.eu/environment/nature/natura2000/index_en.htm (accessed November 10, 2018).

Fabricius, K., and De'ath, G. (2001). Environmental factors associated with the spatial distribution of crustose coralline algae on the great barrier reef. *Coral Reefs* 19, 303–309. doi: 10.1007/s003380000120

Fithian, W., Elith, J., Hastie, T., and Keith, D. A. (2015). Bias correction in species distribution models: pooling survey and collection data for multiple species. *Methods Ecol. Evol.* 6, 424–438. doi: 10.1111/2041-210X.12242

Foster, M. S. (2001). Rhodoliths: between rocks and soft places. *J. Phycol.* 37, 659–667. doi: 10.1046/j.1529-8817.2001.00195.x

Foster, M. S., Amado Filho, G. M., Kamenos, N. A., Riosmena-Rodríguez, R., Steller, D. L., Lang, M. A., et al. (2013). "Rhodoliths and Rhodolith Beds," in *Research and Discoveries: The Revolution of Science through Scuba*, (Washington: Smithsonian Contributions to the Marine Sciences), 143–155.

Fox, C. J., Valcic, L., and Veszelovsxki, A. (2015). *Evidence Gathering in Support of Sustainable Scottish Inshore Fisheries: Work Package 4 Final Report A Pilot Study to Define the Footprint and Activities of Scottish Inshore Fisheries by Identifying Target Fisheries, Habitats and Associated Fish Stocks*. Scotland: Marine Alliance for Science and Technology Scotland.

Freeman, L., Kleypas, J. A., and Miller, A. J. (2013). *PLoS ONE* 8:e82404. doi: 10.1371/journal.pone.0082404

Friedlander, A. M., Caselle, J. E., Ballesteros, E., Brown, E. K., Turchik, A., and Sala, E. (2014). The real bounty: marine biodiversity in the pitcairn Islands. *PLoS One* 9:e100142. doi: 10.1371/journal.pone.0100142

Gallon, R. K., Robuchon, M., Leroy, B., Le Gall, L., Valero, M., and Feunteun, E. (2014). Twenty years of observed and predicted changes in subtidal red seaweed assemblages along a biogeographical transition zone: inferring potential causes from environmental data. *J. Biogeogr.* 41, 2293–2306. doi: 10.1111/jbi.12380

Grall, J., and Hall-Spencer, J. M. (2003). Problems facing maerl conservation in Brittany. *Aquat. Conserv. Mar. Freshw. Ecosyst.* 13, S55–S64. doi: 10.1002/aqc.568

Gubbay, S., Sanders, N., Haynes, T., Janssen, J. A. M., Airoldi, L., Battelli, C., et al. (2016). *European Red list of habitats*. Luxembourg: Publications Office of the European Union.

Hall-Spencer, J., White, N., Gillespie, E., Gillham, K., and Foggo, A. (2006). Impact of fish farms on maerl beds in strongly tidal areas. *Mar. Ecol. Prog. Ser.* 326, 1–9. doi: 10.3354/meps326001

Hall-Spencer, J. M., Kelly, J., and Maggs, C. A. (2008). *Assessment of Maerl Beds in the OSPAR Area and the Development of A Monitoring Program*. Ireland: Department of the Environment HaLG, Ireland.

Hall-Spencer, J. M., Kelly, J., and Maggs, C. A. (2010). *OSPAR Commission Background Document for Maerl beds*. London: OSPAR Commission.

Hastings, A., Byers, J. E., Crooks, J. A., Cuddington, K., Jones, C. G., Lambrinos, J. G., et al. (2007). Ecosystem engineering in space and time. *Ecol. Lett.* 10, 153–164. doi: 10.1111/j.1461-0248.2006.00997.x

Hijmans, R. (2017). *Package "Dismo."*. Available online at: https://www.rdocumentation.org/packages/dismo/versions/1.1-4 (accessed August 28, 2019).

Hoegh-Guldberg, O., Mumby, P. J., Hooten, A. J., Steneck, R. S., Greenfield, P., Gomez, E., et al. (2007). Coral reefs under rapid climate change and ocean acidification. *Science* 318, 1737–1742. doi: 10.1126/science.1152509

Hughes, T. P., Rodrigues, M. J., Bellwood, D. R., Ceccarelli, D., Hoegh-Guldberg, O., McCook, L., et al. (2007). Phase shifts. herbivory, and the resilience of coral reefs to climate change. *Curr. Biol.* 17, 360–365. doi: 10.1016/j.cub.2006.12.049

IPCC (2014). *Climate Change 2014: Synthesis Report. Contribution of Working Groups I, II and III to the Fifth Assessment Report of the Intergovernmental Panel on Climate Change*. Available online at: https://www.ipcc.ch/report/ar5/syr/ (accessed February 3, 2020).

Jackson, C. M., Kamenos, N. A., Moore, P. G., and Young, M. (2004). Meiofaunal bivalves in maerl and other substrata; their diversity and community structure. *Ophelia* 58, 49–60.

JNCC (2016). *UK BAP Priority Habitats*. Available online at: http://jncc.defra.gov.uk/page-5718 (accessed November 10, 2018).

Jorda, G., Marbà, N., Bennett, S., Santana-Garcon, J., Agusti, S., and Duarte, C. M. (2020). Ocean warming compresses the three-dimensional habitat of marine life | Nature Ecology & Evolution. *Nat. Ecol. Evol.* 4, 109–114. doi: 10.1038/s41559-019-1058-0

Júnior, P. D. M., and Nóbrega, C. C. (2018). Evaluating collinearity effects on species distribution models: An approach based on virtual species simulation. *PLoS One* 13:e0202403. doi: 10.1371/journal.pone.0202403

Kamenos, N., and Law, A. (2010). Temperature Controls on Coralline Algal Skeletal Growth. *J. Phycol.* 46, 331–335. doi: 10.1111/j.1529-8817.2009.00780.x

Kamenos, N., Moore, G., and Hall-Spencer, J. M. (2004). Small-scale distribution of juvenile gadoids in shallow inshore waters; what role does maerl play? *ICES J. Mar. Sci.* 61, 422–429. doi: 10.1016/j.icesjms.2004.02.004

Kamenos, N. A., Burdett, H. L., Aloisio, E., Findlay, H. S., Martin, S., Longbone, C., et al. (2013). Coralline algal structure is more sensitive to rate, rather than the magnitude, of ocean acidification. *Glob. Change Biol.* 19, 3621–3628. doi: 10.1111/gcb.12351

Kamenos, N. A., Perna, G., Gambi, M. C., Micheli, F., and Kroeker, K. J. (2016). Coralline algae in a naturally acidified ecosystem persist by maintaining control of skeletal mineralogy and size. *Proc. R. Soc. B Biol. Sci.* 283:20161159. doi: 10.1098/rspb.2016.1159

Kamenos, N. A., Strong, S., Shenoy, D., Wilson, S., Hatton, A., and Moore, P. (2008b). Red coralline algae as a source of marine biogenic dimethylsulphoniopropionate. *Mar. Ecol. Prog. Ser.* 372, 61–66. doi: 10.3354/meps07687

Kroeker, K. J., Micheli, F., and Gambi, M. C. (2012). Ocean acidification causes ecosystem shifts via altered competitive interactions. *Nat. Clim. Change* 3, 156–159. doi: 10.1038/nclimate1680

Legrand, E., Riera, P., Lutier, M., Coudret, J., Grall, J., and Martin, S. (2017). Species interactions can shift the response of a maerl bed community to ocean acidification and warming. *Biogeosciences* 14, 5359–5376. doi: 10.5194/bg-14-5359-2017

Lynham, J., Nikolaev, A., Raynor, J., Vilela, T., and Villaseñor-Derbez, J. C. (2020). Impact of two of the world's largest protected areas on longline fishery catch rates. *Nat. Commun* 11, 1–9.

Macreadie, P. I., Anton, A., Raven, J. A., Beaumont, N., Connolly, R. M., Friess, D. A., et al. (2019). The future of blue carbon science. *Nat. Commun.* 10, 1–13. doi: 10.1038/s41467-019-11693-w

Mao, J., Burdett, H. L., McGill, R. A. R., Newton, J., Gulliver, P., and Kamenos, N. A. (2020). Carbon burial over the last four millennia is regulated by both climatic and land use change. *Glob. Change Biol.* 26, 2496-2504. doi: 10.1111/gcb.15021

Marine Scotland. (2018). *Improving Protection Given to Priority Marine Features Outside the Marine Protected Area Network*. Available online at: https://www.gov.scot/publications/improving-protection-given-pmfs-outside-mpa-network/pages/8/ (accessed January 30, 2020).

Martin, S., and Gattuso, J.-P. (2009). Response of Mediterranean coralline algae to ocean acidification and elevated temperature. *Glob. Change Biol.* 15, 2089–2100. doi: 10.1111/j.1365-2486.2009.01874.x

Martin, S., and Hall-Spencer, J. M. (2017). "Effects of Ocean Warming and Acidification on Rhodolith/Maërl Beds," in *Rhodolith/Maërl Beds: A Global Perspective Coastal Research Library*, eds R. Riosmena-Rodriguez, W. Nelson, and J. Aguirre (Berlin: Springer).

Martínez, B., Radford, B., Thomsen, M. S., Connell, S. D., Carreño, F., Bradshaw, C. J. A., et al. (2018). Distribution models predict large contractions of habitat-forming seaweeds in response to ocean warming. *Divers. Distrib.* 24, 1350–1366. doi: 10.1111/ddi.12767

McCoy, S. J., and Kamenos, N. A. (2015). Coralline algae (Rhodophyta) in a changing world: integrating ecological, physiological, and geochemical responses to global change. *J. Phycol.* 51, 6–24. doi: 10.1111/jpy.12262

Merow, C., Smith, M. J., and Silander, J. A. (2013). A practical guide to MaxEnt for modeling species' distributions: what it does, and why inputs and settings matter. *Ecography* 36, 1058–1069. doi: 10.1111/j.1600-0587.2013.07872.x

Muscarella, R., Galante, P. J., Soley-Guardia, M., Boria, R. A., Kass, J. M., Uriarte, M., et al. (2018). *ENMeval: Automated Runs and Evaluations of Ecological Niche Models*. Available online at: https://cran.r-project.org/web/packages/ENMeval/index.html (accessed November 22, 2018).

Muscarella, R., Galante, P. J., Soley-Guardia, M., Boria, R. A., Kass, J. M., Uriarte, M., et al. (2014). ENMeval: an R package for conducting spatially independent evaluations and estimating optimal model complexity for Maxent ecological niche models. *Methods Ecol. Evol.* 5, 1198–1205. doi: 10.1111/2041-210X.12261

National Species Reintroduction Forum (2014). *The Scottish Code for Conservation Translocations*. Available online at: https://www.nature.scot/sites/default/files/Publication%202014%20-%20The%20Scottish%20Code%20for%20Conservation%20Translocations.pdf (accessed March 23, 2020).

Nelson, W. A. (2009). Calcified macroalgae - critical to coastal ecosystems and vulnerable to change: a review. *Mar. Freshw. Res.* 60:787. doi: 10.1071/MF08335

Noisette, F., Duong, G., Six, C., Davoult, D., and Martin, S. (2013a). Effects of elevated pCO2 on the metabolism of a temperate rhodolith Lithothamnion corallioides grown under different temperatures. *J. Phycol.* 49, 746–757. doi: 10.1111/jpy.12085

Noisette, F., Egilsdottir, H., Davoult, D., and Martin, S. (2013b). Physiological responses of three temperate coralline algae from contrasting habitats to near-future ocean acidification. *J. Exp. Mar. Biol. Ecol.* 448, 179–187. doi: 10.1016/j.jembe.2013.07.006

Pan, B. J., Vernet, M., Reynolds, R. A., and Mitchell, B. G. (2019). The optical and biological properties of glacial meltwater in an Antarctic fjord. *PLoS One* 14:e0211107. doi: 10.1371/journal.pone.0211107

Pardo, C., Guillemin, M.-L., Peña, V., Bárbara, I., Valero, M., and Barreiro, R. (2019). Local coastal configuration rather than latitudinal gradient shape clonal diversity and genetic structure of phymatolithon calcareum maerl beds in North European Atlantic. *Front. Mar. Sci.* 6:149. doi: 10.3389/fmars.2019.00149

Pardo, C., Lopez, L., Peña, V., Hernández-Kantún, J., Gall, L. L., Bárbara, I., et al. (2014a). A Multilocus species delimitation reveals a striking number of species of coralline algae forming maerl in the OSPAR maritime area. *PLoS One* 9:e104073. doi: 10.1371/journal.pone.0104073

Pardo, C., Peña, V., Bárbara, I., Valero, M., and Barreiro, R. (2014b). Development and multiplexing of the first microsatellite markers in a coralline red alga (Phymatolithon calcareum, Rhodophyta). *Phycologia* 53, 474–479. doi: 10.2216/14-031.1

Pavlova, A., Beheregaray, L. B., Coleman, R., Gilligan, D., Harrisson, K. A., Ingram, B. A., et al. (2017). Severe consequences of habitat fragmentation on genetic diversity of an endangered Australian freshwater fish: a call for assisted gene flow. *Evol. Appl.* 10, 531–550. doi: 10.1111/eva.12484

Pearson, R. G. (2010). Species' Distribution Modeling for Conservation Educators and Practitioners. *Lessons Conserv.* 3, 54–89.

Pearson, R. G., Raxworthy, C. J., Nakamura, M., and Peterson, A. T. (2007). Predicting species distributions from small numbers of occurrence records: a test case using cryptic geckos in Madagascar. *J. Biogeogr.* 34, 102–117. doi: 10.1111/j.1365-2699.2006.01594.x

Peña, V., and Barbara, I. (2009). Distribution of the Galician maerl beds and their shape classes (Atlantic Iberian Peninsula): proposal of areas in future conservation actions. *Cah. Biol. Mar.* 50, 335–368.

Peña, V., Barbara Criado, I., Grall, J., Maggs, C. A., and Hall-Spencer, J. (2014). The diversity of seaweeds on maerl in the NE Atlantic. *Mar. Biodivers.* 44, 533–551. doi: 10.1007/s12526-014-0214-7

Perry, F., Jackson, A., and Garrard, S. L. (2017a). "Lithothamnion glaciale Maerl," in *Marine Life Information Network: Biology and Sensitivity Key Information Reviews*, eds H. Tyler-Walters and K. Hiscock (Plymouth: Marine Biological Association of the United Kingdom).

Perry, F., Jackson, A., Garrard, S. L., and Hiscock, K. (2017b). "Phymatolithon calcareum Maerl," in *Marine Life Information Network: Biology and Sensitivity Key Information Reviews*, ed. H. Tyler-Walters (Plymouth: Marine Biological Association of the United Kingdom).

Phillips, S. J., Dudík, M., and Schapire, R. E. (2006). *Maxent Software for Modeling Species Niches and Distributions*. Available online at: http://biodiversityinformatics.amnh.org/open_source/maxent (accessed January 20, 2019).

Porter, J. S., Austin, W. E. N., Burrows, M. T., Davies, G., Kamenos, N., Riegel, S., et al. (2020). *Blue Carbon Audit of Scottish Waters*. Available online at: https://www.researchgate.net/publication/338585272_Blue_Carbon_Audit_of_Orkney_Waters (accessed March 12, 2020).

Porzio, L., Buia, M. C., and Hall-Spencer, J. M. (2011). Effects of ocean acidification on macroalgal communities. *J. Exp. Mar. Biol. Ecol.* 400, 278–287. doi: 10.1016/j.jembe.2011.02.011

Qui-Minet, Z. N., Coudret, J., Davoult, D., Grall, J., Mendez-Sandin, M., Cariou, T., et al. (2019). Combined effects of global climate change and nutrient enrichment on the physiology of three temperate maerl species. *Ecol. Evol.* 9, 13787–13807. doi: 10.1002/ece3.5802

R Core Team (2019). *R: A Language and Environment for Statistical Computing*. Vienna: R Foundation for Statistical Computing.

Riosmena-Rodriguez, R. (ed.) (2016). *"The Role of Rhodolith/Maërl Beds in Modern Oceans," in Rhodolith/maerl Beds: A Global Perspective*. New York, NY: Springer, 3–26.

Riosmena-Rodriguez, R., Nelson, W. A., and Aguirre, J. (eds) (2016). *Rhodolith/maerl Beds: A Global Perspective*. New York, NY: Springer.

Roberts, C. M., O'Leary, B. C., McCauley, D. J., Cury, P. M., Duarte, C. M., Lubchenco, J., et al. (2017). Marine reserves can mitigate and promote adaptation to climate change. *Proc. Natl. Acad. Sci. U.S.A.* 114, 6167–6175. doi: 10.1073/pnas.1701262114

Schoenrock, K. M., Bacquet, M., Pearce, D., Rea, B. R., Schofield, J. E., Lea, J., et al. (2018). Influences of salinity on the physiology and distribution of the Arctic coralline algae, Lithothamnion glaciale (Corallinales, Rhodophyta). *J. Phycol.* 54, 690–702. doi: 10.1111/jpy.12774

Scottish Government (2018). *Priority Marine Features*. Available online at: http://www2.gov.scot/Topics/marine/marine-environment/mpanetwork/PMF (accessed January 11, 2019).

Scottish Government (2019). *Improving protection given to Priority Marine Features Outside the Marine Protected Area Network - Scottish Government - Citizen Space*. Available online at: https://consult.gov.scot/marine-scotland/priority-marine-features/ (accessed January 30, 2020).

Scottish Natural Heritage (2019a). *GeMS - Scottish Priority Marine Features (PMF)*. Available online at: https://gateway.snh.gov.uk/natural-spaces/dataset.jsp?dsid=GEMS-PMF (accessed August 28, 2019).

Scottish Natural Heritage (2019b). *Loch nam Madadh SAC*. Available online at: https://sitelink.nature.scot/site/8301 (accessed December 18, 2018).

Sheehan, E. V., Bridger, D., and Attrill, M. J. (2015). The ecosystem service value of living versus dead biogenic reef. *Estuar. Coast. Shelf Sci.* 154, 248–254. doi: 10.1016/j.ecss.2014.12.042

Smale, D. A. (2020). Impacts of ocean warming on kelp forest ecosystems. *New Phytol.* 225, 1447–1454. doi: 10.1111/nph.16107

Steen, B. (2019). Modelling hot spot areas for the invasive alien plant *Elodea nuttallii* in the EU. *Manag. Biol. Invasions* 10, 151–170. doi: 10.3391/mbi.2019.10.1.10

Steller, D. L., Riosmena-Rodríguez, R., Foster, M. S., and Roberts, C. A. (2003). Rhodolith bed diversity in the Gulf of California: the importance of rhodolith structure and consequences of disturbance. *Aquat. Conserv. Mar. Freshw. Ecosyst.* 13, S5–S20. doi: 10.1002/aqc.564

Suggett, D. J., Camp, E. F., Edmondson, J., Boström-Einarsson, L., Ramler, V., Lohr, K., et al. (2019). Optimizing return-on-effort for coral nursery and outplanting practices to aid restoration of the great barrier reef. *Restor. Ecol.* 27, 683–693. doi: 10.1111/rec.12916

Sunday, J. M., Fabricius, K. E., Kroeker, K. J., Anderson, K. M., Brown, N. E., Barry, J. P., et al. (2017). Ocean acidification can mediate biodiversity shifts by changing biogenic habitat. *Nat. Clim. Change* 7, 81–85. doi: 10.1038/nclimate3161

Teagle, H., and Smale, D. A. (2018). Climate-driven substitution of habitat-forming species leads to reduced biodiversity within a temperate marine community. *Divers. Distrib.* 24, 1367–1380. doi: 10.1111/ddi.12775

The Council of the European Communities (1992). *Council Directive 92/43/EEC of 21 May 1992 on the Conservation of Natural Habitats and of Wild Fauna and Flora*. Available online at: https://eur-lex.europa.eu/legal-content/EN/TXT/?uri=CELEX:01992L0043-20070101 (accessed January 10, 2019).

Tyberghein, L., Verbruggen, H., Pauly, K., Troupin, C., Mineur, F., and Clerck, O. D. (2012). Bio-ORACLE: a global environmental dataset for marine species

distribution modelling. *Glob. Ecol. Biogeogr.* 21, 272–281. doi: 10.1111/j.1466-8238.2011.00656.x

van der Heijden, L. H., and Kamenos, N. A. (2015). Reviews and syntheses: calculating the global contribution of coralline algae to total carbon burial. *Biogeosciences* 12, 6429–6441. doi: 10.5194/bg-12-6429-2015

Veloz, S. D. (2009). Spatially autocorrelated sampling falsely inflates measures of accuracy for presence-only niche models. *J. Biogeogr.* 36, 2290–2299. doi: 10.1111/j.1365-2699.2009.02174.x

Verbruggen, H., Tyberghein, L., Belton, G. S., Mineur, F., Jueterbock, A., Hoarau, G., et al. (2013). Improving transferability of introduced species' distribution models: new tools to forecast the spread of a highly invasive seaweed. *PLoS One* 8:e68337. doi: 10.1371/journal.pone.0068337

Wernberg, T., Smale, D. A., and Thomsen, M. S. (2012). A decade of climate change experiments on marine organisms: procedures, patterns and problems. *Glob. Change Biol.* 18, 1491–1498. doi: 10.1111/j.1365-2486.2012.02656.x

Wilson, S., Blake, C., Berges, J. A., and Maggs, C. A. (2004). Environmental tolerances of free-living coralline algae (maerl): implications for European marine conservation. *Biol. Conserv.* 120, 279–289. doi: 10.1016/j.biocon.2004.03.001

Conflict of Interest: The authors declare that the research was conducted in the absence of any commercial or financial relationships that could be construed as a potential conflict of interest.

frontiers in Marine Science

ORIGINAL RESEARCH
published: 08 October 2020
doi: 10.3389/fmars.2020.567228

Ocean Acidification Mitigates the Negative Effects of Increased Sea Temperatures on the Biomineralization and Crystalline Ultrastructure of *Mytilus*

Antony M. Knights[1], Matthew J. Norton[1], Anaëlle J. Lemasson[1,2] and Natasha Stephen[3]*

[1] *Marine Biology and Ecology Research Centre, School of Biological and Marine Sciences, University of Plymouth, Plymouth, United Kingdom,* [2] *Wild Planet Trust (Paignton Zoo), Paignton, United Kingdom,* [3] *Plymouth Electron Microscopy Centre, University of Plymouth, Plymouth, United Kingdom*

Negative impacts of global climate change are predicted for a range of taxa. Projections predict marked increases in sea surface temperatures and ocean acidification (OA), arguably placing calcifying organisms at most risk. While detrimental impacts of environmental change on the growth and ultrastructure of bivalve mollusk shells have been shown, rapid and diel fluctuations in pH typical of coastal systems are often not considered. *Mytilus edulis*, an economically important marine calcifier vulnerable to climate change, were exposed to current and future OA (380 and 1000 ppm pCO_2), warming (17 and 20°C), and ocean acidification and warming (OAW) scenarios in a seawater system incorporating natural fluctuations in pH. Both macroscopic morphometrics (length, width, height, volume) and microscopic changes in the crystalline structure of shells (ultrastructure) using electron backscatter diffraction (EBSD) were measured over time. Increases in seawater temperature and OAW scenarios led to increased and decreased shell growth respectively and on marginal changes in cavity volumes. Shell crystal matrices became disordered shifting toward preferred alignment under elevated temperatures indicating restricted growth, whereas *Mytilus* grown under OAW scenarios maintained single crystal fabrics suggesting OA may ameliorate some of the negative consequences of temperature increases. However, both elevated temperature and OAW led to significant increases in crystal size (grain area and diameter) and misorientation frequencies, suggesting a propensity toward increased shell brittleness. Results suggest adult *Mytilus* may become more susceptible to biological determinants of survival in the future, altering ecosystem structure and functioning.

Keywords: multiple stressors, climate change, biomineralization, mussels, environmental variability, functioning

OPEN ACCESS

Edited by:
Ben P. Harvey,
University of Tsukuba, Japan

Reviewed by:
Tomihiko Higuchi,
The University of Tokyo, Japan
Laura Ramajo,
Universidad Católica del Norte, Chile

****Correspondence:***
Antony M. Knights
aknights@plymouth.ac.uk

Specialty section:
This article was submitted to Global Change and the Future Ocean, a section of the journal Frontiers in Marine Science

Received: *29 May 2020*
Accepted: *25 August 2020*
Published: *08 October 2020*

Citation:
Knights AM, Norton MJ, Lemasson AJ and Stephen N (2020) Ocean Acidification Mitigates the Negative Effects of Increased Sea Temperatures on the Biomineralization and Crystalline Ultrastructure of Mytilus. Front. Mar. Sci. 7:567228. doi: 10.3389/fmars.2020.567228

INTRODUCTION

Over the last century, atmospheric concentrations of CO_2 have increased at an unprecedented rate resulting in changing environmental conditions on both land and sea. In the ocean, the increased absorption of CO_2 due to higher atmospheric partial pressures is altering chemical reactions and driving declines in pH and (CO_3^{2-}) (Doney et al., 2009) – a phenomenon referred to as ocean

acidification (OA). At current CO_2 emission rates, by 2100 atmospheric CO_2 concentrations are predicted to exceed 1000 ppm in some instances (Stocker et al., 2013), leading to reductions in pH of between 0.3 and 0.4 units from today's conditions (Doney et al., 2009). For marine life, changes in pH can have significant, detrimental effects on their structure and functioning (Lemasson et al., 2017a, 2018) including abnormal larval development (Kurihara et al., 2007; Kurihara, 2008), increased pressure on acid-base regulatory mechanisms (Lindinger et al., 1984; Thomsen and Melzner, 2010; Scanes et al., 2017) and changes to behavior (Queiros et al., 2015; Sadler et al., 2018).

For calcifying species, OA can be especially problematic due to disruption of the biomineralization process that is so crucial to the development of shells, exoskeletons and tests. In bivalve mollusks, the shell often consists of two polymorphs of calcium carbonate: the outer prismatic layer comprising calcite crystals, and the inner nacre layer comprising aragonite crystal tablets (Gazeau et al., 2013). Both polymorphs are formed within the extrapallial space following the catalytic conversion of CO_2 to bicarbonate by the enzyme carbonic anhydrase (Marin and Luquet, 2004). This catalysis is a crucial process for calcium carbonate crystal nucleation, growth and orientation (Nakahara, 1991; Choi and Kim, 2000; Olson et al., 2013). Under normal conditions, these crystals are arranged as horizontal sheets (Checa et al., 2006; Hahn et al., 2012) but under predicted future climate conditions, crystal formation can become disordered and the crystals themselves misorientated or porous (Hahn et al., 2012; Fitzer et al., 2014a,b; Li et al., 2015; Meng et al., 2019; **Figure 1**). It is argued that these changes will have negative consequences for shell integrity and material properties (e.g., Beniash et al., 2010; Fitzer et al., 2015b), impacting the potential for mollusks to withstand physical and biological stress (Sadler et al., 2018).

The effects of OA on mollusk shell calcification and ultrastructure have largely been considered under fixed pH conditions; the experimental pH treatments are tightly controlled within a small pre-defined range and considerable negative consequences for organisms have been shown (e.g., Dupont et al., 2013). Yet increasingly, *in situ* measurements of pH in a range of coastal marine habitats including estuaries, kelp forests, coral reefs, and upwelling regions (Hofmann et al., 2011) reveal considerable natural fluctuations in pH (of up to 0.8 units) over short (diel) timescales (e.g., Lemasson et al., 2018). Where studies have incorporated pH fluctuations within their experiments either experimentally or by sampling organisms from sites with varying degrees of environmental fluctuation (Dufault et al., 2012; Comeau et al., 2014; Frieder et al., 2014; Ramajo et al., 2019), the impacts of OA have been less severe, perhaps due to transient exposure to less acidified conditions (Wahl et al., 2016) or that organisms originating from sites with naturally higher fluctuations in pH may be more tolerant or locally adapted to OA (Pansch et al., 2014).

Increasingly, studies are beginning to include the potential interactive effects of temperature in order to better simulate the ocean acidification and warming (OAW) environmental scenarios predicted for the end of the century. These studies have largely focused on macro-morphological change but often results appear contradictory or indicate a degree of context specificity (*sensu* Pansch et al., 2014); differences that may be driven by location, species, or life-history stage. For example, Lagos et al. (2016) found elevated temperatures mitigate negative impacts of OA on shell growth in *Argopecten purpuratus*. In *Littorina littorea*, Melatunan et al. (2013) found elevated temperature or reduced pH were equally detrimental to growth but effects increased in severity when combined, and Lemasson et al. (2018) found elevated temperature but not OA affected growth in oysters.

Relatively few studies have assessed the combined effects of OAW scenarios on shell ultrastructure. Independently, temperature has been shown to induce significant crystal misorientation (Olson et al., 2013), changes in thickness (Olson and Gilbert, 2012; Gilbert et al., 2017) and alteration in the overall ultrastructure (Füllenbach et al., 2014). These studies, however, have mainly been in the context of paleo-environmental proxies which arguably have limited relevance to the current, rapid changes in temperature driven by anthropogenic activities. Of the studies that have investigated the combined effects of OA and warming (e.g., Fitzer et al., 2014b, 2015b; Li et al., 2015), the evidence suggests that elevated temperatures can exacerbate ultrastructure disruption caused by elevated pCO_2, although the chosen experimental conditions are not necessarily those marine organisms are expected to face in the next century.

Understanding change in the morphological characteristics of shell ultrastructure, such as changes in crystal orientation, the occurrence of coincident site lattice (CSL) boundaries between crystals, and crystal size, may provide important insights in to how organisms will respond to future climate change. Misorientation – the difference in orientation between adjacent crystals – is expected to be relatively rare under low stress conditions as the organic matrix is able to maintain a well-ordered ultrastructure. Under environmental stress (e.g., OAW scenarios), that organic matrix may breakdown leading to disordered ultrastructure and higher instances of crystal misorientation (Olson et al., 2013). Crystal misorientation can lead to an increased frequency of CSL boundaries; the boundary where the positions of a proportion of lattice sites coincide at the boundary segments between two adjacent crystals (Fortes, 1972). Some material science studies have found that low angle grain boundaries and low Sigma (Σ)-value CSL boundaries can influence material properties with increases in hardness and resistance to the spread of intergranular cracks (Lehockey et al., 2004; Arafin and Szpunar, 2009). An increased frequency of certain CSL boundaries in biomineralized structures such as calcified mollusk shells, may be an important determinant of resistance to mechanical stresses like those experienced by bivalves under predation pressure from decapods and gastropods (Elner, 1978; Sadler et al., 2018). Changes in crystal size may also indicate impacts of environmental conditions on crystal nucleation and growth

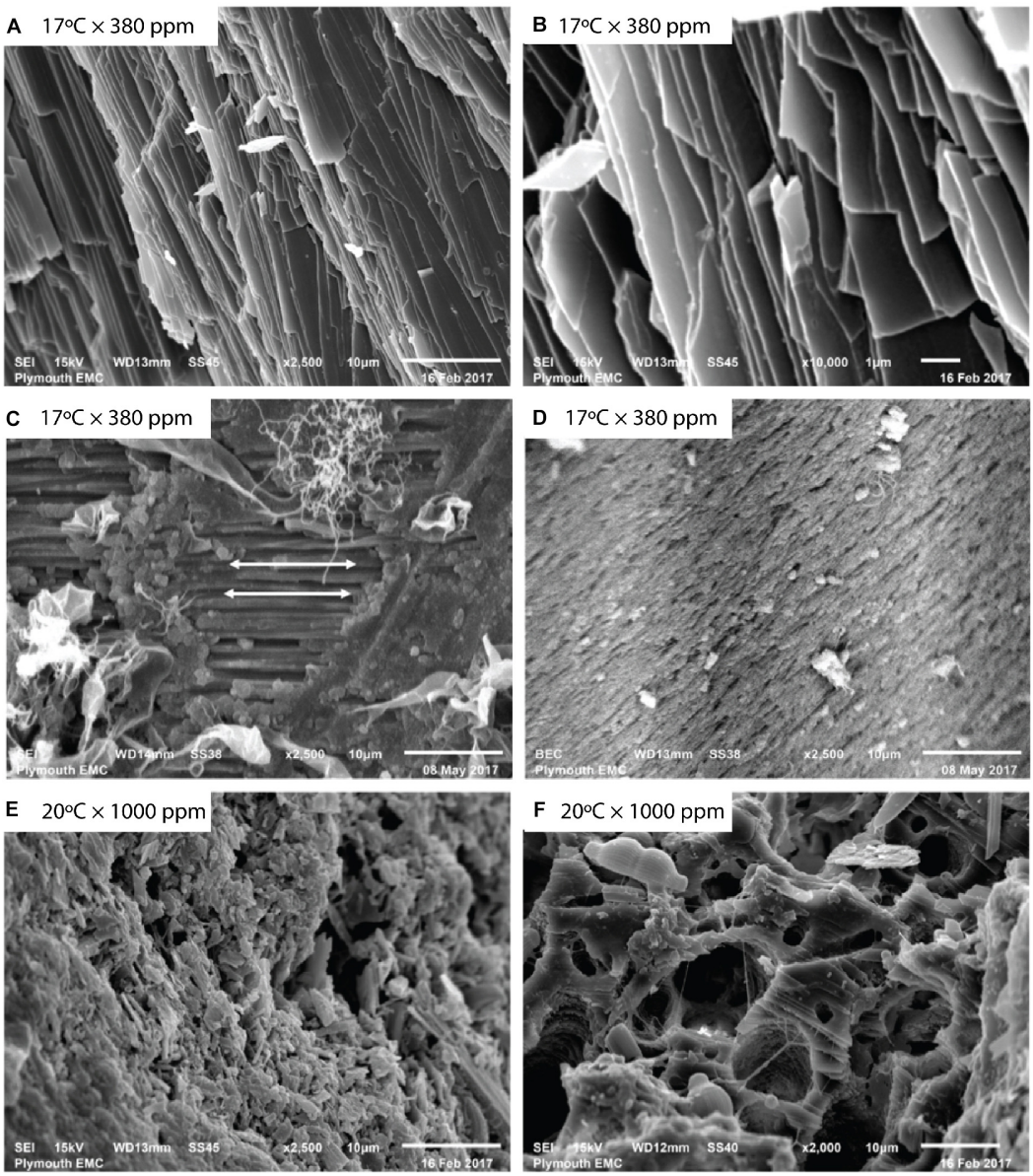

FIGURE 1 | *Mytilus* sp. valves imaged using backscattered electron (BSE) imaging. Unprepared baseline *Mytilus* **(A,B)** show naturally occurring aligned crystalline structures at **(A)** 2500×, and **(B)** 10,000× magnification before specimen preparation. Prepared baseline specimens **(C,D)** at 2500× magnification reveal differences in prismatic and nacre layers showing **(C)** aligned crystalline structure as indicated by arrows, and **(D)** more porous structure with lack of an observable regular crystalline alignment. *Mytilus* exposed to elevated temperature and pCO_2 **(E,F)** show **(E)** disrupted, irregular structure, and **(F)** a fragmented, porous nature.

mechanisms. Such changes have been shown over paleo-geological timescales (e.g., Olson and Gilbert, 2012; Gilbert et al., 2017) but have yet to be considered in the context of rapid environmental change that marine organisms are experiencing today.

This study investigated the extent to which the combination of elevated pCO_2 concentrations and temperature can alter the growth and ultrastructure of *Mytilus* sp. Using an experimental mesocosm system able to replicate future OAW scenarios that encompasses natural fluctuations in pH, we compare changes in (i) whole organism shell growth, and (ii) crystal orientation, size, and lattice boundary formations using cutting-edge electron backscatter diffraction techniques (EBSD).

MATERIALS AND METHODS

Mussel Culture

Mussels were collected from Queen Anne's Battery, Plymouth (50°36′40.82″N, 4°13′11.61″W), cleared of epibionts with a metal scraper, and transported back to the lab in buckets

of seawater. Animals were placed in tanks containing UV-treated filtered seawater collected from the sampling location within 1 h of collection and allowed to acclimate to laboratory conditions (salinity −29.7 ± 2.3; temperature −17°C ± 0.20; pH 8.00 ± 0.04) for 2 weeks. After acclimation, 36 mussels were randomly allocated to 12 chambers (3 mussels per chamber) for 8-week. These chambers were filled with fresh UV-treated filtered sea water, also collected from the sampling location. Mean salinity was marginally higher (32.6 ± 1.3) than in the acclimation treatment as a result of natural fluctuations in salinity due to rainfall and riverine inputs. Each chamber represented one of four environmental scenarios (n = 3). By the end of the century, future climate change scenarios predict increases in sea surface temperature of 2–4°C and increases in atmospheric pCO_2 of ∼600–800 ppm (IPCC, 2014) depending on the emissions (RCP) scenario. Here, we adopted a temperature increase of 3°C and pCO_2 increase of 620 ppm, resulting in the following four combinations: (1) 17°C × 380 ppm pCO_2; (2) 17°C × 1000 ppm pCO_2; (3) 20°C × 380 ppm pCO_2; and (4) 20°C × 1000 ppm pCO_2. Temperature treatments were maintained using recirculating thermostatically controlled heated water baths (Aqua Medic, United Kingdom) bubbled with air or 1000 ppm CO_2-enriched air (see Lemasson et al., 2018). CO_2 concentrations were controlled using a CO_2 gas analyzer (LI-COR LI-820, United States). Natural fluctuations in pH result from this approach as pCO_2 concentrations remain static and pH changes occur as a result of fluctuations in atmospheric pressure, although these fluctuations in pH were relatively small with a maximum standard deviation of 0.1 pH units in any treatment (**Supplementary Table S1**). Seawater pH (SevenExcellence Multi-parameter pH probe), temperature (Omega HH802U temperature probe) and salinity (HI96822 Seawater Refractometer) were tested daily and total alkalinity (TitraLab© AT1000 series workstation) and pCO_2 (Corning 965 TCO_2 Analyser) were measured three times per week. Mussels were fed every other day with 10 mL of Shellfish Diet 1800 at a concentration of ∼4500 cell mL^{-1} (Thomsen and Melzner, 2010; Fitzer et al., 2014b). Four biometric parameters: total wet mass, shell length, shell width, and shell height were measured before and after an 8-week exposure period.

Body volume (cm^3) of all individuals (N = 36) was calculated using the volume of water displaced (mL) by the mussel in a volumetric cylinder containing sea water (density of 1.025 g/cm^3 at 20°C, salinity = 35). This approach controls for any water retained within the mantle. Displacement (mL) of an individual was measured at time zero (t_0) and after 8-week (t_8) of exposure to all experimental treatments. Sea water density was measured using a hand-held digital refractometer (D&D, The Aquarium Solution Ltd., United Kingdom). Shell dimensions (length, width, height) were measured using digital calipers (Mitutoyo, Japan) to the nearest 0.1 mm, also at t_0 and t_8 (**Figure 2A**).

Ultrastructure Data Sampling Procedure

After 8-week, all mussels were euthanized and the soft tissue removed. Two mussels per treatment were randomly chosen from the control (17°C × 380 ppm pCO_2), elevated temperature (20°C × 380 ppm pCO_2), and elevated temperature and pCO_2 treatment (20°C × 1000 ppm pCO_2) and a cross-section from the lip area of each mussel removed using a high-speed cutting wheel (Dremel, United States). Mussels from a control temperature and elevated pCO2 treatment (17°C × 1000 ppm pCO_2) were not used for EBSD analysis due to logistical constraints and given that this scenario is not expected under future climate scenarios. Cross-sectional cuts were specifically made to allow examination of the ultrastructure between the prismatic and nacre layers (**Figure 2B**) along the growth direction in the most recently formed shell material (Checa et al., 2006; Hahn et al., 2012).

Shell samples were mounted in epoxy resin (Struers Epofix), ground [Buehler Carbimet Grit^{TM} 600 (P1200) pad] and sequentially polished with 6 μm then 1 μm diamond suspensions (Buehler MetaDi®) until a glossy appearance was achieved. Samples were then polished using a vibratory polisher (Buehler VibroMet2®) with a 0.05 μm polishing suspension (MasterPrep^{TM}) diluted in distilled water. Samples were examined under an optical microscope (Meiji Techno EMZ-13TR, Infinity 1) to check the quality of the polished surface (**Figure 1**). Samples were preserved in ethanol before carbon sputter-coating (Quorum Technologies Q150T ES, United Kingdom).

Samples were examined in a variable-pressure scanning electron microscope (SEM) (JEOL 6610 VP-SEM, Japan) under high vacuum at 15 kV. Magnification, spot size, and working distance were modified between samples to optimize data acquisition. Crystallographic data were obtained using a Nordlys Nano EBSD detector with AZtec software, and analyzed using HKL CHANNEL5 post-processing software (Oxford Instruments, United Kingdom). Grains were detected using a minimum pixel number of 10 (default setting) and a critical misorientation angle of 3° as the defining criteria (Goetz et al., 2011).

Ultrastructure Parameters

Differences in the ultrastructure between samples were assessed using a combination of inverse pole figure (IPF) orientation maps, contoured pole figures, frequency distributions of grain boundary misorientation angles, Σ-value CSL boundaries, grain area, and grain diameter metrics. IPF maps using the z-direction (IPFz; perpendicular to the sample surface) as the sample reference direction were used to demonstrate patterns of variability in orientation in shell samples. IPF maps present patterns of crystallographic orientation using different colors to illustrate different orientations of EBSD measurement pixels relative to a fixed orientation. In a well-ordered ultrastructure, IPF maps would be expected to show similar orientations throughout much of the mapped site, or with different orientations restricted to definable regions. The majority of grains should appear to face a similar direction along the sample surface. In a more disordered ultrastructure, the mapped sites would be expected to show a wide variation in orientation with the direction that the grains face, relative to the sample surface, appearing more random.

Contoured pole figures (1 point per grain analysis) were used to demonstrate the variation in crystallographic orientation of individual grains relative to different planes. Ordered/orientated

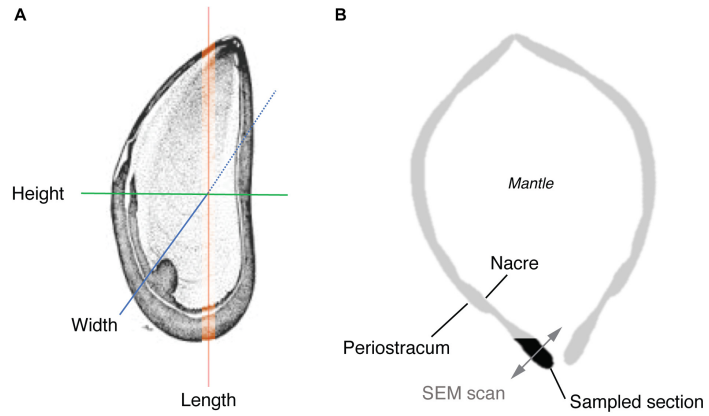

FIGURE 2 | Schematic illustrating **(A)** dimensional features (excluding volume) measured in the macro-morphometric study, and **(B)** transverse section of a mussel showing the location of the shell section used in EBSD analysis and direction of EBSD scans.

crystal lattices form clusters around specific orientations (i.e., single crystal fabrics), which indicates uninhibited growth, whereas disordered/misorientated crystal lattices demonstrate "preferred alignment" indicating inhibited growth. The probability of grain orientation angles (multiple uniform densities; MUD) are illustrated using pole figures.

The frequency distribution of grain boundary misorientation angles demonstrates variation in co-orientation between adjacent grains. Misorientation angle is defined as the rotation angle required to map the lattice of the boundary segment of a grain to the lattice of the adjacent boundary segment (Oxford Instruments, 2015) and the frequency distributions of the Σ values of CSL boundaries can demonstrate variation in co-orientation and fracture resistance between grains. The Σ values reflect the proportion of coincident lattice sites between the two boundary segments. For example, in Σ3 boundaries, one out of every three lattice sites are coincident between the boundary segments (Fortes, 1972). IPFz maps were annotated with the positions of grain and CSL boundaries to demonstrate the distribution of different misorientation angle ranges and Σ values, respectively.

Grain size was used to test for changes in grain formation and growth. Both grain area and diameter were included as measures of grain size, and plotted as frequency distributions, to account for the potential effect of grain shape on the latter.

Three regions (subsets) were defined for each treatment to further explore the variability in ultrastructure parameters within a single shell sample. Each region was chosen to assess crystalline structure in the outer periostracum layer (subset 1), center (subset 2), and inner nacre layer (subset 3) to determine if different regions of the shell responded differently to environmental stresses (**Figure 2B** shows the transverse EBSD scan direction). Statistical tests were only conducted between subsets from the same sample.

Data and Statistical Analysis

Changes in growth and body volume were analyzed using a three-factor linear mixed-effects model to test for significant changes in body volume and growth over time in response to temperature (17 and 20°C) and pCO_2 (380 and 1000 ppm) concentration. Temperature and pCO_2 were included as fixed factors, and "individual" was included as a random factor to account for potential differences in intra-individual responses to experimental conditions within each tank. Model reduction was performed to test for the effect of the random factor, using Akaike information criterion (AIC) to test for significance differences between the maximum (including the random variable) and reduced (excluding the random variable) model predictive power. In all analyses, there was no significant increase in AIC indicating no difference in response among individuals.

Differences in grain boundary misorientation angles, Σ-value of CSL boundaries, grain orientation angle (from pole plots), grain area and grain diameter were compared using planned pairwise Kolmogorov–Smirnov tests to compare frequency distributions (Sokal and Rohlf, 1995). All statistical tests were performed in the open source software, R (R Development Core Team, 2017) and the package "nlme" (Pinheiro et al., 2020).

RESULTS

Mussel Volume and Growth

There were significant changes in body volume depending on temperature and pCO_2 conditions after 8-week ($F_{1,32}$ = 11.9, $p < 0.01$). Mussel body volume reduced under either elevated temperature (20°C) or pCO_2 (1000 ppm), but marginally increased under control (0.13 ± 0.09 mL) and elevated temperature and pCO_2 conditions (0.05 ± 0.02 mL) (**Figure 3**).

There were significant reductions in both shell width and length under the OAW scenario (20°C × 1000 ppm; width: $F_{1,32}$ = 9.2, $p < 0.01$; length: $F_{1,32}$ = 5.6, $p < 0.05$) of 1.05 ± 0.48 mm and 0.86 ± 0.44 mm, respectively. There was no change in morphometrics under control (17°C × 380 ppm), increased temperature or increased pCO_2 conditions (**Figures 3B,C**). There was no significant change in shell height among treatments ($F_{1,32}$ = 0.56, *ns*, **Figure 3D**), although trends suggest a decrease in shell height especially

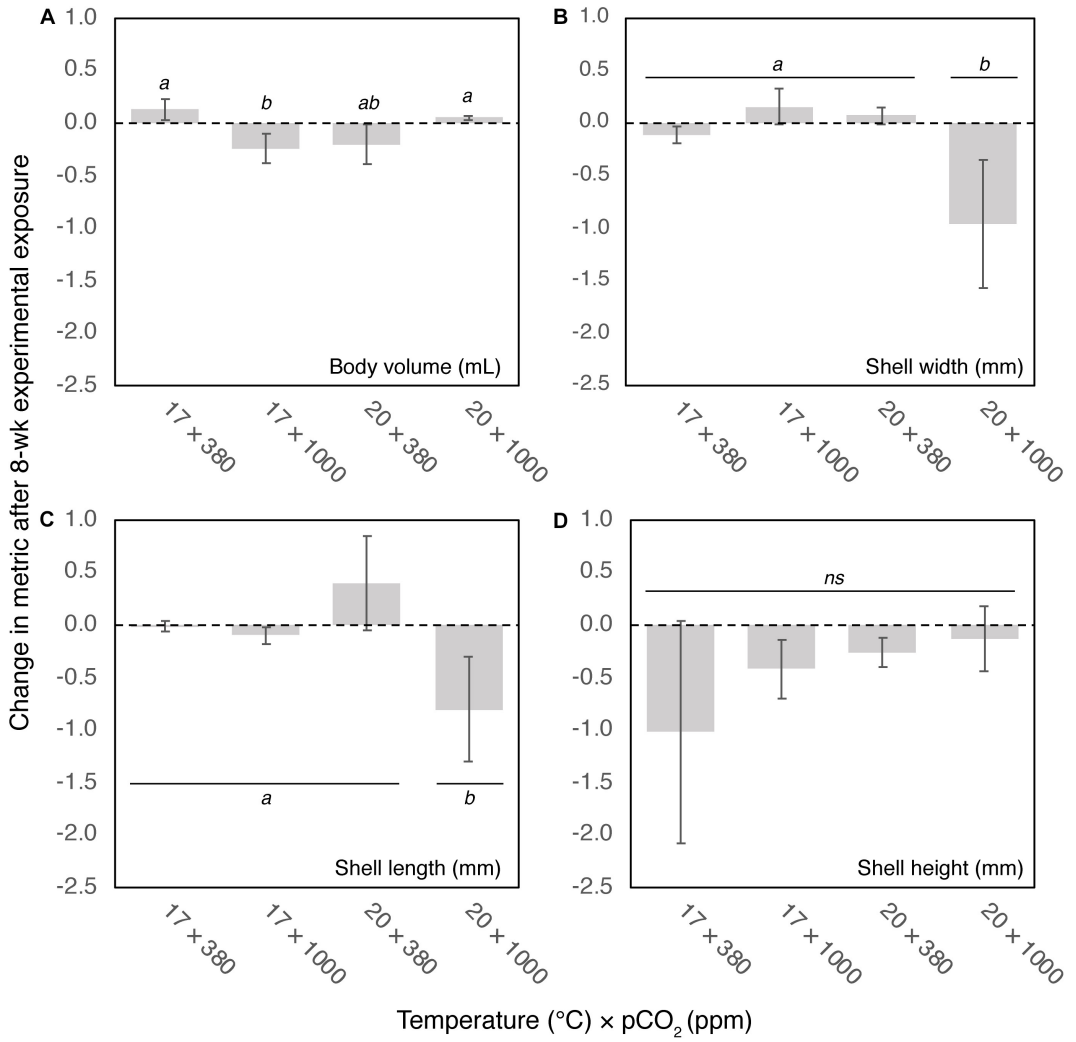

FIGURE 3 | Change in **(A)** body volume (mL), **(B)** shell width (mm), **(C)** length (mm), and **(D)** height (mm) after 8-week exposure to four climate scenarios. Error bars show standard error. Results of *post hoc* pairwise comparisons are shown, where shared letters indicate no significant difference between pairwise groups ($p > 0.05$), and different letters indicate significant differences ($p < 0.05$) between pairwise groups.

under control conditions, albeit reduction among individuals being highly variable.

Ultrastructure Parameters

Grain Area and Diameter

There were significant differences in the frequency distributions of grain areas and diameters among all experimental treatments after 8-week (Kolmogorov–Smirnov paired comparisons; $p < 0.001$ for all comparisons). Both grain area and diameters tended toward smaller dimensions (left skew; **Figure 4**). Grain areas and diameters were smallest in the control treatment (17°C × 380 ppm), largest in the elevated temperature treatment (20°C × 380 ppm), and of intermediate size in the OAW (20°C × 1000 ppm) treatment. Median grain areas were 3.6 × and 2.2 × larger, and diameters 1.9 × and 1.5 × larger, in 20°C × 380 ppm and 20°C × 1000 ppm treatments respectively than in the control treatment (**Figure 4**). While median grain area was lower in the OAW scenario than the temperature only treatment, the maximum grain area observed in mussels from the OAW treatment was up to 7.8 × larger (12,887 μm^2 vs. 1680 μm^2) and 16.5 × larger than the temperature only (20°C × 380 ppm) and control treatments, respectively (**Figure 4**).

Crystallographic Orientation and Disorientation

Change in crystallographic orientation and increased prevalence of misorientation angles were revealed by EBSD (**Figure 5**). Under control conditions, crystal orientation was largely well-ordered with clear evidence of single crystal fabrics (uninhibited growth) across all crystal planes (**Figure 6**). There were few deviations from the expected crystallographic orientation angle of 3–10° and a low prevalence of high misorientation angles (16% > 20°). Under elevated temperature (20°C × 380 ppm)

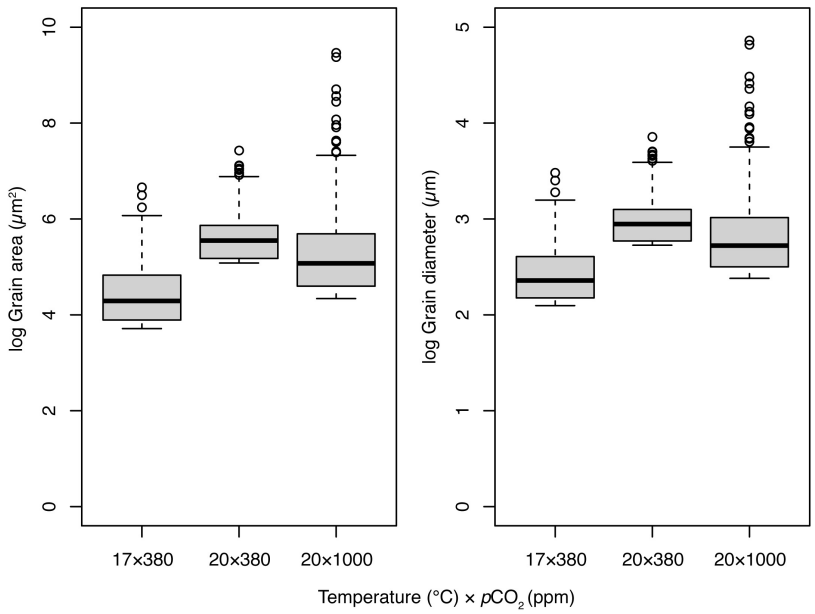

FIGURE 4 | Distribution of grain areas (μm^2) and diameters (μm) within regional subsets of *Mytilus* sp. exposed to three temperature (°C) and pCO_2 climate scenarios for 8-week. Thick lines of boxplots represent the median value, hinge lengths (end of box) represent the 25 and 75% quartiles from the median, and whiskers represent the 1.5 times the interquartile range (IQR) beyond the hinge. Outliers are shown as black circles.

and OAW (20° × 1000 ppm) scenarios, crystals along the 0001 plane also showed propensity toward single crystal fabrics; the orientation of the crystals in the elevated temperature scenario were also rotated.

The 11-20 and 10-10 planes of the elevated temperature treatment exhibited a major shift toward preferred alignment and a higher prevalence (∼23.1%) of misorientated angles (>20°) at the grain boundaries (Kolmogorov–Smirnov tests, $p < 0.01$; **Figures 5**, **6**). This shift toward larger misorientation angles (>20°) was even more apparent in the OAW-treated mussels (41%), although crystals appeared to continue to grow as a single crystal fabric in all planes (**Figure 6**).

Comparison of growth between the external-facing (prismatic) layer and internal-facing (nacreous) revealed differing responses to changed environmental conditions. Focusing on the 11-20 plane only (although a similar pattern was also apparent in the 10-10 plane), *Mytilus* reared in elevated temperatures only (20°C × 380 ppm) showed evidence of restricted growth (preferred alignment) across the entire transverse section of the shell, in particular, within the nacreous region (**Figure 7H**). In comparison, *Mytilus* sp. grown under control (**Figurse 7A,D,G**) and OAW conditions continued to demonstrate single crystal fabric (uninhibited) growth, if not, with marginally lower "intensity" (**Figures 7C,F,I**).

Coincident Site Lattice Boundaries

Coincident site lattice boundaries were most frequent in the elevated temperature treatment (20°C × 380 ppm) followed by the OAW scenario and then the control treatment (**Figures 5B,D,F**). CSL boundaries in the OAW and control samples were restricted to isolated patches, whereas under elevated temperature only, CSL boundaries were distributed throughout the region, although there was no significant difference in the occurrence of these boundaries among treatments.

DISCUSSION

By the end of the century, future climate change scenarios predict increases in sea surface temperature of ∼4°C and increases in atmospheric pCO_2 of ∼600–800 ppm (IPCC, 2014). Exposure of the commercially valuable mussel species, *Mytilus*, to conditions predicted for 2100 led to changes in body volume and shell growth at the macroscale, and alteration of shell crystallization (ultrastructure) at the microscale, although negative consequences mostly occurred under temperature as a single stressor rather than in combination with increases in pCO_2. Results suggest an antagonistic relationship between temperature and pCO_2 stressors on biological functioning of *Mytilus*.

Body volume was reduced under elevated temperature or elevated pCO_2 treatments, but marginally increased under control conditions or when both temperature and pCO_2 were elevated. In contrast, shell length and width reduced under elevated temperature and pCO_2 (20°C × 1000 ppm) conditions, but marginally increased under elevated temperatures (20°C) only. Body volume can act as a proxy measure for the condition of the mussel; change in the mass of soft tissue filling the mantle alters the shell: tissue: mantle-volume ratio and thus water displacement, thereby indicating change in energy utilization over time in somatic tissues development

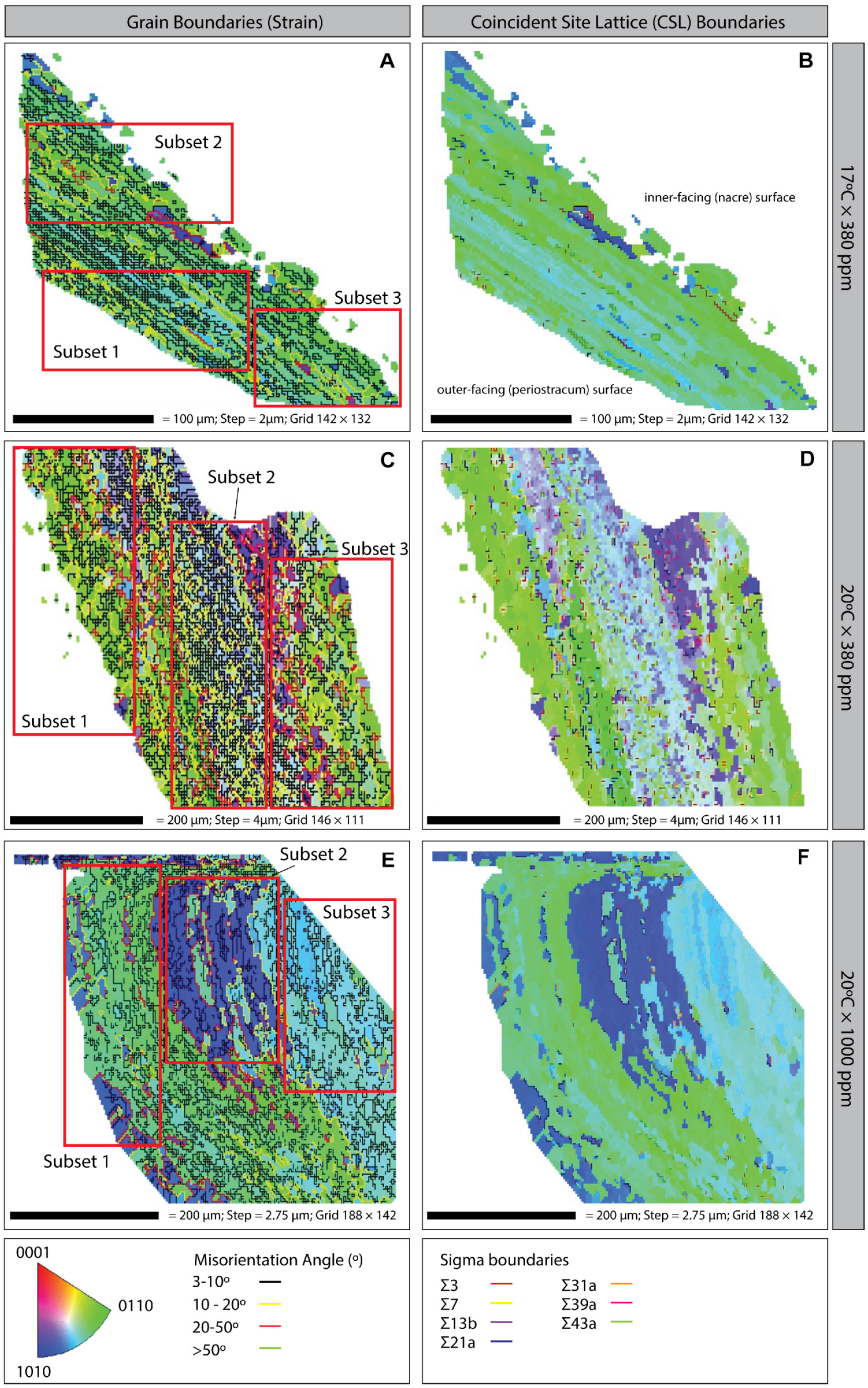

FIGURE 5 | Inverse pole figure (IPF) maps with grain boundaries (left column) and coincident site lattice (CSL; right column) boundaries of *Mytilus* sp. shell samples grown under three climate scenarios: **(A,B)** 17°C × 380 ppm (Control); **(C,D)** 20°C × 380 ppm (Ocean warming without acidification); and **(E,F)** 20°C × 1000 ppm (Ocean warming with acidification). Bottom: Crystal orientation color inset key; grain boundary misorientation (strain) angles; and CSL Sigma boundaries (right column). All plots are orientated in the same way i.e., the left-hand side of the image is the outer-facing periostracum surface and the right-hand side is the inner-facing (nacre) surface (as illustrated on panel **B**).

or maintenance (e.g., Melzner et al., 2011; Huning et al., 2013). The reductions in volume associated with elevated water temperature or pCO_2 might initially suggest an increased metabolic cost to individuals preventing soft issue maintenance, but concurrent increases in shell width and length instead suggest a reallocation of energy toward shell maintenance

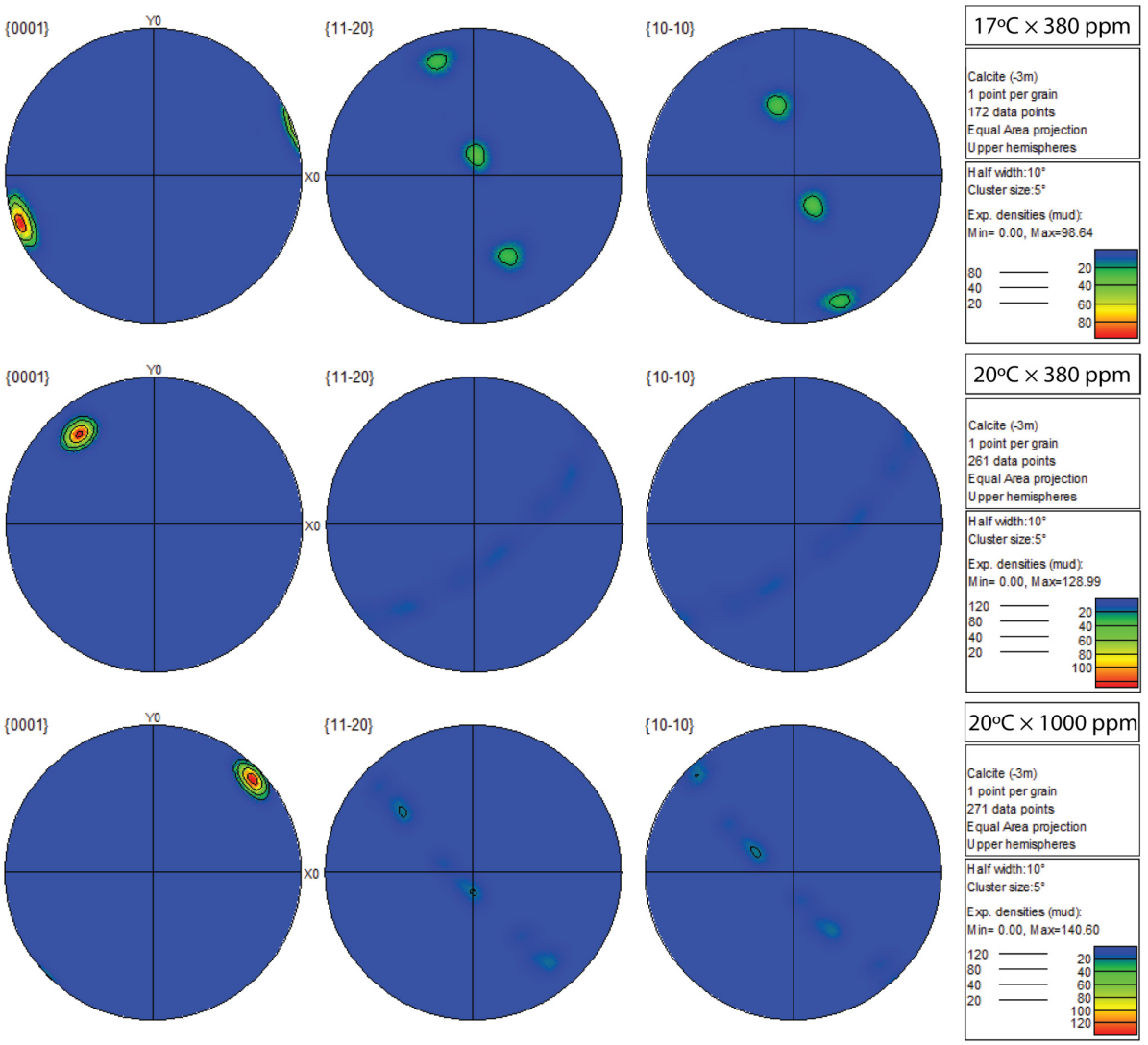

FIGURE 6 | Contoured pole figures (1 point per grain analysis) showing variation in crystallographic orientation along three crystal planes (0001; 11-20; 10-10) in *Mytilus* sp. grown for 8-week under three climate scenarios (top: 17°C × 380 ppm; middle: 20°C × 380 ppm; bottom: 20°C × 1000 ppm). The clear single-crystal fabric observed in the control data (top row) becomes more diffuse along both short axes ({11-20} and {10-10}) as temperature (20°C × 380 ppm), or temperature and CO_2 (20°C × 1000 ppm) increases.

under these single stressor conditions. Previous studies have shown organisms can induce shell thickening (Bibby et al., 2007; Melatunan et al., 2013) or repair damage to their shells (Coleman et al., 2014) through reallocation of energy to specific physiological processes, although OAW scenarios can alter this response. For instance, Li et al. (2016) showed that OAW implemented a compensatory acid-base mechanism, metabolic depression, and up-regulation of physiological responses leading to change in calcification rates, the calcium and carbon content within shells, as well as change in shell ultrastructure. Here, the notable decreases in shell length and width under the elevated temperature and pCO_2 (20°C × 1000 ppm) scenario support these previous findings, suggesting depression of some energetically expensive processes (i.e., soft tissue maintenance) and up-regulation of other physiological and biochemical functions. The observed increases in shell length and width under elevated pCO_2 and ambient temperature conditions (17°C × 1000 ppm) also suggests that mussels may have some capacity to up-regulate biomineralization to maintain or grow shell material under OA (Bibby et al., 2007; Melatunan et al., 2013; Coleman et al., 2014, but see Leung et al., 2020); a process that may be driven by an up-regulation of ion and proton transport genes associated with organic matrix formation (Glazier et al., 2020).

There were also changes in the ultrastructure of mussels grown under future climate conditions. Under elevated temperature, the shell ultrastructure became disordered shifting from single crystal fabrics toward preferred alignment suggesting "restricted"

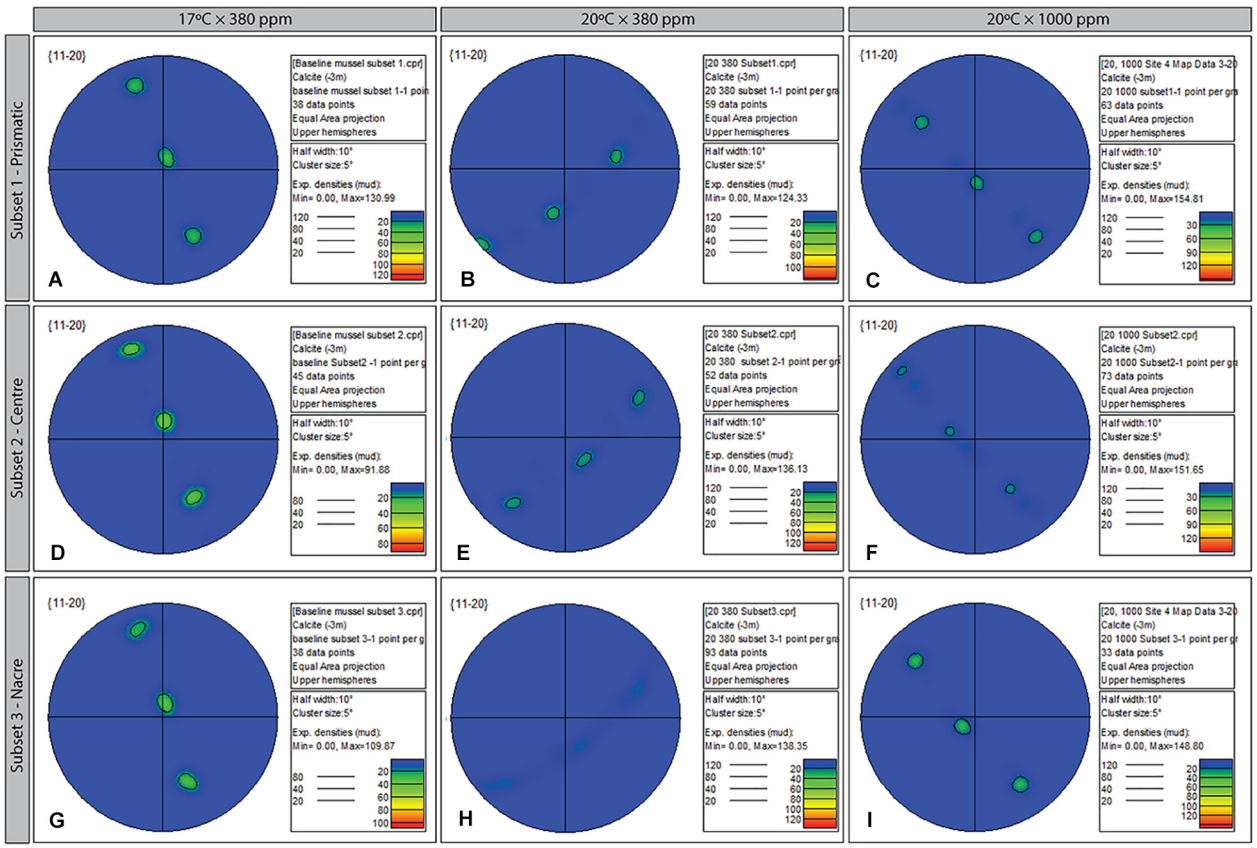

FIGURE 7 | Contoured pole figures (1 point per grain analysis) showing variation in crystallographic orientation along the 11-20 crystal plane in three regions (prismatic; center; and nacreous layers) of the ultrastructure of *Mytilus* sp. grown for 8-week under three climate scenarios: Control **(A,D,C)**; Elevated Temperature **(B,E,H)**; and Elevated Temperature and pCO_2 **(C,F,I)**. The MUD value for the three treatments varies from 98.64 (baseline, 17 × 380) to 154.81 (subset 1, 20 × 1000).

growth, whilst area and diameter of individual grains became significantly larger. In contrast, under elevated temperature and pCO_2, crystalline structures remained ordered as a single crystal fabric, in the same way as control mussels, suggesting OA conditions may be mitigating the effect of temperature. Both future scenarios led to increased frequencies of crystal misorientation; an indicator of stress that signifies the formation of microcracks and weakening of the shell. Previous studies have shown bivalves grown under increasing pCO_2 produce a stiffer, harder calcite (prismatic) layer that is more brittle, whereas the aragonite (nacre) layer may become less stiff and softer (Beniash et al., 2010; Fitzer et al., 2015a) but see Hiebenthal et al. (2013), Mackenzie et al. (2014). While not tested here, the elongation of the crystals grown under elevated temperature and OA (20°C × 1000 ppm) suggests greater crystal malleability, not just within the nacre region of the shell but across the entire transverse section of the shell. Our results are therefore, in part, contradictory to previous studies that have reported disordered shell ultrastructure under elevated pCO_2 in *Mytilus* (Hahn et al., 2012; Fitzer et al., 2014a,b, 2016) and other mollusks (Beniash et al., 2010); an effect argued to be further exacerbated under elevated temperature (Fitzer et al., 2014b). It should be noted, however, that our experimental future climate temperatures (20°C) were considerably higher than those used in Fitzer et al. (2014b).

Change in the physiological mechanisms that underpins ultrastructure composition remain poorly understood (Li et al., 2016). A link between ultrastructure disruption and reduced expression of calcification proteins under elevated pCO_2 has been proposed (e.g., Huning et al., 2013; Fitzer et al., 2014b), although shell matrix protein candidate genes and the expression of carbonic anhydrase – the latter of which catalyzes the interconversion of bicarbonate and CO_2 – appear less affected by elevated CO_2 (Huning et al., 2013). Furthermore, our understanding of the interaction between protein expression, functioning, and $CaCO_3$ formation remains limited (see Glazier et al., 2020 for a recent study in corals). A number of models have been proposed including: changes in epitaxial growth, the formation of "mineral bridges" between crystals, or alteration of the *c*-axis (0001 plane) orientation during the earlier stages of crystal formation (Choi and Kim, 2000; Checa et al., 2006; Fryda et al., 2010; Olson et al., 2013; Maier et al., 2014). Clarification of changes in the physiological mechanisms including gene functioning and regulation under future climate scenarios may

shed light on the capacity of marine species, and especially calcifiers, to mitigate the effects of environmental change.

Our mesocosm system uses fixed input concentrations of CO_2 and we do not attempt to modify these concentrations using feedback loops to control (fix) pH. Consequently, the ocean chemistry in our test system behaves in the same way as *in situ* seawater would i.e., a change in atmospheric pressure can lead to changes in surface water pCO_2 over short timescales (Burgers et al., 2017) and fluctuations in pH (see Lemasson et al., 2018). Fluctuations can also arise from close proximity to CO_2 vents (Hall-Spencer et al., 2008), the introduction of acidified water from coastal upwelling (Feely et al., 2008; Booth et al., 2012), and freshwater inputs (Aguilera et al., 2013; Waldbusser and Salisbury, 2014). Photosynthesis, respiration and the calcification and dissolution of biomineralized structures can also remove and release carbonate (CO_3^{2-}) ions (Anthony et al., 2011). In marine systems, individuals may therefore be exposed to rapid and acute perturbations of pH rather than long-term, chronic exposure to reduced pH as simulated in some mesocosm experiments with conditions varying over spatio-temporal scales. The impact of OA and warming may therefore vary greatly across spatial and temporal scales (e.g., Kurihara et al., 2007; Kurihara, 2008; Thomsen and Melzner, 2010; Fitzer et al., 2015a; Lemasson et al., 2018). Any response may also be context specific and dependent upon individual factors such as the acclimatory capacity and/or evolutionary origins of the target organism (Matoo et al., 2013 and references therein; Ramajo et al., 2019; Britton et al., 2019), capacity to perform biomineralization under variable environmental conditions (Day et al., 2000), or susceptibility to dissolution depending on the mineralogy of their shells (Melzner et al., 2011; Olson et al., 2013). Indeed, current evidence indicates that natural pH fluctuations can influence the impacts of OA on bio-mineralizing organisms (Wahl et al., 2016) or have no effect, even among species within the same genera (Frieder et al., 2014; Lemasson et al., 2017b, 2018).

Should change to the ultrastructural integrity and strength of individuals occur, there are potentially important ramifications for the fitness and survivorship of bivalve mollusks in the future. Given the common role of bivalves as ecosystem engineers (*sensu* Jones et al., 1994) in supporting biodiversity, a reduction in shell strength may lead to greater susceptibility to predation and wider multitrophic impacts. For instance, predators of *Mytilus* sp. (e.g., *Carcinus maenas, Nucella lapillus*) typically use crushing or boring to penetrate the shell (Elner, 1978; Sadler et al., 2018). Furthermore, predators of bivalve mollusks may themselves become susceptible to OA through impacts on fitness (Whiteley, 2011; Landes and Zimmer, 2012; Sadler et al., 2018), feeding structures (Landes and Zimmer, 2012) and predatory behavior (Dixson et al., 2010; Queiros et al., 2015; Sadler et al., 2018).

In recent years, there has been a burgeoning of studies assessing the effects of future climate change scenarios on the fitness, physiology, and provision of ecosystem services in a plethora of marine species at both the macroscale, and increasingly, microscale. Many earlier studies have shown detrimental impacts of OA and warming scenarios on species performance, but increasingly, others do not (see Clark et al., 2020). Here, our results indicate that future predictions of sea surface temperature are likely to have detrimental effects on the ultrastructure of *Mytilus* sp., but when combined with atmospheric pCO_2 concentrations predicted for 2100, those negative effects will be in part, ameliorated. These results further muddy the waters in terms of forming generic conclusions about the impact of climate change on marine organisms. It is important to recognize that in many instances, daily fluctuations in pCO_2 will be experienced by organisms in surface waters, that will change over spatial and temporal scales depending on environment. This presents challenges when making predictions of a general response of organisms to future climate conditions. We therefore propose that understanding how organisms respond to small and large-scale spatio-temporal fluctuations in future environmental conditions is the next challenge to predicting impacts and further disentangling the consequences of climate change.

DATA AVAILABILITY STATEMENT

The datasets presented in this article are not readily available because the dataset contains yet to be processed data and is therefore not freely available for use. Requests to access the datasets should be directed to AK, aknights@plymouth.ac.uk.

AUTHOR CONTRIBUTIONS

AK, NS, and AL devised the research and wrote the draft manuscript. MN and AL ran OAW experiments. MN and NS performed SEM analysis. All authors contributed to the article and approved the submitted version.

FUNDING

Funding support was provided by the School of Biological and Marine Sciences and the Faculty of Science and Engineering to AK and NS.

ACKNOWLEDGMENTS

We thank the editor and two reviewers for their comments that have helped to improve this manuscript. Thanks to Glenn Harper for SEM technical support within Plymouth Electron Microscopy Centre, as well as Rob Hall (School of Geography, Earth and Environmental Sciences) for specimen preparation support.

SUPPLEMENTARY MATERIAL

The Supplementary Material for this article can be found online at: https://www.frontiersin.org/articles/10.3389/fmars.2020.567228/full#supplementary-material

TABLE S1 | Summary of monitoring data from replicate chambers under different temperature and pCO_2 treatments in a seawater system. All parameters are displayed as mean (±SD).

REFERENCES

Aguilera, V. M., Vargas, C. A., Manriquez, P. H., Navarro, J. M., and Duarte, C. (2013). Low-pH freshwater discharges drive spatial and temporal variations in life history traits of neritic copepod *Acartia tonsa*. *Estuaries Coasts* 36, 1084–1092. doi: 10.1007/s12237-013-9615-2

Anthony, K. R. N., Kleypas, J. A., and Gattuso, J. P. (2011). Coral reefs modify their seawater carbon chemistry - implications for impacts of ocean acidification. *Glob. Change Biol.* 17, 3655–3666. doi: 10.1111/j.1365-2486.2011.02510.x

Arafin, M. A., and Szpunar, J. A. (2009). A new understanding of intergranular stress corrosion cracking resistance of pipeline steel through grain boundary character and crystallographic texture studies. *Corros. Sci.* 51, 119–128. doi: 10.1016/j.corsci.2008.10.006

Beniash, E., Ivanina, A., Lieb, N. S., Kurochkin, I., and Sokolova, I. M. (2010). Elevated level of carbon affects metabolism and shell formation in oysters *Crassostrea virginica*. *Mar. Ecol. Prog. Ser.* 419, 95–108. doi: 10.3354/meps08841

Bibby, R., Cleall-Harding, P., Rundle, S., Widdicombe, S., and Spicer, J. (2007). Ocean acidification disrupts induced defences in the intertidal gastropod *Littorina littorea*. *Biol. Lett.* 3, 699–701. doi: 10.1098/rsbl.2007.0457

Booth, J. A. T., McPhee-Shaw, E. E., Chua, P., Kingsley, E., Denny, M., Phillips, R., et al. (2012). Natural intrusions of hypoxic, low pH water into nearshore marine environments on the California coast. *Cont. Shelf Res.* 45, 108–115. doi: 10.1016/j.csr.2012.06.009

Britton, D., Mundy, C. N., McGraw, C. M., Revill, A. T., and Hurd, C. L. (2019). Responses of seaweeds that use CO2 as their sole inorganic carbon source to ocean acidification: differential effects of fluctuating pH but little benefit of CO2 enrichment. *ICES J. Mar. Sci.* 76, 1860–1870. doi: 10.1093/icesjms/fsz070

Burgers, T. M., Miller, L. A., Thomas, H., Else, B. G. T., Gosselin, M., and Papakyriakou, T. (2017). Surface water pCO2 variations and sea-air CO2 fluxes during summer in the Eastern Canadian Arctic. *J. Geophys. Res. Oceans* 122, 9663–9678. doi: 10.1002/2017jc013250

Checa, A. G., Okamoto, T., and Ramirez, J. (2006). Organization pattern of nacre in Pteriidae (Bivalvia: Mollusca) explained by crystal competition. *Proc. R. Soc. B Biol. Sci.* 273, 1329–1337. doi: 10.1098/rspb.2005.3460

Choi, C. S., and Kim, Y. W. (2000). A study of the correlation between organic matrices and nanocomposite materials in oyster shell formation. *Biomaterials* 21, 213–222. doi: 10.1016/s0142-9612(99)00120-9

Clark, T. D., Raby, G. D., Roche, D. G., Binning, S. A., Speers-Roesch, B., Jutfelt, F., et al. (2020). Ocean acidification does not impair the behaviour of coral reef fishes. *Nature* 577, 370–375. doi: 10.1038/s41586-019-1903-y

Coleman, D. W., Byrne, M., and Davis, A. R. (2014). Molluscs on acid: gastropod shell repair and strength in acidifying oceans. *Mar. Ecol. Prog. Ser.* 509, 203–211. doi: 10.3354/meps10887

Comeau, S., Edmunds, P. J., Spindel, N. B., and Carpenter, R. C. (2014). Diel pCO2 oscillations modulate the response of the coral *Acropora hyacinthus* to ocean acidification. *Mar. Ecol. Prog. Ser.* 501, 99–111. doi: 10.3354/meps10690

Day, E. G., Branch, G. M., and Viljoen, C. (2000). How costly is molluscan shell erosion? A comparison of two patellid limpets with contrasting shell structures. *J. Exp. Mar. Biol. Ecol.* 243, 185–208. doi: 10.1016/s0022-0981(99)00120-3

Dixson, D. L., Munday, P. L., and Jones, G. P. (2010). Ocean acidification disrupts the innate ability of fish to detect predator olfactory cues. *Ecol. Lett.* 13, 68–75. doi: 10.1111/j.1461-0248.2009.01400.x

Doney, S. C., Fabry, V. J., Feely, R. A., and Kleypas, J. A. (2009). Ocean acidification: the other CO2 problem. *Annu. Rev. Mar. Sci.* 1, 169–192.

Dufault, A. M., Cumbo, V. R., Fan, T. Y., and Edmunds, P. J. (2012). Effects of diurnally oscillating pCO(2) on the calcification and survival of coral recruits. *Proc. R. Soc. B Biol. Sci.* 279, 2951–2958. doi: 10.1098/rspb.2011.2545

Dupont, S., Dorey, N., Stumpp, M., Melzner, F., and Thorndyke, M. (2013). Long-term and trans-life-cycle effects of exposure to ocean acidification in the green sea urchin *Strongylocentrotus droebachiensis*. *Mar. Biol.* 160, 1835–1843. doi: 10.1007/s00227-012-1921-x

Elner, R. W. (1978). Mechanics of predation by shore crab, *Carcinus maenas* (L), on edible mussel, *Mytilus edulis* L. *Oecologia* 36, 333–344. doi: 10.1007/bf00348059

Feely, R. A., Sabine, C. L., Hernandez-Ayon, J. M., Ianson, D., and Hales, B. (2008). Evidence for upwelling of corrosive" acidified" water onto the continental shelf. *Science* 320, 1490–1492. doi: 10.1126/science.1155676

Fitzer, S. C., Chung, P., Maccherozzi, F., Dhesi, S. S., Kamenos, N. A., Phoenix, V. R., et al. (2016). Biomineral shell formation under ocean acidification: a shift from order to chaos. *Sci. Rep.* 6:21076.

Fitzer, S. C., Cusack, M., Phoenix, V. R., and Kamenos, N. A. (2014a). Ocean acidification reduces the crystallographic control in juvenile mussel shells. *J. Struct. Biol.* 188, 39–45. doi: 10.1016/j.jsb.2014.08.007

Fitzer, S. C., Phoenix, V. R., Cusack, M., and Kamenos, N. A. (2014b). Ocean acidification impacts mussel control on biomineralisation. *Sci. Rep.* 4: 6218.

Fitzer, S. C., Vittert, L., Bowman, A., Kamenos, N. A., Phoenix, V. R., and Cusack, M. (2015a). Ocean acidification and temperature increase impact mussel shell shape and thickness: problematic for protection? *Ecol. Evol.* 5, 4875–4884. doi: 10.1002/ece3.1756

Fitzer, S. C., Zhu, W. Z., Tanner, K. E., Phoenix, V. R., Kamenos, N. A., and Cusack, M. (2015b). Ocean acidification alters the material properties of *Mytilus edulis* shells. *J. R. Soc. Interface* 12:20141227. doi: 10.1098/rsif.2014.1227

Fortes, M. A. (1972). Coincidence site lattices. *Phys. Status Solidi B Basic Res.* 54, 311–319. doi: 10.1002/pssb.2220540131

Frieder, C. A., Gonzalez, J. P., Bockmon, E. E., Navarro, M. O., and Levin, L. A. (2014). Can variable pH and low oxygen moderate ocean acidification outcomes for mussel larvae? *Glob. Change Biol.* 20, 754–764. doi: 10.1111/gcb.12485

Fryda, J., Klicnarova, M., Frydova, B., and Mergl, M. (2010). Variability in the crystallographic texture of bivalve nacre. *Bull. Geosci.* 85, 645–662. doi: 10.3140/bull.geosci.1217

Füllenbach, C. S., Schonë, B. R., and Branscheid, R. (2014). Microstructures in shells of the freshwater gastropod *Viviparus viviparus*: a potential sensor for temperature change? *Acta Biomater.* 10, 3911–3921. doi: 10.1016/j.actbio.2014.03.030

Gazeau, F., Parker, L. M., Comeau, S., Gattuso, J. P., O'Connor, W. A., Martin, S., et al. (2013). Impacts of ocean acidification on marine shelled molluscs. *Mar. Biol.* 160, 2207–2245. doi: 10.1007/s00227-013-2219-3

Gilbert, P. U. P. A., Bergmann, K. D., Myers, C. E., Marcus, M. A., Devol, R. T., Sun, C. Y., et al. (2017). Nacre tablet thickness records formation temperature in modern and fossil shells. *Earth Planet. Sci. Lett.* 460, 281–292. doi: 10.1016/j.epsl.2016.11.012

Glazier, A., Herrera, S., Weinnig, A., Kurman, M., Gómez, C. E., and Cordes, E. (2020). Regulation of ion transport and energy metabolism enables certain coral genotypes to maintain calcification under experimental ocean acidification. *Mol. Ecol.* 29, 1657–1673. doi: 10.1111/mec.15439

Goetz, A. J., Steinmetz, D. R., Griesshaber, E., Zaefferer, S., Raabe, D., Kelm, K., et al. (2011). Interdigitating biocalcite dendrites form a 3-D jigsaw structure in brachiopod shells. *Acta Biomater.* 7, 2237–2243. doi: 10.1016/j.actbio.2011.01.035

Hahn, S., Rodolfo-Metalpa, R., Griesshaber, E., Schmahl, W. W., Buhl, D., Hall-Spencer, J. M., et al. (2012). Marine bivalve shell geochemistry and ultrastructure from modern low pH environments: environmental effect versus experimental bias. *Biogeosciences* 9, 1897–1914. doi: 10.5194/bg-9-1897-2012

Hall-Spencer, J. M., Rodolfo-Metalpa, R., Martin, S., Ransome, E., Fine, M., Turner, S. M., et al. (2008). Volcanic carbon dioxide vents show ecosystem effects of ocean acidification. *Nature* 454, 96–99. doi: 10.1038/nature07051

Hiebenthal, C., Philipp, E. E. R., Eisenhauer, A., and Wahl, M. (2013). Effects of seawater pCO2 and temperature on shell growth, shell stability, condition and cellular stress of Western Baltic Sea *Mytilus edulis* (L.) and *Arctica islandica* (L.). *Mar. Biol.* 160, 2073–2087. doi: 10.1007/s00227-012-2080-9

Hofmann, G. E., Smith, J. E., Johnson, K. S., Send, U., Levin, L. A., Micheli, F., et al. (2011). High-frequency dynamics of ocean pH: a multi-ecosystem comparison. *PLoS One* 6:e28983. doi: 10.1371/journal.pone.0028983

Huning, A., Melzner, F., Thomsen, J., Gutowska, M. A., Kramer, L., Frickenhaus, S., et al. (2013). Impacts of seawater acidification on mantle gene expression patterns of the Baltic Sea blue mussel: implications for shell formation and energy metabolism. *Mar. Biol.* 160, 1845–1861. doi: 10.1007/s00227-012-1930-9

IPCC (2014). *Climate Change 2014: Synthesis Report. Contribution of Working Groups I, II and III to the Fifth Assessment Report of the Intergovernmental Panel on Climate Change*. Geneva: IPCC.

Jones, C. G., Lawton, J. H., and Shachak, M. (1994). Organisms as ecosystem engineers. *Oikos* 69, 373–386. doi: 10.2307/3545850

Kurihara, H. (2008). Effects of CO2-driven ocean acidification on the early developmental stages of invertebrates. *Mar. Ecol. Prog. Ser.* 373, 275–284. doi: 10.3354/meps07802

Kurihara, H., Kato, S., and Ishimatsu, A. (2007). Effects of increased seawater pCO2 on early development of the oyster *Crassostrea gigas*. *Aquat. Biol.* 1, 91–98. doi: 10.3354/ab00009

Lagos, N. A., Benitez, S., Duarte, C., Lardies, M. A., Broitman, B. R., Tapia, C., et al. (2016). Effects of temperature and ocean acidification on shell characteristics of *Argopecten purpuratus*: implications for scallop aquaculture in an upwelling-influenced area. *Aquacult. Environ. Interact.* 8, 357–370. doi: 10.3354/aei00183

Landes, A., and Zimmer, M. (2012). Acidification and warming affect both a calcifying predator and prey, but not their interaction. *Mar. Ecol. Prog. Ser.* 450, 1–10. doi: 10.3354/meps09666

Lehockey, E. M., Brennenstuhl, A. M., and Thompson, I. (2004). On the relationship between grain boundary connectivity, coincident site lattice boundaries, and intergranular stress corrosion cracking. *Corros. Sci.* 46, 2383–2404. doi: 10.1016/j.corsci.2004.01.019

Lemasson, A. J., Fletcher, S., Hall-Spencer, J. M., and Knights, A. M. (2017a). Linking the biological impacts of ocean acidification on oysters to changes in ecosystem services: a review. *J. Exp. Mar. Biol. Ecol.* 492, 49–62. doi: 10.1016/j.jembe.2017.01.019

Lemasson, A. J., Kuri, V., Hall-Spencer, J. M., Fletcher, S., Moate, R., and Knights, A. M. (2017b). Sensory qualities of oysters unaltered by a short exposure to combined elevated pCO2 and temperature. *Front. Mar. Sci.* 4:352. doi: 10.3389/fmars.2017.00352

Lemasson, A. J., Hall-Spencer, J. M., Fletcher, S., Provstgaard-Morys, S., and Knights, A. M. (2018). Indications of future performance of native and non-native adult oysters under acidification and warming. *Mar. Environ. Res.* 142, 178–189. doi: 10.1016/j.marenvres.2018.10.003

Leung, J. Y., Russell, B. D., and Connell, S. D. (2020). Linking energy budget to physiological adaptation: how a calcifying gastropod adjusts or succumbs to ocean acidification and warming. *Sci. Total Environ.* 715:136939. doi: 10.1016/j.scitotenv.2020.136939

Li, S., Huang, J., Liu, C., Liu, Y., Zheng, G., Xie, L., et al. (2016). Interactive effects of seawater acidification and elevated temperature on the transcriptome and biomineralization in the pearl oyster *Pinctada fucata*. *Environ. Sci. Technol.* 50, 1157–1165. doi: 10.1021/acs.est.5b05107

Li, S. G., Liu, C., Huang, J. L., Liu, Y. J., Zheng, G. L., Xie, L. P., et al. (2015). Interactive effects of seawater acidification and elevated temperature on biomineralization and amino acid metabolism in the mussel *Mytilus edulis*. *J. Exp. Biol.* 218, 3623–3631. doi: 10.1242/jeb.126748

Lindinger, M. I., Lauren, D. J., and Mcdonald, D. G. (1984). Acid-base balance in the sea mussel, *Mytilus edulis*. III: effects of environmental hypercapnia on intra- and extracellular acid-base balance. *Mar. Biol. Lett.* 5, 371–381.

Mackenzie, C. L., Ormondroyd, G. A., Curling, S. F., Ball, R. J., Whiteley, N. M., and Malham, S. K. (2014). Ocean warming, more than acidification, reduces shell strength in a commercial shellfish species during food limitation. *PLoS One* 9:e86764. doi: 10.1371/journal.pone.0086764

Maier, B. J., Griesshaber, E., Alexa, P., Ziegler, A., Ubhi, H. S., and Schmahl, W. W. (2014). Biological control of crystallographic architecture: hierarchy and co-alignment parameters. *Acta Biomater.* 10, 3866–3874. doi: 10.1016/j.actbio.2014.02.039

Marin, F., and Luquet, G. (2004). Molluscan shell proteins. *C. R. Palevol* 3, 469–492. doi: 10.1016/j.crpv.2004.07.009

Matoo, O. B., Ivanina, A. V., Ullstad, C., Beniash, E., and Sokolova, I. M. (2013). Interactive effects of elevated temperature and CO2 levels on metabolism and oxidative stress in two common marine bivalves (*Crassostrea virginica* and *Mercenaria mercenaria*). *Comp. Biochem. Physiol. A Mol. Integr. Physiol.* 164, 545–553. doi: 10.1016/j.cbpa.2012.12.025

Melatunan, S., Calosi, P., Rundle, S. D., Widdicombe, S., and Moody, A. J. (2013). Effects of ocean acidification and elevated temperature on shell plasticity and its energetic basis in an intertidal gastropod. *Mar. Ecol. Prog. Ser.* 472, 155–168. doi: 10.3354/meps10046

Melzner, F., Stange, P., Trubenbach, K., Thomsen, J., Casties, I., Panknin, U., et al. (2011). Food supply and seawater pCO2 impact calcification and internal shell dissolution in the blue mussel *Mytilus edulis*. *PLoS One* 6:e24223. doi: 10.1371/journal.pone.0024223

Meng, Y., Guo, Z., Yao, H., Yeung, K. W., and Thiyagarajan, V. (2019). Calcium carbonate unit realignment under acidification: a potential compensatory mechanism in an edible estuarine oyster. *Mar. Pollut. Bull.* 139, 141–149.

Nakahara, H. (1991). "Nacre formation in bivalve and gastropod molluscs," in *Mechanisms and Phylogeny of Mineralization in Biological Systems*, eds S. Suga and H. Nakahara (Tokyo: Springer), 343–350.

Olson, I. C., Blonsky, A. Z., Tamura, N., Kunz, M., Pokroy, B., Romao, C. P., et al. (2013). Crystal nucleation and near-epitaxial growth in nacre. *J. Struct. Biol.* 184, 454–463.

Olson, I. C., and Gilbert, P. U. P. A. (2012). Aragonite crystal orientation in mollusk shell nacre may depend on temperature. The angle spread of crystalline aragonite tablets records the water temperature at which nacre was deposited by *Pinctada margaritifera*. *Faraday Discuss.* 159, 421–432.

Oxford Instruments (2015). *EBSD Explained: from Data Acquisition to Advanced Analysis*. Abingdon: Oxford Instruments.

Pansch, C., Schaub, I., Havenhand, J., and Wahl, M. (2014). Habitat traits and food availability determine the response of marine invertebrates to ocean acidification. *Glob. Change Biol.* 20, 765–777.

Pinheiro, J., Bates, D., DebRoy, S., Sarkar, D., and R Core Team (2020). *nlme: Linear and Nonlinear Mixed Effects Models. R package version 3.1-144*.

Queiros, A. M., Fernandes, J. A., Faulwetter, S., Nunes, J., Rastrick, S. P. S., Mieszkowska, N., et al. (2015). Scaling up experimental ocean acidification and warming research: from individuals to the ecosystem. *Glob. Change Biol.* 21, 130–143.

R Development Core Team (2017). *R: A Language and Environment for Statistical Computing*. Vienna: R Foundation for Statistical Computing.

Ramajo, L., Lagos, N. A., and Duarte, C. M. (2019). Seagrass *Posidonia oceanica* diel pH fluctuations reduce the mortality of epiphytic forams under experimental ocean acidification. *Mar. Pollut. Bull.* 146, 247–254.

Sadler, D. E., Lemasson, A. J., and Knights, A. M. (2018). The effects of elevated CO2 on shell properties and susceptibility to predation in mussels *Mytilus edulis*. *Mar. Environ. Res.* 139, 162–168.

Scanes, E., Parker, L. M., O'Connor, W. A., Stapp, L. S., and Ross, P. M. (2017). Intertidal oysters reach their physiological limit in a future high-CO2 world. *J. Exp. Biol.* 220, 765–774.

Sokal, R. R., and Rohlf, F. J. (1995). *Biometry*, 3rd Edn. New York, NY: W.H. Freeman and Company.

Stocker, T., Qin, D., Plattner, G., Tignor, M., Allen, S., Boschung, J., et al. (2013). *IPCC, 2013: Climate Change 2013: the Physical Science Basis. Contribution of Working Group I to the Fifth Assessment Report of the Intergovernmental Panel on Climate Change*. Cambridge: Cambridge University Press.

Thomsen, J., and Melzner, F. (2010). Moderate seawater acidification does not elicit long-term metabolic depression in the blue mussel *Mytilus edulis*. *Mar. Biol.* 157, 2667–2676.

Wahl, M., Saderne, V., and Sawall, Y. (2016). How good are we at assessing the impact of ocean acidification in coastal systems? Limitations, omissions and strengths of commonly used experimental approaches with special emphasis on the neglected role of fluctuations. *Mar. Freshw. Res.* 67, 25–36.

Waldbusser, G. G., and Salisbury, J. E. (2014). Ocean acidification in the coastal zone from an organism's perspective: multiple system parameters, frequency domains, and habitats. *Annu. Rev. Mar. Sci.* 6, 221–247.

Whiteley, N. M. (2011). Physiological and ecological responses of crustaceans to ocean acidification. *Mar. Ecol. Prog. Ser.* 430, 257–271.

Conflict of Interest: The authors declare that the research was conducted in the absence of any commercial or financial relationships that could be construed as a potential conflict of interest.

frontiers in Marine Science

SYSTEMATIC REVIEW
published: 12 November 2020
doi: 10.3389/fmars.2020.597441

How the Pacific Oyster Responds to Ocean Acidification: Development and Application of a Meta-Analysis Based Adverse Outcome Pathway

*James Ducker and Laura J. Falkenberg**

Simon F.S. Li Marine Science Laboratory, School of Life Sciences, The Chinese University of Hong Kong, Hong Kong, China

Biological fitness relies on processes acting at various levels of organization, all of which can be modified by environmental change. Application of synthesis frameworks, such as the Adverse Outcome Pathway (AOP), can enhance our understanding of the responses to stressors identified in studies at each level, as well as the links among them. However, the use of such frameworks is often limited by a lack of data. In order to identify contexts with sufficient understanding to apply the AOP framework, we conducted a meta-analysis of studies considering ocean acidification effects on calcifying mollusks. Our meta-analysis identified that most studies considered the adult life history stage, bivalve taxonomic group, individual-level changes, and growth- and metabolism-related responses. Given the characteristics of the published literature, we constructed an AOP for the effects of ocean acidification on calcification in an adult bivalve, specifically the Pacific oyster (*Magallana gigas*). By structuring results within the AOP framework, we identify that, at present, the supported pathways by which ocean acidification affects oyster calcification are via the downregulation of cavortin and arginine kinase transcription. Such changes at the molecular level can prompt changes in cellular and organ responses, including altered enzyme activities, lipid peroxidation, and regulation of acid–base status, which have impacts on organism level metabolic rate and, therefore, calcification. Altered calcification may then impact organism mortality and population sizes. We propose that when developed and incorporated in future studies, the AOP framework could be used to investigate sources of complexity including varying susceptibility within and among species, feedback mechanisms, exposure duration and magnitude, and species interactions. Such applications of the AOP framework will allow more effective reflections of the consequences of environmental change, such as ocean acidification, on all levels of biological organization.

Keywords: ocean acidification, marine mollusks, marine molluscs, Adverse Outcome Pathway, carbon dioxide, Pacific oyster

OPEN ACCESS

Edited by:
Jonathan Y. S. Leung, University of Adelaide, Australia

Reviewed by:
Qing Wang, Chinese Academy of Sciences (CAS), China
Vengatesen Thiyagarajan, The University of Hong Kong, Hong Kong

****Correspondence:***
Laura J. Falkenberg
laurafalkenberg@cuhk.edu.hk

Specialty section:
This article was submitted to Global Change and the Future Ocean, a section of the journal Frontiers in Marine Science

Received: *21 August 2020*
Accepted: *05 October 2020*
Published: *12 November 2020*

Citation:
Ducker J and Falkenberg LJ (2020) How the Pacific Oyster Responds to Ocean Acidification: Development and Application of a Meta-Analysis Based Adverse Outcome Pathway. Front. Mar. Sci. 7:597441. doi: 10.3389/fmars.2020.597441

INTRODUCTION

Organism fitness depends on processes acting at various levels of biological organization, all of which are affected by abiotic conditions (Prosser, 1955). The response of organisms to changing environmental conditions is, therefore, governed by cumulative effects across multiple biological levels, from molecular pathways to whole-organism processes. Ultimately, changes in organism fitness will affect population composition, ecosystem structure, and evolutionary potential (Munday et al., 2013; Queirós et al., 2014).

Marine systems around the world are experiencing unprecedented rates of abiotic change, with ocean acidification associated with rapid alterations in environmental conditions (Burrows et al., 2011). It is estimated that the oceans have absorbed almost half of the carbon dioxide emitted globally almost the past two decades (Sabine et al., 2004). Such uptake has resulted in the average oceanic pH declining by 0.1 units compared to preindustrial levels, in a process termed ocean acidification (Caldeira, 2005). In addition to reduced pH, ocean acidification also incorporates other alterations to seawater chemistry, including reduction in the calcium carbonate saturation state and alteration of the global carbon cycle (Zeebe and Wolf-Gladrow, 2001). In the future, seawater pH is predicted to undergo a 0.3–0.4 unit decrease by 2100 (Caldeira and Wickett, 2003; IPCC, 2013). As pH is measured on the logarithmic scale, this corresponds to a doubling in acidity by the end of the century and represents a profound change for future oceans.

Ocean acidification is recognized to negatively impact many calcifying organisms, including mollusks (see reviews by Kroeker et al., 2010; Gazeau et al., 2013 and references therein). Such impacts are of concern given that mollusks fulfill numerous ecological roles (Gazeau et al., 2013), provide an abundance of ecosystem services (Lemasson et al., 2017), and represent an aquaculture industry that was worth US $19 billion globally in 2016 (FAO, 2016). The effects of ocean acidification on calcifying mollusks have been suggested to result largely from impacts on the development of calcified structures, as well as their maintenance via enhanced erosion and dissolution due to the increased porosity of the shells' internal microstructure (e.g., Marshall et al., 2008; Nienhuis et al., 2010; Rodolfo-Metalpa et al., 2011; Fitzer et al., 2015, 2016, 2019; Meng et al., 2018; Byrne and Fitzer, 2019; Leung et al., 2020a). Although calcification represents one of the physiological processes most susceptible to ocean acidification (Kroeker et al., 2010), studies have only relatively recently started to unravel the complex drivers of such effects (e.g., Meng et al., 2018; Clark et al., 2020; Leung et al., 2020b). Currently, the key mechanism impairing calcification under ocean acidification is considered to be the exacerbation of the energetic costs of maintaining internal pH homeostasis under the increased concentration of protons in the surrounding seawater (Barry et al., 2011; Stumpp et al., 2011; Waldbusser et al., 2015; Cyronak et al., 2016; Fitzer et al., 2016). The required reallocation of metabolic resources to maintain calcified structures appears to occur at the detriment of other physiological processes including growth, reproduction, and immune system function (Wood et al., 2008; Scanes et al., 2014; Garilli et al., 2015; Harvey and Moore, 2017; Leung et al., 2017; Telesca et la., 2019). Promisingly, some calcifying mollusks can buffer the effects of acidification through energy reallocation (Leung et al., 2020b), adjusting internal pH (Zhao et al., 2018), and adjusting the mineralogical composition of their shells (Leung et al., 2017, 2020a). It is important to note, however, that such adaptive capacities may be considerably reduced when acidity is modified to more extreme levels, indicating that processes associated with calcification may lack the capacity to overcome the challenges of future acidification (Leung et al., 2020a). Of particular concern are changes occurring in oysters, which are a group of considerable economic and ecological importance (see Lemasson et al., 2017 and references therein). For oysters, acidification is considered to reduce individual fitness by generating energetically costly effects in early life history stages that are then carried over to later stages (Hettinger et al., 2013). Specifically, acidification can decrease larval metamorphosis by up to 30% (Talmage and Gobler, 2009), as it alters the expression of proteins involved in energy production and calcification (Dineshram et al., 2016). Such changes can lead to later life stages experiencing abnormal development, decreased body size, and altered shell properties (Parker et al., 2009; Hettinger et al., 2012; Gazeau et al., 2013).

While a general understanding of the pathways by which ocean acidification influences marine calcifiers is being developed, confidence may be increased where more rigorous synthesis approaches are used. That is, the above description of effects of ocean acidification on calcification is based on a "qualitative literature review" approach, where we selected the portion of evidence we felt best described the process (Falkenberg et al., 2018). A more objective approach could be the application of a conceptual framework that synthesizes the sequential cascade of responses initiated by environmental stressors, specifically the Adverse Outcome Pathway (AOP) framework (Ankley et al., 2010). AOPs were first developed in 1992 to bring together key information on the sequential consequences of toxicants across biological processes (Ankley et al., 2010). The subsequent adoption of AOPs in toxicology has gained momentum (Leist et al., 2017), leading to the design of online databases gathering information on a myriad of stressors and their impacts (Society for Advancement of AOPs, 2020).

To date, the AOP framework has yet to be used to address ocean acidification, with few examples of its application to global change parameters (but see Hooper et al., 2013). Nonetheless, the effects of human-driven global change (e.g., increased temperatures, hypoxia, or ocean acidification) are akin to human-derived toxicants, as they represent potentially lethal threats to organisms. Successful application of the AOP framework within the context of global change will depend on sufficient data availability for different: (a) life history stages, (b) taxonomic groups, (c) biological responses, and (d) response variables. Where the required data exist, application of synthesis frameworks, such as the AOP, can enhance our understanding of the generality of responses identified in studies of each level, as well as the links between those observed from molecular, to physiological, and population levels. Thus, AOPs would provide

a unique and comprehensive tool to address climate-related impacts on ecosystems and the species within them (**Figure 1**; Hooper et al., 2013; Falkenberg et al., 2018).

Here, we explore the potential for developing more accurate predictions of ocean acidification effects on organism fitness based on empirical data using the AOP framework. To identify the contexts in which there would be sufficient understanding to apply the AOP framework, we conducted a meta-analysis of studies considering the effects of ocean acidification on calcifying mollusks. Findings were organized to recognize our understanding of acidification across: (a) life history stages, (b) taxonomic groups, (c) biological levels, and (d) response variables. We then used the identified literature to construct an AOP for calcification in an organism and life stage we found to be well-studied. Where the AOP approach is developed, advanced, and informed by a greater number of studies, it will ultimately enhance our ability to relate findings across levels of biological organization.

METHODS

Literature Search and Suitability Criteria

The meta-analysis followed Preferred Reporting Items for Systematic Reviews and Meta-Analyses (PRISMA) guidelines, which provide an evidence-based set of requirements for conducting and reporting meta-analyses. First, a standardized search for peer-reviewed research articles about the effects of ocean acidification on marine mollusks was conducted on Web of Science, Scopus, and Science Direct in October 2019. The search string used was TS = [("ocean acidification" OR "marine acidification" OR "seawater acidification") AND ("mollusc" OR "mollusk")], the language was restricted to English, and no constraints were placed on the publication year.

The initial search identified 5,850 potentially relevant papers, which were then screened to determine their eligibility. Specifically, studies were narrowed to peer-reviewed research relating to contemporary climate change. Papers included in our analysis are those that considered the effect of a control "ambient" acidification treatment and at least one "future" acidification treatment as based on the author's opinion of "ambient" and "future" levels of ocean acidification. These treatments needed to be achieved using commonly accepted methods, with studies that manipulated carbonate chemistry with acid addition excluded (following criteria outlined by Harvey et al., 2013). All the abstracts were then read from the retained papers, and the full manuscripts obtained for those studies that indicated in their title, abstract, or keywords that relevant data could be collected ($n = 517$ papers). These papers were then read, and 267 papers were included.

For each of the included papers, we extracted information on the considered: (a) life history stages, (b) taxonomic groups, (c) biological levels, and (d) response variable groups. For studies that included more than one life history stage, taxonomic group, biological level, or response variable in the reported experiment(s), all separate life history stages, taxonomic groups, biological levels, and response variables were included as long as they met our overall criteria for inclusion. Response variables were grouped into the most commonly considered metrics (i.e., calcification, survival, growth, reproduction, development, and metabolism) as employed in previous meta-analyses (e.g., Gazeau et al., 2013; Harvey et al., 2013). Additionally, counts of the numbers of life history stages, taxonomic groups, biological levels, and response variables groups were made to determine the number of levels of each characteristic considered in each study.

Statistical Analysis

Chi-squared tests were used to examine differences in the frequency of (a) life history stages, (b) taxonomic groups, (c) biological levels, and (d) response variable groups considered in each study, as well as the frequency of the number of factors listed above (1, 2, or >2 factors). All tests were done in GraphPad Prism v 8.42.

AOP Framework Development

Studies considering the adult Pacific oyster, *Magallana gigas*, were then used to develop an AOP addressing the cascading mechanisms resulting in effects on calcification in response to acidification in adults of this species. This case study was selected as the focal life history stage (adult), taxonomic group (bivalve), biological level (individual), and response variable of interest (calcification) were well-represented in our meta-analysis relative to other levels. To develop the AOP, results from our meta-analysis were grouped according to the biological level of organization and organized into the major outcomes of studies, termed key events (KEs), caused by acidification. The KEs were then organized into a causal sequence starting with the molecular initiating event (MIE) (i.e., the reduction in external pH), progressing through the hierarchical levels of organization, and culminating in the outcomes (referred to as adverse outcomes, AOs, under the AOP terminology) at the organism and population level. Each KE is connected by key event relationships (KERs), which describe how alterations in upstream events (lower levels of organization) relate to the downstream modifications (higher levels of organization). The number of studies supporting each KE for *M. gigas* in the present meta-analysis is indicated. If certain KEs were not supported by these studies, plausible linkages with further evidence from other bivalve species were added. Further information on existing guidelines for constructing AOPs is available on the publicly accessible knowledgebase (Society for Advancement of AOPs, 2020).

RESULTS

There were significant differences in the proportion of studies across: (a) life history stages [$\chi^2_{(df = 3, n = 356)} = 273.371$, $p < 0.0001$; **Figure 2A**], (b) taxonomic groups [$\chi^2_{(df = 4, n = 324)} = 479.696$, $p < 0.0001$; **Figure 2B**], (c) biological levels [$\chi^2_{(df = 4, n = 358)} = 475.324$, $p < 0.0001$; **Figure 2C**], and (d) response variable groups [$\chi^2_{(df = 5, n = 411)} = 160.139$, $p < 0.001$; **Figure 2D**). In terms of life history stages, there was a higher proportion of studies considering adults (60%) than each of the other stages (i.e., embryos, larvae, and juveniles were all <20%;

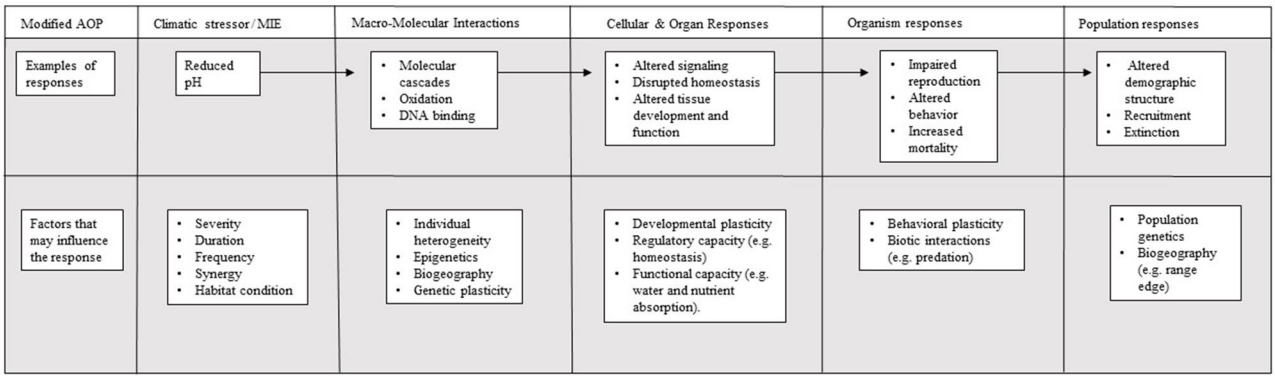

FIGURE 1 | Conceptual diagram of the Adverse Outcome Pathway (AOP) linking the effect of the toxicant, considered to be ocean acidification, with the mechanistic toxicity pathway, and adverse outcomes (based on Ankley et al., 2010).

Figure 2A). While less well-studied than adults, the effects of acidification on earlier life stages is relatively well-understood, as 16% of studies in our review consider larvae and another 15% consider juvenile life stages, comprising 117 studies total (60 and 57 studies, respectively). Across taxonomic groups, almost three-quarters of the studies examined effects on bivalve species (70%), with the next most commonly considered group gastropods (22%) (**Figure 2B**). The majority of studies considered individual level responses (65%; **Figure 2C**), primarily focusing on response variable groups relating to growth (27%), metabolism (26%), survival (16%), and calcification (13%; **Figure 2D**).

The number of levels of each characteristic considered in a study varied across the categories of interest. That is, the majority of studies considered just one life history stage [90%; $\chi^2_{(df=2,n=267)} = 397.011$, $p < 0.0001$; **Figure 3A**], taxonomic group [94%; $\chi^2_{(df=2,n=267)} = 448.472$, $p < 0.0001$; **Figure 3B**], or biological level [73%, $\chi^2_{(df=2,n=267)} = 209.598$, $p < 0.0001$; **Figure 3C**]. In contrast, the number of response variable groups more often considered two or more levels, although there was a significant difference in the number of levels considered [$\chi^2_{(df=2,n=250)} = 11.048$, $p < 0.01$; **Figure 3D**].

The AOP that links the molecular initiating event of reduced seawater pH to the adverse effect of altered calcification and effects at higher levels highlights what is currently understood regarding the related pathways for *M. gigas* (**Figure 4**). A direct pathway supported by the literature on *M. gigas* is via the molecular downregulation of cavortin transcription. A second supported pathway to changes in calcification is via the molecular level change of downregulated genes encoding metabolic pathways, including kinase transcription. These changes lead to the cellular- and organ-level responses of altered enzyme activities and increased lipid peroxidation, which can lead to a depressed metabolic rate that is, in turn, linked with altered calcification. Similarly, the downregulation of genes encoding metabolic pathways can also lead to the deregulation of acid–base status, decreased metabolic rates, and altered calcification rates (although there is no *M. gigas*-specific support for this deregulation). The consequences of altered calcification are also considered in the AOP; altered calcification can potentially prompt organism-level changes in shell thickness that lead to increased mortality and ultimately population level declines.

DISCUSSION

Forecasting the effects of ocean acidification on calcifying organisms, and the associated ecosystems and human societies, will benefit from the use of structured frameworks informed by sufficient experimental evidence. Here, we identified that such an approach may be more suitable for certain groups; in the context of marine mollusks, greater evidence is available for particular life history stages (adults), biological levels (individuals), taxonomic groups (bivalves), and response variables (metabolism, growth, survival, and calcification). Promisingly, there is potential that the existing evidence can be used to inform structured frameworks, such as the Adverse Outcome Pathway. Here, we consider the impact of ocean acidification on a well-represented life stage, biological level, taxonomic group, and response variable, specifically the calcification of individual adult oysters, *M. gigas*. The resulting AOP reveals the extent of repercussions across biological levels as a result of simulated acidification treatments. It allows us to conclude that, at present, the pathways by which ocean acidification is known to impact calcification in *M. gigas* is via the downregulation of cavortin and kinase transcription. As gaps in the existing literature are filled, more complex AOPs will be able to be developed.

Characteristics of Existing Literature Regarding Effects of Ocean Acidification on Mollusks and Their Implications for AOP Development

Characteristics of the existing literature identified in meta-analyses will determine our ability to develop well-informed frameworks. Promisingly, here we identified that a range of response variables were relatively well-represented in the current literature (i.e., growth, metabolism, and survival; **Figure 2D**).

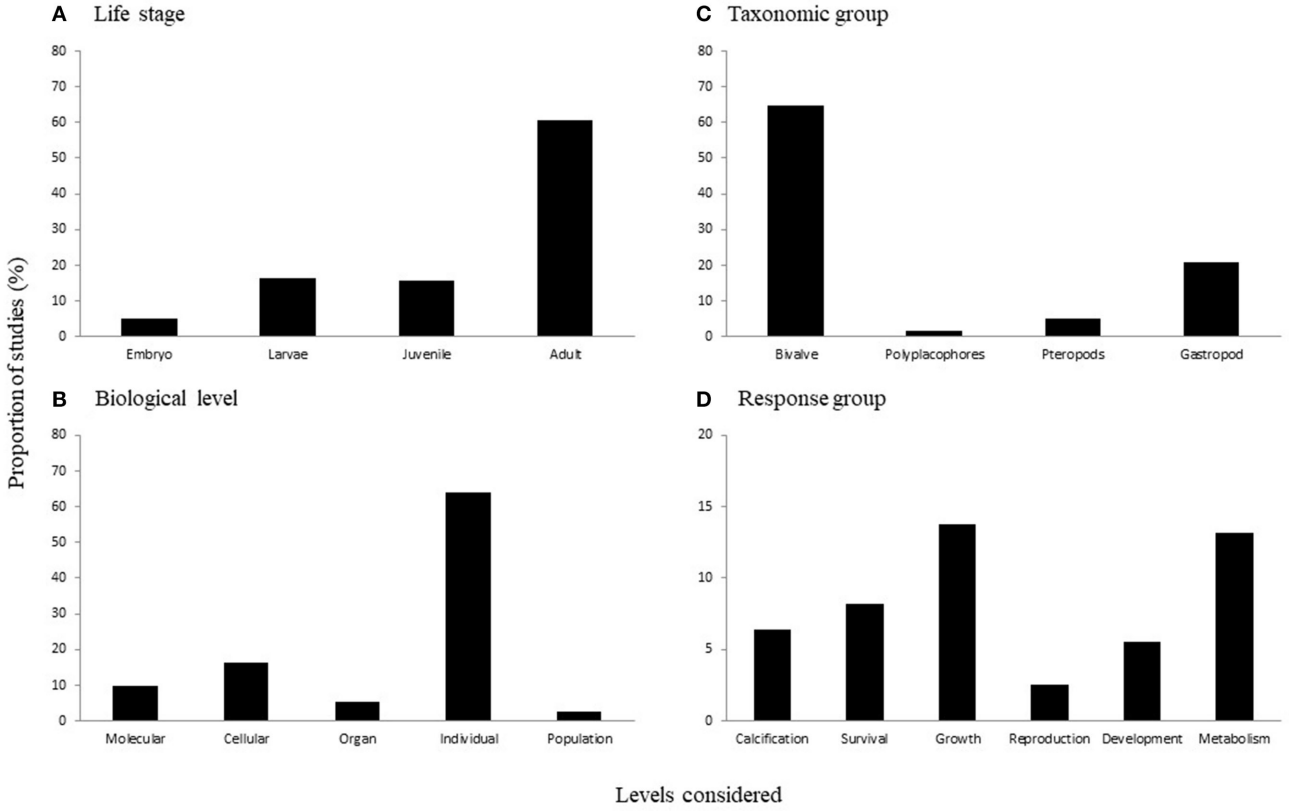

FIGURE 2 | The proportion of studies considering different levels of **(A)** life stages, **(B)** taxonomic groups, **(C)** biological levels, and **(D)** response variable groups. Note the difference in scale on the y-axis of **(D)**.

Moreover, the number of response variables considered in each study was typically two or above, indicating that we are developing an understanding of how responses relate to each other across groups (**Figure 3D**). That is, where a number of response variables are considered, particularly within a single study, this provides key information for subsequent AOPs in terms of how processes affect one another both within, and across, levels of organization.

Our meta-analysis also revealed traits of the existing literature that could be strengthened to enhance the development of future AOPs. In this context, it is worth noting that an emphasis has been placed on considering a single life history stage within each study, typically the adults (**Figures 2A**, **3A**). Such a focus on the adult life stage, and the omission of others, limits our capacity to understand how effects differ across life stages and also how effects on early life stages, such as the embryo, can influence later life stages. For example, studies in our meta-analysis considering early life history stages identified that larvae experienced negative responses in metamorphosis and development (Scanes et al., 2014; Dineshram et al., 2016; Wang et al., 2017) likely due to changes in the expression of proteins related to energy production (Dineshram et al., 2012, 2015, 2016). Similarly, a certain taxonomic group, specifically the bivalves, was the focus of the majority of studies (**Figures 2B**, **3B**), considering that a broader range of taxonomic groups will be important given the potential for varying responses to manifest, even among closely related groups (reviewed by Doney et al., 2009). Moreover, we identified that fewer studies consider "lower" level processes (i.e., molecular or cellular), with the majority focused on those that manifest at the individual level (e.g., growth, respiration; **Figure 2C**). In addition, the majority of studies considered one biological level (**Figure 3C**). Altogether, these traits of the existing literature confer challenges to scaling effects and understanding how responses are connected. For instance, connecting across levels will allow us to understand how responses at the molecular level, such as altered gene expression patterns, may generate outcomes for processes operating at the cellular or organ levels (Harvey et al., 2013). Overall, consideration of the less commonly studied groups identified here—be they life history stages, taxonomic groups, or biological levels—will improve our understanding regarding the generality of responses and, therefore, AOP development.

Considering the Effects of Ocean Acidification Using the AOP Framework

The AOP constructed here for the calcification of the oyster *M. gigas* indicates biological pathways impacted by ocean

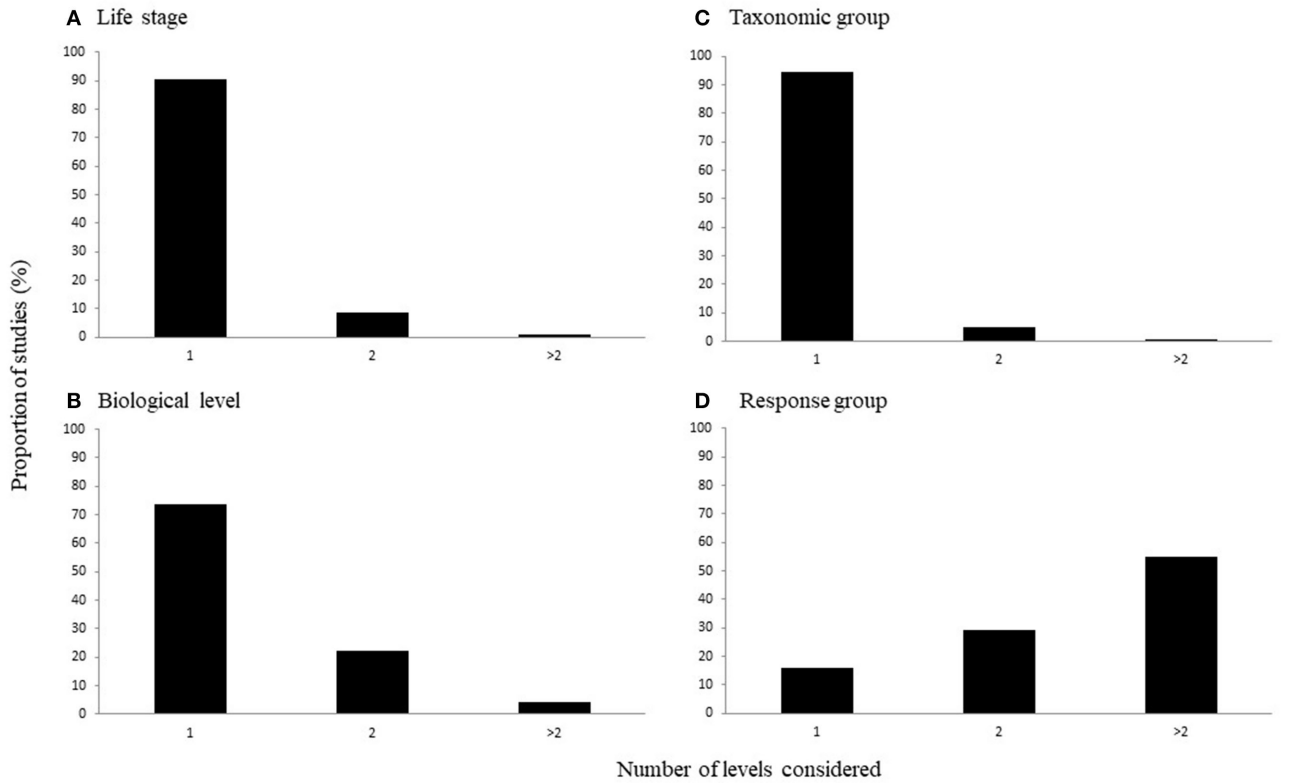

FIGURE 3 | The proportion of studies considering different numbers of levels of **(A)** life stages, **(B)** taxonomic groups, **(C)** biological levels, and **(D)** response variable groups.

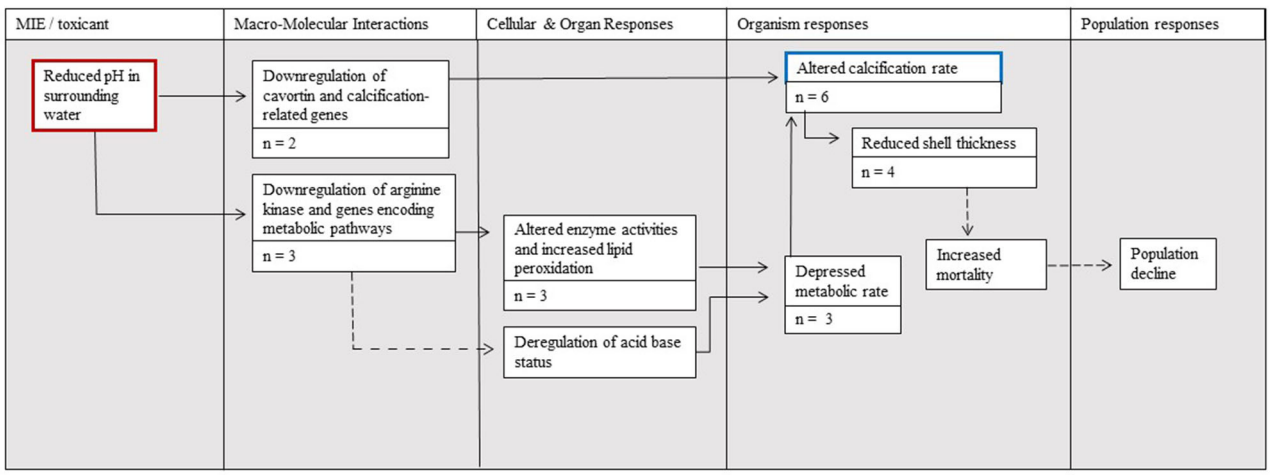

FIGURE 4 | The Adverse Outcome Pathway (AOP) linking the effects of ocean acidification (red border) to calcification (blue border) and its effects on *Magallana gigas* as supported by the studies assembled in the present meta-analysis. The number of studies supporting each step is denoted by $n = X$. Solid arrow lines represent established linkages with quantitative data documented for *M. gigas*, whereas dotted arrow lines represent linkages supported with data considering other bivalves.

acidification (**Figure 4**). In this application of the AOP framework, the reduction in external pH is considered to be the molecular initiating event (MIE). The changes in external pH associated with ocean acidification can then be detected by the oysters through several mechanisms, including signaling peptides (Roggatz et al., 2016), ingestion of acidified water (Jaeckle, 2017),

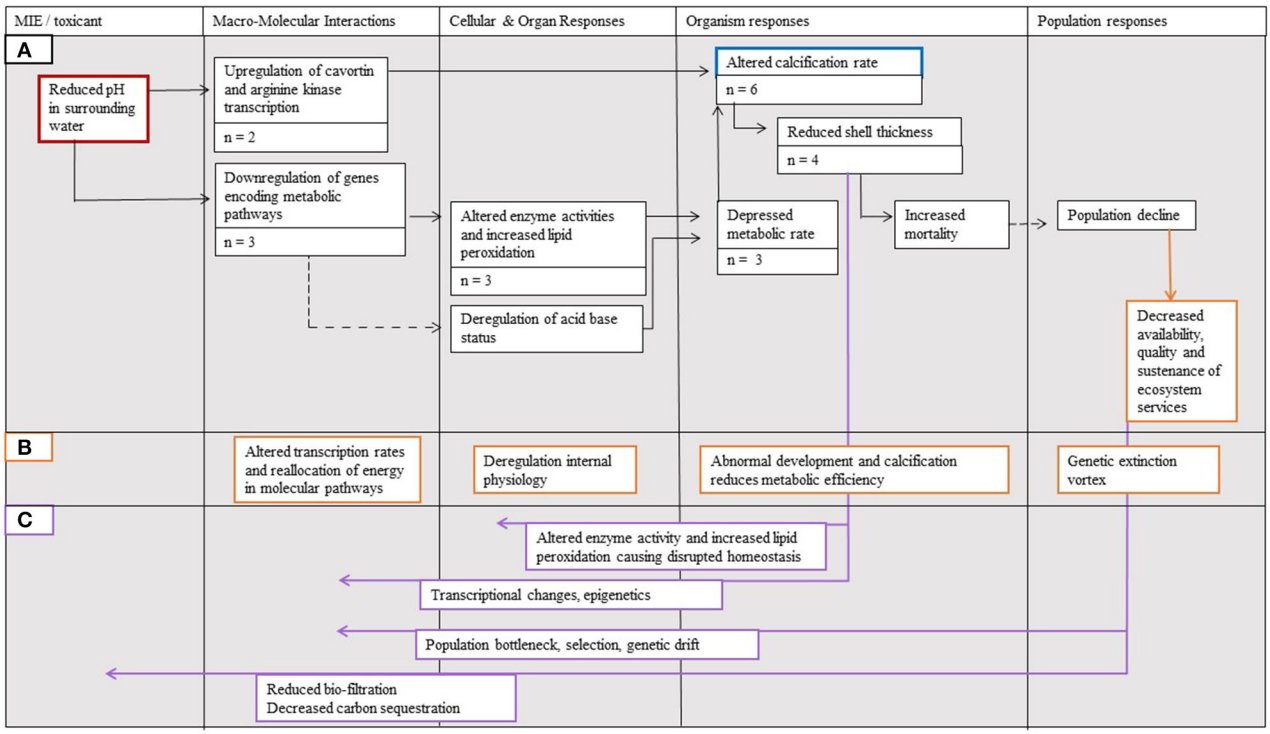

FIGURE 5 | The Adverse Outcome Pathway (AOP) linking the effects of **(A)** ocean acidification (red border) to calcification (blue border) and its effects on *Magallana gigas*, amended to incorporate **(B)** within-level feedback mechanisms (orange borders indicate added examples of responses and arrow lines indicate added pathways), as well as **(C)** interaction effects from higher to lower levels of biological organization (purple arrow lines indicate added pathways). The number of studies supporting each step is denoted $n = X$. Solid arrow lines represent established linkages with quantitative data documented for *M. gigas*, whereas dotted arrow lines represent linkages supported with data considering other bivalves.

or direct contact (O'Donnell et al., 2013). Once detected, the associated molecular signal is then transmitted and received.

When the chemical signal associated with ocean acidification is received, effects can be observed at the molecular level. Anticipated molecular level changes include the decreased expression of genes involved in the calcification process, such as the transcription of cavortin, a gene involved in shell deposition (Itoh et al., 2011; Wei et al., 2015). In addition, the MIE can also lead to molecular changes that result in decreased expression of arginine kinase (AK) and adenosine triphosphate (ATP), which are fundamental components in metabolic pathways (Dineshram et al., 2012; Wei et al., 2015; Evans et al., 2017).

The changes at the molecular level can then generate changes at the cellular and organ level. Here, we anticipate that the downregulation of genes encoding metabolic pathways would lead to changes in enzyme activities, increases in lipid peroxidation, and deregulation of the acid–base status (e.g., extracellular acidosis). These changes subsequently alter the individual level rates of energetic expenditure and metabolism (Michaelidis et al., 2005; Wang et al., 2017), which are linked with decreased calcification rates.

Impacts on the individual level process of calcification can then scale up to affect "higher" levels of organization. That is, our meta-analysis and subsequent AOP highlight that altered calcification can lead to impaired shells in oysters; for example, ocean acidification has led to a drop in shell hardness and stiffness in the oyster *Magallana angulata* (Meng et al., 2018). Such changes have been shown to result in increased mortality in other bivalves. That is, thinner shells are weaker, which directly increases the prevalence of shell microfractures and reduces shell resistance (Dickinson et al., 2011), increasing the susceptibility of individuals to predation (Fitzer et al., 2016). Indirect effects can, however, alter the direct effect of ocean acidification on shell structure. That is, where energy-rich food is available under ocean acidification, calcifiers can build shells that are thicker, more crystalline, and more mechanically resilient (Leung et al., 2019). Where such resources are not available, these responses not possible, and shells impaired, the increased mortality at the individual level can then lead to a decline in the size of the overall population.

In addition to highlighting what is known regarding the effects of ocean acidification, constructing this AOP also highlighted areas of uncertainty. That is, while the AOP reveals links from the chemical changes driven by ocean acidification through the various levels of biological organization to the population responses, there is still uncertainty regarding many key steps and their effects. This uncertainty occurs despite *M. gigas* representing a relatively well-studied species. Such

uncertainty results as the existing experimental literature makes few connections across levels of biological hierarchy, with extensive variations identified where such connections have been made (e.g., Dineshram et al., 2012; Wei et al., 2015). The strength of links from lower to higher biological levels of organization may also vary, which is not taken into account under the AOP framework. For example, an impact with strong links across levels would be reduced antioxidant activity, which lowers immune system function and directly impacts individual survival (Wang et al., 2017). In contrast, an impact with weaker or less direct links across levels would be a reduction in metabolic efficiency, which represents a malleable response with largely indirect effects on individual fitness through energy reallocation (Cao et al., 2018). Connections across biological levels, therefore, require further consideration as, despite our limited understanding, they are recognized to play a key influence in the overall response of mollusks (Queirós et al., 2014) and other calcifying taxa to environmental change (Calosi et al., 2013; Palumbi et al., 2014).

Recommendations for Future AOP Development

The development of AOPs considering the impacts of environmental stressors associated with global change, such as ocean acidification, provides an opportunity to explore the impacts of more complex scenarios. Some key aspects of complexity that could be considered in future iterations of this framework include varying susceptibility within and among species; feedback mechanisms; stressor duration, magnitude, and co-occurrence; as well as species interactions.

Varying Susceptibility Within and Among Species

In the future, the AOP framework could be used to consider mechanisms underlying varying responses that have been found, for example, between populations across large spatial areas (e.g., Parker et al., 2010; Ginger et al., 2013; Kraft et al., 2014; Falkenberg et al., 2019; Telesca et al., 2019; Clark et al., 2020), among distinct populations of the same species (e.g., Stapp et al., 2016), among closely related species (Vihtakari et al., 2016), and across different taxonomic groups (e.g., Kroeker et al., 2010). For example, recent studies considering a range of ectotherms from different taxonomic groups have suggested that Nab/Kb ATPase, a major cellular ATP consumer (Wieser and Krumschnabel, 2001), may be broadly susceptible to the effects of acidification (Pörtner et al., 2004; Lannig et al., 2010). If AOPs were to be constructed for a range of organisms representing diverse taxonomic groups, and all the pathways included impacts on the Nab/Kb ATPase, it would indicate the general importance of this pathway. In contrast, if the AOPs did not reveal this expected pattern, it would highlight that there are greater differences among taxonomic groups than anticipated. In addition to providing insight into conserved mechanisms across species, AOPs also have the potential to reveal divergent processes that lead to varied responses. For example, the mechanisms that cephalopods and some echinoderms use to maintain internal pH under acidification contrast with the processes used by bivalves. That is, cephalopods and some echinoderms can partially or fully restore their internal pH through the use of extracellular respiratory pigments and accumulation of bicarbonate (Gutowska et al., 2010); in contrast bivalves, which lack these pigments, are unable to adjust their internal pH in this way (Collard et al., 2013). Such differences would be revealed in the AOPs constructed for species of these groups.

Feedback Mechanisms—Between and Within Biological Levels

Despite the broad outcomes of ocean acidification being relatively well-documented, the implications of processes acting between and within biological levels require further consideration (**Figure 5**). Of particular interest are feedbacks moving between biological levels from "higher" to "lower" levels (e.g., compromised immune system affecting metabolic pathways; **Figure 5C**) and within-level feedback cycles (e.g., reduced individual growth affecting energy expenditure affecting reduced individual growth, etc.; **Figure 5B**). Feedback mechanisms between biological levels could be explored using the AOP framework where outcomes at higher levels of biological organization are linked to their consequences for processes at lower levels. An example of such feedbacks includes the effect of reduced organism level metabolic rate altering cellular- and organ-level processes, specifically enzyme activity and increasing lipid peroxidation (Wei et al., 2015; Wang et al., 2017). The AOP framework also provides an opportunity to explore within-level impacts. For instance, at the level of the organism, changes in the process of calcification and development may subsequently affect metabolic rates (e.g., in sea urchin; Stumpp et al., 2011).

Stressor Duration, Magnitude, and Co-occurrence

Developing AOPs with recognition of the features of treatments used, such as the duration, magnitude, and co-occurrence of stressor exposure, will allow for more nuanced understanding of anticipated effects. In terms of duration, it would be useful to incorporate information on whether each of the observed outcomes occurred in a matter of hours, days, weeks, or years, potentially developing separate AOPs for each of these timescales. Where information on the longer timescales is available, this could facilitate inclusion of the evolutionary responses to climate change in AOPs (see Munday et al., 2013 and references therein). Long-term responses to stressors spanning several generations are gaining increased interest, which could allow incorporation of the role of epigenetics (Turner, 2009) and carry over effects (Parker et al., 2010). Another important development will be the incorporation of information regarding the relationship between dose dependency and expected outcomes, an issue that has only relatively recently been addressed (e.g., Hooper et al., 2013). The level of the stressor considered may play a key role in the responses observed as biological responses may be characterized by distinct "thresholds" or sensitivities (e.g., May, 1977). Moreover, the combination of stressor exposure duration and magnitude will be important to consider; exposure to shorter and stronger treatments may lead to considerably different responses than longer and weaker exposures (Kroeker et al., 2010, 2019). Finally, environmental stressors will occur in combination, and this could modify their effects. For instance, the

effects of ocean acidification can be altered where this condition interacts with higher temperature (Leung et al., 2020b) and salinity (Przeslawski et al., 2015) to affect organisms, including those of particular concern, such as oysters (Thiyagarajan and Ko, 2012; Ginger et al., 2014). The effect can also be dependent on other factors, such as life history stage considered, with acidification and temperature found to have positive effects on larval growth but lead to an increase in overall mortality (Parker et al., 2017). Stressor identity is also likely to be influential. When acidification is combined with increased salinity, it has negative effects on attachment and metamorphosis of developing oysters, but such effects were not observed when combined with elevated temperature (Thiyagarajan and Ko, 2012; Ginger et al., 2014). Consequently, an important role of AOPs will be to combine independent AOPs created for each stressor to identify common effects overlapping across separate pathways. In this way, AOPs may be used to better understand the complexity of responses including the duration magnitude and synergy of stressors.

Multiple Species and Their Interactions

The AOPs developed for individual species could be assembled together to form large networks that depict the impacts of stressors on whole ecosystems. Where these links are made, it could allow for species interactions to be incorporated into studies applying the AOP framework. For instance, such a network approach could allow representation of the impacts that result from the degradation of shallow-water oyster reefs to reduce biodiversity and eventually result in profound shifts in composition from a calcareous-dominated system to one dominated by non-calcareous species (Christen et al., 2012; Rossoll et al., 2012). Where such networks are created for a range of sites characterized by similar ecosystems, this could allow improved understanding of the similarities or differences in responses to ocean acidification and the underlying mechanisms. In particular, comparisons of AOPs developed for species and communities in naturally acidified conditions such as volcanic seeps, areas of upwelling, lagoons, and estuaries may be of particular interest for predicting the impacts of future ocean conditions (see studies by Tunnicliffe et al., 2009; Thomsen et al., 2013; Basso et al., 2015).

CONCLUSIONS

Here, we highlight how the AOP framework can be applied to consider the effects of a climate stressor, specifically ocean acidification, on a process of interest in a key organism, specifically oyster calcification. This application highlights that such an approach can effectively bring together key findings from existing literature to demonstrate how responses may manifest. Looking forward, the AOP framework may provide a novel approach to consider mechanisms by which ocean acidification, and other climate drivers, have an effect and alter organism function, ecosystem structure, and benefits provided to human societies.

DATA AVAILABILITY STATEMENT

The raw data supporting the conclusions of this article will be made available by the authors, without undue reservation.

AUTHOR CONTRIBUTIONS

JD and LF contributed to the conception and design of this meta-analysis, AOP, manuscript, and manuscript revision. JD performed the meta-analysis, did the statistical analysis, created the AOP, and produced the figures with guidance from LF. JD prepared the first draft of the manuscript. All authors contributed to the article and approved the submitted version.

ACKNOWLEDGMENTS

We would like to thank Jodie Kei Yu Ip and Cindy B. Tong for their assistance in reviewing papers for the meta-analysis.

REFERENCES

Ankley, G. T., Bennett, R. S., Erickson, R. J., Hoff, D. J., Hornung, M. W., Johnson, R. D., et al. (2010). Adverse outcome pathways: a conceptual framework to support ecotoxicology research and risk assessment. *Environ. Toxicol. Chem.* 29, 730–741. doi: 10.1002/etc.34

Barry, J. P., Widdicombe, S., and Hall-Spencer, J. M. (2011). "Effects of ocean acidification on marine biodiversity and ecosystem function," in *Ocean Acidification*, eds J. P. Gattuso and L. *Lansson (Oxford: Oxford University Press)*, 192–209.

Basso, L., Hendriks, I. E., Rodríguez-Navarro, A. B., Gambi, M. C., and Duarte, C. M. (2015). Extreme pH conditions at a natural CO_2 vent system (Italy) affect growth, and survival of juvenile pen shells (*Pinna nobilis*). *Estuaries Coast* 38, 1986–1999. doi: 10.1007/s12237-014-9936-9

Burrows, M. T., Schoeman, D. S., Buckley, L. B., Moore, P., Poloczanska, E. S., Brander, K. M., et al. (2011). The pace of shifting climate in marine and terrestrial ecosystems. *Science* 334, 652–655. doi: 10.1126/science.1210288

Byrne, M., and Fitzer, S. (2019). The impact of environmental acidification on the microstructure and mechanical integrity of marine invertebrate skeletons. *Conserv. Physiol.* 7:coz062. doi: 10.1093/conphys/coz062

Caldeira, K. (2005). Ocean model predictions of chemistry changes from carbon dioxide emissions to the atmosphere and ocean. *J. Geophys. Res.* 110:C9. doi: 10.1029/2004JC002671

Caldeira, K., and Wickett, M. E. (2003). Anthropogenic carbon and ocean pH. *Nature* 425:365. doi: 10.1038/425365a

Calosi, P., Rastrick, S. P., Lombardi, C., Guzman, H. J., Davidson, L., Jahnke, M., et al. (2013). Adaptation and acclimatization to ocean acidification in marine ectotherms: an *in situ* transplant experiment with polychaetes at a shallow CO_2 vent system. *Philos. T. R. Soc. B.* 368:20120444. doi: 10.1098/rstb.2012.0444

Cao, R., Liu, Y., Wang, Q., Zhang, Q., Yang, D., Liu, H., et al. (2018). The impact of ocean acidification and cadmium on the immune responses of Pacific oyster, *Crassostrea gigas*. *Fish. Shell. Immun.* 81, 456–462. doi: 10.1016/j.fsi.2018.07.055

Christen, N., Calosi, P., McNeill, C. L., and Widdicombe, S. (2012). Structural and functional vulnerability to elevated pCO_2 in marine benthic communities. *Mar. Biol.* 160, 2113–2128. doi: 10.1007/s00227-012-2097-0

Clark, M. S., Peck, L. S., Arivalagan, J., Backeljau, T., Berland, S., Cardoso, J. C. R., et al. (2020). Deciphering mollusc shell production: the roles of genetic mechanisms through to ecology, aquaculture and biomimetics. *Biol. Rev.* doi: 10.1111/brv.12640

Collard, M., Laitat, K., Moulin, L., Catarino, A. I., Grosjean, P., and Dubois, P. (2013). Buffer capacity of the coelomic fluid in echinoderms. *Comp. Biochem. Physiol. A Mol. Int. Physiol.* 166, 199–206. doi: 10.1016/j.cbpa.2013.06.002

Cyronak, T., Schulz, K. G., and Jokiel, P. L. (2016). The Omega myth: what really drives lower calcification rates in an acidifying ocean. *ICES J. Mar. Sci.* 73, 558–562. doi: 10.1093/icesjms/fsv075

Dickinson, G. H., Ivanina, A. V., Matoo, O. B., Pörtner, H. O., Lannig, G., Bock, C., et al. (2011). Interactive effects of salinity and elevated CO_2 levels on juvenile eastern oysters, *Crassostrea virginica*. *J. Exp. Biol.* 215, 29–43. doi: 10.1242/jeb.061481

Dineshram, R., Chandramouli, K., Ko, G. W., Zhang, H., Qian, P., Ravasi, T., and Thiyagarajan, V. (2016). Quantitative analysis of oyster larval proteome provides new insights into the effects of multiple climate change stressors. *Glob. Chang. Biol.* 22, 2054–2068. doi: 10.1111/gcb.13249

Dineshram, R., Q., Q., Sharma, R., Chandramouli, K., Yalamanchili, H. K., et al. (2015). Comparative and quantitative proteomics reveal the adaptive strategies of oyster larvae to ocean acidification. *Proteom* 15, 4120–4134. doi: 10.1002/pmic.201500198

Dineshram, R., Wong, K. K., Xiao, S., Yu, Z., Qian, P. Y., and Thiyagarajan, V. (2012). Analysis of Pacific oyster larval proteome and its response to high-CO_2. *Mar. Pollut. Bull.* 64, 2160–2167. doi: 10.1016/j.marpolbul.2012.07.043

Doney, S. C., Fabry, V. J., Feely, R. A., and Kleypas, J. A. (2009). Ocean acidification: the other CO_2 problem. *Ann. Rev. Mar. Sci.* 1, 169–192. doi: 10.1146/annurev.marine.010908.163834

Evans, T. G., Pespeni, M. H., Hofmann, G. E., Palumbi, S. R., and Sanford, E. (2017). Transcriptomic responses to seawater acidification among sea urchin populations inhabiting a natural pH mosaic. *Mol. Ecol. Resour.* 26, 2257–2275. doi: 10.1111/mec.14038

Falkenberg, L. J., Dupont, S., and Bellerby, R. G. (2018). Approaches to reconsider literature on physiological effects of environmental change: examples from ocean acidification research. *Front. Mar. Sci.* 5:453. doi: 10.3389/fmars.2018.00453

Falkenberg, L. J., Styan, C. A., and Havenhand, J. N. (2019). Sperm motility of oysters from distinct populations differs in response to ocean acidification and freshening. *Sci. Rep.* 9:7970. doi: 10.1038/s41598-019-44321-0

FAO (2016). *The State of World Fisheries and Aquaculture. Meeting the Sustainable Development Goals*. Rome.

Fitzer, S. C., Chan, V. B. S., Meng, Y., Rajan, K. C., Suzuki, M., Not, C., et al. (2019). "Established and emerging techniques for characterizing the formation, structure and performance of calcified structures under ocean acidification," in *Oceanography and Marine Biology: An Annual Review*, eds S. J. Hawkins, A. L. Allcock, A. E. Bates, L. B. Firth, I. P. Smith, S. E. Swearer, and P. A. Todd (Boca Raton; London; New York, NY: CRC Press, Taylor & Francis Group), 57, 89–125.

Fitzer, S. C., Chung, P., Maccherozzi, F., Dhesi, S. S., Kamenos, N. A., Phoenix, V. R., and Cusack, M. (2016). Biomineral shell formation under ocean acidification: a shift from order to chaos. *Sci. Rep.* 6:21076. doi: 10.1038/srep21076

Fitzer, S. C., Zhu, W., Tanner, K. E., Phoenix, V. R., Kamenos, N. A., and Cusack, M. (2015). Ocean acidification alters the material properties of *Mytilus edulis* shells. *J. R. Soc. Interface* 12:20141227. doi: 10.1098/rsif.2014.1227

Garilli, V., Rodolfo-Metalpa, R., Scuderi, D., Brusca, L., Parrinello, D., Rastrick, S. P., et al. (2015). Physiological advantages of dwarfing in surviving extinctions in high-CO_2 oceans. *Nat. Clim. Chang.* 5, 678–682. doi: 10.1038/nclimate2616

Gazeau, F., Parker, L. M., Comeau, S., Gattuso, J., O'Connor, W. A., Martin, S., et al. (2013). Impacts of ocean acidification on marine shelled mollusks. *Mar. Biol.* 160, 2207–2245. doi: 10.1007/s00227-013-2219-3

Ginger, K. W. K., Dineshram, R., Campanati, C., Chan, V. B. S., Havenhand, J., and Thiyagarajan, V. (2014). Interactive effects of ocean acidification, elevated temperature, and reduced salinity on early-life stages of the Pacific oyster. *Environ. Sci. Tech.* 48, 10079–10088. doi: 10.1021/es501611u

Ginger, K. W. K., Vera, C. B. S., Dennis, C. K. S., Adela, L. J., Yu, Z., Thiyagarajan, V., et al. (2013). Larval and post-larval stages of Pacific oyster (*Crassostrea gigas*) are resistant to elevated CO_2. *PLoS. ONE* 8:e34147. doi: 10.1371/journal.pone.0064147

Gutowska, M. A., Melzner, F., Langenbuch, M., Bock, C., Claireaux, G., and Pörtner, H. O. (2010). Acid–base regulatory ability of the cephalopod (*Sepia officinalis*) in response to environmental hypercapnia. *J. Comp. Physiol.* 180, 323–335. doi: 10.1007/s00360-009-0412-y

Harvey, B., and Moore, P. (2017). Ocean warming and acidification prevent compensatory response in a predator to reduced prey quality. *Mar. Ecol. Prog. Ser.* 563, 111–122. doi: 10.3354/meps11956

Harvey, B. P., Gwynn-Jones, D., and Moore, P. J. (2013). Meta-analysis reveals complex marine biological responses to the interactive effects of ocean acidification and warming. *Ecol. Evol.* 3, 1016–1030. doi: 10.1002/ece3.516

Hettinger, A., Sanford, E., Hill, T. M., Lenz, E. A., Russell, A. D., and Gaylord, B. (2013). Larval carry-over effects from ocean acidification persist in the natural environment. *Glob. Chang. Biol.* 19, 3317–3326. doi: 10.1111/gcb.12307

Hettinger, A., Sanford, E., Hill, T. M., Russell, A. D., Sato, K. N. S., Hoey, J., et al. (2012). Persistent carry-over effects of planktonic exposure to ocean acidification in the Olympia oyster. *Ecology* 93, 2758–2768. doi: 10.1890/12-0567.1

Hooper, M. J., Ankley, G. T., Cristol, D. A., Maryoung, L. A., Noyes, P. D., and Pinkerton, K. E. (2013). Interactions between chemical and climate stressors: a role for mechanistic toxicology in assessing climate change risks. *Environ. Toxicol. Chem.* 32, 32–48. doi: 10.1002/etc.2043

IPCC (2013). *Climate Change 2013 - The Physical Science Basis: Working Group I Contribution to the Fifth Assessment Report of the IPCC*. Cambridge: Cambridge University Press.

Itoh, N., Xue, Q., Schey, K. L., Li, Y., Cooper, R. K., and Peyre, J. F. (2011). Characterization of the major plasma protein of the Eastern Oyster, *Crassostrea virginica*, and a proposed role in host defense. *Comp. Biochem. Physiol. B Biochem. Mol. Biol.* 158, 9–22. doi: 10.1016/j.cbpb.2010.06.006

Jaeckle, W. (2017). "Chapter 9: Physiology of Larval Feeding" in *Evolutionary Ecology of Marine Invertebrate Larvae* (Oxford: Oxford Scholarship Online), 124–141. doi: 10.1093/oso/9780198786962.003.0009

Kraft, N. J. B., Adler, P. B., Godoy, O., James, E. C., Fuller, S., and Levine, J. M. (2014). Community assembly, coexistence and the environmental filtering metaphor. *Funct. Ecol.* 29, 592–599. doi: 10.1111/1365-2435.12345

Kroeker, K. J., Bell, L. E., Donham, E. M., Hoshijima, U., Lummis, S., Toy, J. A., and Willis-Norton, E. (2019). Ecological change in dynamic environments: accounting for temporal environmental variability in studies of ocean change biology. *Glob. Chang. Biol.* 26, 54–67. doi: 10.1111/gcb.14868

Kroeker, K. J., Kordas, R. L., Crim, R. N., and Singh, G. G. (2010). Meta-analysis reveals negative yet variable effects of ocean acidification on marine organisms. *Ecol. Lett.* 13, 1419–1434. doi: 10.1111/j.1461-0248.2010.01518.x

Lannig, G., Eilers, S., Pörtner, H. O., Sokolova, I. M., and Bock, C. (2010). Impact of ocean acidification on energy metabolism of oyster, *Crassostrea gigas* – changes in metabolic pathways and thermal response. *Mar. Drugs* 8, 2318–2339. doi: 10.3390/md8082318

Leist, M., Ghallab, A., Graepel, R., Marchan, R., Hassan, R., Bennekou, S. H., et al. (2017). Adverse outcome pathways: opportunities, limitations and open questions. *Arch. Toxicol.* 91, 3477–3505. doi: 10.1007/s00204-017-2045-3

Lemasson, A. J., Fletcher, S., Hall-Spencer, J. M., and Knights, A. M. (2017). Linking the biological impacts of ocean acidification on oysters to changes in ecosystem services: a review. *J. Exp. Mar. Biol. Ecol.* 492, 49–62. doi: 10.1016/j.jembe.2017.01.019

Leung, J. Y. S., Chen, Y., Nagelkerken, I., Zhang, S., Xie, Z., and Connell, S. D. (2020a). Calcifiers can adjust shell building at the nanoscale to resist ocean acidification. *Small* 16:2003186. doi: 10.1002/smll.202003186

Leung, J. Y. S., Doubleday, Z. A., Nagelkerken, I., Chen, Y., Xie, Z., and Connell, S. D. (2019). How calorie-rich food could help marine calcifiers in a CO_2-rich future. *Proc. R Soc. B* 286:20190757. doi: 10.1098/rspb.2019.0757

Leung, J. Y. S., Russell, B. D., and Connell, S. D. (2017). Mineralogical plasticity acts as a compensatory mechanism to the impacts of ocean acidification. *Environ. Sci. Technol.* 51, 2652–2659. doi: 10.1021/acs.est.6b04709

Leung, J. Y. S., Russell, B. D., and Connell, S. D. (2020b). Linking energy budget to physiological adaptation: how a calcifying gastropod adjusts or succumbs to ocean acidification and warming. *Sci. Total. Environ.* 715:136939. doi: 10.1016/j.scitotenv.2020.136939

Marshall, D. J., Santos, J. H., Leung, K. M., and Chak, W. H. (2008). Correlations between gastropod shell dissolution and water chemical properties in a tropical estuary. *Mar. Environ. Res.* 66, 422–429. doi: 10.1016/j.marenvres.2008.07.003

May, R. M. (1977). Thresholds and breakpoints in ecosystems with a multiplicity of stable states. *Nature* 269, 471–477. doi: 10.1038/269471a0

Meng, Y., Guo, Z., Fitzer, S. C., Upadhyay, A., Chan, V. B. S., Li, C., et al. (2018). Ocean acidification reduces hardness and stiffness of the Portuguese oyster shell with impaired microstructure: a hierarchical analysis. *Biogeosciences* 15, 6833–6846. doi: 10.5194/bg-15-6833-2018

Michaelidis, B., Ouzounis, C., Paleras, A., and Pörtner, H. (2005). Effects of long-term moderate hypercapnia on acid-base balance and growth rate in marine mussels *Mytilus galloprovincialis*. *Mar. Ecol. Prog. Ser.* 293, 109–118. doi: 10.3354/meps293109

Munday, P. L., Warner, R. R., Monro, K., Pandolfi, J. M., and Marshall, D. J. (2013). Predicting evolutionary responses to climate change in the sea. *Ecol. Lett.* 16, 1488–1500. doi: 10.1111/ele.12185

Nienhuis, S., Palmer, A. R., and Harley, C. D. (2010). Elevated CO_2 affects shell dissolution rate but not calcification rate in a marine snail. *Proc. R Soc. B* 277, 2553–2558. doi: 10.1098/rspb.2010.0206

O'Donnell, M. J., George, M. N., and Carrington, E. (2013). Mussel byssus attachment weakened by ocean acidification. *Nat. Clim. Change*. 3, 587–590. doi: 10.1038/nclimate1846

Palumbi, S. R., Barshis, D. J., Traylor-Knowles, N., and Bay, R. A. (2014). Mechanisms of reef coral resistance to future climate change. *Science* 344, 895–898. doi: 10.1126/science.1251336

Parker, L. M., O'Connor, W. A., Byrne, M., Coleman, R. A., Virtue, P., Dove, M., et al. (2017). Adult exposure to ocean acidification is maladaptive for larvae of the Sydney rock oyster *Saccostrea glomerata* in the presence of multiple stressors. *Biol. Lett.* 13:20160798. doi: 10.1098/rsbl.2016.0798

Parker, L. M., Ross, P. M., and O'Connor, W. A. (2009). The effect of ocean acidification and temperature on the fertilization and embryonic development of the Sydney rock oyster *Saccostrea glomerata* (Gould, 1850). *Glob. Chang. Biol.* 15, 2123–2136. doi: 10.1111/j.1365-2486.2009.01895.x

Parker, L. M., Ross, P. M., and O'Connor, W. A. (2010). Comparing the effect of elevated pCO_2 and temperature on the fertilization and early development of two species of oysters. *Mar. Biol.* 157, 2435–2452. doi: 10.1007/s00227-010-1508-3

Pörtner, H. O., Langenbuch, M., and Reipschläger, A. (2004). Biological impact of elevated ocean CO_2 concentrations: lessons from animal physiology and earth history. *J. Oceanogr.* 60, 705–718. doi: 10.1007/s10872-004-5763-0

Prosser, C. L. (1955). Physiological variation in animals. *Biol. Rev.* 30, 229–261. doi: 10.1111/j.1469-185X.1955.tb01208.x

Przeslawski, R., Byrne, M., and Mellin, C. (2015). A review and meta-analysis of the effects of multiple abiotic stressors on marine embryos and larvae. *Glob. Chang. Biol.* 21, 2122–2140. doi: 10.1111/gcb.12833

Queirós, A. M., Fernandes, J. A., Faulwetter, S., Nunes, J., Rastrick, S. P., Mieszkowska, N., et al. (2014). Scaling up experimental ocean acidification and warming research: from individuals to the ecosystem. *Glob. Chang. Biol.* 21, 130–143. doi: 10.1111/gcb.12675

Rodolfo-Metalpa, R., Houlbrèque, F., Tambutt,é, É., Boisson, F., Baggini, C., Patti, F. P., et al. (2011). Coral and mollusc resistance to ocean acidification adversely affected by warming. *Nat. Clim. Chang.* 1, 308–312. doi: 10.1038/nclimate1200

Roggatz, C. C., Lorch, M., Hardege, J. D., and Benoit, D. M. (2016). Ocean acidification affects marine chemical communication by changing structure and function of peptide signalling molecules. *Glob. Chang. Biol.* 22, 3914–3926. doi: 10.1111/gcb.13354

Rossoll, D., Bermúdez, R., Hauss, H., Schulz, K. G., Riebesell, U., Sommer, U., and Winder, M. (2012). Ocean acidification-induced food quality deterioration constrains trophic transfer. *PLoS ONE* 7:e34737. doi: 10.1371/journal.pone.0034737

Sabine, C. L., Feely, R. A., Gruber, N., Key, R. M., Lee, K., Bullister, J. L., et al. (2004). The oceanic sink for anthropogenic CO_2. *Science* 305, 367–371. doi: 10.1126/science.1097403

Scanes, E., Parker, L. M., O'Connor, W. A., and Ross, P. M. (2014). Mixed effects of elevated pCO_2 on fertilisation, larval and juvenile development and adult responses in the mobile subtidal scallop *Mimachlamys asperrima* (Lamarck, 1819). *PLoS ONE* 9:93649. doi: 10.1371/journal.pone0093649

Society for Advancement of AOPs (2020). Available online at: https://aopwiki.org/ (accessed October 20, 2019).

Stapp, L. S., Thomsen, J., Schade, H., Bock, C., Melzner, F., Pörtner, H. O., et al. (2016). Intra-population variability of ocean acidification impacts on the physiology of baltic blue mussels (*Mytilus edulis*): integrating tissue and organism response. *J. Comp.Phys. B* 187, 529–543. doi: 10.1007/s00360-016-1053-6

Stumpp, M., Wren, J., Melzner, F., Thorndyke, M., and Dupont, S. (2011). CO_2 induced seawater acidification impacts sea urchin larval development I: elevated metabolic rates decrease scope for growth and induce developmental delay. *Comp. Biochem. Phys. A Mol. Integr. Physiol.* 160, 331–340. doi: 10.1016/j.cbpa.2011.06.022

Talmage, S. C., and Gobler, C. J. (2009). The effects of elevated carbon dioxide concentrations on the metamorphosis, size, and survival of larval hard clams (*Mercenaria mercenaria*), bay scallops (*Argopecten irradians*), and eastern oysters (*Crassostrea virginica*). *Limnol. Oceangr.* 54, 2072–2080. doi: 10.4319/lo.2009.54.6.2072

Telesca, L., Peck, L. S., Sanders, T., Thyrring, J., Sejr, M. K., and Harper, E. M. (2019). Biomineralization plasticity and environmental heterogeneity predict geographical resilience patterns of foundation species to future change. *Glob. Change Biol.* 25, 4179–4193. doi: 10.1111/gcb.14758

Thiyagarajan, V., and Ko, G. W. K. (2012). Larval growth response of the Portuguese oyster (*Crassostrea angulata*) to multiple climate change stressors. *Aquaculture* 370–371, 90–95. doi: 10.1016/j.aquaculture.2012.09.025

Thomsen, J., Casties, I., Pansch, C., Körtzinger, A., and Melzner, F. (2013). Food availability outweighs ocean acidification effects in juvenile *Mytilus edulis*: laboratory and field experiments. *Glob. Chang. Biol.* 19, 1017–1027. doi: 10.1111/gcb.12109

Tunnicliffe, V., Davies, K. T., Butterfield, D. A., Embley, R. W., Rose, J. M., and Chadwick, W. W. Jr. (2009). Survival of mussels in extremely acidic waters on a submarine volcano. *Nat. Geosci.* 2, 344–348. doi: 10.1038/ngeo500

Turner, B. M. (2009). Epigenetic responses to environmental change and their evolutionary implications. *Philos. Trans. R Soc. Lond. B Biol. Sci.* 364, 3403–3418. doi: 10.1098/rstb.2009.0125

Vihtakari, M., Havenhand, J., Renaud, P. E., and Hendriks, I. E. (2016). Variable individual- and population-level responses to ocean acidification. *Front. Mar. Sci.* 3:51. doi: 10.3389/fmars.2016.00051

Waldbusser, G. G., Hales, B., Langdon, C. J., Haley, B. A., Schrader, P., Brunner, E. L., et al. (2015). Ocean acidification has multiple modes of action on bivalve larvae. *PLoS ONE* 10:e128376. doi: 10.1371/journal.pone.0128376

Wang, X., Wang, M., Jia, Z., Qiu, L., Wang, L., Zhang, A., et al. (2017). A carbonic anhydrase serves as an important acid-base regulator in Pacific oyster *Crassostrea gigas* exposed to elevated CO_2: implication for physiological responses of mollusk to ocean acidification. *Mar. Biotechnol.* 19, 22–35. doi: 10.1007/s10126-017-9734-z

Wei, L., Wang, Q., Wu, H., Ji, C., and Zhao, J. (2015). Proteomic and metabolomic responses of Pacific oyster *Crassostrea gigas* to elevated pCO_2 exposure. *J. Proteom.* 112, 83–94. doi: 10.1016/j.jprot.2014.08.010

Wieser, W., and Krumschnabel, G. (2001). Hierarchies of ATP-consuming processes: direct compared with indirect measurements, and comparative aspects. *Biochem. J.* 355:389. doi: 10.1042/bj3550389

Wood, H. L., Spicer, J. I., and Widdicombe, S. (2008). Ocean acidification may increase calcification rates, but at a cost. *Proc. R Soc. B* 275, 1767–1773. doi: 10.1098/rspb.2008.0343

Zeebe, R. E., and Wolf-Gladrow, D. W. (2001). *CO_2 in Seawater: Equilibrium, Kinetics, Isotopes*. The Netherlands: Elsevier. doi: 10.1016/s0422-9894(01)x8001-x

Zhao, L., Milano, S., Walliser, E. O., and Schöne, B. R. (2018). Bivalve shell formation in a naturally CO_2-enriched habitat: unraveling the resilience mechanisms from elemental signatures. *Chemosphere* 203, 132–138. doi: 10.1016/j.chemosphere.2018.03.180

Conflict of Interest: The authors declare that the research was conducted in the absence of any commercial or financial relationships that could be construed as a potential conflict of interest.

frontiers in Marine Science

ORIGINAL RESEARCH
published: 27 November 2020
doi: 10.3389/fmars.2020.581160

Potential Acclimatization and Adaptive Responses of Adult and *Trans*-Generation Coral Larvae From a Naturally Acidified Habitat

Haruko Kurihara[1], Yuri Suhara[1], Izumi Mimura[1] and Yimnang Golbuu[2]*

[1] *Department of Science, University of the Ryukyus, Nishihara, Japan,* [2] *Palau International Coral Reef Center, Koror, Palau*

Coral reefs are one of the most susceptible ecosystems to ocean acidification (OA) caused by increasing atmospheric carbon dioxide (CO_2). OA is suspected to impact the calcification rate of corals as well as multiple early life stages including larval and settlement stages. Meanwhile, there is now a strong interest in evaluating if organisms have the potential for acclimatization or adaptation to OA. Here, by taking advantage of a naturally acidified site in Nikko Bay, Palau where corals are presumably exposed to high CO_2 conditions for their entire life history, we tested if adult and the next-generation larvae of the brooder coral *Pocillopora acuta* originating from the high-CO_2 site are more tolerant to high CO_2 conditions compared to the individuals from a control site. Larvae released from adults collected from the high-CO_2 site within the bay and a control site outside the bay were reciprocally cultivated under experimental control or high-CO_2 seawater conditions to evaluate their physiology. Additionally, reciprocal transplantation of adult *P. acuta* corals were conducted between the high-CO_2 and control sites in the field. The larvae originating from the control site showed lower Chlorophyll-*a* content and lipid percentages when reared under high-CO_2 compared to control seawater conditions, while larvae originating from the high-CO_2 site did not. Additionally, all 10 individuals of adult *P. acuta* from control site died when transplanted within the bay, while all *P. acuta* corals within the bay survived at both control and high-CO_2 site. Furthermore, *P. acuta* within the bay showed higher calcification and net photosynthesis rates when exposed to the condition they originated from. These results are one of the first results that indicate the possibility that the long-living corals could enable to show local adaptation to different environmental conditions including high seawater pCO_2.

Keywords: coral, high-CO_2, local adaptation, trans-generation acclimatization, naturally acidified site

OPEN ACCESS

Edited by:
Ben P. Harvey,
University of Tsukuba, Japan

Reviewed by:
Christian Pansch,
Åbo Akademi University, Finland
Naoko Isomura,
Okinawa College, Japan

****Correspondence:***
Haruko Kurihara
harukoku@sci.u-ryukyu.ac.jp;
harukoku@e-mail.jp

Specialty section:
This article was submitted to Global Change and the Future Ocean, a section of the journal Frontiers in Marine Science

Received: *08 July 2020*
Accepted: *15 October 2020*
Published: *27 November 2020*

Citation:
Kurihara H, Suhara Y, Mimura I and Golbuu Y (2020) Potential Acclimatization and Adaptive Responses of Adult and Trans-Generation Coral Larvae From a Naturally Acidified Habitat. Front. Mar. Sci. 7:581160. doi: 10.3389/fmars.2020.581160

INTRODUCTION

Coral reefs are highly susceptible to ocean acidification (OA) which is caused by increasing concentrations of atmospheric carbon dioxide (CO_2; Hoegh-Guldberg et al., 2007). Seawater pH is expected to decrease by about 0.2–0.4 units compared to present levels of 8.1 by the end of this century according to the RCP scenarios (IPCC, 2014). Because the seawater calcium carbonate saturation (Ω) decreases with OA, the calcification rate of most calcifiers including

corals, is expected to decrease in the future ocean (Kleypas et al., 2005; Chan and Connolly, 2013). Additionally, OA has been reported to impact multiple life stages of corals, including fertilization (Albright and Mason, 2013), larval (Nakamura et al., 2011; Putnam et al., 2013), and settlement (Doropoulos et al., 2012), suggesting strong impacts of OA on corals and coral reef ecosystems.

Meanwhile, more recent studies reported that the responses of marine calcifiers to OA could vary among species and even among populations or individuals within a species (Kroeker et al., 2010; McCulloch et al., 2012). These findings stimulate ideas about acclimatization or adaptation potential of organisms to OA (Pandolfi et al., 2011; Kelly and Hofmann, 2012; Sunday et al., 2014; Vargas et al., 2017). Indeed, some experimental studies demonstrated potential existence of genetic variations (e.g., sea urchins: Sunday et al., 2011) or phenotypic plasticity (e.g., corals: Putnam et al., 2016) to high pCO_2 environment. Additionally, acclimatization by "*trans*-generational plasticity" such that offspring of parents exposed to OA can show higher tolerance to OA have also been indicated (Munday, 2014; Lamare et al., 2016; Thomsen et al., 2017). When the parents of anemone fish were cultured under high pCO_2, it was found that the effects of high pCO_2 were absent or reversed in terms of the survival or size of their juveniles (Miller et al., 2012). Putnam and Gates (2015) studied the *trans*-generational acclimatization potential of the coral *Pocillopora damicornis* to high pCO_2 and temperature conditions, and found that the exposure of coral parents to those conditions may alleviate stress in next-generation larval stages. However, one of the limitations of these studies are that the exposure time of parents to the OA condition is restricted to a limited period of time or life stages (e.g., 1.5 months for the coral *P. damicornis*). Although evolution experiments studying the processes of adaptation to high pCO_2 using short generation organisms such as phytoplankton are now available (Lohbeck et al., 2012), we still lack for understanding multigeneration effects of OA on particularly long-living organisms such as corals (Torda et al., 2017). In this context, organisms living in naturally acidified sites such as on CO_2 vents (Hall-Spencer et al., 2008; Fabricius et al., 2011; Inoue et al., 2013) and sheltered lagoon (Shamberger et al., 2014; Golbuu et al., 2016) can be an ideal model to test adaptation potential and *trans*-generation responses to high pCO_2 (Calosi et al., 2013; Harvey et al., 2016; Welch and Munday, 2017).

Here we focused on the coral *Pocillopora acuta* living in Nikko Bay, Palau, where the seawater shows naturally low pH and high pCO_2 conditions with the aim of testing for the first time if adult and the next-generation larval stages of corals exposed to low pH for their entire life cycle show potential adaptation response to the OA. Seawater pH within Nikko Bay is 0.2–0.3 lower than that outside the bay, which is suggested to be caused by the net decomposition and net calcification by the organisms within the bay (Shamberger et al., 2014; Golbuu et al., 2016; Kurihara et al., unpublished data). The seawater residence time within the bay is also known to exceed 70 days (Golbuu et al., 2016), suggesting that the organisms within the bay may be genetically isolated from outside the bay (e.g., vermetid *Cerasignum maximum*: Soliman et al., 2019). This is likely so for *P. acuta* a brooder species, which releases larvae that mostly settled within 1–2 days (Kopp et al., 2016); they are thus suggested to have less dispersion capacity compared to spawning corals (Isomura and Nishihira, 2001; Nishikawa et al., 2003). This species has recently been identified as a cryptic species of coral *P. damicornis* complex (Schmidt-Roach et al., 2013).

In this study we tested if the adults and the larvae of *P. acuta* originating from the high-CO_2 site within Nikko Bay are more tolerant to high pCO_2 conditions compared to the adult and larvae from the control site outside the bay, respectively. To examine this hypothesis, we first conducted a reciprocal cultivation of larvae released from high-CO_2 and control site corals *P. acuta* under experimental control or high pCO_2 seawater conditions and evaluated their physiology including photosynthesis, respiration, zooxanthella density, chlorophyll-*a* (Chl-*a*) concentration, and lipid content. Additionally, reciprocal transplantation of adult colonies was conducted between the high-CO_2 and control site in the field, to evaluate their fitness by examining survival rate and physiology including calcification, photosynthesis, and respiration rate.

MATERIALS AND METHODS

Coral Collection for Larval Experiment

Five different colonies of the coral *P. acuta* were collected from each of two sites (high-CO_2 and control site, both 4–5 m depth) in Palau on March 15, 2018 that have different seawater pCO_2 concentrations. The high-CO_2 site was within Nikko Bay (7°19′13.2″N, 134°30′00.6″ E) where seawater pCO_2 is naturally high (1,123 μatm/pH 7.77) and represents the value expected by the end of this century (RCP 8.5 IPCC). The control site was outside of Nikko Bay (7°18′15.3″N, 134°30′01.4″ E) where seawater pCO_2 shows normal concentrations (mean±SD: 416 ± 73 μatm/pH 8.15 ± 0.06, n = 3, **Table 1**) equivalent to present conditions (**Table 1**). The high pCO_2 and low pH condition within the bay is suggested to be caused mainly by high dissolved inorganic carbon (DIC) and low alkalinity resulting from net decomposition and net calcification by the organisms within the bay which has a high seawater residence time (Shamberger et al., 2014; Golbuu et al., 2016; Kurihara et al., unpublished data). In addition to seawater pCO_2, the average seawater temperature was also slightly higher (about 1.0°C) and the light intensity significantly lower within Nikko Bay compared to the control site (**Supplementary Figure 1**). The bottom seawater pH and salinity at both sites were measured by casts of a multi-parameter water quality sensor (AAQ-RINKO, JFE Advantech Co., Ltd., Japan). Bottom seawater samples were also collected three times using a Van Don water sampler for the measurement of total alkalinity (TA) and nutrient concentrations. Seawater TA was measured using an auto burette titrator (ATT-05, KIMOTO, Japan) with precision evaluated by analyzing certified reference materials (CRMs) supplied by the A. Dickson laboratory, Scripps Institution of Oceanography. Seawater for nutrient concentration analysis (4 replicates per sampling) was filtered through pre-combusted filters and frozen until measurement using an AACS II (BRAN+LUEBBE,

TABLE 1 | Seawater carbon chemistry and nutrient concentration measured at control and CO_2 site at field where the adult corals for the larval experiment was collected and seawater carbon chemistry during the larval experiments in laboratory.

		Temperature	Salinity	pH (NBS scale)	pCO_2	TA (μmol Kg^{-1})
Field	Control site	29.3 ± 0.3	33.6 ± 0.03	8.15 ± 0.06	416 ± 73	2115 ± 4.5
	CO2 site	30.1 ± 0.4	33.1 ± 0.1	7.77 ± 0.02	1123 ± 83	2069 ± 14
Experiment	Control	29.2 ± 0.7	33.7 ± 0.12	8.09 ± 0.12	504 ± 164	2106 ± 6.5
	CO2	29.3 ± 0.7	33.6 ± 0.16	7.74 ± 0.15	1301 ± 465	2110 ± 7
		NO_3^{2-}+NO_2^-	NH_4^{3+}	PO_4^{3-}	Light intensity	
Field	Control site	0.1 ± 0.05	0.5 ± 0.3	0.03 ± 0.01	336 ± 341	
	CO2 site	0.5 ± 0.2	0.3 ± 0.2	0.07 ± 0.02	71 ± 95	

Seawater pCO2 was calculated by measured temperature, salinity pH (NBS scale) and total alkalinity (TA). Mean ± SD n = 3 for field data and n = 16 for experiment data for carbon chemistry. n = 12 for nutrient analysis.

Table 1). Seawater temperature and light intensity were recorded using temperature data logger (U22-001, HOBO V2, Onset Corp., United States) and light quantum (DEFI-L, JFE Advantech Co., Ltd., Japan) data loggers installed at each site for around 2 weeks (**Supplementary Figure 1**).

Experimental Set-Up for Larval Experiment

After collection, all corals were immediately brought to the Palau International Coral Reef Center (PICRC) and each 5 colonies was placed individually within 10 aquaria (36 × 22 × 26 cm) in which seawater pCO_2 was maintained at the comparable condition as where the corals were collected (control condition: 504 ± 164 μatm/pH 8.09 ± 012; high-CO_2 condition: 1301 ± 465 μatm/pH 7.74 ± 0.15, n = 16) (**Table 1**). Seawater pCO_2 was controlled by bubbling running seawater pumped from the ocean in front of PICRC with air mixed with either CO_2 gas or air only. Flow rates of CO_2 gas and air were controlled by mass flow controllers (SEC-E40, HoribaSTEC, Japan). Seawater pH (NBS scale) and salinity were measured, respectively, using a pH sensor (SenTix 940-3) and salinity sensor (TetraCon 925) connected to a multi-parameter portable meter (WTW Multi 3420, Germany). Seawater was sampled from aquaria for TA measurement and seawater pCO_2 and DIC was calculated using the CO2sys program of Lewis and Wallace (1998).

Coral Larvae

Two days after coral sampling, corals started to release larvae, which peaked on March 20 and 21 and lasted for about 1 week. Coral larvae were collected each day in a plastic container with a plankton mesh side installed at side of each aquaria every night (19:00) such that seawater exiting the aquaria flowed into the containers. Larval collection last for 6 days. The next morning (6:00), all larvae released at the same day from the adult colonies that were collected from the same site condition (control or high-CO_2 site) were pooled, and about each 150 larvae released from control or high-CO_2 site adults were allocated into plastic container (750 ml) filled with the same control or high-CO_2 seawater used for adults. Although we lose the genetical differentiation, larvae released from different colonies were pooled to get enough number of samples for the following measurements. Those larvae that following measurements were conducted the same day the larvae were collected, were designated as the Day 0 sample (2 treatments: larvae released from corals from the control and high-CO_2 sites and reared under the same control or high-CO_2 seawater conditions, respectively). After collecting larvae for Day 0, each 150 larvae released from control and high-CO_2 sites adults were reciprocated into containers (3–4 containers per treatment according to the released number of larvae) containing either control or high-CO_2 seawater and cultured for 5 days, designated as the Day 5 sample (4 treatments: larvae released from coral from the control and high-CO_2 sites and reared, reciprocally, under both control and high-CO_2 seawater conditions, respectively). The same procedure written above was repeated for 6 days using the larvae released from control and high-CO_2 sites adults each day. Seawater within the containers was changed every day and seawater temperatures were controlled by keeping the containers within a running seawater bath. The following measurement were conducted for the Day 0 and Day 5 samples, respectively.

Larval Metabolic Activity

Light photosynthesis and dark respiration rate of the Day 0 and Day 5 larvae samples were measured for all treatments. The symbiotic zooxanthella of pocilloporid corals such as *P. acuta* are known to be transmitted directly from the adult to the larvae (Atoda, 1947). Ten larvae from each treatment were held in air-tight 2 ml glass vials containing pre-filtered control or high-CO_2 seawater. After 20 min acclimatization, oxygen concentrations were measured with a fiber optic oxygen electrode (FIBOX 3, PreSens) for 5 min every 30 min under LED light (83 ± 5 μmol photon m^{-2} s^{-1}) or dark conditions. This measurement was conducted for 9–12 replicates consisting of 10 larvae for each of the 2 and 4 treatments at Day 0 and Day 5, respectively.

Larval Zooxanthella Density and Chlorophyll-*a* Concentration

To evaluate the density of zooxanthella and chlorophyll-*a* (Chl-*a*) concentration in the larvae, each 10 larvae group used for the photosynthesis and respiration rate measurement were pooled into a 1.5 ml microtube, and homogenized with a micro-homogenizer. Thereafter, 150 μl of filtered seawater was added, mixed again and 50 μl of the homogenized sample was used for counting zooxanthellae numbers by a hemocytometer. The

remaining 100 μl sample was filtered through pre-combusted (450°C, 4 h) GF/F glass filters, and Chl-*a* was extracted within a N,N-dimethylformamide (DMF) solutions, and measured using a Trilogy fluorometer (Turner Design) following Holm-Hansen et al. (1965) method.

Adult Zooxanthella Density and Chlorophyll-*a* Concentration

Since we found differences in the zooxanthella density and Chl-*a* concentration in coral larvae from the control and high-CO_2 sites, we also evaluated the density of zooxanthella and Chl-*a* concentration of adult colonies. A piece of an additional 4 colonies of *P. acuta* were sampled from each site after all the larval experiments were complited. After collection, they were immediately brought to PICRC and the tissue from each coral piece was removed using a waterpik and filtered seawater. After homogenizing the seawater containing the coral tissue, the sample was centrifuged three times and zooxanthellae numbers counted using a hemocytometer. Additionally, a known amount of the sample was filtered through pre-combusted (450°C, 4 h) GF/F glass filters, extracted with DMF and Chl-*a* measured using the Trilogy fluorometer. The surface area of each piece was measured using the aluminum foil technique (Marsh, 1970) and the zooxanthella density and Chl-*a* concentration was standardized by surface area.

Larval Dry Weight

To evaluate the larval dry weight, each 20 larvae from Day 0 and Day 5 samples were collected on pre-combusted and pre-weighted GF/F glass filters (450°C, 4 h) from each of the 2 and 4 treatments at Day 0 and Day 5, respectively. Filters were frozen at −80°C and then freeze-dried and weighted, and the weight per larvae was calculated. Each filter with 20 larvae were used as a replicate, and the replicate number per treatment was 4 to 13 (see **Figure 4** for detail).

Larval Lipid

To evaluate the lipid content, 50 larvae from Day 0 and Day 5 samples were collected on pre-combusted and pre-weighted GF/F glass filters (450°C, 4 h) for each of the 2 and 4 treatments at Day 0 and Day 5, respectively. Filters were frozen at −80°C until lipid analysis. Each filter with 50 larvae were used as a replicate, and the numbers of filter replications per treatment was 3 to 6 (see **Figure 5**). All filters were first freeze-dried, weighted and the lipids extracted following Harii et al. (2010). Briefly, lipids were extracted within a 6:4 dichloromethane:methanol solution, and concentrated by removing water with Na_2SO_4 and the amount of extracted lipid weighted. The amount of lipid was calculated as the percentage of lipid per larvae by dividing the extracted lipid weight by the dry weight of 50 larvae and the number of larvae.

Adult Experiment

To evaluate the possibility of any acclimatization or adaptation responses of adult colonies, 10 different colonies of *P. acuta* were collected from the same sites that corals were sampled for larval collection; the high-CO_2 site within Nikko Bay and the control site outside the bay in February 2017. All colonies collected were immediately brought to PICRC, and two nubbins of about 5–7 cm^2 were taken from each colony and glued to plastic screws. Two days later, the buoyant wet weigh of all 40 *P. acuta* nubbins were measured with an electronic balance (0.1 mg precision, HR-200, A&D, Japan) according to Davies (1989). Thereafter, each 20 nubbins (10 nubbins originated from control and 10 nubbins from high-CO_2 sites) were set into a mesh panel (ca. 1 m^2), and the nubbins were reciprocally transplanted back to each of the high-CO_2 and control sites till October 2017. This transplantation period was decided so that the corals experience the two different seasons (dry season: February to May and wet season: July to September) at Palau (Watanabe et al., 2006). Seawater carbon chemistry at each site was measured six times during the transplantation as explained above (**Table 2**).

After 7 months, all nubbins were re-collected, and brought back to PICRC for photosynthesis rate, dark respiration rate and buoyant wet weight measurements. Additionally, seawater from each site was collected to use for the following photosynthesis and respiration rate measurements. Although most coral nubbins were alive, all of the 10 nubbins that were collected at the control site (outside of Nikko Bay) and transplanted to the high-CO_2 site (within Nikko Bay) died, and hence we could not take any measurement for those nubbins.

Photosynthesis and dark respiration were measured in 500 ml air-tight glass chamber with stir bars during the daytime under meta-halide lump (250 μmol photon m^{-2} s^{-1}), and during the nighttime under dark conditions, respectively. Each glass container was filled with the seawater from the same site the corals were retrieved from and submerged within a water bath to control seawater temperatures. Oxygen concentrations were measured with a fiber optic oxygen electrode (FIBOX 3, PreSens) for 1 min every 15 min. After photosynthesis and dark respiration measurement, the buoyant wet weight of all nubbins was measured, and calcification rates were calculated based on the change in dry weight measured before transplantation. All photosynthesis, dark respiration and calcification rates were normalized by surface area.

Statistical Analysis

The larval data measured at Day 0 were analyzed with a student *t*-test between the two sites the parental colonies were collected from (control and high-CO_2 sites). When the data did not meet the assumption of normality, data was analyzed with a Wilcoxon rank test. The larval data measured at Day 5 were analyzed by 2-way ANOVA (Type III was used for all unbalanced designed data) with fixed factors of the site that parental colonies were collected from (control and high-CO_2 site) and the environment larval were cultured under (control and high-CO_2 conditions) and their interactions. For the photosynthesis, dark respiration and calcification rates of adult corals, because we could not get data for the nubbins from the control site transplanted to the high-CO_2 site, data were analyzed with restricted maximum likelihood (REML) with the 3 treatments (from control-transplanted to control, from CO_2-transplanted to CO_2, from CO_2-transplanted to control) as a fixed factor and colonies as a random effect. Variables with significant interactions

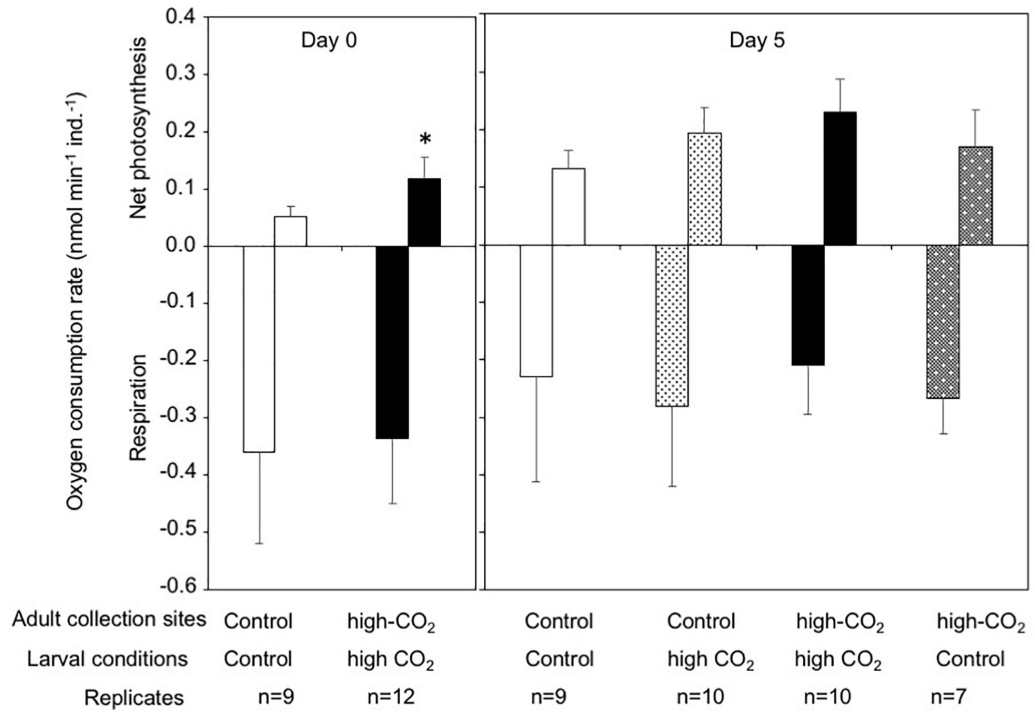

FIGURE 1 | Net photosynthesis and respiration rates of *Pocillopora acuta* larvae released from adults collected at control (white bar) and high-CO_2 sites (black bar) at Day 0, and at Day 5 after larvae from the control site were reared under control (white bar) or high CO_2 (light gray) conditions, and larvae from high-CO_2 site were reared under high CO_2 (black bar) or control (dark gray) conditions. At Day 0, differences among larvae from control and high-CO_2 sites were compared by *t*-test, and asterisk shows significant differences. At Day 5, both net photosynthesis and respiration did not show significant differences among larvae originating from control and high CO_2 parents, or among larvae cultured under control and high CO_2 conditions. The replicate number are shown as *n* in the graph. Average ± SD.

were examined further with Tukey's honest significant differences (HSD) test. Assumptions of normality and variables were tested and transformed for analysis when necessary. Statistical analysis was carried out in R (R.2.7.2).

RESULTS

Larval Experiment

The larval net photosynthesis rate measured at Day 0 just after released from the adults collected at the high-CO_2 site within Nikko Bay was significantly higher than larvae from the control site adults (student *t*-test, $t = -4.7$, $p = 0.0001$, **Figure 1**). Respiration rates were not significantly different among the two larval groups (student *t*-test, $t = -0.4$, $p = 0.69$). After the larvae were reciprocally cultivated at control or high CO_2 seawater for 5 days, photosynthesis rate of the larvae cultured at high-CO_2 was significantly higher than control seawater regardless of the seawater conditions where they originated from [$F_{(1,32)} = 8.68$, $p = 0.005$], with no interaction (**Figure 1** and **Table 3**). Respiration rate did not differ based on origin of the parents, or the culture condition, with no interaction between the two factors [$F_{(1,32)} = 1.65$, $p = 0.20$, **Figure 1** and **Table 3**].

Zooxanthella densities of larvae released from adults originating from the high-CO_2 site were significantly higher compared to larvae from control adults at Day 0 (*t*-test, $t = -3.2$, $p = 0.003$, **Figure 2**). A similar trend was also observed at Day 5, where zooxanthella densities in the larvae originating from high-CO_2 adults were significantly higher compared to larvae from control adults, regardless of the seawater conditions they were cultured under [$F_{(1,36)} = 9.31$, $p = 0.004$], with no interaction [$F_{(1,36)} = 1.86$, $p = 0.18$, **Figure 2** and **Table 3**]. Chl-*a* concentrations did not differ among larvae released from adults originating from control and high-CO_2 sites at Day 0 (Wilcoxon-rank test, $p = 0.09$, **Figure 2**). However, at Day 5, Chl-*a* of the larvae originating from high-CO_2 adults was significantly higher than control larvae [$F_{(1,32)} = 59.9$, $p < 0.001$], with a significant interaction among parent origin and the seawater condition that larvae were cultured under [$F_{(1,32)} = 10.25$, $p = 0.003$, **Table 3**]. The Chl-*a* of larvae released from control adults cultured under high-CO_2 seawater was significantly lower than the other larvae (Tukey's HSD, **Figure 2**). In addition to the larvae, both zooxanthella density (*t*-test, $t = -5.6$, $p = 0.001$) and Chl-*a* (*t*-test, $t = -2.4$, $p = 0.05$) of adult corals originating from the high-CO_2 site were significantly higher than in adults originating from the control site (**Figure 3**).

The dry weight of the larvae released from control adults was significantly higher than the larvae released from high-CO_2 adults at Day 0 (Wilcoxon-rank test, $p = 0.02$, **Figure 4**). However, after 5 days of culture, the dry weight of larvae

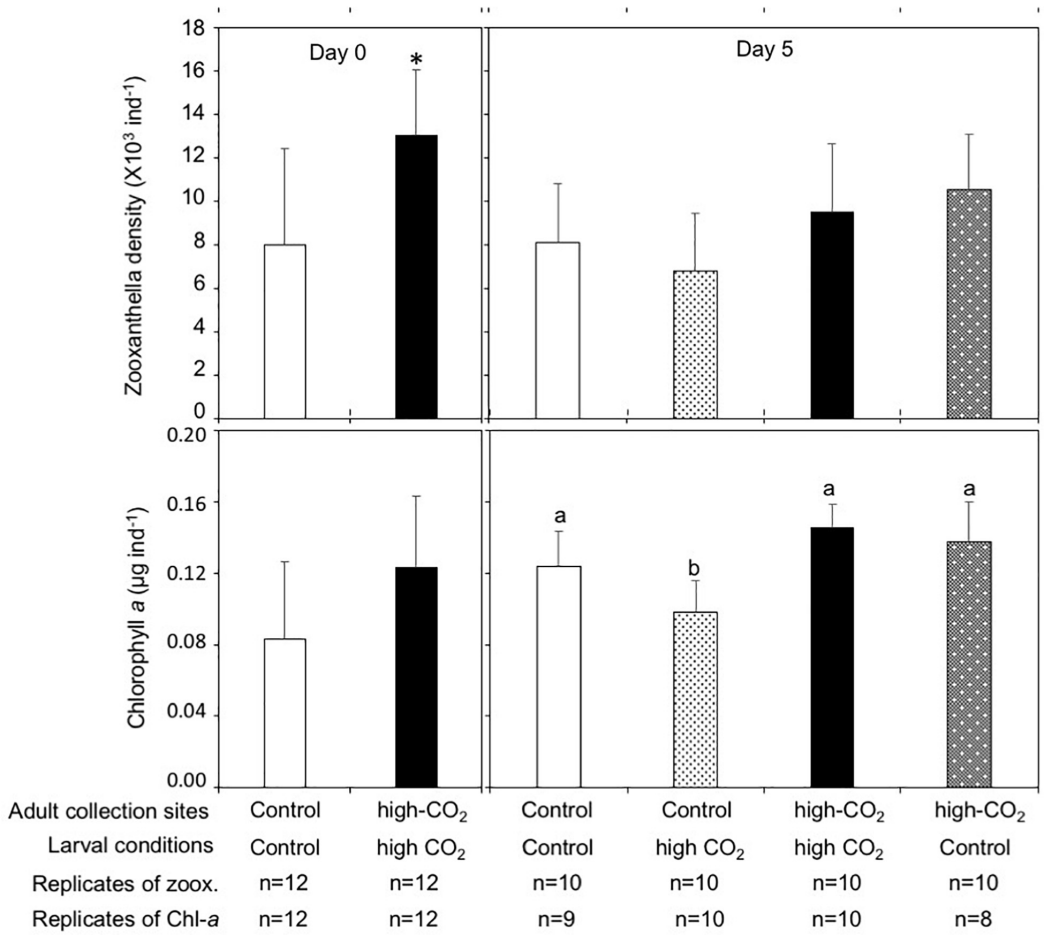

FIGURE 2 | Zooxanthella density and Chl-*a* concentrations in *Pocillopora acuta* larvae released from adults collected at control (white bar) and high-CO_2 (black bar) sites at Day 0, and at Day 5 after being reciprocally reared under control or high CO_2 conditions. At Day 0 differences among larvae from control and high-CO_2 sites were compared by *t*-test and Wilcoxon-test, respectively. Asterisk shows significant differences among control and high CO_2. At Day 5, both zooxanthella density [$F_{(1,36)}$ = 9.31, p = 0.004] and Chl-*a* [$F_{(1,36)}$ = 59.9, $p < 0.001$] of the larvae originating from high CO_2 adults were significantly higher compared to larvae originating from control adults. Additionally, Chl-*a* showed a significant interaction among the parent origin and the seawater condition that larvae were cultured under [$F_{(1,32)}$ = 10.2, p = 0.003, **Table 3**]. Different letters show significant differences among treatment by Tukey's HSD. The replicate number are shown as *n* in the graph. Average ± SD.

did not show any significant differences among parent origin [$F_{(1,18)}$ = 0.23] and the seawater condition that larvae were cultured under [$F_{(1,18)}$ = 0.95, **Figure 4** and **Table 3**]. Lipid concentrations in larvae released from control and high-CO_2 adults did not show any significant differences at Day 0 (*t*-test, t = 0.9, p = 0.39, **Figure 5**). However, after 5 days of culture, the lipid concentration displayed an interaction effect among the origin of adults and the conditions the larvae were cultured under [$F_{(1,17)}$ = 7.74, p = 0.01, **Figure 5** and **Table 3**]. When the larvae released from adults originating from the control site were cultured under high CO_2 seawater, lipid concentrations were significantly lower than when the larvae were cultured under control conditions (Tukey's HSD, **Figure 5**). Meanwhile, larvae released from adult originating from the high-CO_2 site did not show any difference when cultured under control or high-CO_2 seawater.

Adult Experiment

While only one nubbin collected at the control site and transplanted to the control site died, all 10 nubbins derived from each 10 different colonies collected at control site and transplanted to the high-CO_2 site died after 7 months. No nubbins collected from the high-CO_2 site and transplanted to the control or high-CO_2 sites died. Calcification rates for the nubbins collected from the high-CO_2 site and transplanted to their original high-CO_2 site were significantly higher than the nubbins collected from the high-CO_2 site and transplanted to the control site [REML, $F_{(2,18.5)}$ = 4.60, p = 0.02, **Figure 6**]. Additionally, net photosynthesis rates in the nubbins collected from the high-CO_2 site and transplanted to their original high-CO_2 site was significantly higher than the nubbins transplanted to the control site from both the control and high-CO_2 site [REML, $F_{(2,19.1)}$ = 13.56, p = 0.0002, **Figure 6**].

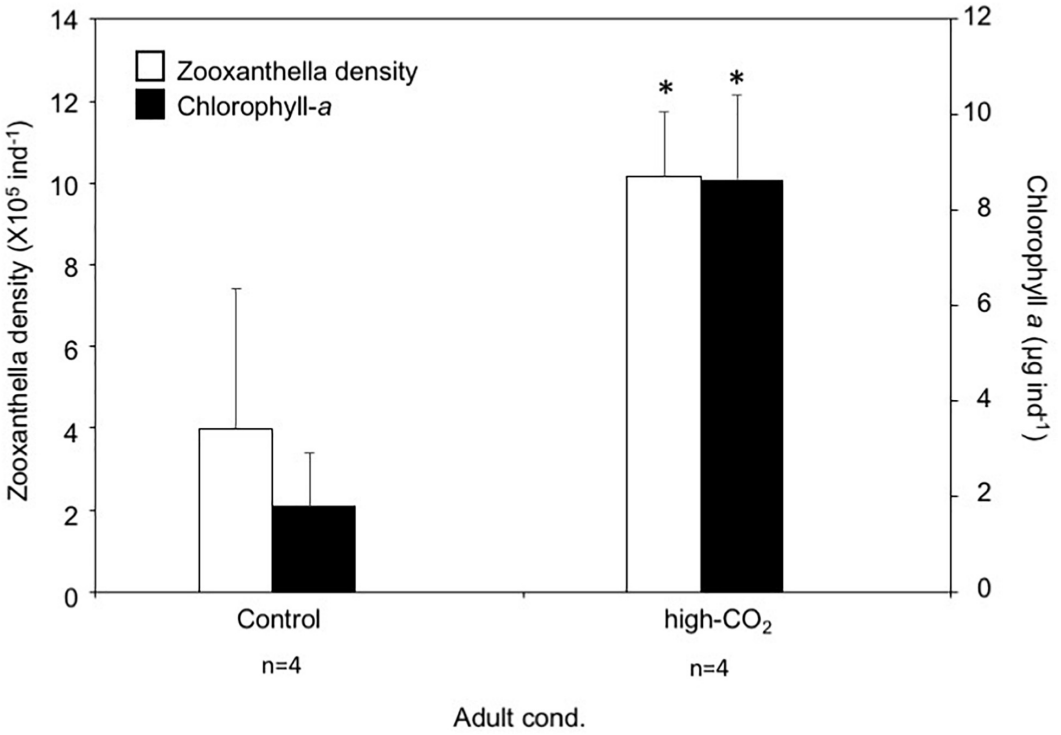

FIGURE 3 | Zooxanthella density and Chl-*a* concentration of *Pocillopora acuta* adults collected at control (white bar) and high-CO_2 (black bar) sites. Asterisks show significant differences among control and high CO_2 adults analyzed by *t*-test. The replicate number are shown as *n* in the graph. Average ± SD.

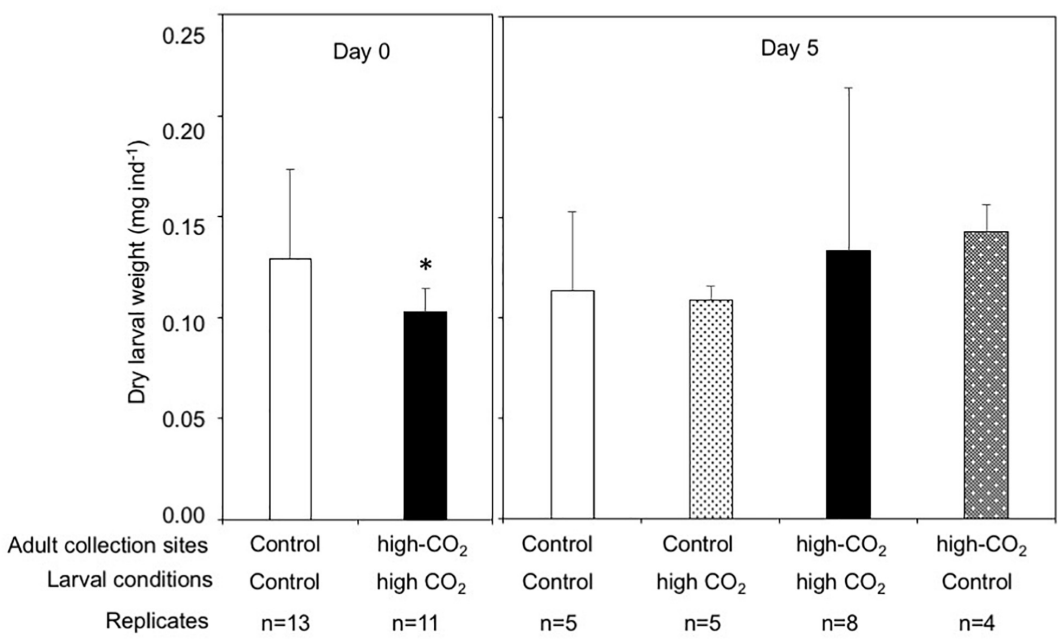

FIGURE 4 | Dry weight of *Pocillopora acuta* larvae released from adult collected at control (white bar) and high-CO_2 (black bar) sites at Day 0, and at Day 5 after being reciprocally reared under control or high CO_2 conditions. At Day 0, differences among larvae from control and high-CO_2 sites were compared by Wilcoxon rank test, and asterisk shows significant differences. At Day 5, dry weight did not show significant differences among larvae originating from control and CO_2 parents, or among larvae cultured at control and CO_2 conditions. The replicate number are shown as *n* in the graph. Average ± SD.

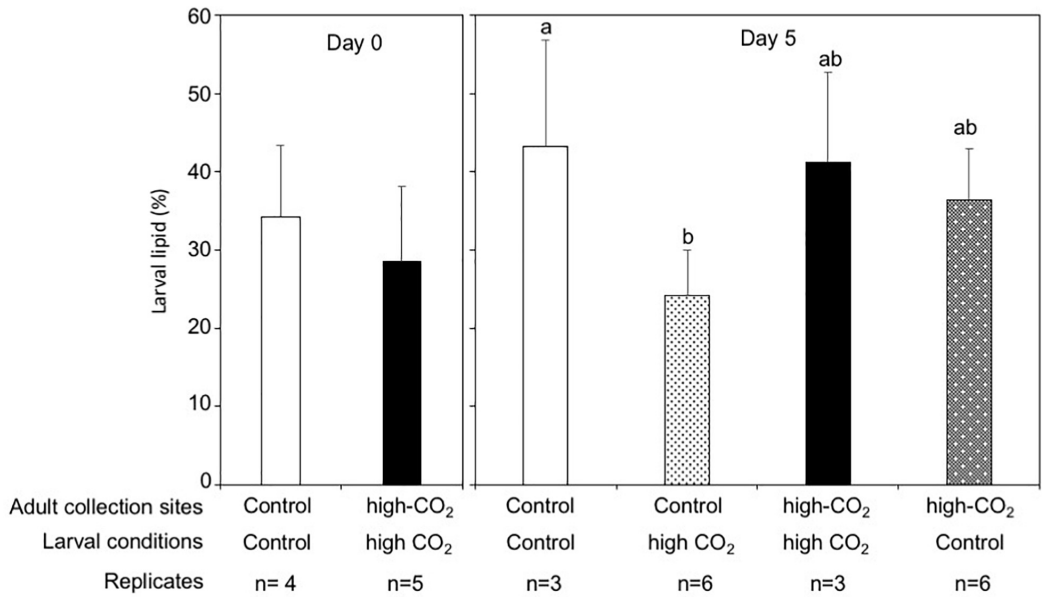

FIGURE 5 | Lipid percentage in *Pocillopora acuta* larvae released from adults collected at control (white bar) and high-CO_2 site (black bar) sites at Day 0, and at Day 5 after being reciprocally reared under control or high CO_2 conditions. At Day 0, differences among larvae from control and high-CO_2 sites were compared by *t*-test. After 5 days of culture, the lipid concentration display an interaction effect among the origin of adult and the condition of seawater the larvae were cultured under [$F_{(1,17)}$ = 7.74, p = 0.01]. Different letters show significant differences among treatment by Tukey's HSD. The replicate number are shown as *n* in the graph. Average ± SD.

TABLE 2 | Seawater carbon chemistry measured at control and CO_2 site at field where the adult corals were reciprocally transplanted for 7 months.

		Temperature	Salinity	pH	*p*CO2	TA (μmol Kg^{-1})
Field	Control site	29.3 ± 0.7	33.5 ± 0.21	8.15 ± 0.04	430 ± 53	2206 ± 23
	CO2 site	30.5 ± 0.6	32.5 ± 0.26	7.79 ± 0.05	886 ± 152	1895 ± 16

Those measurement was conducted for five times. Seawater pCO2 was calculated by measured temperature, salinity pH (NBS scale) and total alkalinity (TA). Mean ± SD n = 6.

DISCUSSION

Although tropical coral reefs provide number of ecological functions and economic values, we still lack information on whether long-living corals have the capacity to show acclimatization or adaptation responses to the environmental change (Torda et al., 2017). Here we first found that adult corals and the next-generation larvae which are potentially exposed for multigeneration to naturally acidified environment show higher fitness under their condition similar to their original sites. These results provide, insights for the potential of corals to acclimatize or adapt to the environmental change including CO_2 conditions.

The *P. acuta* larvae released from adults originating from the high-CO_2 site showed significantly higher photosynthesis rates, which may be due to the higher zooxanthellae density of larvae from the high-CO_2 site compared to those from the control site. Since the adult *P. acuta* colonies originating from the high-CO_2 site also showed higher zooxanthella density compared to the control site colonies, it appears that the amount of zooxanthella in the parent can affect amount transmitted to larvae, suggesting strong parental effects on next generation. Reasons for adult corals from the high-CO_2 site within Nikko Bay showing higher zooxanthellae densities may related to (1) the high seawater pCO_2 concentration, which may enhance primary production, (2) the slightly higher nutrient concentrations (**Table 1**) or (3) the lower light intensity observed within the bay (control site: 336 ± 341 μmol photon m^{-2} s^{-1}, high-CO_2 site: 71 ± 95 μmol photon m^{-2} s^{-1}, **Table 1**, **Supplementary Figure 1**). Previous studies demonstrated increased ammonium concentrations induced proliferation of zooxanthella in both adults (Muller-Parker et al., 1994) and larvae of *P. damicornis* (Gaither and Rowan, 2010). In addition, zooxanthella density has been reported to increase under low light intensity by the increase in the zooxanthella division and decrease in zooxanthella degradation, which has been suggested to be an acclimation strategy of corals to low light environment (Falkowski and Dubinsky, 1981; Stimpson, 1997; Titlyanov et al., 1999). Hence all the above factors can be suggested as reasons for the differences observed in the high-CO_2 adults. For Chl-*a*, although there was no significant differences among control and high-CO_2 larvae at Day 0, after 5 days of culture, the Chl-*a* was significantly lower in larvae originating from the control site

TABLE 3 | Two-way ANOVA table for larval experiments.

		df	*F*	*p*
Net Photosynthesis	Adult	1	2.58	0.11
	Larvae	1	8.68	**0.005**
	Adult×Larvae	1	0.08	0.76
	Error	32		
Dark Respiration	Adult	1	1.62	0.21
	Larvae	1	0.87	0.35
	Adult×Larvae	1	1.65	0.20
	Error	32		
Zooxanthella density	Adult	1	9.31	**0.004**
	Larvae	1	0.71	0.4
	Adult×Larvae	1	1.86	0.18
	Error	36		
Chl-*a*	Adult	1	59.9	**<0.001**
	Larvae	1	1.43	0.23
	Adult×Larvae	1	10.2	**0.003**
	Error	32		
Dry weight	Adult	1	1.50	0.23
	Larvae	1	0.003	0.95
	Adult×Larvae	1	0.02	0.87
	Error	18		
Lipid	Adult	1	7.94	**0.01**
	Larvae	1	0.61	0.44
	Adult×Larvae	1	7.74	**0.01**
	Error	17		

Statistically significant values are shown in bold.

cultured under high-CO_2 conditions, while larvae from the high-CO_2 site did not show any change between control and high-CO_2 conditions. This may suggest that, although larvae from parents living at control corals show some potential stress responses to high pCO_2 seawater, larvae from high-CO_2 corals are able to tolerate a wide range of pCO_2 concentration.

The dry weight of the larvae released from the adults originating from the high-CO_2 site was lower compared to larvae from the control site at the Day 0, suggesting that they were smaller in size or of lower density. Interestingly, the same trend in the production of smaller larval size was observed when the adult of *P. damicornis* adult were culture under high CO_2 and high temperatures for 1.5 months (Putnam and Gates, 2015). Here we measured the dry weight instead of larval size because we found it difficult to measure the swimming larval size correctly, but we expect that the larval dry weight correlates well with their volume. The production of smaller larvae has been suggested to be a potential adaptive plasticity of adults under predictable stressful conditions (Crean and Marshall, 2009; Putnam and Gates, 2015), which can also be the case observed in this study. However, here we did not observe any potential stress responses such as declines of physiological performance in either larvae or adult corals from the high-CO_2 site. Additionally, after 5 days of culture, the dry weight of larvae from all conditions did not show any significant differences, suggesting that the initially low dry weight may not negatively affect the subsequent development of the larvae from the high-CO_2 site. Interestingly, although we were not able to prove statistically because we did not count the number of larvae released per colony, we observed that the summed number of larvae released by the 5 colonies from the high-CO_2 site was larger (total of 1383 larvae from 5 colonies) compared to the control site (total of 875 larvae from 5 colonies, **Figure 7A**). Additionally, same trend was also found for the corals collected on September 2017 (those larvae were not used for the present study) from the same high-CO_2 site (total of 1262 larvae from 5 colonies) compared to the control site (total of 919 larvae from 5 colonies, **Figure 7B**). Although further studies should be conducted before make any firm conclusion, this may suggest that corals from the high-CO_2 site tend to release a larger number of larvae of smaller size compared to the corals at control site, which can be a potential adaptation strategy of the corals living within this high-CO_2 Nikko bay.

Another difference that was found among larvae from the control and high-CO_2 sites was that the larvae from control site cultured under high-CO_2 conditions for 5 days shows significantly lower lipid percentage. Larvae from the high-CO_2 site did not show any differences in lipids among control and high CO_2 conditions. Several studies have indicated that corals may need further energy to compensate for their internal pH when reared under low pH (Cohen and Holocomb, 2009; Allemand et al., 2011; Edmunds, 2011), so excess use of lipid could be expected in larvae from the control site reared under high CO_2. Meanwhile, larvae from the parents originating from the high-CO_2 site seems to be acclimatized or adapted to the high-CO_2 seawater. Larval lipid content has also been suggested to be used as energy for locomotion and mucus secretion (Richmond, 1987; Gaither and Rowan, 2010). Although we did not observe any clear differences in larval locomotion, effects of CO_2 on these biological activities can also be expected (Bergman et al., 2018). In any case, since the lipid content of larvae has been proposed as an important factor affecting the duration of the larval period (Harii et al., 2007), and larvae with larger amounts of lipid may benefit post-settlement by growing faster (Richmond, 1987), larvae from the high-CO_2 site within Nikko Bay are likely to be conferred an advantage compared to larvae from the control site when under high-CO_2 conditions.

In addition to larval responses, reciprocal transplantation of adult corals showed that while all corals originated from Nikko Bay survived when transplanted to either control or high-CO_2 sites at Nikko Bay, *P. acuta* colonies originated from the control site were not able to survive within the bay, suggesting the existence of strong selection within the bay. Though, here we need to take into account the fact that all transplanted corals originated outside and inside the bay were put together at same mesh, there might have other interactive effects that influenced their survival. But, because only the out-side corals transplanted within the bay died, even though the corals originated from out-side and in-side the bay were put randomly at the same mesh, it seem that is more likely that the coral mortality rate was influenced by their origin rather than by the mesh. Additionally, considering the fact that corals within the bay showed higher fitness of

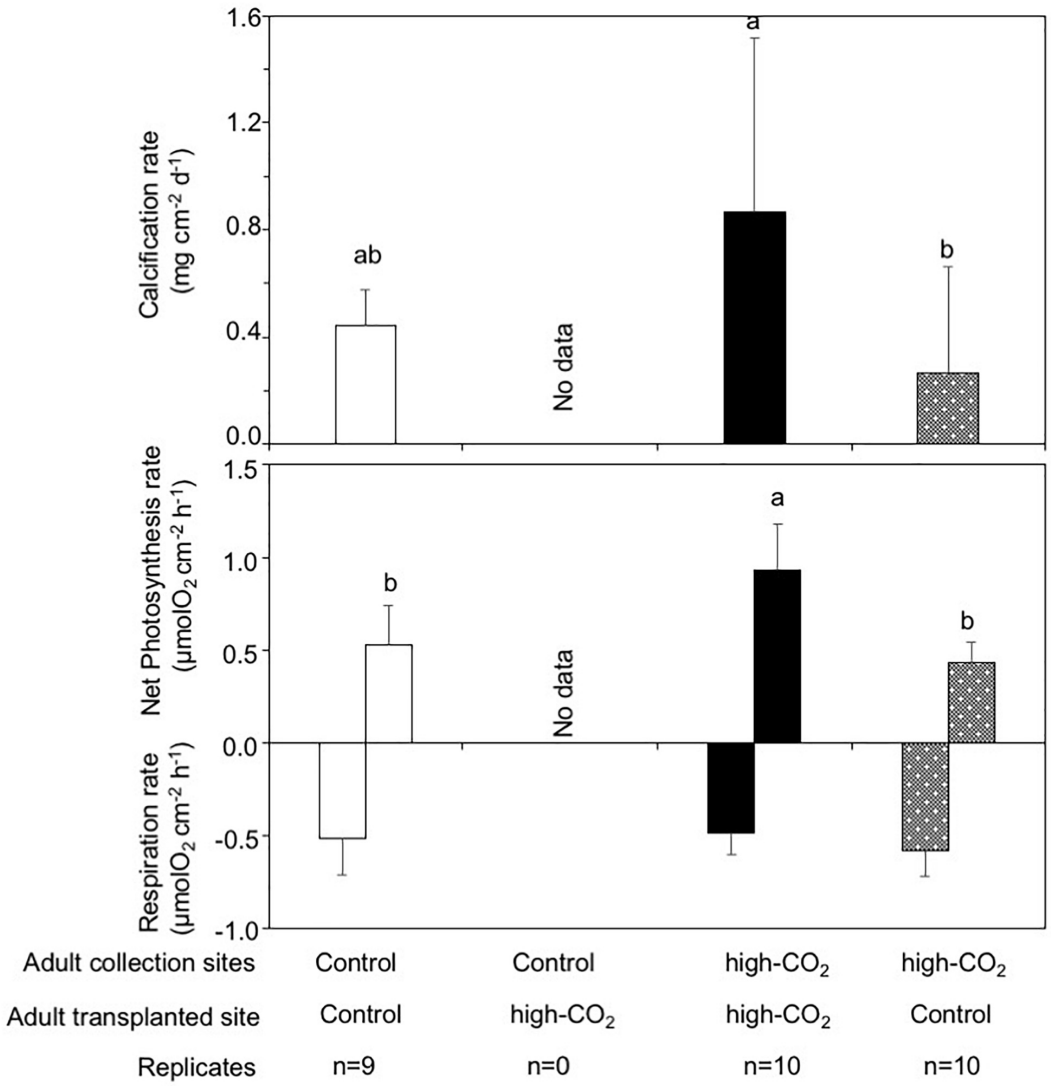

FIGURE 6 | Calcification, net photosynthesis, and respiration of adult corals collected from control and high-CO_2 sites and reciprocally transplanted to control or high-CO_2 site for 7 months. All coral nubbins that were collected from the control site and transplanted to high-CO_2 site died after 7 months. Adult corals collected from the high-CO_2 site and transplanted to their original high-CO_2 site shows significantly higher calcification, net photosynthesis and respiration rates, which are shown by different letters. The replicate number are shown as *n* in the graph. Average ± SD.

high calcification and net photosynthesis rates when exposed to the condition they originated from compared to the control condition, it can be suggested that *P. acuta* living in Nikko Bay are well adapted to the conditions found within the bay. Although we also need to note that not only seawater pCO_2 concentration but also several other conditions, such as light intensity, temperature and nutrient concentrations, all differ between the control site and the high-CO_2 site (**Table 1**). Of particular note, light intensity within the bay was less than half that compared to the control site (**Supplementary Figure 1**), which is mainly due to the higher turbidity (control site: 0.3 ± 0.15 FTU, CO_2 site: 1.8 ± 0.8 FTU). Additionally, seawater temperatures were about 1°C higher within the bay (**Supplementary Figure 1**). Some previous studies indicated that Pocilloporidae corals may have a higher tolerance to high pCO_2 condition compared to other corals such as the Acroporidae (Putnam et al., 2013; Comeau et al., 2014). Hence the low survival of *P. acuta* corals from the control site transplanted into the Nikko Bay may be a response to the synergistic impacts of a range of conditions: high pCO_2, high temperature, and low light. Although we cannot evaluate the genetic mechanisms as here we lack of molecular approaches, Vidal-Dupiol et al. (2013) revealed that several genes related to calcification, heterotrophy and autotrophy were up-regulated in *P. damicornis* adults reared under low pH conditions. Epigenetic phenotypic plasticity to high pCO_2 by DNA methylation has also been found in the coral *P. damicornis* (Putnam et al., 2016) and *Stylophora pistillata* (Liew et al., 2018). Additionally, the

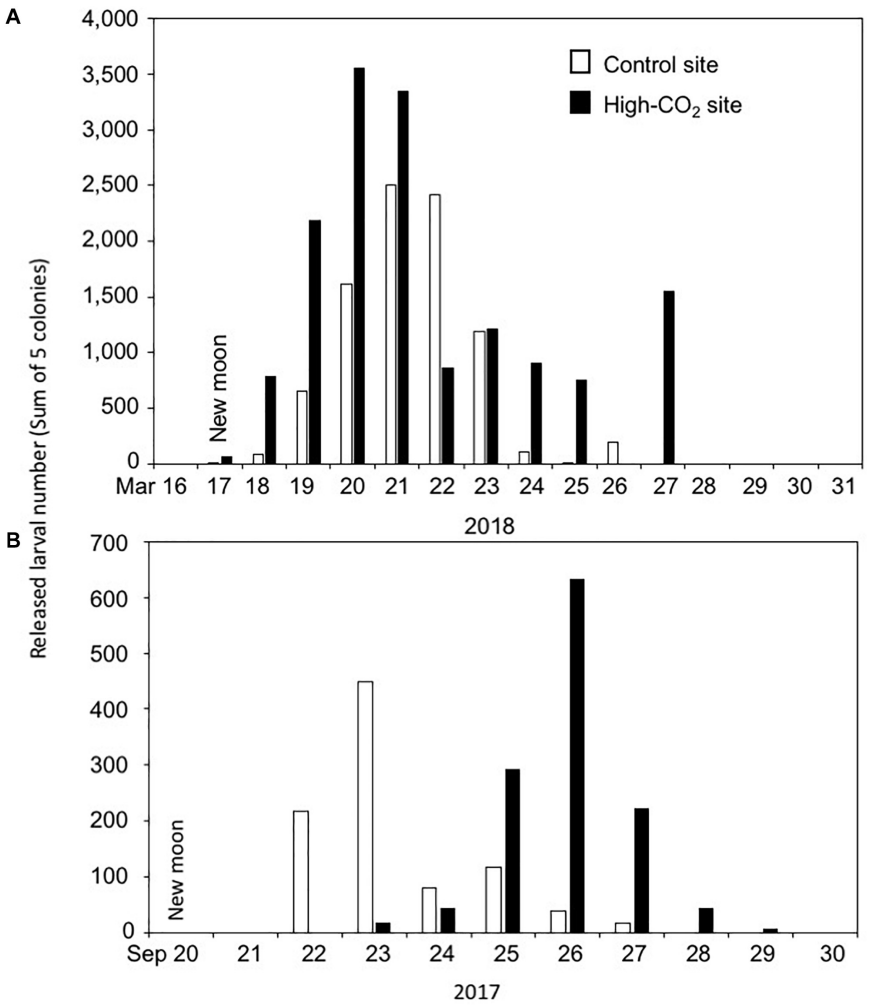

FIGURE 7 | Larval number released each day from the adult corals collected from control and high-CO_2 sites on 2018 **(A)** and 2017 **(B)**. Larval number are the sum of 5 colonies collected from each site. Larvae start to be released around the null moon.

change in expression of several genes in *P. damicornis* larvae reared under OA and high temperature conditions has also been reported (Rivest et al., 2018). Future studies evaluating the potential interactive effects of other environmental factors and the potential genetical differences in corals within the bay are needed for better understanding the mechanisms driving their tolerances.

Although there are several uncertainties, the seawater environmental condition found within Nikko bay has been suggested to be maintained for at least 5000 years (Golbuu et al., 2016). This time period could be long enough for selecting individuals that shows higher fitness to the environmental conditions found within the bay which may have been amplified by the *trans*-generation acclimatization responses. Additionally, gradual change of the environmental condition including seawater pCO_2 found from outside toward the bay (Kurihara et al., unpublished data) may allow the step by step acclimatization of corals to the environment found within the bay. Long-living and high dispersal capacity corals have been suggested to have less capacity of transgenerational epigenetic inheritance to effect rapid phenotypic change to the environmental change (Torda et al., 2017), however, this is one of the first results that indicate the possibility that corals could show local adaptation to high CO_2 and other conditions including high temperature and high turbidity. Though, interpretation of these results should take into account the fact that future OA is expected to occur at whole ocean and at the speed of few decades, the present study gives strong insight for the ability of corals to acclimatize or adapt to different environmental conditions. Future studies evaluating the genetical background of those corals within this bay may give important insights for the potential conservation strategies such as assisted evolution (van Oppen et al., 2017) and understanding the mechanism of organisms to acclimatize and adapt to different environmental conditions, including high pCO_2 seawater concentration.

DATA AVAILABILITY STATEMENT

The raw data supporting the conclusions of this article will be made available by the authors, without undue reservation.

AUTHOR CONTRIBUTIONS

HK designed the study, wrote the draft of the manuscript, and performed the statistical analysis. YS mainly performed the larval experiments. HK and IM performed the adult experiments. All authors contributed to manuscript revision, read, and approved the submitted version.

FUNDING

This work was supported by funding from the Japan Society for the Promotion of Science (JSPS) KAKENHI, grant number: 16H05772, Japan International Cooperation Agency (JICA)-Japan Science and Technology (JST) SATREPS Program, Uruma funding, and Okinawa Research Core for High Innovative Discipline Science Project from the University of the Ryukyus.

ACKNOWLEDGMENTS

We are grateful to all the staff of Palau International Coral Reef Center for their support. We thank Dr. Chuki Hongo for assistances at field works and Dr. Saki Harii for the assistance of lipid measurement.

SUPPLEMENTARY MATERIAL

The Supplementary Material for this article can be found online at: https://www.frontiersin.org/articles/10.3389/fmars.2020.581160/full#supplementary-material

REFERENCES

Albright, R., and Mason, B. (2013). Projected near-future levels of temperature and pCO2 reduce coral fertilization success. *PLoS One* 8:e56468. doi: 10.1371/journal.pone.0056468

Allemand, D., Tambutté, E., Zoccola, D., and Tambutté, S. (2011). "Coral calcification, cells to reefs," in *Coral Reef: An Ecosystem in Transition*, eds Z. Dubinsky and N. Stambler (New York: Springer), 119–150. doi: 10.1007/978-94-007-0114-4_9

Atoda, K. (1947). The larval and postlarval development of some reef-building corals, *Stylophora pistillata* (Esper). *Sci. Rep. Tohoku Univ. Ser.* 4, 48–64.

Bergman, J. L., Harii, S., Kurihara, H., and Edmunds, P. J. (2018). Behavior of brooded coral larvae in response to elevated pCO2. *Font. Mar. Sci.* 5:51.

Calosi, P., Rastrick, S. P. S., Lombardi, C., de Guzman, H. J., Davidson, L., Jahnke, M., et al. (2013). Adaptation and acclimatization to ocean acidification in marine ectotherms: an in situ transplant experiment with polychaetes at a shallow CO2 vent system. *Philos. Trans. R. Soc. Lond. B. Biol. Sci.* 368:20120444. doi: 10.1098/rstb.2012.0444

Chan, N. C. S., and Connolly, S. R. (2013). Sensitivity of coral calcification to ocean acidification: a meta-analysis. *Glob. Change Biol.* 19, 282–290. doi: 10.1111/gcb.12011

Cohen, A., and Holocomb, M. (2009). Why corals care about ocean acidification: uncovering the mechanism. *Oceanography* 22, 118–127. doi: 10.5670/oceanog.2009.102

Comeau, S., Edmunds, N. B., Spindel, N. B., and Carpenter, R. C. (2014). Fast coral reef calcifiers are more sensitive to ocean acidification in short-term laboratory incubations. *Limnol. Oceanogr.* 59, 1081–1091. doi: 10.4319/lo.2014.59.3.1081

Crean, A., and Marshall, D. J. (2009). Coping with environmental uncertainty: dynamic bet hedging as a maternal effect. *Philos. Trans. R. Soc. B* 364, 1087–1096. doi: 10.1098/rstb.2008.0237

Davies, P. S. (1989). Short-term growth measurements of coral using an accurate buoyant weighing technique. *Mar. Biol.* 101, 389–395. doi: 10.1007/bf00428135

Doropoulos, C., Ward, S., Diaz-Pulido, G., Hoegh-Guldburg, O., and Mumby, P. J. (2012). Ocean acidification reduces coral recruitment by disrupting intimate larval-algal settlement interactions. *Ecol. Lett.* 15, 338–346. doi: 10.1111/j.1461-0248.2012.01743.x

Edmunds, P. J. (2011). Zooplanktivory ameliorates the effects of ocean acidification on the reef coral *Porites* spp. *Limnol. Oceanogr.* 23, 2402–2410. doi: 10.4319/lo.2011.56.6.2402

Fabricius, K. E., Langdon, C., Uthicke, S., Humphrey, C., Noonan, S., De'ath, G., et al. (2011). Losers and winners in coral reefs acclimatized to elevated carbon dioxide concentrations. *Nat. Clim. Change* 1, 165–169. doi: 10.1038/nclimate1122

Falkowski, P. G., and Dubinsky, Z. (1981). Light-shade adaptation of *Stylophora pistillata*, a hermatypic coral from the Gulf of Eilat. *Nature* 289, 172–174. doi: 10.1038/289172a0

Gaither, M. R., and Rowan, R. (2010). Zooxanthellar symbiosis in planula larvae of the coral *Pocillopora damicornis*. *J. Exp. Mar. Biol. Ecol.* 386, 45–53. doi: 10.1016/j.jembe.2010.02.003

Golbuu, Y., Gouezo, M., Kurihara, H., Rehm, L., and Wolanski, E. (2016). Long-term isolation and local adaptation in Palau's Nikko Bay help corals thrive in acidic waters. *Coral Reefs* 35, 909–918. doi: 10.1007/s00338-016-1457-5

Hall-Spencer, J. M., Rodolfo-Metalpa, R., Martin, S., Ransome, E., Fine, M., Turner, S. M., et al. (2008). Volcanic carbon dioxide vents show ecosystem effects of ocean acidification. *Nature* 454, 96–99. doi: 10.1038/nature07051

Harii, S., Nadaoka, K., Yamamoto, M., and Iwao, K. (2007). Temporal changes in settlement, lipid content and lipid composition of larvae of the spawning hermatypic coral *Acropora tenuis*. *Mar. Ecol. Prog. Ser.* 346, 89–96. doi: 10.3354/meps07114

Harii, S., Yamamoto, M., and Hoegh-Guldberg, O. (2010). The relative contribution of dinoflagellate photosynthesis and stored lipids to the survivorship of symbiotic larvae of the reef-building corals. *Mar. Biol.* 156, 1215–1224. doi: 10.1007/s00227-010-1401-0

Harvey, B. P., McKeown, N. J., Rastrick, S. P. S., Betoloni, C., Foggo, A., Graham, H., et al. (2016). Individual and population-level responses to ocean acidification. *Sci. Rep.* 6:20194.

Hoegh-Guldberg, O., Mumby, P. J., Hooten, A. J., Steneck, R. S., Greenfield, P., Gomez, E., et al. (2007). Coral reefs under rapid climate change and ocean acidification. *Science* 318, 1737–1742.

Holm-Hansen, O., Lorenzen, C. J., Holmes, R. W., and Strickland, J. D. H. (1965). Fluorometric determination of chlorophyll. *J. Cos. Perm. Int. Explor. Mer.* 30, 3–15. doi: 10.1093/icesjms/30.1.3

Inoue, S., Kayanne, H., Yamamoto, S., and Kurihara, H. (2013). Spatial community shift from hard to soft corals in acidified water. *Nat. Clim. Change* 3, 683–687. doi: 10.1038/nclimate1855

IPCC (2014). "Climate change 2014: synthesis report," in *Proceedings of the Contribution of Working Group I, II and III to the Fifth Assessment Report of the Intergovermental Panel on Climate Change*, (Geneva: IPCC).

Isomura, N., and Nishihira, M. (2001). Size variation of planulae and its effect on the lifetime of planulae in three pocilloporid corals. *Coral Reefs* 20, 309–315. doi: 10.1007/s003380100180

Kelly, M. W., and Hofmann, G. E. (2012). Adaptation and the physiology of ocean acidification. *Funct. Ecol.* 27, 980–990. doi: 10.1111/j.1365-2435.2012.02061.x

Kleypas, J. A., Feely, R. A., Fabry, V. J., Langdon, C., Sabine, C. L., and Robbins, L. L. (2005). *Impacts of Ocean Acidification on Coral Reefs and Other Marine Calcifiers: A Guide for Future Research, Report of a Workshop Held 18-20 April 2005*. St. Petersburg, FL: NSF, NOAA, and the U.S. Geological Survey.

Kopp, C., Domart-Coulon, I., Barthelemy, D., and Meibom, A. (2016). Nutritional input from dinoflagellate symbionts in reef-building corals is minimal during planula larval stage. *Sci. Adv.* 2:e1500681. doi: 10.1126/sciadv.1500681

Kroeker, K. J., Kordas, R. L., Crim, R. N., and Singh, G. G. (2010). Meta-analysis reveals negative yet variable effects of oean acidification on marine organisms. *Ecol. Lett.* 12, 1419–1434. doi: 10.1111/j.1461-0248.2010.01518.x

Lamare, M. D., Liddy, M., and Uthicke, S. (2016). In situ developmental responses of tropical sea urchin larvae to ocean acidification conditions at naturally elevated pCO2 vent sites. *Proc. R. Soc. B* 283:20161506. doi: 10.1098/rspb.2016.1506

Lewis, E., and Wallace, D. (1998). "Program developed for CO_2 system calculations," in *ORNL/CDIAC-105 Carbon Dioxide Information Analysis Center, Oak Ridge National Laboratory* (Oak Ridge, TX: U.S. Department of Energy).

Liew, Y. J., Zoccola, D., Li, Y., Tambutté, E., Venn, A. A., Michell, C. T., et al. (2018). Epigenome-associated phenotypic acclimatization to ocean acidification in a reef-building coral. *Sci. Adv.* 6:eaar8028. doi: 10.1126/sciadv.aar8028

Lohbeck, K. T., Riebesell, U., and Reusch, T. B. H. (2012). Adaptive evolution of a key phytoplankton species to ocean acidification. *Nat. Geosci.* 5, 346–351. doi: 10.1038/ngeo1441

Marsh, J. A. (1970). Primary productivity of reef-building calcacerous red algae. *Ecology* 51, 255–263. doi: 10.2307/1933661

McCulloch, M., Falter, J., Trotter, J., and Montagna, P. (2012). Coral resilience to ocean acidification and global warming through pH up-regulation. *Nat. Clim. Change* 2, 623–627. doi: 10.1038/nclimate1473

Miller, G. M., Watson, S.-A., Donelson, J. M., McCormick, M. I., and Munday, P. L. (2012). Parental environment mediates impacts of increased carbon dioxide on a coral reef fish. *Nat. Clim. Change* 2, 858–861. doi: 10.1038/nclimate1599

Muller-Parker, G., McCloskey, L. R., Hoegh-Gulberg, O., and McAuley, P. J. (1994). Effect of ammonium enrichment on animal and algal biomass of the coral *Pocillopora damicornis*. *Pac. Sci.* 48, 273–283.

Munday, P. L. (2014). Transgeneration acclimation of fishes to climate change and ocean acidification. *F1000Prime Rep.* 6:MC4229724.

Nakamura, M., Ohki, S., Suzuki, A., and Sakai, K. (2011). Coral larvae under ocean acidification: survival, metabolism, and metamorphosis. *PLoS One* 6:e14521. doi: 10.1371/journal.pone.0014521

Nishikawa, A., Katoh, M., and Sakai, K. (2003). Larval settlement rates and gene flow of broadcast spawning (Acropora tenuis) and planula-brooding (*Stylophora pistillata*) corals. *Mar. Ecol. Prog. Ser.* 256, 87–97. doi: 10.3354/meps256087

Pandolfi, J. M., Connolly, S. R., Marshall, D. J., and Cohen, A. L. (2011). Projecting coral reef future under warming and ocean acidification. *Science* 333, 418–422. doi: 10.1126/science.1204794

Putnam, H. M., Davidson, J. M., and Gates, R. D. (2016). Ocean acidification influences host DNA methylation and phenotypic plasticity in environmentally susceptible corals. *Evol. Appl.* 9, 1165–1178. doi: 10.1111/eva.12408

Putnam, H. M., and Gates, R. D. (2015). Preconditioning the reef-building coral Pocillopora damicornis and the potential for trans-generational acclimatization in coral larvae under future climate change conditions. *J. Exp. Biol.* 218, 2365–2372. doi: 10.1242/jeb.123018

Putnam, H. M., Mayfield, A. B., Fan, T. Y., Chen, C. S., and Gates, R. D. (2013). The physiological and molecular responses of larvae from the reef-building coral *Pocillopora damicornis* exposed to near-future increases in temperature and pCO2. *Mar. Biol.* 160, 2157–2173. doi: 10.1007/s00227-012-2129-9

Richmond, R. H. (1987). Energetics, competency, and long-distance dispersal of planulae larvae of the coral *Pocillopora damicornis*. *Mar. Biol.* 93, 527–533. doi: 10.1007/bf00392790

Rivest, E. B., Kelly, M. W., DeBiasse, M. B., and Hofmann, G. E. (2018). Host and symbionts in *Pocillopora damicornis* larvae display different transcriptomic responses to ocean acidification and warming. *Front. Mar. Sci.* 5:186. doi: 10.3389/fmars.2018.00186

Schmidt-Roach, S., Lundgren, P., Miller, K. J., Gerlach, G., Noreen, A. M. E., and Andreakis, N. (2013). Assessing hidden species diversity in the coral *Pocillopora darmicornis* from Eastern Australia. *Coral Reefs* 32, 161–172. doi: 10.1007/s00338-012-0959-z

Shamberger, K. E. F., Cohen, A. L., Golbuu, Y., McCorkle, D. C., Lentz, S. J., and Barley, H. C. (2014). Diverse coral communities in naturally acidified waters of a Western Pacific reef. *Geophys. Res. Lett.* 41, 499–504. doi: 10.1002/2013gl058489

Soliman, T., Fernandez-Silva, I., Kise, H., Kurihara, H., and Reimer, J. D. (2019). Population differentiation across small distances in a coral reef-associated vermetid (*Ceraesignum maximum*) in Palau. *Coral Reefs* 38, 1159–1172. doi: 10.1007/s00338-019-01849-x

Stimpson, J. (1997). The annual cycle of density of zooxanthellae in the tissues of field and laboratory-held *Pocillopora damicornis* (Linnaeus). *J. Exp. Mar. Biol. Ecol.* 214, 35–48. doi: 10.1016/s0022-0981(96)02753-0

Sunday, J. M., Calosi, P., Dupont, S., Munday, P. L., Stillman, J. H., and Reusch, T. B. H. (2014). Evolution in an acidifying ocean. *Trends Ecol. Evol.* 29, 117–125. doi: 10.1016/j.tree.2013.11.001

Sunday, J. M., Crim, R. N., Harley, C. D. G., and Hart, M. W. (2011). Quantifying rates of evolutionary adaptation in response to ocean acidification. *PLoS One* 6:e22881. doi: 10.1371/journal.pone.0022881

Thomsen, J., Stapp, L. S., Haynert, K., Schade, H., Danelli, M., Lannig, G., et al. (2017). Naturally acidified habitat selects for ocean acidified-tolerant mussels. *Sci. Adv.* 3:e1602411. doi: 10.1126/sciadv.1602411

Titlyanov, E. A., Titlyanova, T. V., Tsukahara, J., Van Woesik, R., and Yamazato, K. (1999). Experimental increases of zooxanthellae density in the coral *Stylophora pistillata* elucidate adaptive mechanisms for zooxanthellae regulation. *Symbiosis* 26, 347–362.

Torda, G., Donelson, J. M., Aranda, M., Barshis, D. J., Bay, L., Berumen, M. L., et al. (2017). Rapid adaptive responses to climate change in corals. *Nat. Clim. Change* 7, 627–636. doi: 10.1038/nclimate3374

van Oppen, M. J. H., Gates, R. D., Blackall, L. L., Cantin, N., Chakravarti, L. J., Chan, W. Y., et al. (2017). Shifting paradigms in restoration of the world's coral reefs. *Glob. Change Biol.* 23, 3437–3448.

Vargas, C. A., Lagos, N. A., Lardies, M. A., Duarte, C., Manríquez, P. H., Anguilera, V. M., et al. (2017). Species-specific responses to ocean acidification should account for local adaptation and adaptive plasticity. *Nat. Ecol. Evol.* 1:0084.

Vidal-Dupiol, J., Zoccola, D., Tambutté, E., Grunau, C., Cosseau, C., Smith, K. M., et al. (2013). Genes related to ion-transport and energy production are upregulated in response to CO2-driven pH decrease in corals: new insights from transcriptome analysis. *PLoS One* 8:e58652. doi: 10.1371/journal.pone.0058652

Watanabe, A., Kayanne, H., Hata, H., Kudo, S., Nozaki, K., Kato, K., et al. (2006). Analysis of the seawater CO2 system in the barrier reef-lagoon system of Palau using total alkalinity-dissolved inorganic carbon diagrams. *Limnol. Oceanogr.* 51, 1614–1628. doi: 10.4319/lo.2006.51.4.1614

Welch, M. J., and Munday, P. L. (2017). Heritability of behavioural tolerance to high CO2 in a coral reef fish is masked by nonadaptive phenotypic plasticity. *Evol. Appl.* 10, 682–693. doi: 10.1111/eva.12483

Conflict of Interest: The authors declare that the research was conducted in the absence of any commercial or financial relationships that could be construed as a potential conflict of interest.

frontiers in Marine Science

ORIGINAL RESEARCH
published: 15 January 2021
doi: 10.3389/fmars.2020.600836

Greater Mitochondrial Energy Production Provides Resistance to Ocean Acidification in "Winning" Hermatypic Corals

Sylvain Agostini[1], Fanny Houlbrèque[2], Tom Biscéré[2], Ben P. Harvey[1], Joshua M. Heitzman[1], Risa Takimoto[1], Wataru Yamazaki[1], Marco Milazzo[3] and Riccardo Rodolfo-Metalpa[2]*

[1] Shimoda Marine Research Center, University of Tsukuba, Shimoda, Japan, [2] ENTROPIE, IRD, Université de la Réunion, CNRS, IFREMER, Université de Nouvelle-Calédonie, Nouméa, France, [3] Dipartimento di Scienze della Terra e del Mare, Università Di Palermo, Palermo, Italy

OPEN ACCESS

Edited by:
Peng Jin, University of Guangzhou, China

Reviewed by:
Xiangcheng Yuan, South China Sea Institute of Oceanology (CAS), China
Fiorella Prada, University of Bologna, Italy

***Correspondence:**
Sylvain Agostini
agostini.sylvain@shimoda.tsukuba.ac.jp

Specialty section:
This article was submitted to Global Change and the Future Ocean, a section of the journal Frontiers in Marine Science

Received: *31 August 2020*
Accepted: *23 December 2020*
Published: *15 January 2021*

Citation:
Agostini S, Houlbrèque F, Biscéré T, Harvey BP, Heitzman JM, Takimoto R, Yamazaki W, Milazzo M and Rodolfo-Metalpa R (2021) Greater Mitochondrial Energy Production Provides Resistance to Ocean Acidification in "Winning" Hermatypic Corals. Front. Mar. Sci. 7:600836. doi: 10.3389/fmars.2020.600836

Coral communities around the world are projected to be negatively affected by ocean acidification. Not all coral species will respond in the same manner to rising CO_2 levels. Evidence from naturally acidified areas such as CO_2 seeps have shown that although a few species are resistant to elevated CO_2, most lack sufficient resistance resulting in their decline. This has led to the simple grouping of coral species into "winners" and "losers," but the physiological traits supporting this ecological assessment are yet to be fully understood. Here using CO_2 seeps, in two biogeographically distinct regions, we investigated whether physiological traits related to energy production [mitochondrial electron transport systems (ETSAs) activities] and biomass (protein contents) differed between winning and losing species in order to identify possible physiological traits of resistance to ocean acidification and whether they can be acquired during short-term transplantations. We show that winning species had a lower biomass (protein contents per coral surface area) resulting in a higher potential for energy production (biomass specific ETSA: ETSA per protein contents) compared to losing species. We hypothesize that winning species inherently allocate more energy toward inorganic growth (calcification) compared to somatic (tissue) growth. In contrast, we found that losing species that show a higher biomass under reference pCO_2 experienced a loss in biomass and variable response in area-specific ETSA that did not translate in an increase in biomass-specific ETSA following either short-term (4–5 months) or even life-long acclimation to elevated pCO_2 conditions. Our results suggest that resistance to ocean acidification in corals may not be acquired within a single generation or through the selection of physiologically resistant individuals. This reinforces current evidence suggesting that ocean acidification will reshape coral communities around the world, selecting species that have an inherent resistance to elevated pCO_2.

Keywords: ocean acidification, hermatypic corals, mitochondrial electron transport activity, biomass, resistance

INTRODUCTION

Ocean acidification and ocean warming are threatening the existence of coral reefs. The latest IPCC report warns that if meaningful reductions in CO_2 emissions does not happen soon, 99% of coral reefs could disappear by the end of the century (IPCC, 2018). The effects of ocean warming on hermatypic corals are readily observable with a dramatic increase in the frequency and severity of massive coral bleaching events in recent years (Hughes et al., 2018). Recent studies have shown that ocean acidification has already reduced the community calcification rates of reefs. For instance, Albright et al. (2016) chemically manipulated seawater carbonate chemistry of a section of a reef to attain pre-industrial carbonate concentration and aragonite saturation state levels, increasing reef net calcification by *ca.* 7%. Ultimately ocean acidification may cause some reefs to shift to net dissolution in the near future (Eyre et al., 2018). Hermatypic corals and other calcifying organisms are considered among the most vulnerable to ocean acidification, as the decrease in oceanic pH and carbonate ions concentration makes the precipitation of calcium carbonate (aragonite in the case of corals) more energetically costly (Cohen and Holcomb, 2009).

In hermatypic corals, the calcification process occurs in a semi-isolated space located between the calicoblastic tissue and the already formed skeleton. At this site of calcification, corals elevate the aragonite saturation state by expelling protons, pumping in calcium ions and maintaining a high concentration of carbonates. This tight regulation of the calcifying fluid chemistry allows corals to maintain high calcification rates and for some species to even maintain an elevated saturation state of the calcifying fluid under reduced seawater $\Omega_{aragonite}$ (Holcomb et al., 2014; McCulloch et al., 2017). However, this regulation comes at a cost as the active ion transport required to maintain the elevated pH (Holcomb et al., 2014) and/or calcium ions (DeCarlo et al., 2018) is achieved via the activity of Calcium-ATPase (Zoccola et al., 2004). In addition, bicarbonate ion concentration and the resulting aragonite saturation state are also tightly regulated through the activities of multiple enzymes and ion transporters (Bhattacharya et al., 2016). The energy required for the activity of those enzymes and transporters is produced by the coral host in the form of ATP through the mitochondrial electron transport system (ETSA) and oxidative phosphorylation of the respiration process (Chalker and Taylor, 1975; Galli and Solidoro, 2018).

The dependence of calcification on the capacity of energy (ATP activities) production is supported by the observation of a high number of mitochondria in the calicoblastic tissue (Tambutté et al., 2007), the suppression of light calcification by oxidative phosphorylation inhibitors (Chalker and Taylor, 1975), the expression of the enzymes and transporter involved in calcification which is limited to calicoblastic cells, and the correlation between the ETSA activities with calcification rates in both healthy and bleached corals (Agostini et al., 2013, 2016; Higuchi et al., 2018). Electron transport system activities can be measured by isolating fragmented mitochondrial membranes of the host tissue, and measuring the reduction of an artificial tetrazolium substrate (by the mitochondrial complex II) in the presence of a saturating concentration of the coenzyme NADH (Packard, 1971; Agostini et al., 2013). The transfer of electrons from complex II is deemed to be the slowest reaction in the chain and therefore would limit the following reaction including the production of ATP. Therefore, ETSA can be used to assess the coral potential for energy production (i.e., ATP).

Most studies on the effects of ocean acidification on coral calcification are conducted in laboratories under highly controlled environments and over relatively short timescales (Gattuso et al., 2015). Short experimental durations (days to weeks) do not allow corals to acquire complete acclimation to high pCO_2 conditions and are clearly insufficient for achieving adaptation (multi-generation evolution) or ecological adaptation (selection of resistant species and/or individuals) to these conditions (Riebesell et al., 2010). Natural analogues such as volcanic CO_2 seeps have increasingly been used to complement laboratory experiments (Hall-Spencer et al., 2008), allowing the physiological study of corals that have fully acclimatized to elevated pCO_2 throughout at least their entire post-settlement lives (Noonan et al., 2018). At such natural analogues for future conditions, ocean acidification has drastically decreased the coverage and diversity of corals (Fabricius et al., 2011; Inoue et al., 2013; Enochs et al., 2015; Agostini et al., 2018). Since corals found in the acidified areas of CO_2 seeps are ecologically adapted to the elevated pCO_2 conditions (i.e., capable of surviving), those species for which individuals are found in reasonable numbers have been designated as winning species, while those that are very rare or absent from the elevated pCO_2 areas are the losing species (*sensu* Fabricius et al., 2011).

The dichotomy of a species being either a "winner" or a "loser" may be inappropriate to encapsulate the range of effects of ocean acidification on hermatypic corals, but it has facilitated the distinction between traits that contribute toward the resistance of corals to ocean acidification. Here we present a study using two CO_2 seeps, one located in the coral reefs off the coast of Normanby Island in Papua New Guinea, and the other in the coral communities off the coast of Shikine Island in Japan. The aim of the study was to highlight general physiological traits that distinguished winning species that are resistant to ocean acidification (present in the elevated pCO_2 areas) from losing species that are sensitive to ocean acidification (almost or entirely absent in the elevated pCO_2 areas but common in the control sites at ambient pCO_2). The physiological traits studied were protein contents as a proxy for tissue biomass, and coral host mitochondrial electron transport system activities (ETSA) as a proxy for energy production, either normalized by coral tissue surface area or coral host protein contents. ETSA normalized by tissue surface area (surface area-specific ETSA) represents the potential energy production while ETSA normalized by protein contents of coral tissue (biomass-specific ETSA) represents the biomass specific potential energy production. Three hypotheses were tested (**Figure 1**).

(1) *Inherent physiological traits of coral species resistant to ocean acidification:* Are inherent physiological traits related to biomass and energy production linked with the resistance to ocean acidification? This hypothesis was

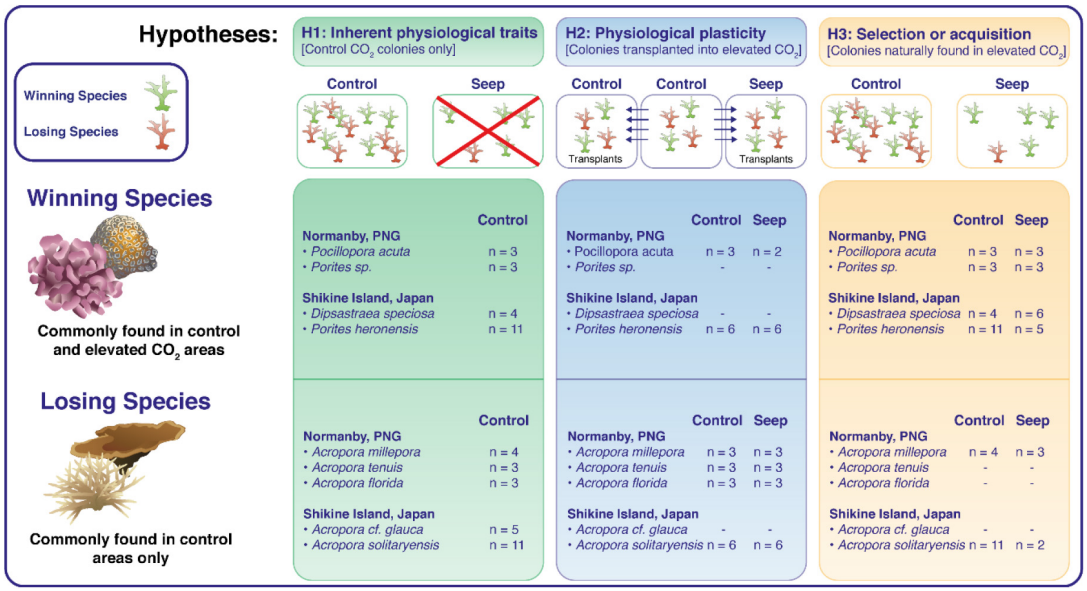

FIGURE 1 | Physiological traits (Protein per surface, surface area-specific ETSA and biomass-specific ETSA) of coral specimens belonging to winning species and losing species were used to test three hypotheses. (1) Inherent physiological traits of coral species resistant to ocean acidification: Physiological traits of corals in control areas; (2) Physiological plasticity as an acclimation response to ocean acidification: Physiological traits of corals transplanted from control areas into control and elevated pCO_2 areas (seep); (3) Selection or acquisition of resistance to ocean acidification: Physiological traits of corals found naturally in both elevated pCO_2 (seep) and control areas (*n* indicates the number of coral specimens used for each species and each CO_2 condition).

tested by measuring traits in individuals sampled in control areas only, thereby excluding potential stress responses and any acclimation/adaptation to elevated pCO_2 conditions.

(2) *Physiological plasticity as an acclimation response to ocean acidification:* Can resistance to ocean acidification be acquired over a short timescale (4–5 months) *via* physiological plasticity? This was tested by conducting transplantation experiments of winning and losing coral species from the control areas to the same control areas, and from the control areas to the elevated pCO_2 areas.

(3) *Selection or acquisition of resistance to ocean acidification:* Can the physiological traits required to tolerate ocean acidification be acquired either during the lifetime of individuals or through the selection of resistant individuals? This was tested by assessing the changes in protein contents and ETSA of winning and losing species that are naturally found in both the elevated pCO_2 areas and nearby (non-acidified) control areas.

MATERIALS AND METHODS

Sampling Sites

The study was conducted at two well-known CO_2 seeps. Previous studies at these two sites showed that the main driver of the difference in benthic communities between control and elevated pCO_2 sites was the increase in pCO_2. No difference in depth, total alkalinity, and temperature were found between sites (Uthicke and Fabricius, 2012; Fabricius et al., 2014; Agostini et al., 2018; Harvey et al., 2019; Witkowski et al., 2019; Cattano et al., 2020). At both seeps, the released gas is composed of more than 97% CO_2 with minimal concentrations in toxic gas such as hydrogen (Fabricius et al., 2011; Agostini et al., 2015). The first seep is located on the coast of Normanby Island in Papua New Guinea, and it has been extensively described in Fabricius et al. (2011) and following papers. The control area close to the CO_2 seep is a well-developed fringing reef showing a high diversity and coverage of corals. This control site experienced pH_T (mean ± SD) of 7.96 ± 0.03, corresponding to a pCO_2 of 468 ± 37 ppm and $\Omega_{aragonite}$ of 3.25 ± 0.17. In comparison, only few species of corals were found in the elevated pCO_2 area, with the coral community clearly dominated by massive *Porites* spp., although a few massive or sub-massive Favids, and a few branching corals of different species were present where space was available. The carbonate chemistry at this elevated pCO_2 area was: pH_T (mean ± SD) 7.66 ± 0.22, corresponding to a pCO_2 of 1,429 ± 1,027 ppm and $\Omega_{aragonite}$ of 1.83 ± 0.69. The second seep system used in this study is located off the shore of Shikine Island in Japan which was first described in Agostini et al. (2015, 2018) and following papers. Situated at a latitude of 34°N, this site is at the transition between sub-tropical and temperate zones. Due to the oceanographic context of the region, waters off Shikine Island show low CO_2 concentrations with pCO_2 often dropping down to 300 ppm. Large tabular Acroporids, sub-massive and encrusting corals (e.g., Favids and Porites) inhabit the control areas of these warm temperate reefs. In contrast, the area close to the seeps shows a very low abundance of corals and an ecosystem mostly dominated by turf algae (Harvey et al., 2019). There, the only corals recorded are a few small colonies of *Porites heronensis*, *Dipsastraea speciosa* and two small colonies of *Acropora solitaryensis*. This

area close to the seeps, hereafter "elevated pCO_2 area" has the following carbonate chemistry conditions: pH_T (mean ± SD) of 7.81 ± 0.09 corresponding to a pCO_2 of 769 ± 225 ppm and a $\Omega_{aragonite}$ of 1.76 ± 0.28. In contrast, the control areas located in an adjacent bay to the seeps are at ambient seawater carbonate chemistry: pH_T (mean ± SD) of 8.14 ± 0.06, pCO_2 of 309 ± 46 ppm and $\Omega_{aragonite}$ of 3.30 ± 0.35 (Harvey et al., 2018). Coral sampling and transplantation were conducted at both the Normanby and Shikine study sites, and in both the elevated pCO_2 and control areas.

Coral Samples

A total of 107 coral samples across 12 species were used, with 47 (across 7 species) sampled in Papua New Guinea under CITES permit 016132, and 60 (across 5 species) sampled in Shikine Island under permit Tokyo Prefecture 29-12. Fragments (5–10 cm^2 in size) of individual colonies were randomly sampled using chisel and hammer by a SCUBA diver. Care was taken to remove potentially attached algae or fauna. All colonies sampled were healthy and did not show signs of bleaching or tissue necrosis. Each coral species was categorized as a winning species if they were commonly found in the elevated CO_2 zones, or as a losing species if they were commonly found in the control zones but were absent or very rare from the elevated CO_2 zones. Previous literature available on the distribution of coral species for the two locations was also taken into consideration, namely Fabricius et al. (2011) and Agostini et al. (2018) for the Normanby Island and Shikine Island seeps, respectively. **Figure 1** summarizes all the species and coral specimens that were used.

(1) Inherent physiological traits of coral species resistant to ocean acidification: Physiological traits of corals in control areas

For the analyses designed to test hypothesis (1) Inherent physiological traits of coral species resistant to ocean acidification, fragments from colonies of the losing species *Acropora millepora*, *Acropora florida*, and *Acropora tenuis* for the Normanby site, and *Acropora cf glauca* and *Acropora solitaryensis* for the Shikine site, were sampled from the control areas. These were compared to traits measured on specimens from winning species sampled always at the control areas, *Pocillopora acuta* and massive *Porites* spp. for the Normanby site and *Dipsastrea speciosa* and *Porites heronensis* for the Shikine site.

(2) Physiological plasticity as an acclimation response to ocean acidification: Physiological Traits of corals transplanted from control areas into control and elevated pCO_2 areas

To test hypothesis 2, we transplanted corals from the control areas into the elevated CO_2 areas as well as into the same control site, the latter to test for transplantation effects. In Normanby, three losing species: *A. millepora* (control n = 4 and elevated pCO_2 n = 3), *A. tenuis* (control n = 3 and elevated pCO_2 n = 3), *A. florida* (control: n = 3 and elevated pCO_2 n = 3), and one winning species: *P. acuta* (control n = 3 and elevated pCO_2 n = 2), were transplanted from the 1st October 2016 to the 23rd January 2017. At the Shikine site, 12 individuals from the losing species *A. solitaryensis* and 12 individuals from the winning species *P. heronensis* were transplanted from the 22nd February 2018 to the 19th July 2018 into each site (n = 6 at each site for each species). Large fragments (>10 cm^2 in surface area) of healthy colonies of the various species were haphazardly sampled from the control areas using chisel and hammer, avoiding the base of the colonies and parts with clearly visible lesions. The fragments were glued to PVC tiles using epoxy glue and randomly attached to metallic grids (90 × 60 cm) that were fixed 10–20 cm above the seabed using metallic anchors at a depth of 3–6 m at the respective sites. In Normanby, the samples were collected and immediately transplanted. In Shikine, the transplantation field setup was done 1 month after sampling the coral fragments. During that month, the fragments were allowed to recover from the sampling in outdoor aquarium with running seawater at the Shimoda Marine Research Center, University of Tsukuba, Japan. At the end of the transplantation period, coral fragments were retrieved and measured on board the research vessels.

(3) Selection or acquisition of resistance to ocean acidification: Physiological traits of corals found naturally in both elevated pCO_2 and control areas

For the analyses designed to test hypothesis 3, we compared the physiological traits of winning and losing species where colonies could be found in both the control and elevated pCO_2 area. Although winning species could be found and collected easily in both areas (*P. acuta*, massive *Porites* spp. at the Normanby site, and *D. speciosa* and *P. heronensis* at the Shikine site), only the losing species *A. millepora* (Normanby site) and *A. solitaryensis* (Shikine site) could be collected in both areas. Physiological traits of the specimens found in control and elevated pCO_2 areas were compared. In addition, the traits of the specimens naturally found in the elevated pCO_2 area were compared to the traits of corals transplanted from the control areas to the elevated pCO_2 areas during the transplantation experiment.

ETSA and Protein Measurements Methods

The sampled fragments of colonies were immediately treated after collection, either aboard the M/B Chertan in Normanby, or at the Shikine Island Field Station (Shimoda Marine Research Center, University of Tsukuba) on Shikine Island. Coral tissue was removed using a custom air-gun connected to a source of compressed air in 10 ml of 0.2 μm filtered ice-cold seawater. Symbiodiniacea were pelleted by centrifugation (600 g, 15 min) and the coral host ETSA and protein contents were measured using the supernatant. All steps were conducted on ice to limit the degradation of the mitochondrial ETSAs. ETSA were measured under saturating concentrations of the NADH and NADPH coenzymes, in the presence of the artificial substrate INT ([4-iodophenyl]-3-[4-nitrophenyl]-5-phenyl-2H-tetrazolium chloride), following the protocols detailed in Agostini et al. (2013) with the following modifications. Filtered seawater instead of phosphate buffer saline was used for the blanks and for dissolving the reagents, and ETSA were extracted by placing

1 ml of the tissue slurry supernatant in 1.5 ml microtube in a sonic bath at 100 KHz for 10 min. For protein contents, 1 ml of the supernatant was stored at −20°C until measurement, which was carried out using the Bradford method (Bradford, 1976). Coral surface areas were determined by the wax method (Stimson and Kinzie, 1991).

Statistical Analysis

For all hypotheses the same physiological traits were used as response variables: protein contents (coral surface area normalized protein concentration), surface area-specific ETSA (coral surface area normalized ETSA), and biomass-specific ETSA (ETSA normalized by the host protein contents). For hypothesis 1, we tested for differences in those physiological traits between winning and losing species using a generalized linear mixed model (Gamma, link: identity) with resistance as a fixed effect (two levels: "Winning" and "Losing") and location (two levels: "Shikine," "Normanby") as a random effect in order to account for the associated variability. For hypothesis 2, we assessed the effect of a short-term exposure to elevated pCO_2 (4 months at the Normanby and 5 months at the Shikine seeps) compared to control conditions, for both winning and losing species. This used a generalized linear mixed model (Gamma, link: identity) with resistance (two levels: "Winning" and "Losing") and CO_2 condition (two levels: "Control," "elevated pCO_2") as fixed effects, and species as a random effect.

For hypothesis 3, we tested for the differences in physiological traits for coral specimens found naturally in the elevated pCO_2 areas compared to those found in the control areas, for both winning and losing species. This used a generalized linear mixed model (Gamma, link: identity) with resistance (two levels: "Winning" and "Losing") and CO_2 condition (two levels: "Control," "elevated pCO_2") as fixed effects, and species as a random effect. Finally, the response to elevated pCO_2 observed for coral specimens used in hypothesis 2 ("short exposure") and hypothesis 3 ("life-long exposure") were compared using a generalized linear mixed model (Gamma, link: identity) with resistance (two levels: "Winning" and "Losing") and exposure duration (two levels: "short exposure," "life-long exposure") as fixed effects and species as a random effect. All analysis and visualizations were performed with the R statistical programming languages (R Core Team, 2020) using the RStudio IDE[1] and the following packages: tidyverse (Wickham et al., 2019), ggplot2 (Wickham, 2016, p. 2), rstatix (Kassambara, 2020), patchwork (Pedersen, 2019), and lme4 (Bates et al., 2015). The code and raw data are available at https://gitlab.com/agoremix/oa-resistance.

RESULTS

(1) Inherent physiological traits of coral species resistant to ocean acidification: Physiological traits of corals in control areas

The amount of protein normalized per coral surface area was more than twofold higher in losing species compared to winning species (175 ± 20 and 73 ± 15 μg cm^{-2}, respectively; GLMM, resistance: t-value = 5.510, $p < 0.001$; **Figure 2A** and **Supplementary Tables 1, 2.1**). Mean surface area-specific ETSA was higher for losing species compared to winning species

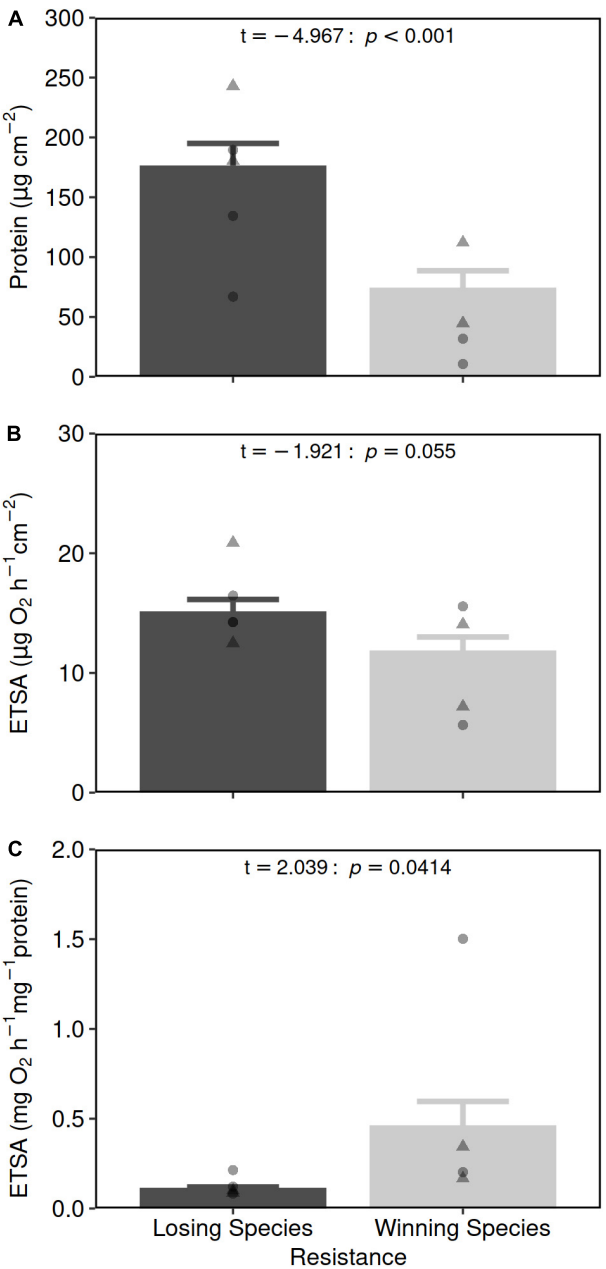

FIGURE 2 | Protein per surface **(A)**, ETSA per coral surface area **(B)** and ETSA per protein contents **(C)** (mean ± SE) in losing (black bars, sensitive to OA, n = 26) and winning coral species (**gray** bars, resistant to OA, n = 21), collected in the control areas. Individual points show the mean value per species with circles for species from the Normanby site and triangles for species from the Shikine site (see **Supplementary Table 1**). Two-way GLMM (Resistance with Location as a random factor) results are presented in the top-right of each panel (see **Supplementary Table 2** for more detailed statistics).

[1]https://rstudio.com/

(15.0 ± 1.1 and 11.8 ± 1.2 μg O_2 h^{-1} cm^{-2}, respectively, **Figure 2B** and **Supplementary Table 1**) but the difference was marginally non-significant (GLMM, resistance: t-value = −1.921, p = 0.055; **Supplementary Table 2.2**). This resulted in the biomass-specific ETSA being fourfold greater in the winning species compared to the losing species (0.46 ± 0.14 and 0.11 ± 0.01 mg O_2 h^{-1} mg^{-1} protein, respectively, GLMM, t-value = 2.039, p = 0.041; **Figure 2C** and **Supplementary Tables 1, 2.3**).

(2) Physiological plasticity as an acclimation response to ocean acidification: Physiological traits of corals transplanted from control areas into control and elevated pCO_2 areas

The four losing species tested (*Acropora millepora*, *Acropora tenuis*, *Acropora florida*, and *Acropora solitaryensis*) on average showed ∼40% decrease in their protein contents (**Figure 3A** and **Supplementary Table 3**) following a 4 or 5 months acclimation to elevated pCO_2 conditions (from 147 ± 17 μg cm^{-2} at the control sites to 87 ± 13 μg cm^{-2} at the elevated pCO_2 sites). The two winning species did not exhibit such a decrease, maintaining their protein contents at 87 ± 17 and 97 ± 15 μg cm^{-2} after transplantation to the control and elevated pCO_2 sites, respectively (GLMM: CO_2 condition x resistance, t-value = 2.064, p = 0.039; **Supplementary Table 4.1**).

The response of surface area-specific ETSA (**Figure 3B** and **Supplementary Table 3**) following a 4–5 months acclimation to elevated pCO_2 conditions showed a similar pattern to protein contents, with losing species showing a decrease in activity (from 13.3 ± 1.4 μg O_2 h^{-1} cm^{-2} at the control areas to 9.6 ± 1.5 μg O_2 h^{-1} cm^{-2} at the elevated pCO_2 areas), and winning species showing relatively little change (10.1 ± 1.5 μg O_2 h^{-1} cm^{-2} at the control sites to 9.2 ± 1.1 μg O_2 h^{-1} cm^{-2} at the elevated pCO_2 sites). The different responses exhibited by winning and losing species following transplantation into elevated pCO_2 conditions resulted in a significant interaction (GLMM: CO_2 condition x resistance, t-value = 811.0, $p < 0.001$; **Supplementary Table 4.2**).

For biomass-specific ETSA (**Figure 3C** and **Supplementary Table 3**), two patterns were observed with either a trend of increasing activity (*Acropora tenuis*, *Acropora florida*, and *Pocillopora acuta*) or remaining at similar levels of activity (*Acropora solitaryensis, Dipsastraea speciosa*, and *Porites heronensis*). However overall there was no significant response following transplantation into elevated pCO_2 conditions, regardless of the resistance of the species (GLMM: CO_2 condition, t-value = 1.747, p = 0.081; resistance, t-value = 0.393, p = 0.695; CO_2 condition × resistance, t-value = −0.573, p = 0.567; **Supplementary Table 4.3**).

(3) Selection or acquisition of resistance to ocean acidification: Physiological traits of corals found naturally in both elevated pCO_2 and control areas

For those coral specimens found naturally, only the losing species showed a difference in the amount of protein per surface area between control and elevated pCO_2 areas (**Figure 4A** and **Supplementary Table 5**). The mean amount of protein for those specimens collected at the elevated pCO_2 areas (86 ± 12 μg cm^{-2}) was half that of the specimens collected at the control areas (183 ± 26 μg cm^{-2}). This decrease was consistent for the two losing species tested: *A. millepora* and *A. solitaryensis*, at the Normanby and Shikine CO_2 seeps, respectively. The

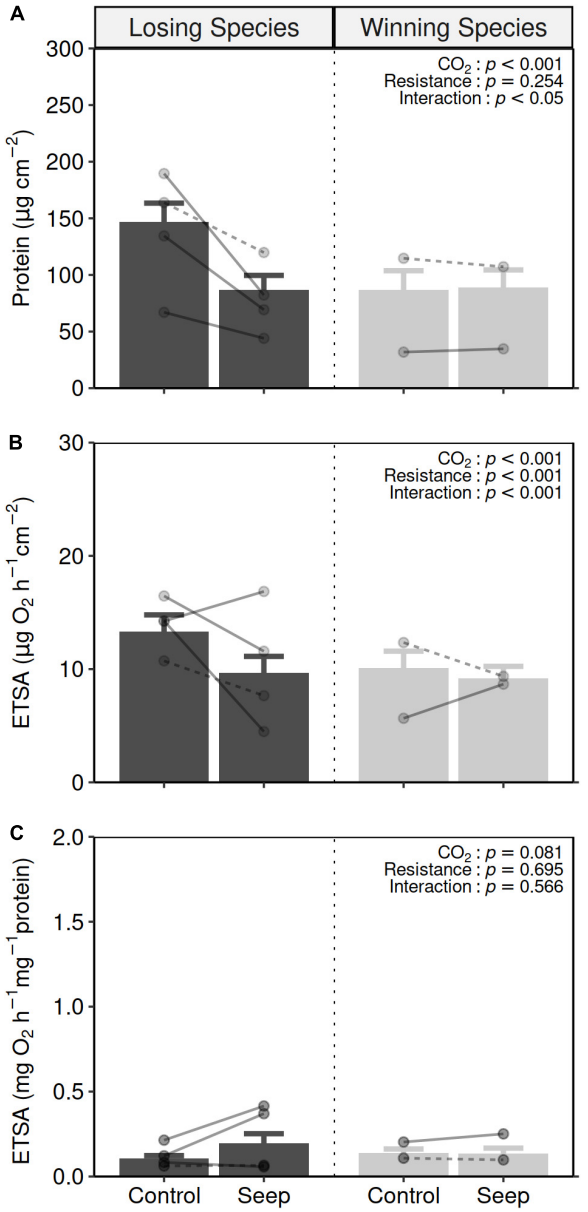

FIGURE 3 | Mean (±SE) protein per surface **(A)**, ETSA per coral surface area **(B)** and ETSA per protein contents **(C)** in losing species (black bars), and winning species (gray bars) specimens transplanted from the control areas to the control areas (control) and elevated pCO_2 areas (seep) for 4–5 months (losing species specimens: control n = 14, seep n = 5; winning species specimens: control n = 20, seep = 16). Points and lines show the mean and response per species with dashed and plain lines representing species from Shikine and Normanby CO_2 seeps, respectively (see **Supplementary Table 3**). Two-way GLMM: CO_2 condition x resistance with Species as a random factor) results are presented in the top-right of each panel (see **Supplementary Table 4** for more detailed statistics).

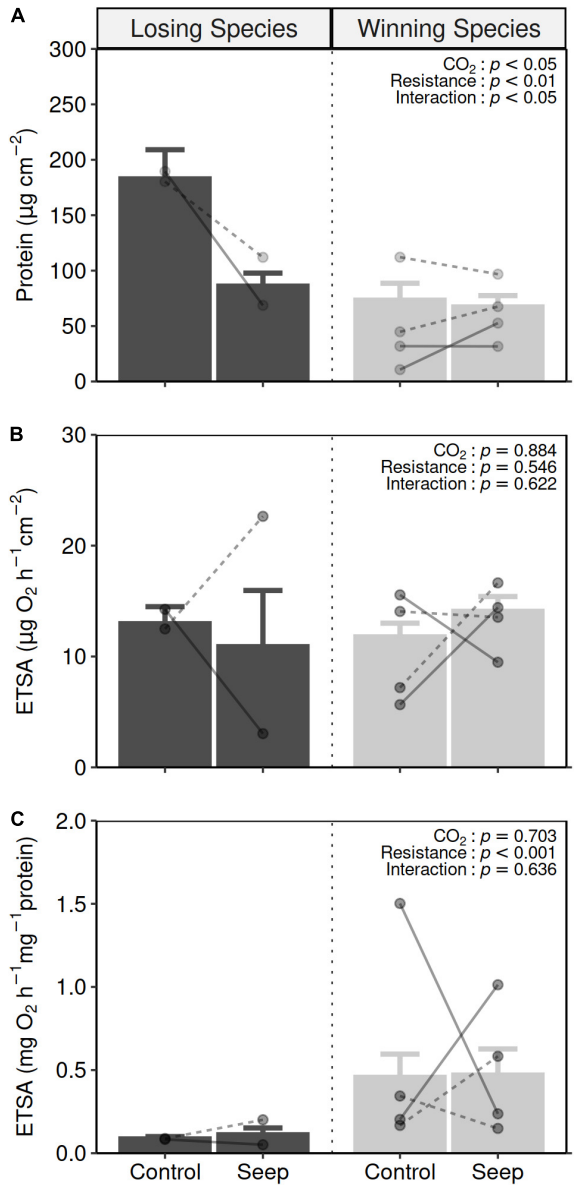

FIGURE 4 | Mean (±SE) protein per surface **(A)**, ETSA per coral surface area **(B)** and ETSA per protein contents **(C)** in losing species (black bars) and winning species (gray bars) species sampled at the control areas (control) and elevated pCO_2 areas (seep) (losing species specimens: control $n = 14$, seep $n = 5$; winning species specimens: control $n = 20$, seep $= 16$). Points and lines show the mean and response per species with dashed and plain lines representing species from Shikine and Normanby sites, respectively (see **Supplementary Table 5**). Two-way GLMM (CO_2 condition x resistance with Species as a random factor) results are presented in the top-right of each panel (see **Supplementary Table 6** for more detailed statistics).

mean amount of protein for winning species remained the same between specimens collected at the elevated pCO_2 and control areas (GLMM, CO_2 condition x resistance, t-value = 2.435, $p = 0.015$; **Supplementary Table 6.1**).

The response of ETSA in coral specimens exposed to life-long elevated pCO_2 conditions varied greatly among species. The amount of surface area-specific ETSA (**Figure 4B** and **Supplementary Table 5**) did not differ between specimens sampled in either control or elevated pCO_2 areas (GLMM, CO_2 condition: t-value = −0.146, $p = 0.884$) for both the winning nor losing coral species (GLMM, resistance: t-value = −0.603, $p = 0.546$) with no significant interaction (CO_2 condition x resistance: t-value = 0.493, $p = 0.622$; **Supplementary Table 6.2**). Biomass-specific ETSA (**Figure 4C** and **Supplementary Table 5**) were five times higher in the winning species (0.46 ± 0.14 mg O_2 h^{-1} mg^{-1} protein) compared to the losing species (0.093 ± 0.014 mg O_2 h^{-1} mg^{-1} protein) (GLMM, resistance, t-value = 3.519, $p = 0.0004$) but did not differ between CO_2 conditions for neither winning or losing species (GLMM, CO_2 condition: t-value = 0.381, $p = 0.703$; CO_2 condition x resistance: t-value = −0.473, $p = 0.636$; **Supplementary Table 6.1**).

The response to life-long exposure to elevated pCO_2 (hypothesis 3) was consistent with the response observed during the transplantation of specimens from control areas to elevated pCO_2 areas (hypothesis 2) (**Supplementary Tables 3, 5** and **Supplementary Figure 1**). No significant differences were observed in the response of coral specimens to the different periods of exposure to elevated pCO_2 for the mean amount of protein (GLMM, Exposure Condition, t-value = 0.685, $p = 0.4936$; **Supplementary Figure 1A** and **Supplementary Table 7.1**), surface area-specific ETSA (GLMM, Exposure Condition, t-value = −1.400, $p = 0.1615$; **Supplementary Figure 1A** and **Supplementary Table 7.2**), or biomass-specific ETSA (GLMM, Exposure Condition, t-value = −0.433, $p = 0.665$; **Supplementary Figure 1A** and **Supplementary Table 7.3**), in either losing or winning species (no significant interactions; GLMM, $p > 0.05$; **Supplementary Tables 5, 7**).

DISCUSSION

Climate change and ocean acidification will likely transform coral communities leaving only the most resistant species (Hughes et al., 2018) and individuals (Matsuda et al., 2020). Natural analogues such as CO_2 seeps can reveal ecological shifts in the composition of coral communities and highlight which physiological traits are associated with a higher resistance to ocean acidification. Here we found that resistant winning species had a lower biomass per coral surface area compared to losing species, while at similar levels of mitochondrial electron transport activities (ETSA). This resulted in a higher ETSA per biomass in the winning species. These traits were interpreted as the capacity of winning species to allocate more energy toward inorganic growth compared to losers which allocate more energy toward somatic growth. These traits are inherent to winning species and were not acquired following exposure to elevated pCO_2 since they were observed in specimens that were found in both the control and elevated pCO_2 areas. This capacity could generally not be acquired by the losing species, whether through physiological plasticity (following 4–5 months or lifelong acclimation to elevated pCO_2 conditions) or through the selection of specimens that show physiological traits associated with resistance to ocean acidification (a high biomass-specific energy production

potential) (see **Figure 5**). The responses following acclimation to elevated pCO_2 differed among species, with some winning species showing changes in their energy allocation depending on the pCO_2 levels they were maintained under. This demonstrates that winning species are still affected by ocean acidification, with their response either corresponding to some acclimation mechanisms that aims to increase their fitness under elevated pCO_2 or a negative impact of ocean acidification on their physiology. This highlights that the dichotomy of "winner" versus "loser" as previously proposed is too restrictive, and while informative, it does not accurately reflect the variety of responses and acclimation strategies of corals to ocean acidification.

A higher biomass or tissue thickness can provide more protection at the site of calcification (Jokiel, 2011; Rodolfo-Metalpa et al., 2011; Strahl et al., 2015; Kline et al., 2019) which allows for a better control of the aragonite saturation state and maintenance of inorganic growth under elevated pCO_2 conditions (Trotter et al., 2011; Holcomb et al., 2014). Individuals that can survive within the naturally acidified environment represent individuals whose physiological traits conferred them with sufficient resistance to ocean acidification as well as being ecologically capable of competing for primary space. In our study, the winning species exhibited a lower biomass in terms of their protein content normalized per coral tissue surface area. For example, despite their imperforated skeleton and low tissue biomass Pocilloporids are considered as resistant to ocean acidification (Comeau et al., 2014). Conversely, the higher protein contents found in losing species suggests that these species may require a larger amount of energy for somatic growth and the maintenance of this biomass (Kaniewska et al., 2015). This suggests that the amount of biomass covering the skeleton does not directly relate to a species' resistance to ocean acidification, instead the costly maintenance of biomass could reduce the ecological fitness of losing species under elevated pCO_2.

The mitochondrial ETSA, which represents the maximum potential rate of the respiratory electron transfer and therefore production of ATP, was similar or even slightly higher (albeit non-significantly) for the losing species compared to winning species when normalized by coral surface area. This finding reinforces the unexpected result that winning coral species do not achieve a greater resistance to ocean acidification through an increased biomass and/or availability of energy. Instead, the lower biomass and similar ETSA per coral surface area resulted in higher ETSA per biomass in the winning species. The resistance of winning coral species to ocean acidification could be linked with a different allocation strategy of energy between inorganic growth and somatic growth, with winning species allocating a greater amount of energy toward inorganic growth. As ocean acidification increases the energetic cost of calcification (Cohen and Holcomb, 2009), a higher energy production potential (ETSA) could allow for a stronger maintenance of the aragonitic saturation state at the site of calcification, enabling the maintenance of inorganic growth even under elevated pCO_2 (McCulloch et al., 2012). This increased energetic potential relative to biomass would additionally support other metabolic processes important for the resistance against ocean acidification, such as high fecundity (Albright, 2011), protein synthesis (Edmunds and Wall, 2014), or the maintenance of other anabolic pathways (Kaniewska et al., 2015).

In the present study, coral species that are sensitive to ocean acidification showed a decrease in their biomass regardless of whether they were acclimatized for 4–5 months or exposed for their entire lifetime to elevated pCO_2. Similar decreases in biomass have been observed across multiple studies (Edmunds and Wall, 2014; Strahl et al., 2015; Wall et al., 2017) with the response attributed to an impairment of protein anabolism due to elevated pCO_2. Two of the losing coral species (*A. florida* and *A. tenuis*) transplanted into the elevated pCO_2 conditions exhibited similar traits to the winning species, which themselves

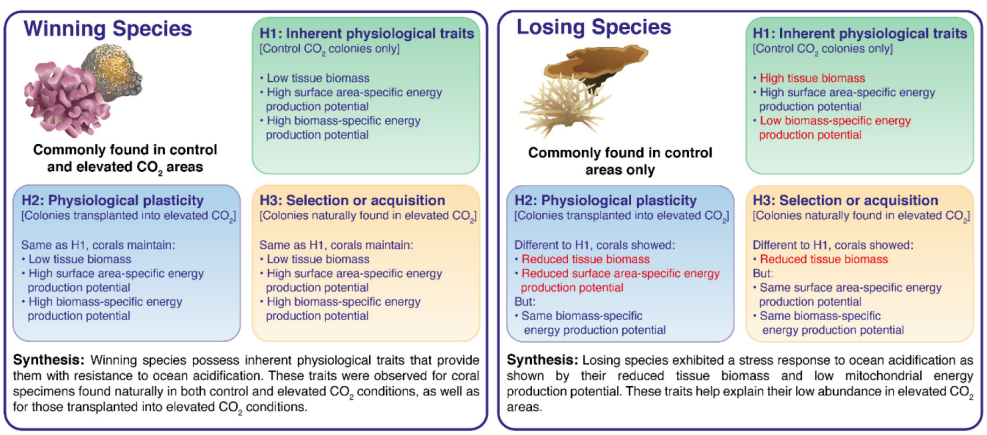

FIGURE 5 | Synthesis and interpretation of the main results for hypothesis (1) Inherent physiological traits of coral species resistant to ocean acidification: Physiological traits of corals in control areas, Hypothesis (2) Physiological plasticity as an acclimation response to ocean acidification: Physiological traits of corals transplanted from control areas into control and elevated pCO_2 areas, and Hypothesis (3) Selection or acquisition of resistance to ocean acidification: Physiological traits of corals found naturally in both elevated pCO_2 and control areas.

were unaffected by the change in pCO_2. This suggests that certain losing species are capable of demonstrating some physiological plasticity related to energy allocation. However this was not observed for the two other species (*A. solitaryensis* and *A. millepora*) tested and this plasticity did not translate into an overall increase in the biomass-specific energy production potential. Our observations support that resistance to ocean acidification cannot be acquired within a single generation (Comeau et al., 2019). Physiological traits of corals transplanted to elevated pCO_2 areas did not differ from those exhibited by corals that were found and sampled in the elevated pCO_2 areas: losing species exhibited a decrease in biomass which did not translate into an increase in biomass-specific energy production potential compared to winning species that were mostly unaffected by the elevated pCO_2. As specimens from losing species are rarely found in the elevated pCO_2 areas as well as often being of smaller size, this suggest that such short-term plasticity through the downregulation of metabolic processes may not be viable in the long term.

Although the different acclimation periods to elevated pCO_2 altered the specific responses of the species, the general patterns observed here were mostly consistent for corals tested in two radically different biogeographic regions, the coral reefs of Papua New Guinea and the marginal warm-temperate coral communities of Japan. The lower aragonite saturation state found in high latitudes suggests that the coral species there could have a higher tolerance to ocean acidification (Kleypas, 1999; Yara et al., 2012). However, the parameters tested in our study did not reveal a remarkable difference in terms of energy allocation between tropical and temperate coral species. This suggest that other traits, either physiological or ecological, may contribute toward the resistance to ocean acidification.

The importance of calcification and somatic growth in determining the resistance of scleractinian corals to ocean acidification remains poorly understood. Our findings suggest that species resistant to ocean acidification have a lower maintenance cost for biomass compared to more sensitive species. This could allow for more energy to be allocated toward inorganic growth providing them with an ecological advantage under high CO_2. The losing species did not exhibit these physiological traits and could not even acquire them through physiological plasticity or the selection of individuals. Instead, losing species exhibit a stress response under elevated pCO_2 whereby their biomass cannot be maintained. Taken together, unless adaptation rapidly occurs, losing species will lack the resistance required to survive future acidification, leaving only those species that possess an inherent resistance to ocean acidification. Such radical selection will likely result in a major loss of diversity and associated functioning in coral communities around the world.

DATA AVAILABILITY STATEMENT

The datasets presented in this study can be found in online repositories. The names of the repository/repositories and accession number(s) can be found below: https://gitlab.com/agoremix/oa-resistance and Zenodo repository (https://doi.org/10.5281/zenodo.4415127).

AUTHOR CONTRIBUTIONS

SA, MM, FH, and RR-M contributed to conception and design of the study. SA, MM, FH, RR-M, and TB conducted the experiment and field survey in Papua New Guinea. SA, BH, RT, JH, and WY conducted the experiment and field survey in Japan. SA wrote the first draft of the manuscript. All authors contributed to manuscript revision, read, and approved the submitted version.

FUNDING

Fieldwork and analyses at the Shikine and Normanby seeps were supported by JSPS KAKENHI Grant in Aids (Grant No: 17K17621), and by the French National Research Agency (ANR, project CARIOCA no. ANR15CE02-0006-01, 2015). We acknowledge funding support from the Ministry of Environment, Government of Japan (Suishinhi: 4RF-1701).

ACKNOWLEDGMENTS

We thank Yasutaka Tsuchiya and the technical staff at Shimoda Marine Research Center and aboard RV Tsukuba II, University of Tsukuba for their assistance and the JF agencies of Izu/Shimoda (Shizuoka prefecture) and Nijima/Shikine Island (Tokyo prefecture) for their support. We are grateful to the local populations of Normanby for the access to their reef, and to the National Research Institute, the Milne Bay Provincial Research Committee, and the Conservation and Environment Protection Authority of Papua New Guinea for permits. This publication contributes toward the International Education and Research Laboratory Program, University of Tsukuba. Images used in **Figures 1** and **5** are courtesy of the Integration and Application Network, University of Maryland Center for Environmental Science (ian.umces.edu/symbols/).

SUPPLEMENTARY MATERIAL

The Supplementary Material for this article can be found online at: https://www.frontiersin.org/articles/10.3389/fmars.2020.600836/full#supplementary-material

REFERENCES

Agostini, S., Fujimura, H., Fujita, K., Suzuki, Y., and Nakano, Y. (2013). Respiratory electron transport system activity in symbiotic corals and its link to calcification. *Aquat. Biol.* 18, 125–139. doi: 10.3354/ab00496

Agostini, S., Fujimura, H., Hayashi, H., and Fujita, K. (2016). Mitochondrial electron transport activity and metabolism of experimentally bleached hermatypic corals. *J. Exper. Mar. Biol. Ecol.* 475, 100–107. doi: 10.1016/j.jembe.2015.11.012

Agostini, S., Harvey, B. P., Wada, S., Kon, K., Milazzo, M., Inaba, K., et al. (2018). Ocean acidification drives community shifts towards simplified non-calcified habitats in a subtropical-temperate transition zone. *Sci. Rep.* 8:11354. doi: 10.1038/s41598-018-29251-29257

Agostini, S., Wada, S., Kon, K., Omori, A., Kohtsuka, H., Fujimura, H., et al. (2015). Geochemistry of two shallow CO_2 seeps in Shikine Island (Japan) and their potential for ocean acidification research. *Reg. Stud. Mar. Sci.* 2, 45–53. doi: 10.1016/j.rsma.2015.07.004

Albright, R. (2011). Reviewing the effects of ocean acidification on sexual reproduction and early life history stages of reef-building corals. *J. Mar. Biol.* 2011:473615. doi: 10.1155/2011/473615

Albright, R., Caldeira, L., Hosfelt, J., Kwiatkowski, L., Maclaren, J. K., Mason, B. M., et al. (2016). Reversal of ocean acidification enhances net coral reef calcification. *Nature* 531, 362–365. doi: 10.1038/nature17155

Bates, D., Mächler, M., Bolker, B., and Walker, S. (2015). Fitting linear mixed-effects models using lme4. *J. Statist. Softw.* 67:104235. doi: 10.18637/jss.v067.i01

Bhattacharya, D., Agrawal, S., Aranda, M., Baumgarten, S., Belcaid, M., Drake, J. L., et al. (2016). Comparative genomics explains the evolutionary success of reef-forming corals. *eLife* 5:e13288. doi: 10.7554/eLife.13288

Bradford, M. (1976). A rapid and sensitive method for the quantitation of microgram quantities of protein utilizing the principle of protein-dye binding. *Analyt. Biochem.* 72, 248–254. doi: 10.1016/0003-2697(76)90527-90523

Cattano, C., Agostini, S., Harvey, B. P., Wada, S., Quattrocchi, F., Turco, G., et al. (2020). Changes in fish communities due to benthic habitat shifts under ocean acidification conditions. *Sci. Total Environ.* 725:138501. doi: 10.1016/j.scitotenv.2020.138501

Chalker, B. E., and Taylor, D. L. (1975). Light-enhanced calcification, and the role of oxidative phosphorylation in calcification of the coral *Acropora cervicornis*. *Proc. R. Soc. B Biol. Sci.* 190, 323–331. doi: 10.1098/rspb.1975.0096

Cohen, A., and Holcomb, M. (2009). Why corals care about ocean acidification: uncovering the mechanism. *Oceanography* 22, 118–127. doi: 10.5670/oceanog.2009.102

Comeau, S., Cornwall, C. E., DeCarlo, T. M., Doo, S. S., Carpenter, R. C., and McCulloch, M. T. (2019). Resistance to ocean acidification in coral reef taxa is not gained by acclimatization. *Nat. Clim. Chang.* 9, 477–483. doi: 10.1038/s41558-019-0486-489

Comeau, S., Edmunds, P. J., Spindel, N. B., and Carpenter, R. C. (2014). Fast coral reef calcifiers are more sensitive to ocean acidification in short-term laboratory incubations. *Limnol. Oceanogr.* 59, 1081–1091. doi: 10.4319/lo.2014.59.3.1081

DeCarlo, T. M., Comeau, S., Cornwall, C. E., and McCulloch, M. T. (2018). Coral resistance to ocean acidification linked to increased calcium at the site of calcification. *Proc. R. Soc. B* 285:20180564. doi: 10.1098/rspb.2018.0564

Edmunds, P. J., and Wall, C. B. (2014). Evidence that high pCO_2 affects protein metabolism in tropical reef corals. *Biol. Bull.* 227, 68–77. doi: 10.1086/BBLv227n1p68

Enochs, I. C., Manzello, D. P., Donham, E. M., Kolodziej, G., Okano, R., Johnston, L., et al. (2015). Shift from coral to macroalgae dominance on a volcanically acidified reef. *Nat. Clim.* 5, 1083–1088. doi: 10.1038/nclimate2758

Eyre, B. D., Cyronak, T., Drupp, P., Carlo, E. H. D., Sachs, J. P., and Andersson, A. J. (2018). Coral reefs will transition to net dissolving before end of century. *Science* 359, 908–911. doi: 10.1126/science.aao1118

Fabricius, K. E., De'ath, G., Noonan, S., and Uthicke, S. (2014). Ecological effects of ocean acidification and habitat complexity on reef-associated macroinvertebrate communities. *Proc. R. Soc. B* 281:20132479. doi: 10.1098/rspb.2013.2479

Fabricius, K. E., Langdon, C., Uthicke, S., Humphrey, C., Noonan, S., De'ath, G., et al. (2011). Losers and winners in coral reefs acclimatized to elevated carbon dioxide concentrations. *Nat. Clim. Chang.* 1, 165–169. doi: 10.1038/nclimate1122

Galli, G., and Solidoro, C. (2018). ATP supply may contribute to light-enhanced calcification in corals more than abiotic mechanisms. *Front. Mar. Sci.* 5:68. doi: 10.3389/fmars.2018.00068

Gattuso, J.-P., Magnan, A., Billé, R., Cheung, W. W. L., Howes, E. L., Joos, F., et al. (2015). Contrasting futures for ocean and society from different anthropogenic CO_2 emissions scenarios. *Science* 349:aac4722. doi: 10.1126/science.aac4722

Hall-Spencer, J. M., Rodolfo-Metalpa, R., Martin, S., Ransome, E., Fine, M., Turner, S. M., et al. (2008). Volcanic carbon dioxide vents show ecosystem effects of ocean acidification. *Nature* 454, 96–99. doi: 10.1038/nature07051

Harvey, B. P., Agostini, S., Kon, K., Wada, S., and Hall-Spencer, J. M. (2019). Diatoms dominate and alter marine food-webs when CO_2 rises. *Diversity* 11:242. doi: 10.3390/d11120242

Harvey, B. P., Agostini, S., Wada, S., Inaba, K., and Hall-Spencer, J. M. (2018). Dissolution: the achilles' heel of the triton shell in an acidifying ocean. *Front. Mar. Sci.* 5:371. doi: 10.3389/fmars.2018.00371

Higuchi, T., Yuyama, I., and Agostini, S. (2018). "Physiology of winter coral bleaching in temperate zone," in *Proceedings of the COAST Symposium*, Bordeaux.

Holcomb, M., Venn, A. A., Tambutté, E., Tambutté, S., Allemand, D., Trotter, J., et al. (2014). Coral calcifying fluid pH dictates response to ocean acidification. *Sci. Rep.* 4:5207. doi: 10.1038/srep05207

Hughes, T. P., Anderson, K. D., Connolly, S. R., Heron, S. F., Kerry, J. T., Lough, J. M., et al. (2018). Spatial and temporal patterns of mass bleaching of corals in the *Anthropocene*. *Science* 359, 80–83. doi: 10.1126/science.aan8048

Inoue, S., Kayanne, H., Yamamoto, S., and Kurihara, H. (2013). Spatial community shift from hard to soft corals in acidified water. *Nat. Clim. Chang.* 3, 683–687. doi: 10.1038/nclimate1855

IPCC (2018). *Global Warming of 1.5°C., eds V. Masson-Delmotte, P. Zhai, H. O. Pörtner, D. Roberts, J. Skea, P.R. Shukla, et al.* Available online at: http://www.ipcc.ch/report/sr15/ (accessed January 18, 2019).

Jokiel, P. L. (2011). The reef coral two compartment proton flux model: a new approach relating tissue-level physiological processes to gross corallum morphology. *J. Exper. Mar. Biol. Ecol.* 409, 1–12. doi: 10.1016/j.jembe.2011.10.008

Kaniewska, P., Chan, C.-K. K., Kline, D., Ling, E. Y. S., Rosic, N., Edwards, D., et al. (2015). Transcriptomic changes in coral holobionts provide insights into physiological challenges of future climate and ocean change. *PLoS One* 10:e0139223. doi: 10.1371/journal.pone.0139223

Kassambara, A. (2020). *rstatix: Pipe-Friendly Framework for Basic Statistical Tests*. Available online at: https://CRAN.R-project.org/package=rstatix (accessed December 31, 2020).

Kleypas, J. A. (1999). Geochemical consequences of increased atmospheric carbon dioxide on coral reefs. *Science* 284, 118–120. doi: 10.1126/science.284.5411.118

Kline, D. I., Teneva, L., Okamoto, D. K., Schneider, K., Caldeira, K., Miard, T., et al. (2019). Living coral tissue slows skeletal dissolution related to ocean acidification. *Nat. Ecol. Evol.* 3, 1438–1444. doi: 10.1038/s41559-019-0988-x

Matsuda, S., Huffmyer, A., Lenz, E. A., Davidson, J., Hancock, J., Przybylowski, A., et al. (2020). Coral bleaching susceptibility is predictive of subsequent mortality within but not between coral species. *Front. Ecol. Evol.* 8:178. doi: 10.3389/fevo.2020.00178

McCulloch, M., Falter, J., Trotter, J., and Montagna, P. (2012). Coral resilience to ocean acidification and global warming through pH up-regulation. *Nat. Clim.* 2, 623–627. doi: 10.1038/nclimate1473

McCulloch, M. T., D'Olivo, J. P., Falter, J., Holcomb, M., and Trotter, J. A. (2017). Coral calcification in a changing world and the interactive dynamics of pH and DIC upregulation. *Nat. Commun.* 8:15686. doi: 10.1038/ncomms15686

Noonan, S. H. C., Kluibenschedl, A., and Fabricius, K. E. (2018). Ocean acidification alters early successional coral reef communities and their rates of community metabolism. *PLoS One* 13:e0197130. doi: 10.1371/journal.pone.0197130

Packard, T. (1971). The measurement of respiratory electron-transport activity in marine phytoplankton. *J. Mar. Res.* 29, 235–244.

Pedersen, T. L. (2019). *patchwork: The Composer of Plots*. Available online at: https://CRAN.R-project.org/package=patchwork (accessed December 31, 2020).

R Core Team (2020). *R: A Language and Environment for Statistical Computing*. Vienna: R Foundation for Statistical Computing.

Riebesell, U., Fabry, V. J., Hansson, L., and Gattuso, J.-P. (2010). *Guide to Best Practices in Ocean Acidification Research and Data Reporting*, eds U. Riebesell, V. J. Fabry, L. Hansson, and J.-P. Gattuso (Luxembourg: Publications Office of the European Union).

Rodolfo-Metalpa, R., Houlbrèque, F., Tambutté, É, Boisson, F., Baggini, C., Patti, F. P., et al. (2011). Coral and mollusc resistance to ocean acidification adversely affected by warming. *Nat. Clim. Chang.* 1, 308–312. doi: 10.1038/nclimate1200

Stimson, J., and Kinzie, R. A. (1991). The temporal pattern and rate of release of zooxanthellae from the reef coral *Pocillopora damicornis* (Linnaeus) under nitrogen-enrichment and control conditions. *J. Exper. Mar. Biol. Ecol.* 153, 63–74. doi: 10.1016/S0022-0981(05)80006-80001

Strahl, J., Stolz, I., Uthicke, S., Vogel, N., Noonan, S. H. C., and Fabricius, K. E. (2015). Physiological and ecological performance differs in four coral taxa at a volcanic carbon dioxide seep. *Compar. Biochem. Physiol. Part A* 184, 179–186. doi: 10.1016/j.cbpa.2015.02.018

Tambutté, E., Allemand, D., Zoccola, D., Meibom, A., Lotto, S., Caminiti, N., et al. (2007). Observations of the tissue-skeleton interface in the scleractinian coral *Stylophora pistillata*. *Coral Reefs* 26, 517–529. doi: 10.1007/s00338-007-0263-265

Trotter, J., Montagna, P., McCulloch, M., Silenzi, S., Reynaud, S., Mortimer, G., et al. (2011). Quantifying the pH 'vital effect' in the temperate zooxanthellate coral *Cladocora caespitosa*: validation of the boron seawater pH proxy. *Earth Planet. Sci. Lett.* 303, 163–173. doi: 10.1016/j.epsl.2011.01.030

Uthicke, S., and Fabricius, K. E. (2012). Productivity gains do not compensate for reduced calcification under near-future ocean acidification in the photosynthetic benthic foraminifer species *Marginopora vertebralis*. *Glob. Chang. Biol.* 18, 2781–2791. doi: 10.1111/j.1365-2486.2012.02715.x

Wall, C. B., Mason, R. A. B., Ellis, W. R., Cunning, R., and Gates, R. D. (2017). Elevated pCO_2 affects tissue biomass composition, but not calcification, in a reef coral under two light regimes. *R. Soc. Open. Sci.* 4:170683. doi: 10.1098/rsos.170683

Wickham, H. (2016). *ggplot2: Elegant Graphics for Data Analysis*, 2nd Edn, New York, NY: Springer-Verlag.

Wickham, H., Averick, M., Bryan, J., Chang, W., McGowan, L., François, R., et al. (2019). Welcome to the Tidyverse. *J. Open Source Softw.* 4:1686. doi: 10.21105/joss.01686

Witkowski, C. R., Agostini, S., Harvey, B. P., Meer, M. T. J., van der Sinninghe Damste, J. S., and Schouten, S. (2019). Validation of carbon isotope fractionation in algal lipids as a pCO_2 proxy using a natural CO_2 seep (Shikine Island, Japan). *Biogeosci. Discuss.* 16, 4451–4461. doi: 10.5194/bg-16-4451-2019

Yara, Y., Vogt, M., Fujii, M., Yamano, H., Hauri, C., Steinacher, M., et al. (2012). Ocean acidification limits temperature-induced poleward expansion of coral habitats around Japan. *Biogeosci. Discuss.* 9, 7165–7196. doi: 10.5194/bgd-9-7165-2012

Zoccola, D., Tambutté, E., Kulhanek, E., Puverel, S., Scimeca, J.-C., Allemand, D., et al. (2004). Molecular cloning and localization of a PMCA P-type calcium ATPase from the coral *Stylophora pistillata*. *Biochim. Biophys. Acta* 1663, 117–126. doi: 10.1016/j.bbamem.2004.02.010

Conflict of Interest: The authors declare that the research was conducted in the absence of any commercial or financial relationships that could be construed as a potential conflict of interest.

frontiers in Marine Science

ORIGINAL RESEARCH
published: 21 January 2021
doi: 10.3389/fmars.2020.588938

Impacts of Acclimation in Warm-Low pH Conditions on the Physiology of the Sea Urchin *Heliocidaris erythrogramma* and Carryover Effects for Juvenile Offspring

*Januar Harianto[1], Joshua Aldridge[2], Sergio A. Torres Gabarda[2], Richard J. Grainger[1] and Maria Byrne[1]**

[1] School of Life and Environmental Sciences, The University of Sydney, Sydney, NSW, Australia, [2] Sydney Institute of Marine Science, Mosman, NSW, Australia

OPEN ACCESS

Edited by:
Jonathan Y. S. Leung, University of Adelaide, Australia

Reviewed by:
Mary A. Sewell, The University of Auckland, New Zealand
Karen Chan, Swarthmore College, United States
Narimane Dorey, UMR8539 Laboratoire de météorologie Dynamique (LMD), France

***Correspondence:**
Maria Byrne
maria.byrne@sydney.edu.au

Specialty section:
This article was submitted to Global Change and the Future Ocean, a section of the journal Frontiers in Marine Science

Received: *29 July 2020*
Accepted: *14 December 2020*
Published: *21 January 2021*

Citation:
Harianto J, Aldridge J, Torres Gabarda SA, Grainger RJ and Byrne M (2021) Impacts of Acclimation in Warm-Low pH Conditions on the Physiology of the Sea Urchin Heliocidaris erythrogramma and Carryover Effects for Juvenile Offspring. Front. Mar. Sci. 7:588938. doi: 10.3389/fmars.2020.588938

Ocean warming (OW) and acidification (OA) affects nearly all aspects of marine organism physiology and it is important to consider both stressors when predicting responses to climate change. We investigated the effects of long-term exposure to OW and OA on the physiology of adults of the sea urchin, *Heliocidaris erythrogramma*, a species resident in the southeast Australia warming hotspot. The urchins were slowly introduced to stressor conditions in the laboratory over a 7-week adjustment period to three temperature (ambient, +2°C, +3°C) and two pH (ambient: pH_T 8.0; −0.4 units: pH_T 7.6) treatments. They were then maintained in a natural pattern of seasonal temperature and photoperiod change, and fixed pH, for 22 weeks. Survival was monitored through week 22 and metabolic rate was measured at 4 and 12 weeks of acclimation, feeding rate and ammonia excretion rate at 12 weeks and assimilation efficiency at 13 weeks. Acclimation to +3°C was deleterious regardless of pH. Mortality from week 6 indicated that recent marine heatwaves are likely to have been deleterious to this species. Acclimation to +2°C did not affect survival. Increased temperature decreased feeding and increased excretion rates, with no effect of acidification. While metabolic rate increased additively with temperature and low pH at week 4, there was no difference between treatments at week 12, indicating physiological acclimation in surviving urchins to stressful conditions. Regardless of treatment, *H. erythrogramma* had a net positive energy budget indicating that the responses were not due to energy limitation. To test for the effect of parental acclimation on offspring responses, the offspring of acclimated urchins were reared to the juvenile stage in OW and OA conditions. Parental acclimation to warming, but not acidification altered juvenile physiology with an increase in metabolic rate. Our results show that incorporation of gradual seasonal environmental change in long-term acclimation can influence outcomes, an important consideration in predicting the consequences of changing climate for marine species.

Keywords: climate change, metabolic rate, scope for growth, ocean acidification, ocean warming, transgeneration, Echinoidea, Echinodermata

INTRODUCTION

Many of the key challenges in predicting the ecological consequences of climate change stem from the fact that organisms are confronted with multiple biotic and abiotic stressors, which often interact (Boyd and Brown, 2015; Przeslawski et al., 2015; Boyd et al., 2017; Goldenberg et al., 2017). The impacts of global warming and ocean acidification are intricately linked as approximately 90% of the Earth's heat and 25% of anthropogenic CO_2 emissions are absorbed directly into the ocean (Gattuso et al., 2015). Further, marine heatwaves (MHW) are a major climate change stress in many regions (Babcock et al., 2019; Holbrook et al., 2019).

Ocean warming (OW) increases the body temperature of marine ectotherms, affecting metabolism and most biological processes (Brown et al., 2004; Somero, 2012). Concurrently, ocean acidification (OA) alters the carbonate saturation states in sea water which may alter the metabolic costs associated with acid–base regulation and calcification, with evidence of reduced biomineral production and hypercapnia (Byrne et al., 2013; Kroeker et al., 2013; Thomsen et al., 2015; Byrne and Fitzer, 2019). Given that warming and acidification both influence key metabolic processes, stressor interactions are inevitable with biological responses affected in unexpected ways (Kordas et al., 2011; Boyd and Brown, 2015; Boyd et al., 2017). This highlights the uncertainty as to our understanding of the drivers of ecosystem change in a high CO_2 world. For example, increased temperature affects both oxygen demand and the supply of oxygen in water (Pörtner, 2010; Christensen et al., 2011; Schulte, 2015) and may limit oxygen delivery, restricting metabolism and exacerbating the energetic demands elicited by OA (Dillon et al., 2010; Deutsch et al., 2015; Lefevre, 2016).

Exposure to combined warming and acidification often causes negative impacts that are either additive (e.g., increased metabolism in sea urchins, Carey et al., 2016) or synergistic (e.g., increased photosynthesis in foraminifera, Schmidt et al., 2014). However, positive or neutral responses have also been observed, such as in the development and thermal windows of echinoderm larvae (Karelitz et al., 2016) and the growth of sea urchins and mussels (Keppel et al., 2015; Dworjanyn and Byrne, 2018), and reproduction in many taxa (Harvey et al., 2013). Warming can ameliorate the negative effects of acidification on biological processes such as calcification, but within limits (Sheppard Brennand et al., 2010; Dworjanyn and Byrne, 2018). Critical gaps remain in our understanding of the ability of marine species to acclimatize or adapt to global change stressors within and across generations as most studies involve short-term acute experiments where the stress is immediate and so is delivered at a pace unrealistic with respect to global change. Organisms respond differently to more gradual introduction to a stressor and long-term acclimation (Dupont et al., 2013; Byrne et al., 2020; Uthicke et al., 2020). In general, acclimation to increased temperature decreases thermal sensitivity over time (Seebacher et al., 2014), and if this coincides with gamete development, can have positive carryover effects in conveying stress resilience to offspring (Pechenik, 2018; Byrne et al., 2020).

Warming and/or acidification have broadly deleterious effects on sea urchin growth, behavior, metabolism, reproduction and immune defense and disease, with response magnitude influenced by the stressor levels used (Byrne et al., 2011a,b, 2013; Brothers et al., 2016; Carey et al., 2016; Delorme and Sewell, 2016; Sweet et al., 2016; Manríquez et al., 2017; Dworjanyn and Byrne, 2018; Byrne and Fitzer, 2019; Byrne and Hernández, 2020). Global change experiments with sea urchins and other marine invertebrates that incorporate an acclimation period show that outcomes differ from the acute, shock-type approach (e.g., Dupont et al., 2013; Munguia and Alenius, 2013; Bellworthy et al., 2019; Uthicke et al., 2020). For *Strongylocentrotus droebachiensis*, a decrease in fecundity was observed after 4 months exposure to acidification (−0.3 pH units), but not after 16 months (Dupont et al., 2013). For *Sterechinus neumayeri*, exposure to warming (+2°C) and acidification (−0.3 to −0.5 units) over 2 years diminished the negative effects of these stressors on metabolism and reproduction (Suckling et al., 2015; Morley et al., 2016). For *Echinometra* sp. a 20-month exposure to warming (+1°C, +2°C) and acidification (−0.2 to −0.3 units) had no effects on growth, respiration and reproduction (Uthicke et al., 2020). Similar acclimatory responses are reported for corals (*Stylophora pistillata*) and crustaceans (*Paradella dianae*) exposed to warming and acidification (Munguia and Alenius, 2013; Bellworthy et al., 2019).

Acclimation as an important mechanism of phenotypic plasticity to adjust to changing habitat conditions within and across generations (Ghalambor et al., 2007). Parental stress history can influence stress responses in offspring (Byrne et al., 2020). The temperature at which gametes develop determines the thermal tolerance of fertilization and offspring development in a range of species (Byrne, 2011; Byrne et al., 2011b). However, the progeny of *S. intermedius* were negatively affected by parental exposure (15 months) to warming (Zhao et al., 2018). Acclimation of *S. droebachiensis* in OA (14 months) through gonad maturation had some positive carryover effects for surviving offspring, although mortality was high (Dupont et al., 2013). In *S. purpuratus* acclimation in OA conditions (4.5 months) increased embryonic growth and altered the transcriptome (Wong et al., 2018), but it is not known if these responses are negative or positive. For *Echinometra* sp. acclimation of parents to warming and acidification had negative carryover effects for larvae (Karelitz et al., 2020).

We examined the combined effects of warming and acidification in an acclimation experiment with the sea urchin *Heliocidaris erythrogramma* and outcomes for offspring reared in these stressors. This species is ecologically important in structuring subtidal habitats across temperate Australia through its grazing ecology (Keesing, 2020). In the southeast region *H. erythrogramma* resides in a hotspot where habitat warming is the global change stressor of primary concern (Babcock et al., 2019). In a preconditioning single stressor acclimation study, where temperature was gradually increased (+2–4°C) followed by a 14-week exposure, this species exhibited some capacity to acclimate to moderate warming (+2°C) but struggled to survive at a higher (+4°C) temperature increase (Harianto et al., 2018). Here, we build on this research using a preconditioning period that involved a gradual introduction to warming (+2°C, +3°C) and acidification (−0.4 pH units) levels over 7 weeks in the flow-through aquaria to facilitate adjustment of the urchins to

new conditions. This was followed by >5 months of acclimation under a natural pattern of seasonal temperature (offset at +2°C and +3°C) and photoperiod change at two pH levels (ambient pH_T 8.0; −0.4 units: pH_T 7.6). The treatments are commensurate with current and ongoing warming projections for the region, although recent MHWs which have extended for months have resulted in temperature increase at the levels used here (Oliver et al., 2018; Babcock et al., 2019).

Over 22-weeks we monitored survival and metabolic rate was measured at weeks 4 and 12 to evaluate physiological responses over two experimental periods and assess the acclimation response. Feeding, assimilation efficiency, excretion and survival were also recorded. As maintaining energy is key to long-term survival, the physiological parameter data were used to model scope for growth (SfG). This bioenergetics framework is used to quantify performance and energy budgets and has been applied to assess the impacts of warming and/or acidification on marine invertebrates including gastropods and sea urchins (Hill and Lawrence, 2006; Zhang et al., 2015, 2016; Delorme and Sewell, 2016). We used the SfG model to explore whether changes in the energy budget may be associated with the responses of *H. erythrogramma*. This approach allowed us to integrate multiple physiological traits under a single response metric to achieve a better understanding of the vulnerability of *H. erythrogramma* to warming and acidification.

We maintained *H. erythrogramma* for 22 weeks through the period of intense gonad development of local populations (September–December, see Laegdsgaard et al., 1991), a physiologically demanding period (Powell et al., 2020) to assess how they would survive in treatments and generate gametes with which to generate F1 progeny. The fast development of this species which metamorphoses within a week was used as a model to investigate carryover effects of parental acclimation. Offspring were reared to the juvenile in OW and OA conditions and their metabolic rate and growth were measured to determine if parental stress history altered these parameters.

We hypothesized that: (1) gradual introduction to warming and acidification conditions followed by acclimation would enhance tolerance to these stressors as seen in high survivorship (2) increased temperature and acidification would interact to affect metabolic rate, feeding rate and ammonia excretion rate (3) physiological adjustments to warming and acidification would be evident over acclimation time and (4) that there would be interactions between parental acclimation environment and offspring metabolic rate. Finally, as warming trends in the region are linked to increased disease in *H. erythrogramma* and that +4°C is close to the thermal tolerance of this species (Sweet et al., 2016; Harianto et al., 2018), we expected to see deleterious effects compounded over time at the upper level of warming used (+3°C).

MATERIALS AND METHODS

Specimen Collection and Experimental Treatments

Heliocidaris erythrogramma (44.15 ± 3.25 mm test diameter, n = 100) were collected from the subtidal (2–3 m depth) and selected for size at low tide, at Milk Beach (33°51′23.3″S, 151°16′1.1″E) and Bottle and Glass Point (33°50′52.7″S, 151°16′12.4″E) in June 2014. Sea surface temperature (SST) at the time was 15.3°C. The urchins were transported to the Sydney Institute of Marine Science (SIMS) in Chowder Bay and were held in aquaria (80 L) supplied with ambient flow-through, filtered sea water (FSW, 70 μm, 1.5 L min^{-1}). After 1 week, they were randomly allocated into six treatments, based on three temperature profiles (ambient +0°C, elevated +2°C and +3°C, adjusted weekly according to the mean SST profile determined from 5 years of *in situ* data (**Supplementary Figure 1**) and two constant pH levels (ambient: pH_T 8.0, low: pH_T 7.6). For each treatment, we used three replicate tanks (28 L) with 10 urchins per tank. The flow-through conditions ensured that the entire volume of the tanks was turned over 15 times per day.

Experiments were conducted in a controlled temperature room for precise adjustments of water temperature and pH in the flow through delivery system. Room lighting was adjusted weekly to reflect the diurnal sunrise/sunset cycle using a digital 24-h timer. Adjustments to water parameters were made in header tanks before the water was channeled to treatment tanks with the high flow-through rate reducing tank effects. Each header tank was supplied with FSW (20 μm) using a thermocouple-solenoid feedback system that mixed warm (25°C) and cold (14.5°C) filtered FSW (20 μm) in a 2 L mixing chamber to supply temperature-controlled water consistently. Each header tank was also equipped with a heater (75 W, EHEIM GmbH & Co KG, Germany) attached to a temperature controller (model 7028/3, TUNZE Aqraientechnik GmbH, Germany) as a second level of temperature control. Sea water pH was maintained using a mixed CO_2 system, where a thermally compensated, low-flow controller valve (Parker Hannifin, OH, United States) and a proportional–integral–derivative controller, updated every 10 s, were used to precisely inject food-grade CO_2 (BOC, Australia) into ambient air that had been scrubbed of CO_2. The CO_2-mix was bubbled vigorously and continuously into all header tanks using ceramic diffusers. The header tanks, diffusers and treatment tanks were checked, changed and cleaned frequently.

Increased temperature and acidification levels were changed gradually over 7 weeks and no mortality occurred. Temperature was increased at a rate of 1°C every 6 days until target temperatures were achieved. Sea water pH was lowered at a rate of −0.1 pH_T units every week. These manipulations were performed on a staggered schedule so that all treatments achieved target conditions in the same week (**Figure 1A**). After 7 weeks the treatment temperatures were (mean ± SD) ambient (15.6 ± 0.4°C), +2°C (17.6 ± 0.4°C) and +3°C (18.6 ± 0.3°C). During the acclimation period, temperature levels were regulated to achieve the mean weekly temperature over the same period (**Figure 1A**) determined from reference data collected from loggers deployed in the *H. erythrogramma* habitat (2009–2014) (**Supplementary Figure 1**). Treatment temperatures were generally kept within ±0.4°C (max, min) of reference temperatures (see **Supplementary Table 2**), while mean measured pH values over the same period were pH_T 8.0 ± 0.02 SD and pH_T 7.64 ± 0.09 SD. Treatment temperatures and photoperiod followed the natural change that occurs from

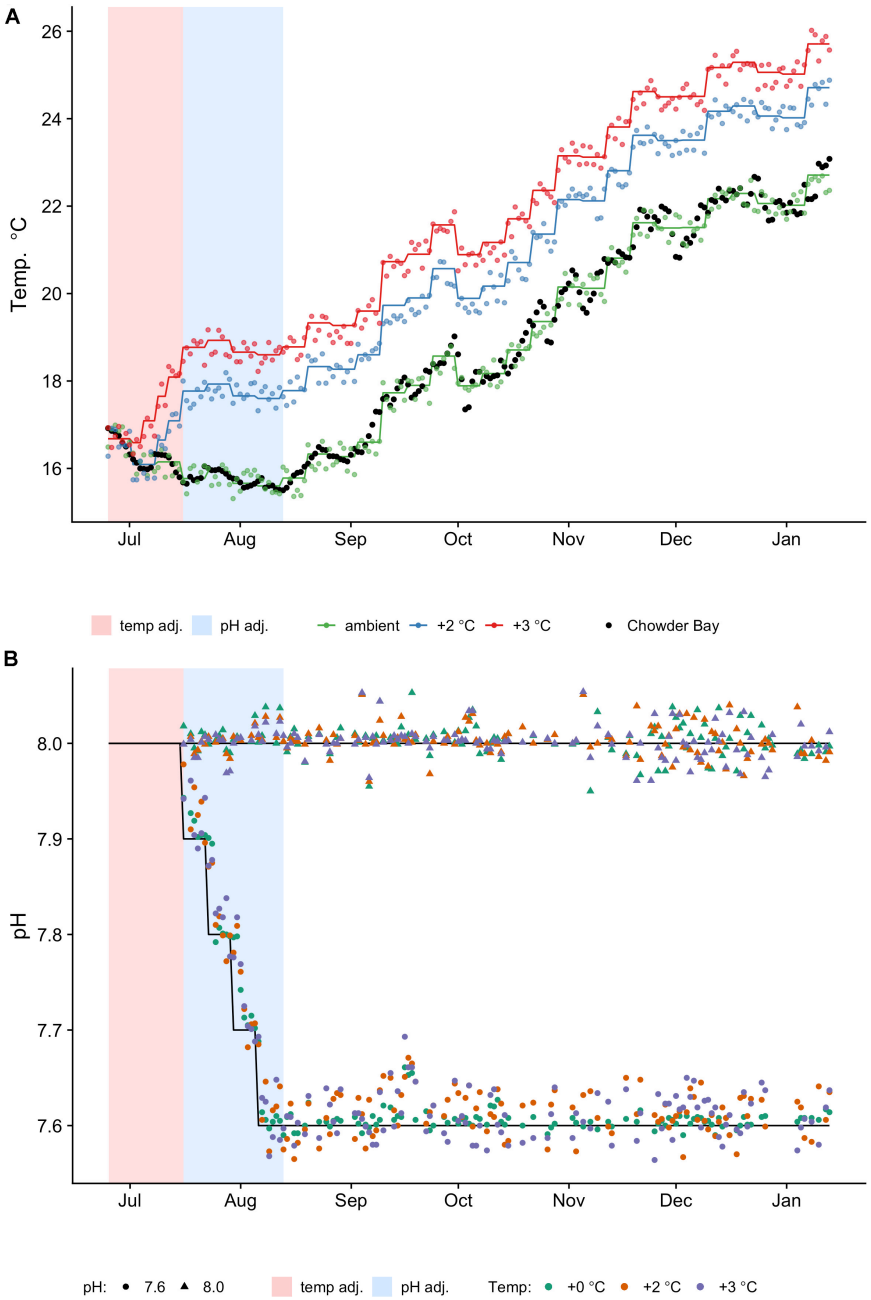

FIGURE 1 | Temperature **(A)** and pH **(B)** profiles and measurements taken daily. One replicate tank for every treatment was selected at random for measurements. Shaded regions are the pre-acclimation adjustment periods for temperature (pink) and pH (blue), respectively. **(A)** Colored lines represent the planned temperature profiles (ambient, +2°C, +3°C), which change every week and the dots represent actual temperatures measured (see also **Supplementary Table 1**). Black dots are the reference temperatures collected from *in situ* loggers deployed in Chowder Bay from 2009 to 2014, averaged by day (see **Supplementary Figure 1**). **(B)** Black lines represent the reference profiles of constant pH_T levels (8.0, 7.6) and initial adjustments. Actual measurements are indicated by shapes (triangle: 8.0; circle: 7.6). The actual mean measured pH values were pH_T 8.0 (SD = 0.02, n = 378) and pH_T 7.64 (SD = 0.09, n = 384). Colors represent the temperature group (see legend).

winter to summer. During the period of gonad growth, around which this study was scheduled, day length changes from 10 h in July to 14 h in December (data from Sydney Observatory). Because temperature affects CO_2 solubility and temperatures were changing every week, the system maintained constant pH_T (not CO_2 ppm) within each treatment (**Figure 1B**). With the pH encountered in the subtidal environment at Chowder Bay, there is little seasonal change, with most variation associated with diurnal flux (range pH_T 7.9–8.07; Runcie et al., 2018). For the experiment we used pH_T 7.6 as representative of a projected pH scenario of a decrease in ocean pH by up to 0.4 pH units by 2100 (Collins et al., 2013).

Temperature was logged using PT1000 resistance temperature detectors attached to a Graphtec multifunction logger (model GL840, Graphtec Corporation). Sea water pH was measured every 1–2 days to assess how acclimation treatments were tracking (**Figure 1B**) and was determined spectrophotometrically on the total scale with a custom-built pH sampling system connected to an Ocean Optics USB4000+ fiber optic spectrometer, using m-Cresol dye indicator (Acros Argonics, catalog number 110585000, Lot A0321770) and calculated according to Liu et al. (2011). The measurements were calibrated to certified reference material (CRM) for CO_2 in sea water (Batch 139) following SOP 6b in Dickson et al. (2007). In addition, temperature, pH and salinity of the tanks across treatments were independently checked every 1–2 days using a Canter 376 RTD thermometer, a Vernier LabQuest 2 salinity sensor and a WTW Multi 3420 pH probe, respectively, to test for consistent conditions. The pH probe was calibrated using high precision buffers (pH 4, 7 and 10, ProSciTech).

For analysis of total alkalinity (A_T), water samples (330 mL) were taken randomly from experimental tanks every 2 to 3 weeks (n = 36 samples across all treatments). A_T was determined by potentiometric titration (907 Titrando, Metrohm), calibrated using sea water CRMs (Batch 139, Dickson et al., 2007). Carbonate chemistry parameters pCO_2, calcite and aragonite saturation states ΩCa and ΩAr were calculated using the "seacarb" package in R (Gattuso et al., 2020) using the constants for K_1 and K_2 from Lueker et al. (2000), the constant for K_f from Perez and Fraga (1987) and the constant for K_s from Dickson (1990), as recommended by Dickson et al. (2007) (**Supplementary Table 1**).

Animal Maintenance and Monitoring

The sea urchins were fed on a mixed diet of *Ecklonia radiata* and *Sargassum* spp. suspended in kelp-based agar (MSC CO, Kyeongnam, Korea). To prepare the food, the algae were rinsed in fresh water, dried at 50°C for 48 h, and then ground into fine powder and mixed with agar powder (1:4 by weight). This was then mixed with FSW (20 μm) (1:10 by weight) at ∼80°C. The agar was left to cool and solidify for 45 min and then cut into 1 to 2 cm^2 cubes. The urchins were fed twice a week by placing three to four cubes on top of each individual ensuring that each animal received the same amount of food in excess during the experimental period. They were checked daily for survival and condition (e.g., spine loss, bald patch disease, see Sweet et al., 2016) over 22 weeks (155 days). Dead individuals were removed immediately. Uneaten food and feces were removed every 2 days.

As the experimental period coincided with the time when local *H. erythrogramma* populations undergo gonad development to spawning, and we employed a seasonal temperature and daylength cycle in our experiments, we expected spontaneous gamete release to occur. During the spawning season, which starts in October and would be expected to continue through the experimental period (Laegdsgaard et al., 1991), the tanks were monitored for released eggs. Spawning is readily detected as *H. erythrogramma* releases large, buoyant eggs that become trapped at the water surface. As appears typical for *H. erythrogramma* (Byrne, pers. obs.), spawning occurred at night in all treatments. We could not determine how many individuals spawned and so the observations were recorded as an indication that the animals were close to their natural physiological/reproductive cycle but were not statistically analyzed.

Metabolic Rate

Routine weight-specific metabolic rate, MO_2 was estimated by intermittent-flow respirometry at two time-points (week 4 and 12), using a random sample of 10 specimens from tanks across each treatment that were not fed for 5 days prior to measurement. They were transferred individually into 1 L respirometry chambers in individual water baths. Each chamber contained an oxygen sensor spot (SP-PSt3-NAU, PreSens GmbH, Germany) for the detection of dissolved oxygen concentration using an external multi-channel sensor (OXY-10-mini, PreSens). A magnetic stirrer ensured even mixing of water. The specimens were allowed to adjust to the chambers under flow-through conditions for 30 min prior to respirometry measures. At week 4, the temperatures were 16.6, 18.6, and 19.6°C and at week 12, were 20.7, 22.7 and 23.7°C for the ambient, +2 and +3°C treatments, respectively.

To measure oxygen uptake, the chambers were sealed, and dissolved oxygen (DO, $mgO_2\ L^{-1}$) was measured every 10 s until a 10% decrease in DO was recorded. The chamber was then flushed, and the measurement repeated. Background respiration was determined by recording FSW-only blanks (n = 8) to correct the recordings for background respiration and instrument drift. At the end of each measurement, sea water weight was calculated by deducting chamber, stir bar and urchin wet weights from the total weight of the chamber, and then converted to volume using sea water density estimated from current temperature, salinity and barometric air pressure (Fofonoff and Millard, 1983).

Weight-specific MO_2 ($mgO_2\ L^{-1}\ h^{-1}\ kg^{-1}$) was calculated manually using the R package 'respR' (Harianto et al., 2019) and the equation (Lighton, 2008):

$$MO_2 = \frac{\Delta O_2 V}{W}$$

where ΔO_2 is the linear regression of O_2 concentration over time ($mg\ L^{-1}\ h^{-1}$), V is the volume of the sea water available (L) and W is the wet weight of the urchin (kg).

Ammonia Excretion

Ammonia excretion rate was determined at 12 weeks after respiration experiments. Ten specimens were randomly selected from each treatment and transferred into 1 L chambers supplied with flow-through FSW at the same treatment conditions and left to rest for at least 45 min. Initial water samples were carefully collected (50 mL, 0,22 μm) and frozen. The chambers were then sealed and left in the water baths for 3 h before final water samples were collected. Background ammonia levels were determined by repeating the procedure without a specimen (n = 3 $treatment^{-1}$). The water samples were immediately frozen and stored in the dark until they were analyzed spectrophotometrically (within 10 days) for total ammonia (Parsons et al., 1984). Spectrophotometric readings

were obtained at 640 nm on a microplate reader (CLARIOstar Microplate Reader, BMG LABTECH, Offenburg, Germany) and calibrated using daily blanks and a standard ammonium solution. Ammonia excretion rate (U, μg kg^{-1} h^{-1}) was calculated according to the equation:

$$U = \frac{N_c}{W \cdot T}$$

where N_C is the concentration of ammonia (μg at–N L^{-1}), W is the weight of the specimen in kg and T is the time elapsed in hours. Ammonia concentration (N_C) is determined using the equation:

$$N_C = \frac{3 \cdot V}{E_s - E_b}$$

where E_s and E_b are the standard and corrected spectrophotometric extinction values of the blue indophenol color formed with ammonia, respectively, and V is the volume of the chamber (L). The precision of this technique (±0.1 μg at–N L^{-1}) was determined using the equation (Parsons et al., 1984):

$$h = \pm {0.1}\Big/{n^{\frac{1}{2}}}$$

where h is the precision at the 1 μg at–N L^{-1} level, and n is the number of determinations.

Feeding Rate and Assimilation Efficiency

Feeding trials were conducted in week 13 where the temperatures were 20.1, 22.1, and 23.1°C for the ambient, +2 and +3°C treatments, respectively. Ten random specimens from each treatment were transferred into individual tanks (4 L) supplied with flow-through FSW (6 L h^{1}) at the same treatment conditions. They were starved for 6 days in their new environments before feeding trials commenced, using the same agar-based food mixture used in routine feeding. The initial wet weight of the diet was determined, and the food was added to each tank in excess. Food-only autogenic controls were used to determine background changes in agar composition (n = 24).

After 48 h, unconsumed food was carefully collected and oven dried at 80°C for 48 h, and then reweighed. Fecal pellets were also collected for calculations of assimilation efficiency (see below). The specimens were removed from the tanks, blotted briefly with a paper towel, and weighed. To convert the initial wet weight (W_{wet}) of the food to their dry-weight equivalents, the wet:dry ratio of the food was determined in a regression analysis of wet to dry weights (W) (n = 60, r^2 = 0.82, $p < 0.01$), and determined as:

$$W_{dry} = (0.1529 \times W_{wet}) - 0.036$$

Feeding rate (C, mg day^{-1} kg^{-1}), was calculated by subtracting the final dry weight (W_{T1}) from the initial dry weight (W_{T0}), with adjustments for background changes and specimen weight (W_{sp}) and adjusted by time (T):

$$C = \frac{W_{T0} - W_{T1}}{W_{sp} \cdot T}$$

Fecal samples were dried at 60°C for 48 h and weighed. These samples were then ashed in a muffle furnace at 500°C for 2–3 h and re-weighed to determine their ash-free dry weight (AFDW). Assimilation efficiency (A) was calculated using the Conover method (Conover, 1966):

$$A = \left[\frac{F - E}{(1 - E) \cdot F}\right] \times 100\%$$

where F and E denote the AFDW:dry weight fraction measured in the diet and the feces, respectively. All weights were determined using the same analytical balance accurate to 0.0001 g.

Scope for Growth (SfG) Parameters

To explore the influence of temperature and pH stressors on the growth potential of *H. erythrogramma*, we constructed an SfG model using data from respirometry and ammonia analyses (week 12) and feeding trials (week 13). Details of parameter data, coding and analysis are provided in the **Supplementary Data**. Oxygen consumption was converted to energy equivalent values to calculate the energy lost in respiration per day (R_E) using a conversion factor of 14.14 J mg^{-1} O_2 (Elliott and Davison, 1975). A conversion factor of 0.025 J g^{-1} ammonia (Elliott and Davison, 1975) was used to estimate the energy equivalent of the energy lost due to ammonia excretion per day (U_E). The energy available from food (C_E) was calculated with bomb-calorimetry using an automatic adiabatic bomb calorimeter (Gallenkamp, London). The calorimeter was calibrated for the heat of combustion of 1 g of benzoic acid (26.493 kJ g^{-1}) to determine the approximate effective heat capacity of both the bomb chamber and the mass of the water within the calorimeter chamber (C_S Mean 10.27 ± 0.07 kJ°C, n = 3).

The diet was dried in an oven at 60°C to remove moisture. Approximately 1 g of the diet was used each time to determine gross energy by combustion and an average value (12.67 ± 0.25 S.D. kJ g^{-1}, n = 6) was obtained using the equation:

$$C_E = \frac{\Delta T \times C_S}{W_S}$$

where ΔT (°C) is the change in temperature – detected using a Beckmann thermometer – between the initial and post-combustion of the sample, C_S is the effective heat capacity of the system (bomb chamber and water), and W_S is the weight of the diet sample (g).

To calculate scope for growth (SfG) we used the equation adapted from Winberg (1960):

$$SfG = C_E \cdot A - (R_E + U_E)$$

where C_E is the energy obtained from diets, A is the assimilation efficiency, R_E is the energy lost in respiration and U_E is the energy lost due to ammonia excretion. All energy-related units are in kJ g^{-1} day^{-1}, while assimilation efficiency is a proportion.

Spawning and Offspring Rearing

The gametes of *H. erythrogramma* that had been acclimated to two temperature (ambient, +2°C) and two pH levels (pH_T 8.0, pH_T 7.6) were used to generate offspring. There were insufficient spawners in the +3°C treatments to use for this experiment. The urchins were induced to spawn by injection of 0.5 ml of 0 M KCl.

Although they had previously spawned during acclimation (see below), *H. erythrogramma* has continuous gamete production over the breeding period (Laegdsgaard et al., 1991). Gametes from at least three females and five males from each parental acclimation group were pooled and 500–1000 of the pooled eggs were placed in custom-built plankton kreisels, 100 ml volume (**Supplementary Figure 2**) in a controlled temperature room. There were three kreisels for each of 16 treatments, four temperatures (18°C, 20°C, 22°C, 24°C), two parental temperature conditions (ambient, +2°C) and the two parental pH levels (pH_T 8.0, pH_T 7.6) established as above and in a fully factorial design in a flow-through experimental water delivery system, with a header tank system similar to the adult experiment, with full turnover of water every 2 min to maintain conditions and circulation of larvae. The four temperatures reflect the range that the larvae encounter during the breeding season and recent warm summers and also included the thermal environment of the parents (21–24°C range). The eggs were fertilized ($\sim 10^4$ sperm mL^{-1}) and fertilization was checked after 5 min by examining counts of 100 randomly selected eggs to ensure >90% fertilization. The flow-through system (50 mL min^{-1}) was turned on to start the flow of experimental water and to wash away excess sperm. The kreisels had a 50 μm mesh covered outflow ports allowing constant flow of treatment water and gentle agitation of the embryos.

Heliocidaris erythrogramma has rapid development and by day 3.5–4 the larvae in all treatments were competent to settle as they had developed the five primary podia that are used to settle on the substrate. By day 4.5–5 most larvae had settled on the surface of the kreisels and completed metamorphosis to the juvenile which involves resorption of the larval tissue as juvenile structures develop. We did not document larval development as previous studies have shown that *H. erythrogramma* can develop normally in the temperature and pH conditions used, albeit with differential mortality of sensitive genotypes (Byrne et al., 2011a). Our primary interest was to span metamorphosis to the F1 advanced juveniles at 14 days old. It was not possible to follow mortality as dead embryos and larvae disintegrate quickly and were washed out of the system. Temperature and pH were monitored daily in kreisels across treatments (**Supplementary Table 3**). For A_T, sea water samples (330 mL) were taken randomly from experimental treatments three times over the 2 weeks. Other carbonate chemistry parameters (**Supplementary Table 3**) were determined as described above.

Metabolic rate, MO_2 of the juveniles was estimated using constant volume respirometry on day 14, 9–10 days after settlement. The respirometry chambers were 2 ml borosilicate glass vials with silicon septum lids (Thomas Scientific, United States). Oxygen concentration within the glass vials was measured using needle microsensors (PreSens) attached to 4 and 10 channel meters (OXY-10 and OXY-4 micro, PreSens). From each kreisel 50 juveniles were randomly collected and placed in the respirometry chamber filled with 0.22 μm FSW at the same treatment conditions they were reared in. Background respiration was measured in 4–6 vials containing only treatment water, measured separately for each group of juveniles. Thus, we had 50 juveniles in each of the three replicates for 16 treatments. Respirometry experiments ran for 12–15 h in the dark and oxygen concentrations did not drop below 85% air saturation at the end of the measurements. Temperatures were kept constant using water baths. The juveniles were photographed using an Olympus microscope and digital camera and test diameter was measured using ImageJ (NIH). Metabolic rates were scaled to the average test diameter per kreisel (pmol O_2 h^{-1} $juvenile^{-1}$ μm^{-1}).

Statistical Analyses

Analyses were performed in R (v 3.4.5). The survival time for each specimen was determined by the number of days from time zero (when the acclimation period started) to the end of the experiment, a total period of 155 days. Survival data were analyzed using Kaplan–Meier log-rank analysis, with right censoring, to determine whether temperature and pH affect survival time. In addition, a Cox proportional hazards model (Cox, 1972) was fitted using survival as a function of temperature and pH to assess the effects of each stressor on mortality risk. The fitted Cox regression met the assumption of proportional hazards (Schoenfeld residual tests, Grambsch and Therneau, 1994; $p = 0.673$). As no interactions were found between temperature and pH (Cox proportional hazards regression, $z = 0.61$, df = 3, $p = 0.54$), the analysis was repeated with only the main effects tested. *Post hoc* tests for the differences between treatments were determined using pairwise tests of significance corrected using the Benjamini–Hochberg (BH) false discovery rate method (Benjamini and Hochberg, 1995).

Metabolic rate data were first analyzed by constructing a generalized linear mixed model of metabolic rate as a function of relative temperature (ambient, +2°C, +3°C) and pH (8.0, 7.6). To avoid the potential effect of survival bias, the two measurement time points (week 4 and 12) were analyzed separately. Feeding rate and ammonia excretion rate data were also analyzed as above with the response variable as a function of temperature and pH. For all analyses, the nested effects of tank, temperature within tank and pH within tank were added as a random parameter in the models, and then tested using a likelihood ratio test on random effects, which were all not significant ($p \geq 0.9$ for all tests). To test for interactions, the nested terms were excluded from the final linear models to prevent confounding (Schielzeth and Nakagawa, 2013). ANOVA was performed on the linear models using Type III sums of squares when interactions were present, or Type II sums of squares when they were not (Langsrud, 2003).

For metabolic rate data, there were no statistically significant interactions between temperature and pH at 4 weeks ($F_{2,54} = 0.2$, $p = 0.93$), thus the data were re-analyzed to test for main effects only. For feeding and ammonia excretion rate data, there were no statistically significant interactions between temperature and pH ($F_{2,47} = 1.07$, $p = 0.35$ and $F_{2,54} = 2.31$, $p = 0.11$, respectively) and so the interaction term was also excluded before ANOVA was performed on each model. Prior to modeling tests, data were checked visually and statistically (if necessary) for normality using the Shapiro–Wilk test of normality (Royston, 1983), and homogeneity of variances using the Fligner–Killeen Test (Conover et al., 1981). Where treatment

conditions were indicated to be significantly different, estimated marginal means (EMM, i.e., Least-Squares Means) were used to develop linear estimates, and then analyzed using the *post hoc* Tukey Highest Significant Difference (HSD) test to identify the significance between temperature-pH combinations. Significance was determined at $p \leq 0.05$ for all tests.

For SfG, as the parameters used to construct the model were obtained from different individual sea urchins (i.e., the urchins were not tagged) and so the metric was calculated using treatment-averaged parameters (thus, $n = 1$), as in previous sea urchin studies (Stumpp et al., 2011; Delorme and Sewell, 2016). We constructed the SfG model using all the physiological parameter data to provide an overall indicative assessment of the impacts of the acclimation treatments on *H. erythrogramma*, but statistical analyses were not performed.

Interactions between parental treatments and offspring metabolic rate and size data were compared using analysis of covariance (ANCOVA). Parental temperature and pH were categorical variables, offspring temperature and pH were continuous covariates, and all possible interactions between all variables were included. The random effect of kreisel was tested using the 'lmer()' function in the 'lme4' package, which was not significant (general linear mixed-effects model, $p > 0.05$). Therefore, ANCOVA was performed using the 'car' package, with type III error to test for main effects and the interaction terms. For metabolic rate, there were no significant three-way interactions ($p < 0.05$), thus the terms were removed and the model reanalyzed. For growth, there were no two or three-way interactions, thus the model was analyzed for main effects only using type II error.

RESULTS

Survival

There was a significant effect of treatment on survival (logrank test, $\chi_2 = 61.23$, df = 3, $p < 0.001$) (**Figure 2**). As single stressors, the +2°C and decreased pH treatments (pH_T 7.6) did not affect survival (>80% survival at 22 weeks). The +3°C, treatments resulted in decreased survival regardless of pH level ($p < 0.001$, hazard ratio: 17.2, 95% CI: 5.27–56.25). These treatments intersected the median survival threshold after 14–20 weeks (**Figure 2**). Cox proportional hazards analysis showed a greater risk of mortality in urchins exposed to increased temperature compared with decreased pH (hazard ratios of 3.38 and 0.47, respectively). *Post hoc* results (pairwise tests, BH-corrected) showed that urchins acclimated to +3°C had significantly lower survival compared to all other treatments ($p < 0.01$ for all pairwise combinations), with no significant differences in all other pairwise comparisons. At week 22, urchins acclimated to +3°C and pH 7.6 had the lowest survival at 33% (**Figure 2**).

Metabolic Rate

After 4 weeks of acclimation, the metabolic rate of *H. erythrogramma* was significantly influenced by increased temperature ($F_{2,54} = 15.9$, $p < 0.001$) and decreased pH ($F_{1,54} = 23.4$, $p < 0.001$) with no interaction between stressors (**Table 1**). Generally, metabolic rate increased by up to 35% with warming and 25% with reduced pH. At week 4, the combined effects of warming and acidification were additive, increasing metabolic rate by up to 56% (**Figure 3A**). *Post hoc* comparisons of estimated marginal means using Tukey's HSD showed that 10 of 15 pairwise comparisons differed significantly as shown in the pairwise-value plot (**Supplementary Figure 3**).

At 12 weeks of acclimation, metabolic rate responses were significantly affected by warming ($F_{2,51} = 9.49$, $p < 0.001$) and acidification ($F_{1,51} = 16.37$, $p < 0.001$), with a significant interaction between these stressors ($F_{2,51} = 10.5$, $p < 0.001$; **Table 1**) resulting in an antagonistic effect on metabolic rate (**Figure 3B**). Thus, at week 12 warming and decreased pH elevated metabolic rate by 9% and 18%, respectively, and in combination reduced metabolic rate by up to 3%. *Post hoc* comparisons of estimated marginal means using Tukey's HSD showed that two of 15 pairwise comparisons differed significantly (**Supplementary Figure 3**). At pH 7.6, the +0°C and +3°C groups differed significantly ($p < 0.001$), and at +0°C, the pH 8.0 and pH 7.6 groups differed significantly ($p < 0.01$). No other pairwise differences were statistically significant (**Supplementary Figure 3**).

Feeding and Ammonia Excretion Rates

Feeding rate was significantly influenced by increased temperature ($F_{2,49} = 13.5$, $p < 0.001$), but not pH, with no interaction between temperature and pH (**Table 2** and **Figure 4A**). Tukey's HSD pairwise comparisons showed that feeding tended to decrease with increasing temperature, and that +2°C and +3°C decreased feeding at pH_T 7.6 ($p = 0.001$ and $p = 0.008$, respectively), but not at pH_T 8.0.

Urchins acclimated to elevated temperature treatments had significantly higher ammonia excretion rates ($F_{2,56} = 8.94$, $p < 0.001$; **Figure 4B**), with no effect of decreased pH and no interaction between temperature and pH (**Table 2**). Tukey's HSD showed that at ambient pH_T 8.0, acclimation to +2°C increased ammonia excretion by 1.3-fold (df = 54, $p = 0.016$), but not at +3°C ($p = 0.099$). At pH_T 7.6, acclimation to +2°C did not significantly affect ammonia excretion ($p = 0.29$), but acclimation to pH_T 7.6 and +3°C, increased excretion 1.5-fold ($p = 0.016$).

Scope for Growth

The scope for growth model for *H. erythrogramma*, incorporating metabolic rate, feeding rate, ammonia excretion rate and assimilation efficiency data, showed that there was a net positive energy budget under all experimental scenarios of warming and acidification after 12 weeks of acclimation (SfG > 0, **Figure 5**). Further, the energy acquired through feeding (with food in excess) contributed to most (>90%) of the energy budget (**Table 3**). While *H. erythrogramma* acclimated to low pH recorded a 16% increase in SfG (1.17 kJ g^{-1} day^{-1}), exposure to +2°C and +3°C reduced overall SfG by 31–41%. In urchins acclimated to both stressors, overall SfG was reduced the most by 42–45%.

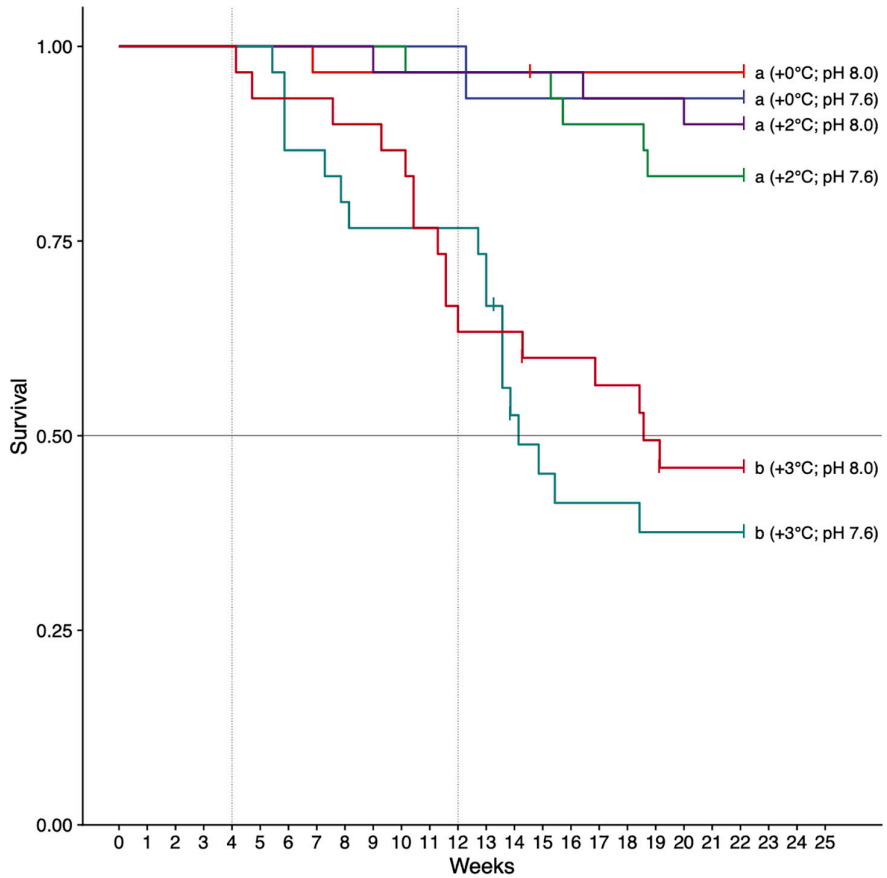

FIGURE 2 | Survival of *H. erythrogramma* acclimated to three temperature (ambient, +2°C, +3°C) and two pH_T (8.0, 7.6) levels in six treatments. Letters indicate treatments that differed (pairwise tests, with Benjamini–Hochberg [BH] false discovery rate corrections, $p < 0.05$). The horizontal line is the median survival threshold; vertical lines show times of data collection at 4 and 12 weeks of acclimation.

Spawning

Synchronous spawning occurred overnight on 7 and 24 October (week 7 and 10, respectively) with the first event occurring all treatments and the second spawning event only occurring in the +3°C treatments and combined +2°C/7.6 pH_T treatments. These events involved males and females as indicated by the presence of developing embryos which progressed through larval and juvenile stages (data not shown).

TABLE 1 | Analysis of variance on the effects of increased temperature and decreased pH on the metabolic rate data from *Heliocidaris erythrogramma* after acclimation in three temperature (ambient, +2°C, +3°C) and two pH_T (8.0, 7.6) treatments analyzed separately after 4 and 12-weeks.

Source	Sum sq	df	*F*-value	*P*
4 weeks				
Temperature	42.26	2	16.419	**<0.001**
pH	31.10	1	24.172	**<0.001**
Residuals	72.06	51		
12 weeks				
Temperature	10.39	2	9.491	**<0.001**
pH	8.97	1	16.370	**<0.001**
Temperature:pH	11.46	2	10.460	**<0.001**
Residuals	27.92	51		

There were no significant interactions between temperature and pH at week 4 and so the interaction term was removed. Significant P-values are highlighted in ***bold****.*

Offspring Metabolic Rate and Size

There was a significant interaction between parental temperature treatment and offspring metabolic response to temperature (GLMM ANCOVA, $F_{3,22} = 24.78$, $p < 0.001$; **Table 4**). Juvenile metabolic rate increased significantly with temperature ($F_{1,22} = 11.06$, $p < 0.003$; **Table 4**). Parental acclimation to increased temperature (2°C above ambient) resulted in increased juvenile metabolism at higher temperature (**Figure 6**). At 24°C, the difference in metabolic rates between juvenile groups was up to 30% depending on whether their parents had been acclimated to increased temperature. Parental acclimation to acidification had no effect on juvenile metabolic rate ($F_{1,22} = 1.68$, $p = 0.21$). Low pH, regardless of parental environment, had no effect on juvenile metabolic rate ($F_{1,22} = 0.24$, $p = 0.63$).

With respect to offspring test diameter, pH_T 7.6 caused a statistically significant reduction in juvenile size of about 4% from 404 mm ± 2.25 (SE) to 387 ± 1.86 (SE) ($F_{1,953} = 38.1$, $p < 0.001$;

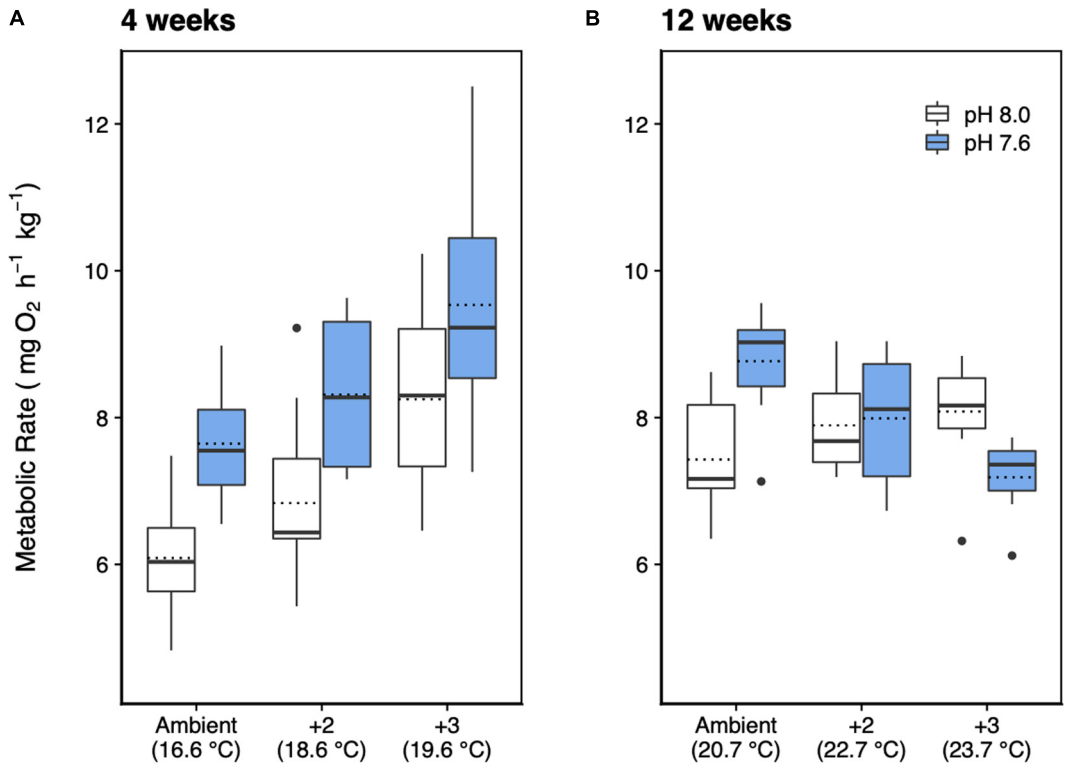

FIGURE 3 | Metabolic rate of *H. erythrogramma* acclimated for **(A)** 4 and **(B)** 12 weeks in three temperature (ambient, +2°C, +3°C) and two pH_T (white: 8.0, blue: 7.6) levels in six treatments. The top and bottom of the boxes represent the interquartile range (IQR) between the 25th and 75th percentile (Q1 and Q3, respectively). The horizontal line represents the median (Q2), the horizontal dotted line represents the mean, and the vertical lines (whiskers) represent the range of the data computed as follows: less than Q1 – 1.5 IQR (bottom whisker); greater than Q3 + 1.5 IQR (top whisker).

Supplementary Figure 4), regardless of parental acclimation to warming ($F_{1,953} = 0.003$, $p = 0.95$) or acidification ($F_{1,953} = 1.99$, $p = 0.16$). Temperature had no effect ($F_{1,953} = 1.32$, $p = 0.27$).

DISCUSSION

Long-term acclimation to warming and acidification, in parallel with the seasonal cycle of temperature and photoperiod, affected the survival, feeding, metabolism and ammonia excretion rates of *H. erythrogramma*. The high temperature offset (+3°C) caused significant mortality while the other treatments did not affect survival. For metabolic rate, temperature and pH did not interact at 4 weeks of acclimation, but significant, antagonistic interactions were detected at 12 weeks, where at pH_T 7.6, metabolic rate decreased with increasing temperature. It appears that while the effect of temperature and pH were clear at 4 weeks where pH had a significant effect on metabolic rate and +3°C influenced almost every treatment, these differences in variation became less distinct after 12 weeks of acclimation. Scope for growth values were positive in all treatments, indicating that energy surplus (excess food) was adequate to support energy demands. We found no evidence of interactive effects of the two stressors on survival, feeding rate and ammonia excretion. Parental acclimation to warming (+2°C), but not acidification altered the physiology of juvenile offspring with an increase in metabolic rate.

Warming (+3°C) regardless of pH was the main driver of mortality risk (∼3-fold) in *H. erythrogramma*, while low pH was associated with a much lower risk of death (∼0.5-fold). The latter is similar to that found previously for this species (Byrne et al., 2009, 2011a; Harianto et al., 2018). Interestingly, in the +3°C treatments, ∼25% mortality occurred by week 10 when the highest temperature treatment had reached 24°C.

TABLE 2 | Analysis of variance on the effects of increased temperature and decreased pH on feeding and ammonia excretion rate data from *Heliocidaris erythrogramma* after 12 weeks acclimation in three temperature (ambient, +2°C, +3°C) and two pH_T (8.0, 7.6) treatments.

Source	Sum sq	df	*F*-value	*P*
Feeding				
Temperature	0.0019	2	13.5	**<0.001**
pH	0.000098	1	1.25	0.27
Residuals	0.0035	49		
Ammonia excretion				
Temperature	8353.3	2	8.95	**<0.001**
pH	425.6	1	0.91	0.34
Residuals	26135.6	56		

The non-significant interaction term (Temperature:pH) was removed.

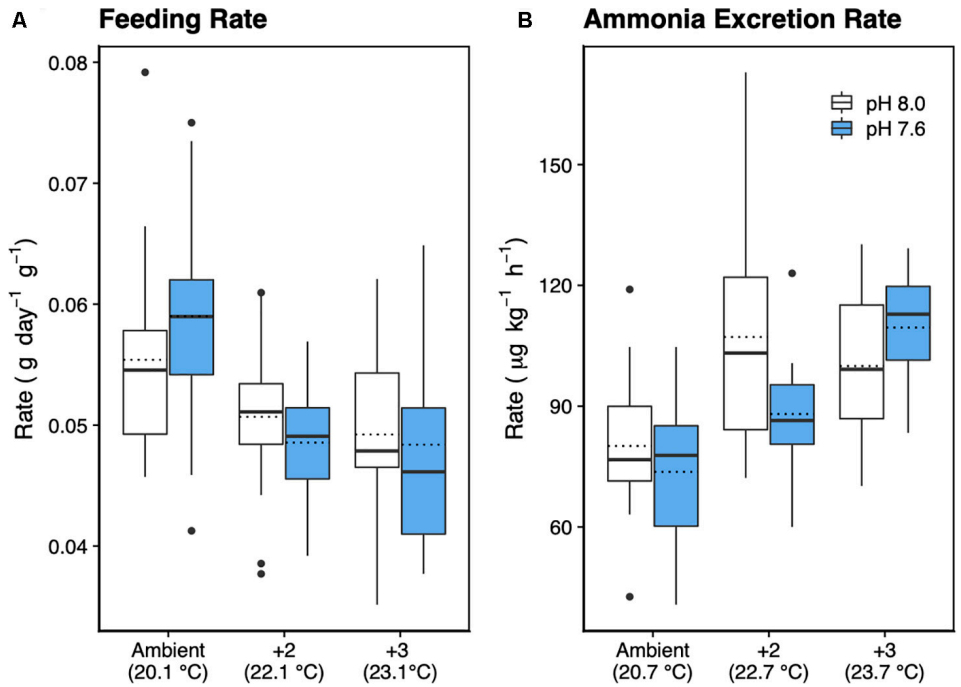

FIGURE 4 | Feeding rate in dry food weight **(A)** and **(B)** ammonia (NH_3) excretion rate of *H. erythrogramma* acclimated for 12 weeks in three temperature (ambient, +2°C, +3°C) and two pH_T (white: 8.0, blue: 7.6) levels in six treatments. The top and bottom of the boxes represent the interquartile range (IQR) between the 25th and 75th percentile (Q1 and Q3, respectively). The horizontal line represents the median (Q2), the horizontal dotted line represents the mean, and the vertical lines (whiskers) represent the range of the data computed as follows: Q1 – 1.5 IQR (bottom whisker); greater than Q3 + 1.5 IQR (top whisker).

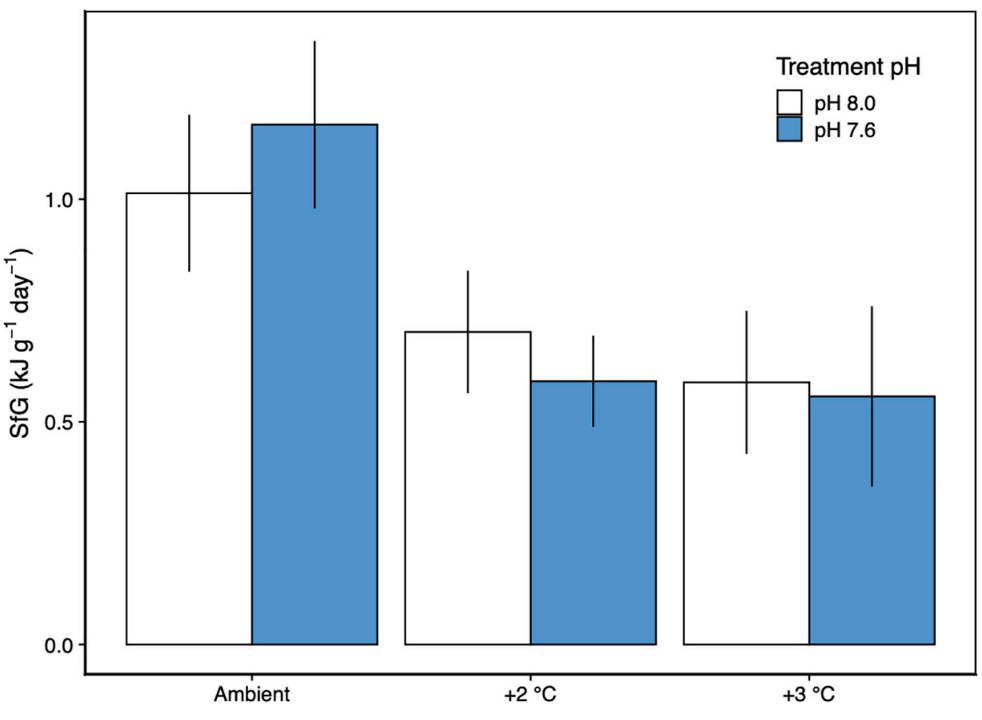

FIGURE 5 | Scope for growth (±SD) of *H. erythrogramma* acclimated to three temperature (ambient, +2°C, +3°C) and two pH_T (white: 8.0, blue: 7.6) levels. The model was determined from measurements of metabolic rate, feeding rate, ammonia excretion rate and assimilation efficiency. $n = 1$.

TABLE 3 | Scope for growth (SfG) in *Heliocidaris erythrogramma*.

Treatment	AE (%)	Feeding	Respiration	Excretion	SfG
+0°C; pH 8.0	69.59	1.61	0.105	0.002	1.013
+0°C; pH 7.6	67.75	1.91	0.124	0.002	1.167
+2°C; pH 8.0	66.91	1.22	0.112	0.003	0.702
+2°C; pH 7.6	67.74	1.04	0.113	0.002	0.591
+3°C; pH 8.0	64.23	1.10	0,114	0.002	0.589
+3°C; pH 7.6	64.30	1.03	0.102	0.003	0.557

The parameters were standardized to the same unit (kJ g^{-1} day^{-1}). Each parameter was obtained after 12–13 weeks of acclimation to three temperature (ambient, +2°C, +3°C) and two pH_T (8.0, 7.6) levels. The parameters used to construct the SfG model were obtained from different sea urchins and so the metric was calculated using treatment-averaged parameters (thus, n = 1). AE, ammonia excretion.

TABLE 4 | Generalized linear models (GLMM) analyses of covariance (ANCOVA, Type III) on the effect of parental acclimation environment (ambient, +2°C, +3°C; pH_T 8.0, pH_T 7.6) and offspring rearing treatment (18°C, 20°C; 22°C, 24°C; pH_T 8.0, pH_T 7.6) on juvenile metabolic rate in *H. erythrogramma*.

Source	Sum sq	df	*F*-value	*P*
Parent Env (Temp)	78.48	1	24.78	**<0.001**
Parent Env (pH)	5.32	1	1.68	0.21
Offspring (Temp)	35.02	1	11.06	**0.003**
Offspring pH	3.99	1	1.26	0.27
Parent Env (Temp): Parent Env (pH)	1.32	1	0.42	0.53
Parent Env (Temp): Offspring Temp	100.74	1	31.81	**<0.001**
Parent Env (Temp): Offspring pH	0.21	1	0.067	0.8
Parent Env (pH): Offspring Temp	6.49	1	2.05	0.17
Parent Env (pH): Offspring pH	0.75	1	0.24	0.63
Offspring (Temp): Offspring pH	5.290	1	1.67	0.21
Residuals	66.514	21		

Non-significant three-way interactions were removed from the model. Significant P-values are highlighted in ***bold****. Env, environment; Temp, temperature.*

This was not expected as temperatures below 24°C were not lethal after several months in previous studies (Carey et al., 2016; Harianto et al., 2018). However, 24°C which occurred ∼3 weeks later in the +2°C treatments – did not cause similar levels mortality. This points to the influence of timing of the increased temperature and the normal biological cycle. Warm conditions early may have created a mismatch between the photoperiod and temperature cues that control physiological processes associated with seasonal reproduction (Laegdsgaard et al., 1991). Successful spawning at the correct time in the +2°C treatment reflects gametogenic entrainment by the daylength cue with the onset of gamete release fine-tuned by temperature (Laegdsgaard et al., 1991). It appears that the earlier arrival of "summer" temperatures in the +3°C treatment was stressful. *Heliocidaris erythrogramma* matures from winter to spring, a metabolically intensive period as nutrients accumulate in the gonads (Laegdsgaard et al., 1991; Byrne and Sewell, 2019; Powell et al., 2020). Spontaneous spawning occurred in all treatments at the expected time and the gametes were fertile. This indicated that normal gametogenesis occurred, likely due to incorporation of seasonal temperature and photoperiod conditions, factors known to entrain gonad development in *H. erythrogramma* (Laegdsgaard et al., 1991), as also found for *Echinometra* sp. maintained in climate change conditions in conjunction with the seasonal cycle of light and temperature (Uthicke et al., 2020). In contrast, gonad development is inhibited or impaired in *H. erythrogramma* (Harianto et al., 2018) and other sea urchin species when in held in constant elevated temperature treatments (Uthicke et al., 2014; Brothers and McClintock, 2015; Delorme and Sewell, 2016; Morley et al., 2016).

For *H. erythrogramma* the thermal offset above ambient had negative consequences at +3°C, but not at +2°C. Our expectation that gradual introduction to warming conditions and acclimation would enhance tolerance to increased temperature seemed to be met in the +2°C treatment. The effect of the 1°C difference in sensitivity would not have been detected if seasonal profile of environmental change and prolonged acclimation were not incorporated into our investigation. This shows that understanding the effects of seasonal change on biological processes is vital for predicting how species will respond to ocean warming (Kreyling and Beier, 2013; Thompson et al., 2013). With respect to current interest in adaptive potential and the strong influence of environmental conditions on gonad development, this is a key consideration for marine climate change studies investigating carryover effects from parent to offspring (Karelitz et al., 2019, 2020; Byrne et al., 2020). For a better understanding of the impact of natural change in pH in the *H. erythrogramma* habitat as might be altered by ocean acidification, it would have also been interesting to incorporate the day–night diurnal change in pH with an offset. However, the source population only experiences a range of ∼0.07 pH units (Runcie et al., 2018).

As single stressors, increased temperature and reduced pH had a clear, positive effect on the metabolic rate of *H. erythrogramma* after 4 and 12 weeks of acclimation. This was expected. It is well-known that temperature modulates physiological activity in ectotherms (Brown et al., 2004; Dillon et al., 2010; Somero, 2012), and pH affects acid–base physiology associated with maintaining homeostasis in echinoderms (Catarino et al., 2012; Collard et al., 2013). Combined warming and acidification resulted in an increase in metabolic rate of *H. erythrogramma* at week 4 when the treatments were 16.6°C, 18.6°C and 19.6°C. There were no interactions between stressors, which was a similar outcome to a previous study where this species was kept in constant warm-low pH conditions (+5°C, −0.4 pH_T) for 8 weeks (Carey et al., 2016). However, after 12 weeks, there was an antagonistic interaction between temperature and pH resulting in decreased metabolic rate, likely due to metabolic depression. Metabolic depression is a known stress response of many organisms faced with deleterious conditions as lowering of metabolism is an effective mechanism to conserve energy and maximize fitness in response to extreme temperatures (Storey and Storey, 1990; Guppy and Withers, 1999). Metabolic depression in *H. erythrogramma* was a stress response to exposure to combined warming and acidification over months, as this response was not observed when the sea urchins were exposed to each stressor individually. For *H. erythrogramma* these results indicated that the urchins may have experienced energetic trade-offs between the needs of routine metabolism and important processes such

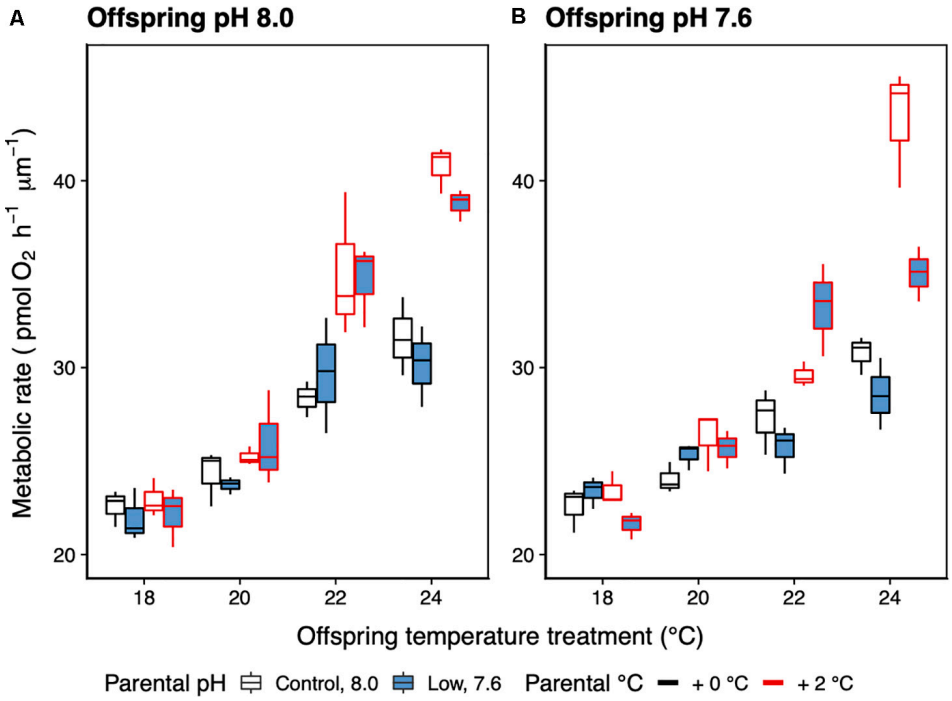

FIGURE 6 | Mean metabolic rate (±SE) of 14-day-old juvenile offspring of *H. erythrogramma* parents that were acclimated for 3 months at two temperature (black outline: ambient, red outline: +2°C) and two pH_T (white: 8.0, blue: 7.6) levels **(A,B)**. The juveniles were reared in a range of temperatures (18–24°C). $n = 3$.

as feeding, reproduction and ATP allocation (Angilletta et al., 2009; Pörtner, 2010; Pan et al., 2015). Our results differ from that found for *Echinometra* sp. where there were no effects on metabolism after a 20-month acclimation to warming (+1°C, +2°C) and acidification (−0.2–0.3 pH units) (Uthicke et al., 2020). Comparison between the two studies is, however, difficult as different stressor levels and respirometry methods were used.

Exposure to low pH over 13 weeks did not significantly affect feeding, excretion and survival rates of *H. erythrogramma*, even when combined with warming (+2°C), suggesting that this species was able to successfully compensate for the potential effects of acidification on these traits and that gradual introduction of stressor levels and acclimation may have facilitated tolerance. Energetic trade-offs would be necessary to maintain acid–base balance, as metabolic rate did not increase with warming and low pH. However, the observed depression of metabolic rate in *H. erythrogramma* due to combined warming and acidification would limit the energy available to maintain these processes. While metabolic depression might be a necessary response to maintain the balance between energy supply and demand (Guppy et al., 1994; Guppy and Withers, 1999; Guderley and St-Pierre, 2002), in the longer term it can lead to a decrease in energy budget and reproduction as seen in gastropods and urchins (Stumpp et al., 2011; Zhang et al., 2015). This reduction of metabolic rate would be expected to impair the ability to persist in the face of habitat warming and acidification. Energetic responses to acidification conditions are also evident in long term studies of *H. erythrogramma*, other sea urchins and other marine invertebrates reared in acidification conditions, a result attributed to energetic constraints as seen in their smaller size, reduced biomineral production and lower gonad production/fecundity (Mos et al., 2016; Hu et al., 2018; Byrne and Fitzer, 2019; Johnson et al., 2020).

With respect to SfG, the levels determined here for *H. erythrogramma* (∼0.5–1.0 kJ g^{-1} day^{-1}) were higher than that obtained for two other sea urchin species *Arbacia punctulata* (0.16–0.19 kJ g^{-1} day^{-1}) and *Lytechinus variegatus* (0.17–0.18 kJ g^{-1} day^{-1}) when subject to feeding and temperature treatments (Hill and Lawrence, 2006). For *H. erythrogramma*, increased temperature appeared to reduce SfG. For *A. punctulata* there was a slight increase in SfG with increased temperature (+8°C), and for *L. variegatus* this level of warming caused a decrease in SfG (Hill and Lawrence, 2006). In contrast, *Evechinus chloroticus* had a lower SfG at control temperature (0.14–0.18 kJ g^{-1} day^{-1}) and this was reduced with increased temperature (+6°C) (0.03–0.05 kJ kg^{-1} day^{-1}; Delorme and Sewell, 2016). It is difficult to compare SfG levels with these studies due to different approach to analyses. In our case all parameters were empirically determined (data and analyses are available as links provided in the section "Data Availability Statement" below).

To date, most long-term warming and acidification experiments with adult echinoderms have not incorporated seasonal change in temperature and daylength (e.g., Suckling et al., 2015; Carey et al., 2016; Morley et al., 2016; Dworjanyn and Byrne, 2018). Morley et al. (2016) presented the longest (40-month) study on the Antarctic sea urchin *Sterechinus neumayeri*. They found that acclimation to stable warming and acidification conditions diminished the negative effects of these

stressors on feeding bioenergetics, with no differences between stress-acclimated (+2°C, −0.3 and −0.5 pH units) and ambient-acclimated sea urchins. After 2 months acclimation to constant warming and acidification conditions (+5°C, −0.5 pH units) Carey et al. (2016) showed evidence of metabolic acclimation in *H. erythrogramma*. In the only other study to incorporate seasonal change in temperature and photoperiod, *Echinometra* sp. exhibited full metabolic rate acclimation after 20 months in warming and acidification conditions (+1°C, +2°C; 0.2–0.3 pH units) although they had elevated ammonium excretion (Uthicke et al., 2020). We also noted increased ammonia excretion at +2°C and +3°C for *H. erythrogramma*. In the single study where a temperature offset (+2°C) from the seasonal trend was used, a 3-month exposure to this experimental treatment was lethal to *Paracentrotus lividus* (∼100% mortality) (Yeruham et al., 2015). This study did not incorporate a gradual introduction to increased temperature.

As expected, the juveniles exhibited an increase in metabolic rate in response to being reared at warmer temperature. In contrast to the feeding larvae of sea urchins and oysters (Stumpp et al., 2011; Parker et al., 2017) as well as larger *H. erythrogramma* (11–80 mm test diameter) (Carey et al., 2016) low pH as a single stressor or together with warming did not cause an increase in the metabolic rate of the juvenile *H. erythrogramma*, with the difference between the present and previous studies was the long pre-acclimation and acclimation times which is likely to have influenced out results. The increase in juvenile metabolic rate in response to warming was accentuated in the offspring of the warm acclimated (+2°C) parents seen in a 30% increase in metabolic rate at 24°C. The increased metabolic rate as a carryover effect of larvae from low pH exposed parents is likely to place a strain on the energy budget of the juveniles and so the response may be maladaptive. A similar response of increased metabolic rate of the larval progeny of warm acclimated parents is reported for *Echinometra* sp., although this was combined with low pH (pH 7.8) and so it is not known if the response was due to increased temperature, increased acidification or the combination (Karelitz et al., 2020). The influence of parental thermal history on offspring thermotolerance is seen in comparison of the performance of *H. erythrogramma* from different latitudes (Byrne et al., 2011b). For the progeny of the +2°C treatment adults there appears to have been transgenerational effects with adult acclimation linked to the offspring thermal stress response, which if occurs in nature may be an important mechanism to facilitate persistence, but for adaptation would need to be conveyed beyond the F1 generation. The larvae that reached the juvenile stage are likely to represent a subset of resilient larvae as well as due to the transgenerational carryover effects of parental conditioning (Byrne et al., 2011a,b, 2020). The resilience of the juvenile stage is likely due to selective mortality of sensitive individuals at the larval stage. Due to the flow through conditions, dead offspring were washed from the system. Larval survivorship data are needed to more fully understand the influence of sensitive and resistant genotypes on overall adaptive capacity. We do not know if thermotolerance would have been seen in progeny of +3°C acclimation parents as there were insufficient spawners. However, as this level of warming incurred high mortality, it is likely that gamete quality would have been marginal with negative effects for development.

Our findings underscore the need for a multifactorial and integrative approach to predicting the effects of climate change stressors on marine species as they show how physiological responses can change the interpretation of sensitivities to climate change (Gunderson et al., 2016). For adult *H. erythrogramma* increased energetic costs of OA may interact with warming to affect metabolism in ways that contrast with single stressor effects and there was a heightened larval metabolism depending on adult acclimation history. The 3°C increase in temperature caused significant levels of adult mortality in our treatments and an indication of reproductive failure, but these effects were not seen in the +2°C treatment. As *H. erythrogramma* showed little tolerance to +4°C in previous studies and recent regional increase in habitat temperature is linked to disease and mortality (Sweet et al., 2016; Harianto et al., 2018) we expected that we might see negative effects at +3°C, as we did. Six weeks at this level of warming approached lethal tolerance limits for *H. erythrogramma*. This indicates that *H. erythrogramma* in the region currently live close to their lethal temperature as they experience MHW and temperatures approaching 25°C (Harianto et al., 2018). However, larval transport of *H. erythrogramma*. to cooler climes will be facilitated by the strong poleward flow (see Byrne et al., 2011b) potentially avoiding the "wrong-way" migration shown elsewhere (Fuchs et al., 2020).

Finally, our results contribute to an increasing body of research (Hu et al., 2018; Byrne et al., 2020) that show the need to consider the influence of acclimation in assessing prospects for phenotypic adjustment and adaptation in marine species in the face of a changing climate.

DATA AVAILABILITY STATEMENT

The raw data supporting the conclusion of this article will be made available by the authors, without undue reservation.

AUTHOR CONTRIBUTIONS

JH and MB devised the project and wrote the manuscript. JH, JA, ST, and RG carried out the experiments. All authors commented on the manuscript.

FUNDING

This research was supported by grants from the ARC (DP150102771) and NSW Environmental Trust 2016RD0159.

ACKNOWLEDGMENTS

The content of the manuscript has been published as part of the thesis of Harianto (2019). We thank the Sydney Institute of

Marine Science (SIMS) for access to facilities and assistance. This is SIMS contribution 265.

SUPPLEMENTARY MATERIAL

The Supplementary Material for this article can be found online at: https://www.frontiersin.org/articles/10.3389/fmars.2020.588938/full#supplementary-material

Supplementary Figure 1 | Mean weekly temperature (±SD) for Chowder Bay from 2009 to 2014. Data were obtained from loggers deployed *in situ* at 3 m depth at the level of the sea urchin habitat and used to design the temperature profile of the elevated temperature treatments (see **Figure 1**). Colors represent the adjustment (blue) and acclimation (red) periods of the experimental treatments, respectively. The shaded region (gray) is the max/min of the temperatures recorded.

Supplementary Figure 2 | Diagram of the kreisel containers used to rear of *H. erythrogramma* to the juvenile stage. Filtered sea water was supplied at a rate of 50 mL min^{-1}. At the water enters the kreisel it generates a continuous circular flow keep the embryos and larvae in suspension until they settle.

Supplementary Figure 3 | A graphical view of pairwise *p*-values from Tukey's Honest Significant Difference (HSD) test, performed on the estimated marginal means (EMM) of treatment groups results, for comparisons of performance of metabolic rate in six treatments of three temperatures (ambient, +2°C, +3°C) and two pH_T levels (8.0, 7.6). Separate analyses were performed at **(A)** 4 weeks and **(B)** 12 weeks. Factor levels are plotted on the vertical axis, and *p*-values are plotted on the horizontal axis. Numbers are the EMM values and vertical lines connect the levels being compared. *P*-values smaller than 0.05 indicate significant differences between paired levels. The *p*-value scale is non-linear.

Supplementary Figure 4 | Mean test diameter (±SE) of 14-day-old juvenile offspring of *H. erythrogramma* parents that were acclimated for 3 months at two temperature (black outline: ambient, red outline: +2°C) and two pH_T (white: 8.0, blue: 7.6) levels. The juveniles were reared in a range of temperatures (18–24°C). $n = 960$.

Supplementary Table 1 | Carbonate system conditions (±SD) during the 22 weeks of acclimation of *Heliocidaris erythrogramma* in six treatments of three temperature (ambient, +2°C, +3°C) and two pH_T (8.0, 7.6) levels. A_T, total alkalinity; DIC, dissolved inorganic carbon, ΩCa and ΩAr, calcite and aragonite saturation states, respectively. $n = 6$.

Supplementary Table 2 | Weekly, sampling-averaged temperatures (°C + SD) for three temperature profile treatments (ambient +0°C, elevated +2°C and +3°C), logged over 22 weeks of acclimation for the sea urchin *Heliocidaris erythrogramma*. Temperatures were adjusted weekly according to the mean SST profile determined from 5 years of *in situ* data (**Supplementary Figure 1**).

Supplementary Table 3 | Carbonate system conditions (±SD) in offspring treatments of four temperatures (18°C, 20°C, 22°C, 24°C) and two pH_T levels (8.0, 7.6). A_T, total alkalinity; DIC, dissolved inorganic carbon, ΩCa and ΩAr, calcite and aragonite saturation states, respectively. $n = 3$.

REFERENCES

Angilletta, M. J., Huey, R. B., and Frazier, M. R. (2009). Thermodynamic effects on organismal performance: is hotter better? *Physiol. Biochem. Zool.* 83, 197–206. doi: 10.1086/648567

Babcock, R. C., Bustamante, R. H., Fulton, E. A., Fulton, D. J., Haywood, M. D., Hobday, A. J., et al. (2019). Severe continental-scale impacts of climate change are happening now: extreme climate events impact marine habitat forming communities along 45% of Australia's coast. *Front. Mar. Sci.* 6:411. doi: 10.3389/fmars.2019.00411

Bellworthy, J., Menoud, M., Krueger, T., Meibpm, A., and Fine, M. (2019). Developmental carry over effects of ocean warming and acidification in corals from a potential climate refugium, the Gulf of Aqaba. *J. Exp. Biol.* 222:jeb186940. doi: 10.1242/jeb.186940

Benjamini, Y., and Hochberg, Y. (1995). Controlling the false discovery rate: a practical and powerful approach to multiple testing. *J. R. Stat. Soc. B* 57, 289–300. doi: 10.1111/j.2517-6161.1995.tb02031.x

Boyd, P. W., and Brown, C. J. (2015). Modes of interactions between environmental drivers and marine biota. *Front. Mar. Sci.* 2:9. doi: 10.3389/fmars.2015.00009

Boyd, P. W., Collins, S., Dupont, S., Fabricius, K., Gattuso, J. P., Havenhand, J., et al. (2017). Experimental strategies to assess the biological ramifications of multiple drivers of global ocean change a review. *Glob. Chang. Biol.* 24, 2239–2261. doi: 10.1111/gcb.14102

Brothers, C. J., Harianto, J., McClintock, J. B., and Byrne, M. (2016). Sea urchins in a high-CO_2 world: the influence of acclimation on the immune response to ocean warming and acidification. *Proc. R. Soc. B* 283:20161501. doi: 10.1098/rspb.2016.1501

Brothers, C. J., and McClintock, J. B. (2015). The effects of climate-induced elevated seawater temperature on the covering behavior, righting response, and Aristotle's lantern reflex of the sea urchin *Lytechinus variegatus*. *J. Exp. Mar. Biol. Ecol.* 467, 33–38. doi: 10.1016/j.jembe.2015.02.019

Brown, J. H., Gillooly, J. F., Allen, A. P., Savage, V. M., and West, G. B. (2004). Toward a metabolic theory of ecology. *Ecology* 85, 1771–1789. doi: 10.1890/03-9000

Byrne, M. (2011). Impact of ocean warming and ocean acidification on marine invertebrate life history stages: vulnerabilities and potential for persistence in a changing ocean. *Oceanog. Mar. Biol. Ann. Rev.* 49, 1–42.

Byrne, M., and Fitzer, S. (2019). The impact of environmental acidification on the microstructure and mechanical integrity of marine invertebrate skeletons. *Conser. Physiol.* 7:coz062. doi: 10.1093/conphys/coz062

Byrne, M., Foo, S. A., Ross, P. M., and Putnam, H. M. (2020). Limitations of cross-and multigenerational plasticity for marine invertebrates faced with global climate change. *Glob. Change Biol.* 26, 80–102. doi: 10.1111/gcb.14882

Byrne, M., and Hernández, J. C. (2020). "Sea urchins in a high CO_2 world: impacts of climate warming and ocean acidification across life history stages," in *Sea Urchins: Biology and Ecology*, 4th Edn, ed. J. M. Lawrence (Amsterdam: Elsevier), 281–297. doi: 10.1016/B978-0-12-819570-3.00016-0

Byrne, M., Ho, M., Selvakumaraswamy, P., Nguyen, H. D., Dworjanyn, S. A., and Davis, A. R. (2009). Temperature, but not pH, compromises sea urchin fertilization and early development under near-future climate change scenarios. *Proc. R. Soc. B* 276, 1883–1888. doi: 10.1098/rspb.2008.1935

Byrne, M., Ho, M. A., Wong, E., Soars, N., Selvakumaraswamy, P., Sheppard Brennand, H., et al. (2011a). Unshelled abalone and corrupted urchins, development of marine calcifiers in a changing ocean. *Proc. R. Soc. B* 278, 2376–2383. doi: 10.1098/rspb.2010.2404

Byrne, M., Selvakumaraswamy, P., Ho, M. A., Woolsey, E., and Nguyen, H. D. (2011b). Sea urchin development in a global change hotspot, potential for southerly migration of thermotolerant propagules. *Deep Sea Res. PT II* 58, 712–719. doi: 10.1016/j.dsr2.2010.06.010

Byrne, M., Lamare, M., Winter, D., Dworjanyn, S. A., and Uthicke, S. (2013). The stunting effect of a high CO_2 ocean on calcification and development in sea urchin larvae, a synthesis from the tropics to the poles. *Philos. Trans. R. Soc. B* 368:20120439. doi: 10.1098/rstb.2012.0439

Byrne, M., and Sewell, M. (2019). Evolution of maternal provisioning strategies in echinoids — selection for high quality juveniles. *Mar. Ecol. Prog. Ser.* 616, 95–106. doi: 10.3354/meps12938

Carey, N., Harianto, J., and Byrne, M. (2016). Sea urchins in a high CO_2 world: partitioned effects of body size, ocean warming and acidification on metabolic rate. *J. Exp Biol.* 219, 1178–1186. doi: 10.1242/jeb.136101

Catarino, A. I., Bauwens, M., and Dubois, P. (2012). Acid-base balance and metabolic response of the sea urchin *Paracentrotus lividus* to different seawater pH and temperatures. *Environ. Sci. Pollut.* 19, 2344–2353. doi: 10.1007/s11356-012-0743-1

Christensen, A. B., Nguyen, H. D., and Byrne, M. (2011). Thermotolerance and the effects of *hypercapnia* on the metabolic rate of the ophiuroid *Ophionereis schayeri*: inferences for survivorship in a changing ocean. *J. Exp. Mar. Biol. Ecol.* 403, 31–38. doi: 10.1016/j.jembe.2011.04.002

Collard, M., Catarino, A. I., Bonnet, S., Flammang, P., and Dubois, P. (2013). Effects of CO_2-induced ocean acidification on physiological and mechanical properties of the starfish *Asterias rubens*. *J. Exp. Mar. Biol. Ecol.* 446, 355–362. doi: 10.1016/j.jembe.2013.06.003

Collins, M., Knutti, R., Arblaster, J., Dufresne, J.-L., Fichefet, T., Friedlingstein, P., et al. (2013). "Long-term climate change: projections, commitments and irreversibility," in *Climate Change 2013: The Physical Science Basis. Contribution of Working Group I to the Fifth Assessment Report of the Intergovernmental Panel on Climate Change*, eds T. F. Stocker, D. Qin, and D. Plattner (Cambridge: Cambridge University Press).

Conover, R. J. (1966). Assimilation of organic matter by zooplankton. *Limnol. Oceanogr.* 11, 338–345. doi: 10.4319/lo.1966.11.3.0338

Conover, W. J., Johnson, M. E., and Johnson, M. M. (1981). A comparative study of tests for homogeneity of variances, with applications to the outer continental shelf bidding data. *Technometrics* 23, 351–361. doi: 10.2307/1268225

Cox, D. R. (1972). Regression models and life-tables. *J. R. Stat. Soc. B* 34, 187–220. doi: 10.1111/j.2517-61611972.tb00899.x

Delorme, N. J., and Sewell, M. A. (2016). Effects of warm acclimation on physiology and gonad development in the sea urchin *Evechinus chloroticus*. *Comp. Biochem. Phys. A* 198, 33–40. doi: 10.1016/j.cbpa.2016.03.020

Deutsch, C., Ferrel, A., Seibel, B., Portner, H. O., and Huey, R. B. (2015). Climate change tightens a metabolic constraint on marine habitats. *Science* 348, 1132–1135. doi: 10.1126/science.aaa1605

Dickson, A. G. (1990). Standard potential of the reaction: AgCl(s) + 1/2H2(g) = Ag(s) + HCl(Aq), and the standard acidity constant of the ion HSO4- in synthetic sea water from 273.15 to 318.15 K. *J. Chem. Thermodyn.* 22, 113–127. doi: 10.1016/0021-9614(90)90074-Z

Dickson, A. G., Sabine, C. L., and Christian, J. R. (2007). *Guide to Best Practices for Ocean CO_2 Measurements*. Sidney: North Pacific Marine Science Organization.

Dillon, M. E., Wang, G., and Huey, R. B. (2010). Global metabolic impacts of recent climate warming. *Nature* 467, 704–706. doi: 10.1038/nature09407

Dupont, S., Dorey, N., Stumpp, M., Melzner, F., and Thorndyke, M. (2013). Long-term and trans-life-cycle effects of exposure to ocean acidification in the green sea urchin *Strongylocentrotus droebachiensis*. *Mar. Biol.* 160, 1835–1843. doi: 10.1007/s00227-012-1921-x

Dworjanyn, S. A., and Byrne, M. (2018). Impacts of ocean acidification on sea urchin growth across the juvenile to mature adult life-stage transition is mitigated by warming. *Proc. R. Soc. B* 285:20172684. doi: 10.1098/rspb.2017.2684

Elliott, J. M., and Davison, W. (1975). Energy equivalents of oxygen consumption in animal energetics. *Oecologia* 19, 195–201. doi: 10.1007/BF00345305

Fofonoff, N. P., and Millard, R. C. (1983). Algorithms for computation of fundamental properties of seawater. *UNESCO Techn. Pap. Mar. Sci.* 44, 53–53.

Fuchs, H. L., Chant, R. J., Hunter, E. J., Curchitser, E. N., Gerbi, G. P., and Chen, E. Y. (2020). Wrong-way migrations of benthic species driven by ocean warming and larval transport. *Nat. Clim. Change* 10, 1052–1056. doi: 10.1038/s41558-020-0894-x

Gattuso, J. P., Epitalon, J. M., Lavigne, H., Orr, J., Gentili, B., Hagens, M., et al. (2020). *Seacarb: Seawater Carbonate Chemistry*. Available online at: https://CRAN.R-project.org/package =seacarb doi: 10.1038/s41558-020-0894-x (accessed May 23, 2020).

Gattuso, J. P., Magnan, A., Billé, R., Cheung, W. W. L., Howes, E. L., Joos, F., et al. (2015). Contrasting futures for ocean and society from different anthropogenic CO_2 emissions scenarios. *Science* 349:aac4722. doi: 10.1126/science.aac4722

Ghalambor, C. K., Mckay, J. K., Carroll, S. P., and Rezenick, D. N. (2007). Adaptive versus non-adaptive phenotypic plasticity and the potential for contemporary adaptation in new environments. *Funct. Ecol.* 21, 394–407. doi: 10.1111/j.1365-2435.2007.01283.x

Goldenberg, S. U., Nagelkerken, I., Ferreira, C. M., Ullah, H., and Connell, S. D. (2017). Boosted food web productivity through ocean acidification collapses under warming. *Glob. Change Biol.* 23, 4177–4184. doi: 10.1111/gcb.13699

Grambsch, P. M., and Therneau, T. M. (1994). Proportional hazards tests and diagnostics based on weighted residuals. *Biometrika* 81, 515–526. doi: 10.2307/2337547

Guderley, H., and St-Pierre, J. (2002). Going with the flow or life in the fast lane: contrasting mitochondrial responses to thermal change. *J. Exp. Biol.* 205, 2237–2249.

Gunderson, A. R., Armstrong, E. J., and Stillman, J. H. (2016). Multiple stressors in a changing world: the need for an improved perspective on physiological responses to the dynamic marine environment. *Annu. Rev. Mar. Sci.* 8, 357–378. doi: 10.1146/annurev-marine-122414-033953

Guppy, M., Fuery, C., and Flanigan, J. (1994). Biochemical principles of metabolic depression. *Comp. Biochem. Phys. B* 109, 175–189. doi: 10.1016/0305-0491(94)90001-9

Guppy, M., and Withers, P. (1999). Metabolic depression in animals: physiological perspectives and biochemical generalizations. *Biol. Rev.* 74, 1–40. doi: 10.1017/S0006323198005258

Harianto, J. (2019). *Physiological Responses of Adult and Juvenile Sea Urchins (Heliocidaris erythrogramma) to Warming and Acidification*. Ph. D thesis, The University of Sydney, Sydney.

Harianto, J., Carey, N., and Byrne, M. (2019). respR—An R package for the manipulation and analysis of respirometry data. *Methods Ecol. Evol.* 10, 912–920. doi: 10.1111/2041-210x.13162

Harianto, J., Nguyen, H. D., Holmes, S. P., and Byrne, M. (2018). The effect of warming on mortality, metabolic rate, heat-shock protein response and gonad growth in thermally acclimated sea urchins (*Heliocidaris erythrogramma*). *Mar. Biol.* 165:96. doi: 10.1007/s00227-018-3353-8

Harvey, B. P., Gwynn-Jones, D., and Moore, P. J. (2013). Meta-analysis reveals complex marine biological responses to the interactive effects of ocean acidification and warming. *Ecol. Evol.* 3, 1016–1030. doi: 10.1002/ece3.516

Hill, S. K., and Lawrence, J. M. (2006). Interactive effects of temperature and nutritional condition on the energy budgets of the sea urchins *Arbacia punctulata* and *Lytechinus variegatus* (Echinodermata: Echinoidea). *J. Mar. Biol. Assoc. U.K.* 8, 783–790. doi: 10.1017/50025315406013701

Holbrook, N. J., Scannell, H. A., Gupta, A. S., Benthuysen, J. A., Feng, M., Oliver, E. C., et al. (2019). A global assessment of marine heatwaves and their drivers. *Nat. Commun.* 10, 1–13. doi: 10.1038/s41467-019-10206-z

Hu, M. Y., Lein, E., Bleich, M., Melzner, F., and Stumpp, M. (2018). Trans-life cycle acclimation to experimental ocean acidification affects gastric pH homeostasis and larval recruitment in the sea star *Asterias rubens*. *Acta Physiol.* 2018:e13075. doi: 10.1111/alpha.13075

Johnson, R., Harianto, J., Thomson, M., and Byrne, M. (2020). The effects of long-term exposure to low pH on the skeletal microstructure of the sea urchin *Heliocidaris erythrogramma*. *J. Exp. Mar. Biol. Ecol.* 523, 151250. doi: 10.1016/j.jembe.2019.151250

Karelitz, S. E., Lamare, M. D., Mos, B., De Bari, H., Dworjanyn, S. A., and Byrne, M. (2019). Impact of growing up in a warmer, lower pH future on offspring performance: transgenerational plasticity in a pan-tropical sea urchin. *Coral Reefs* 38, 1085–1095. doi: 10.1007/s00338-019-01855-z

Karelitz, S. E., Lamare, M. D., Patel, F., Gemmell, N., and Uthicke, S. (2020). Parental acclimation to future ocean conditions increased development rates, but decreases survival in sea urchin larvae. *Mar. Biol.* 167:2. doi: 10.1007/s00227-019-3610-5

Karelitz, S. E., Uthicke, S., Foo, S. A., Barker, M. F., Byrne, M., Pecorino, D., et al. (2016). Ocean acidification has little effect on developmental thermal windows of echinoderms from Antarctica to the tropics. *Glob. Change Biol.* 23, 657–672. doi: 10.1111/gcb.13452

Keesing, J. K. (2020). "*Heliocidaris erythrogramma*," in *Sea Urchins: Biology and Ecology*, 4th Edn, ed. J. M. Lawrence (Amsterdam: Elsevier), 537–552. doi: 10.1016/b978-0-12-819570-3.00030-5

Keppel, E. A., Scrosati, R. A., and Courtenay, S. C. (2015). Interactive effects of ocean acidification and warming on subtidal mussels and sea stars from Atlantic Canada. *Mar. Biol. Res.* 11, 337–348. doi: 10.1080/17451000.2014.932914

Kordas, R. L., Harley, C. D., and O'Connor, M. I. (2011). Community ecology in a warming world: the influence of temperature on interspecific interactions in marine systems. *J. Exp. Mar. Biol. Ecol.* 400, 218–226. doi: 10.1016/j.jembe.2011.02.029

Kreyling, J., and Beier, C. (2013). Complexity in climate change manipulation experiments. *Bioscience* 63, 763–767. doi: 10.1093/bioscience/63.9.763

Kroeker, K. J., Gambi, M. C., and Micheli, F. (2013). Community dynamics and ecosystem simplification in a high-CO_2 ocean. *Proc. Natl. Acad. Sci. U.S.A.* 110, 12721–12726. doi: 10.1073/pnas.1216464110

Laegdsgaard, P., Byrne, M., and Anderson, D. T. (1991). Reproduction of sympatric populations of *Heliocidaris erythrogramma* and *H. tuberculata* (Echinoidea) in New South Wales. *Mar. Biol.* 110, 359–374. doi; 10.1007/BF01344355

Langsrud, Ø (2003). ANOVA for unbalanced data: use Type II instead of Type III sums of squares. *Stat. Comput.* 13, 163–167. doi: 10.1023/A:1023260610025

Lefevre, S. (2016). Are global warming and ocean acidification conspiring against marine ectotherms? A meta-analysis of the respiratory effects of elevated temperature, high CO_2 and their interaction. *Conserv. Physiol.* 4, 1–31. doi: 10.1093/conphys/cow009

Lighton, J. R. B. (2008). *Measuring Metabolic Rates: A Manual for Scientists*. Oxford: Oxford University Press.

Liu, X., Patsavas, M. C., and Byrne, R. H. (2011). Purification and characterization of meta-cresol purple for spectrophotometric seawater pH measurements. *Environ. Sci. Technol.* 45, 4862–4868. doi: 10.1021/es200665d

Lueker, T. J., Dickson, A. G., and Keeling, C. D. (2000). Ocean pCO2 calculated from dissolved inorganic carbon, alkalinity, and equations for K1 and K2: validation based on laboratory measurements of CO_2 in gas and seawater at equilibrium. *Mar. Chem.* 70, 105–119. doi: 10.1016/S0304-4203(00)00022-0

Manríquez, P. H., Torres, R., Matson, P. G., Lee, M. R., Jara, M. E., Seguel, M. E., et al. (2017). Effects of ocean warming and acidification on the early benthic ontogeny of an ecologically and economically important echinoderm. *Mar. Ecol. Prog. Ser.* 563, 169–184. doi: 10.3354/meps11973

Morley, S. A., Suckling, C. C., Clark, M. S., Cross, E. L., and Peck, L. S. (2016). Long-term effects of altered pH and temperature on the feeding energetics of the Antarctic sea urchin, *Sterechinus neumayeri*. *Biodiversity* 17, 34–45. doi: 10.1080/14888386.2016.1174956

Mos, B., Byrne, M., and Dworjanyn, S. A. (2016). Biogenic acidification reduces sea urchin gonad growth and increases susceptibility of aquaculture to ocean acidification. *Mar. Environ. Res.* 112, 39–48. doi: 10.1016/j.marenvres.2015.11.001

Munguia, P., and Alenius, B. (2013). The role of preconditioning in ocean acidification experiments: a test with the intertidal isopod *Paradella diane*. *Mar. Freshw. Behav. Physiol.* 46, 33–44. doi: 10.1080/10236244.2013.788287

Oliver, E. C. J., Donat, M. G., Burrows, M. T., Moore, P. J., Smale, D. A., Alexander, L. V., et al. (2018). Long and more frequent marine heatwaves over the past century. *Nat. Commun.* 9:1324. doi: 10.1038/s41467-018-03732-9

Pan, T. C. F., Applebaum, S. L., and Manahan, D. T. (2015). Experimental ocean acidification alters the allocation of metabolic energy. *Proc. Natl. Acad. Sci. U.S.A.* 112, 4696–4701. doi: 10.1073/pnas.1416967112

Parker, L. M., O'Connor, W. A., Byrne, M., Coleman, R. A., Virtue, P., Dove, M., et al. (2017). Adult exposure to ocean acidification is maladaptive for larvae of the Sydney rock oyster *Saccostrea glomerata* in the presence of multiple stressors. *Biol. Lett.* 13:20160798. doi: 10.1098/rsbl.2016.0798

Parsons, T. R., Maita, Y., and Lalli, C. M. (eds). (1984). "Determination of ammonia (alternative method)," in *A Manual of Chemical & Biological Methods for Seawater Analysis* (Amsterdam: Pergamon), 14–17. doi: 10.1016/b978-0-08-030287-4.50013-x

Pechenik, J. A. (2018). "Latent effects: surprising consequences of embryonic and larval experience on life after metamorphosis," in *Evolutionary Ecology of Marine Invertebrate Larvae*, eds T. J. Carrier, A. M. Reitzel, and A. Heyland (Oxford: Oxford University Press), 208–225.

Perez, F. F., and Fraga, F. (1987). Association constant of fluoride and hydrogen ions in seawater. *Mar. Chem.* 21, 161–168. doi: 10.1016/0304-4203(87)90036-3

Pörtner, H. O. (2010). Oxygen- and capacity-limitation of thermal tolerance: a matrix for integrating climate-related stressor effects in marine ecosystems. *J. Exp. Biol.* 213, 881–893. doi: 10.1242/jeb.037523

Powell, M., Marsh, A. G., and Watts, S. A. (2020). "Biochemical and energy requirements of gonad development in regular sea urchins," in *Sea Urchins: Biology and Ecology*, 4the Edn, eds J. M. Lawrence and J. M. Lawrence (Amsterdam: Elsevier), 51–64. doi: 10.1016/b978-0-12-819570-3.00004-4

Przeslawski, R., Byrne, M., and Mellin, C. (2015). A review and meta-analysis of the effects of multiple abiotic stressors on marine embryos and larvae. *Glob. Change Biol.* 21, 2122–2140. doi: 10.1111/gcb.12833

Royston, J. P. (1983). Some techniques for assessing multivariate normality based on the Shapiro-Wilk W. *J. R. Stat. Soc. C Appl.* 32, 121–133. doi: 10.2307/2347291

Runcie, J. W., Krause, C., Torres Garbarda, S. A., and Byrne, M. (2018). Technical note: continuous fluorescence-based monitoring of seawater pH in situ. *Biogeosciences* 15, 4291–4299. doi: 10.5194/bg-15-4291-2018

Schielzeth, H., and Nakagawa, S. (2013). Nested by design: model fitting and interpretation in a mixed model era. *Methods Ecol. Evol.* 4, 14–24. doi: 10.1111/j.2041-210x.2012.00251.x

Schmidt, C., Kucera, M., and Uthicke, S. (2014). Combined effects of warming and ocean acidification on coral reef foraminifera *Marginopora vertebralis* and *Heterostegina depressa*. *Coral Reefs* 33, 805–818. doi: 10.1007/s00338-014-1151-4

Schulte, P. M. (2015). The effects of temperature on aerobic metabolism: towards a mechanistic understanding of the responses of ectotherms to a changing environment. *J. Exp. Biol.* 218, 1856–1866. doi: 10.1242/jeb.118851

Seebacher, F., White, C. R., and Franklin, C. E. (2014). Physiological plasticity increases resilience of ectothermic animals to climate change. *Nat. Clim. Chang.* 5, 61–66. doi: 10.1038/NCLIMATE2457

Sheppard Brennand, H., Soars, N., Dworjanyn, S. A., Davis, A. R., and Byrne, M. (2010). Impact of ocean warming and ocean acidification on larval development and calcification in the sea urchin *Tripneustes gratilla*. *PLoS One* 5:e11372. doi: 10.1371/journal.pone.0011372

Somero, G. N. (2012). The physiology of global change: linking patterns to mechanisms. *Annu. Rev. Mar. Sci.* 4, 39–61. doi: 10.1146/annurev-marine-120710-100935

Storey, K. B., and Storey, J. M. (1990). Metabolic rate depression and biochemical adaptation in anaerobiosis, hibernation and estivation. *Q. Rev. Biol.* 65, 145–174. doi: 10.1086/416717

Stumpp, M., Wren, J., Melzner, F., Thorndyke, M. C., and Dupont, S. T. (2011). CO_2 induced seawater acidification impacts sea urchin larval development I: elevated metabolic rates decrease scope for growth and induce developmental delay. *Comp. Biochem. Physiol. Part A Mol. Integr. Physiol.* 160, 331–340. doi: 10.1016/j.cbpa.2011.06.022

Suckling, C. C., Clark, M. S., Richard, J., Morley, S. A., Thorne, M. A. S., Harper, E. M., et al. (2015). Adult acclimation to combined temperature and pH stressors significantly enhances reproductive outcomes compared to short-term exposures. *J. Anim. Ecol.* 84, 773–784. doi: 10.1111/1365-2656.12316

Sweet, M., Bulling, M., and Williamson, J. (2016). New disease outbreak affects two dominant sea urchin species associated with Australian temperate reefs. *Mar. Ecol. Prog. Ser.* 551, 171–183. doi: 10.3354/meps11750

Thompson, R. M., Beardall, J., Beringer, J., Grace, M., and Sardina, P. (2013). Means and extremes: building variability into community-level climate change experiments. *Ecol. Lett.* 16, 799–806. doi: 10.1111/ele.12095

Thomsen, J., Haynert, K., Wegner, K. M., and Melzner, F. (2015). Impact of seawater carbonate chemistry on the calcification of marine bivalves. *Biogeosciences* 12, 1543–1571. doi: 10.5194/bg-12-4209-2015

Uthicke, S., Liddy, M., Nguyen, H. D., and Byrne, M. (2014). Interactive effects of near-future temperature I crease and ocean acidification on physiology and gonad development in adult Pacific sea urchin, *Echinometra* sp. A. *Coral Reefs* 33, 831–845. doi: 10.1007/s00338-014-1165-y

Uthicke, S., Patel, F., Karelitz, S., Luter, H. M., Webster, N. S., and Lamare, M. (2020). Key biological responses over two generations of the sea urchin *Echinometra* sp. A under future ocean conditions. *Mar. Ecol. Prog. Ser.* 637, 87–101. doi: 10.3354/meps13236

Winberg, G. G. (1960). Rate of metabolism and food requirements of fishes. *Transl. Ser. Fish. Res. Board Can.* 194, 1–202.

Wong, J., Johnson, K. M., Kelly, M. W., and Hofmann, G. E. (2018). Transcriptomics reveal transgenerational effects in purple sea urchin embryos: adult acclimation to upwelling conditions alters the response of their progeny to differential pCO2 levels. *Mol Ecol.* 27, 1120–1137. doi: 10.1111/mec.14503

Yeruham, E., Rilov, G., Shpigel, M., and Abelson, A. (2015). Collapse of the echinoid *Paracentrotus lividus* populations in the Eastern Mediterranean-result of climate change? *Sci. Rep.* 5, 13479–13479. doi: 10.1038/srep13479

Zhang, H., Shin, P. K. S., and Cheung, S. G. (2015). Physiological responses and scope for growth upon medium-term exposure to the combined effects of ocean acidification and temperature in a subtidal scavenger *Nassarius conoidalis*. *Mar. Environ. Res.* 106, 51–60. doi: 10.1016/j.marenvres.2015.03.001

Zhang, H., Shin, P. K. S., and Cheung, S. G. (2016). Physiological responses and scope for growth in a marine scavenging gastropod, *Nassarius festivus* (Powys, 1835), are affected by salinity and temperature but not by ocean acidification. *ICES J. Mar. Sci.* 73, 814–824. doi: 10.1016/j.marenvres.2015.03.001

Zhao, C., Zhang, L., Shi, D., Ding, J., Yin, D., Sun, J., et al. (2018). Transgenerational effects of ocean warming on the sea urchin *Strongylocentrotus intermedius*. *Ecotox. Environ. Saf.* 151, 212–219. doi: 10.1016/j.marenvres.2015.03.001

Conflict of Interest: The authors declare that the research was conducted in the absence of any commercial or financial relationships that could be construed as a potential conflict of interest.

The reviewer MAS declared a past co-authorship with one of the authors MB to the handling editor.

frontiers in Marine Science

ORIGINAL RESEARCH
published: 19 March 2021
doi: 10.3389/fmars.2021.643377

Increased Thermal Sensitivity of a Tropical Marine Gastropod Under Combined CO_2 and Temperature Stress

*Jay J. Minuti[1], Charlee A. Corra[1,2], Brian S. Helmuth[2] and Bayden D. Russell[1]**

[1] The Swire Institute of Marine Science and School of Biological Sciences, The University of Hong Kong, Hong Kong, China, [2] Marine Science Center, Northeastern University, Nahant, MA, United States

The ability of an organism to alter its physiology in response to environmental conditions offers a short-term defense mechanism in the face of weather extremes resulting from climate change. These often manifest as multiple, interacting drivers, especially pH and temperature. In particular, decreased pH can impose constraints on the biological mechanisms which define thermal limits by throwing off energetic equilibrium and diminishing physiological functions (e.g., in many marine ectotherms). For many species, however, we do not have a detailed understanding of these interactive effects, especially on short-term acclimation responses. Here, we investigated the metabolic plasticity of a tropical subtidal gastropod (*Trochus maculatus*) to increased levels of CO_2 (700 ppm) and heating (+3°C), measuring metabolic performance (Q_{10} coefficient) and thermal sensitivity [temperature of maximum metabolic rate (T_{MMR}), and upper lethal temperature (ULT)]. Individuals demonstrated metabolic acclimation in response to the stressors, with T_{MMR} increasing by +4.1°C under higher temperatures, +2.7°C under elevated CO_2, and +4.4°C under the combined stressors. In contrast, the ULT only increased marginally in response to heating (+0.3°C), but decreased by −2.3°C under CO_2, and −8.7°C under combined stressors. Therefore, although phenotypic plasticity is evident with metabolic acclimation, acute lethal temperature limits seem to be less flexible during short-term acclimation.

Keywords: thermal physiology, ocean warming, ocean acidification, metabolic function, physiological plasticity, acclimation, marine gastropod

OPEN ACCESS

Edited by:
Peng Jin,
University of Guangzhou, China

Reviewed by:
Xiutang Yuan,
Chinese Academy of Sciences (CAS), China
Wei Li,
Huangshan University, China

***Correspondence:**
Bayden D. Russell
brussell@hku.hk

Specialty section:
This article was submitted to Global Change and the Future Ocean, a section of the journal Frontiers in Marine Science

Received: *18 December 2020*
Accepted: *26 February 2021*
Published: *19 March 2021*

Citation:
Minuti JJ, Corra CA, Helmuth BS and Russell BD (2021) Increased Thermal Sensitivity of a Tropical Marine Gastropod Under Combined CO_2 and Temperature Stress. Front. Mar. Sci. 8:643377. doi: 10.3389/fmars.2021.643377

INTRODUCTION

Physiological responses to abiotic conditions, mediated by individual organisms, manifest as population- and ultimately community-level responses. Therefore, identifying the mechanisms by which the survival and fitness of individual organisms change in response to environmental extremes will help determine broader ecosystem effects to ongoing climate change (Pörtner, 2008). Changes in body temperature are often among the most commonly studied responses for ectothermic marine invertebrates as temperature plays a large part in controlling cellular to physiological reactions, which in turn affects metabolism, growth and reproductive rates (Grigaltchik et al., 2012; Sinclair et al., 2016). Even small changes in the environment can cause

a broad range of physiological responses due to variation among and within species (Harley et al., 2017; Wang et al., 2018). In particular, there has been an increasing focus on the physiological impacts of heatwaves, which are increasing in magnitude and frequency, increasing the likelihood that organisms are being subjected to thermal conditions beyond their optimal and lethal limits (Lannig et al., 2010; Sinclair et al., 2016).

Large variation in responses, even within a species, highlights that genetic variation and variability in physiological plasticity can affect the likelihood that populations survive short-term extremes (Wang et al., 2018). Should enough individuals be able to acclimate to novel conditions during extreme events, populations and communities may be able to handle future conditions better than currently predicted (Seebacher et al., 2014). Phenotypic plasticity allows organisms to respond to stressful environmental conditions and is thought to be determined by environmental selection pressure and an organism's sensitivity to change (Parmesan and Yohe, 2003; Hoffmann and Sgró, 2011). For example, intertidal species are naturally exposed to large variation in temperature, regularly being exposed to extremes, and as such are typically already living much nearer their thermal maxima. Consequently, intertidal species generally demonstrate at least phenotypic plasticity in their thermal optima but little capability of increasing upper lethal limits (Stillman and Somero, 2000; Nguyen et al., 2011). In contrast, subtidal organisms are generally considered to live in a relatively stable environment and therefore thought to exhibit lower plasticity but potentially a greater capacity for acclimation.

Importantly, however, we understand considerably less of how organisms acclimate to changes in multiple stressors, particularly temperature and altered pH due to increases in CO_2 concentrations (Gunderson et al., 2016; Kroeker et al., 2017). We know especially little about the ability of subtidal species to modulate their physiology in response to multiple stressors, since until recently it has largely been assumed that subtidal environments are temporally and spatially stable (Bates et al., 2018). With the advent of increased ability to monitor environmental conditions such as temperature and pH at finer temporal and broader spatial scales, it is now apparent that these environments are anything but stable and that underwater "weather" is an important yet relatively understudied feature of the marine environment (Bates et al., 2018). For example, in coastal habitats pH can fluctuate by an entire unit within hours to days (Kelly and Hofmann, 2013; Hofmann et al., 2014). Changes in temperature can likewise occur over a broad range of temporal and spatial scales, from increases of several degrees due to solar heating (or decreases due to upwelling) to seasonal increases of the same magnitude that can last several months (Bates et al., 2018; Pansch et al., 2018). Therefore, understanding the ability of organisms to remodel their physiology is crucial to predict their capacity to respond to, and persist under, combinations of environmental stressors such as increasing CO_2 concentrations and temperature (Hoffmann and Sgró, 2011; Seebacher et al., 2014).

Exposure to elevated CO_2 and temperatures at levels expected in the coming century (or even much sooner) have been shown to have greater effects on marine ectotherms than the stressors in isolation (Byrne, 2011; Byrne and Przeslawski, 2013; Brothers et al., 2016; Carey et al., 2016). For example, tropical urchins (*Echinometra* sp.) suffer far greater reduction in growth and higher metabolic activity when exposed simultaneously to elevated CO_2 (∼860–940 μatm) and temperature (ambient +2 to 3°C) than when either is considered alone (Uthicke et al., 2014). Intertidal limpets not only have higher sensitivity to hotter environments under elevated CO_2 concentrations, but at a population level have greater variation in individual responses to temperature, signifying that some individuals have greater ability to alter their tolerance limits (Wang et al., 2018). Such variable responses ultimately determine the potential for acclimation and plasticity within populations, producing a selective advantage by extending the organism's physiological (fundamental) niche. Critical thermal maximum and minimum (CT_{MAX} and CT_{MIN}) are commonly used to assess the temperature beyond which organisms can no longer supply adequate oxygen to cells to fuel metabolism (Pörtner, 2010). Elevated CO_2 in conjunction with increased temperature can alter thermal acclimation of metabolic capacity by decreasing the CT_{MAX}, potentially resulting in a greater susceptibility to global heating (Manríquez et al., 2019). Whether organisms can shift their maximum threshold temperatures will therefore provide an indication of the extent of the ability of populations and species to respond to rapidly changing environmental conditions.

Here we assessed the acclimation potential of a key grazing subtidal gastropod to elevated levels of CO_2 and temperature, in particular the ability to alter metabolic performance (Q_{10} coefficient), shift their temperature of maximum metabolic rate (T_{MMR}) or their upper lethal temperature (ULT). The gastropod *Trochus maculatus* is commonly found in shallow subtidal habitats in Hong Kong, feeding on a variety of different micro- and macroalgae, playing an important role in maintenance of benthic habitats (Cox and Murray, 2006; Maboloc and Mingoa-Licuanan, 2013). We experimentally tested the influence of elevated CO_2 and temperature on the physiology of *T. maculatus* to determine their acclimation potential in the face of ongoing and future climate change. We tested the hypothesis that whilst elevated temperature would cause a shift in metabolic thresholds, the addition of elevated CO_2 would inhibit this effect. Under ocean heating, an inability to increase upper lethal temperatures, either through phenotypic plasticity or longer-term acclimation, would likely lead to population declines and loss in ecological function.

MATERIALS AND METHODS

Field Collection

Adult gastropods (*Trochus maculatus*) are widely distributed in south-east Asia and the central Western-Pacific Ocean found in shallow coral and rocky reef habitats, and commonly collocated with other benthic grazers such as sea urchins (Cox and Murray, 2006; Maboloc and Mingoa-Licuanan, 2013). In Hong Kong, the sub-tropical climate exposes these organisms to cold winters with lows of ∼16°C, and warm summers, with shallow marine water temperatures having reached a maximum

of 31°C locally (Environmental Protection Department (EPD) Hong Kong, 2019). *T. maculatus* were collected from subtidal rocky substrate (∼1–4 m depth) in Clearwater Bay (Shek Mei Tau), Hong Kong (22°16′58.5″N 114°17′40.6″E) and taken to the Swire Institute of Marine Science (SWIMS) where they were transferred immediately into indoor plastic aquaria (12 L) ($n = 15$ per treatment with 1 individual per tank) with flow-through, sand-filtered seawater at ambient summer conditions (28°C, Hong Kong summer average for subtidal waters). Each aquarium was aerated with ambient air and maintained 12:12 day/night lighting conditions with LED lights fitted above the tanks. Food was provided *ad libitum* as turf-forming and filamentous algae growing on rocks taken from the field collection site during acclimation and experimental treatments.

CO_2 and Temperature Manipulation

We tested the effects of two CO_2 conditions [400 ppm/8.1 pH (control) and 700 ppm/7.8 pH (elevated)] and two temperatures [28°C (control) and 31°C] in fully crossed combinations (n = 15 per treatment) representing the present day and IPCC RCP 6.0 scenario for the year 2100, and the highest locally experienced temperatures. After a 2-week acclimation period to ambient conditions in the laboratory, CO_2 and temperature were raised to treatment conditions gradually over a period of 2 days and maintained for 12 weeks. Aquaria were placed within water baths to help maintain thermal stability, with each aquarium containing a submersible glass heater to control temperature to the pre-designated treatment. Each aquarium was supplied with an independent, intermittent flow-through system which allowed daily water changes with sand-filtered seawater taken from the bay at SWIMS. CO_2 treatment conditions were maintained by bubbling each individual aquarium with air that was pre-mixed to the treatment CO_2 concentration using gas flow meters (Masterflex® Direct-Reading Variable-Area Flowmeters with Valve for Air and CO_2, with Masterflex® Correlated and Direct-Reading Variable Area Flowmeter Multitube Frames Cole-Palmer, Ill, United States). The pH and temperature in each aquarium were monitored using a handheld multiprobe twice per day (Seven2go, Mettler Toledo, OH, United States). Salinity was measured once weekly and water samples were analyzed weekly for total alkalinity using an Alkalinity Titrator (T50, Mettler Toledo, OH, United States). Seawater carbonate parameters [CO_2, bicarbonate (HCO_3^-) and carbonate (CO_3^{2-}) ion concentration] and calcite and aragonite saturation states (**Ω**cal and **Ω**ara) were calculated using CO2SYS program for Excel (Lewis and Wallace, 1998) with constants from Mehrbach et al. (1973) as adjusted by Dickson and Millero (1987) from recorded temperature, pH and TA values (**Table 1**).

Thermal Ramps

After 12 weeks at treatment conditions, n = 10 individuals were subjected to gradually increasing temperatures over a thermal ramp in order to assess how their metabolic rates changes after exposure to treatment conditions, to determine the Q_{10} coefficient, the upper lethal temperature (ULT) and temperature of maximum metabolic rate (T_{MMR}). Individual gastropods were placed into sealed respirometry chambers (0.5 L) with filtered, oxygen saturated seawater which had been CO_2 treated according to the relevant treatment. Each chamber was placed into a water bath set at 17°C (average winter seawater temperature in Hong Kong) with a small water pump placed in the bath to maintain a homogenous temperature. After being left for 30 min for the gastropods to settle, the temperature was increased by 2°C per hour until all animals died (lack of reaction to physical stimulus). After every 1 h (2°C) increment, temperature was held constant for 30 min for the metabolic rate to be recorded. Oxygen concentration within the respirometry chambers was recorded before and after each 30 min incubation using an internal optical oxygen spot measuring system (Fibox4, PreSens). Metabolic rate MO_2 (mg L^{-1} g FW^{-1} h^{-1}) was calculated using the following equation:

$$MO_2 \quad \frac{O_2 V}{w}$$

where ΔO_2 is the linear regression slope of oxygen concentration over time (mg L^{-1} h^{-1}), V is the volume of seawater (L), and W is the fresh weight of the gastropod (g). Blank chambers with no organisms inside were used to account for any possible biological activity in the water and deducted accordingly.

Temperature Coefficient (Q_{10})

The Q_{10} coefficient was calculated using metabolic rate data from the thermal ramp, and calculated from the rates at 10°C below and up to the T_{MMR} [T_{MMR} based off the data from an Exponentially Modified Gaussian Function (EMG) model described below] using the following equation:

$$Q_{10} \quad \left(\frac{R_2}{R_1}\right)^{\frac{10}{T2-T1}}$$

where R is the metabolic rate ($R1$ and $R2$ are the metabolic rate at $T1$ and $T2$, respectively), and T is the temperature (°C).

Morphological Biometrics

We also measured morphological parameters at the beginning and end of the experimental period to test for any physical changes caused by elevated CO_2 (reduced pH), relating to total weight, shell size and shape (n = 15). The total weight of each intact individual (g), height and width were recorded (mm) before and after exposure to the experimental treatments. These dimensions were then used to calculate measures relating to shell shape, i.e., aspect ratio, which was determined as width: height. The values of these measures were calculated for each individual as percentage change between the values at the beginning and end of the experimental exposure period.

Statistical Analysis

Two-factor ANOVAs were used to test for the effects of CO_2 (ambient control vs. elevated) and temperature (control vs. elevated) (fixed and orthogonal) on weight (total weight), shell morphology (height, width) and aspect ratio (width: height) using Euclidean distance in PERMANOVA for PRIMER 7. An Exponentially Modified Gaussian Function (EMG) model

TABLE 1 | Seawater carbonate physio-chemical parameters during the experimental period.

Treatment		Measured			Calculated				
Temp(°C)	(CO_2) (ppm)	pH	Temp (°C)	TA (μmol ml^1)	CO_2 (μatm)	ΩCa	ΩAr	HCO_3^- (μmol kg^{-1})	CO_3^{2-}
28	400	8.08 ± 0.02	27.9 ± 0.01	2,136 ± 13.6	329.9 ± 15.7	5.52 ± 0.12	3.66 ± 0.08	1577.7 ± 21.7	225.3 ± 4.5
	700	7.81 ± 0.01	28.0 ± 0.02	2,225 ± 15.0	721.8 ± 8.90	3.54 ± 0.07	2.34 ± 0.05	1872.7 ± 8.75	143.9 ± 2.99
31	400	8.08 ± 0.02	30.9 ± 0.06	2,144 ± 9.56	330.0 ± 19.4	5.99 ± 0.21	4.01 ± 0.14	1543.7 ± 19.8	242.2 ± 8.67
	700	7.82 ± 0.01	30.8 ± 0.05	2,184 ± 10.1	683.9 ± 18.4	3.88 ± 0.06	2.60 ± 0.04	1798.7 ± 13.5	156.9 ± 2.26

Temperature and pH in each tank were measured daily (n = 15) and Total Alkalinity (TA) in each tank measured weekly (n = 15). CO_2 (μatm), ΩCa, ΩAr, HCO_3^- and CO_3^{2-} were calculated based on the measured parameters using CO2SYS program for Excel (Lewis and Wallace, 1998) with constants from Mehrbach et al. (1973) as adjusted by Dickson and Millero (1987). Values are means ± standard error.

was fitted for metabolic rates over the temperature ramp to extract the T_{MMR}, ULT, and to model the change in metabolic rate over the temperature ramp. Temperature coefficient (Q_{10}) data were analyzed using a two-way ANOVA analysis with Tukey's post-doc test, both of which were performed using RStudio Version 1.1.463 with 95% confidence intervals with all analysis.

RESULTS

Thermal Ramps and Critical Limits

Metabolic rates of the gastropods across thermal ramps were well described by the Exponentially Modified Gaussian Function, demonstrating a positive relationship with temperature up until the temperature of maximum metabolic rate (T_{MMR}) followed by a sharp decline to lethal limits which resulted in mortality (ULT). The T_{MMR} increased from 31.6°C in the control treatment to 35.6°C in the high temperature treatment, 34.3°C in the high CO_2 treatment and 36°C in the combination treatment (**Figure 1** and **Table 2**). The ULT did not increase following exposure to elevated temperature (47.5°C vs. 47.8°C in control and elevated temperature, respectively). In contrast, high CO_2 caused in a decline in the ULT to 45.2°C (−2.3°C decrease), and an even greater decline of 8.7°C in the ULT under the combination of high CO_2 and temperature (38.8°C; **Figure 1** and **Table 2**).

Temperature Coefficient (Q_{10})

Elevated CO_2 negatively affected the temperature coefficients (Q_{10} rates) of *T. maculatus*, with individuals exposed to elevated CO_2 having Q_{10} values >25% lower than under ambient CO_2 [two-way ANOVA, $F_{(1,\ 1)} = 4.3$, $P = 0.04$, **Figure 2** and **Table 2**]. In contrast, there was no significant effect of elevated temperature [two-way ANOVA, $F_{(1,\ 1)} = 0.06$, $P > 0.05$] or for the interaction between temperature and CO_2 [two-way ANOVA, $F_{(1,\ 1)} = 0.79$, $P > 0.05$] on Q_{10} rates.

Morphological Biometrics

As could be expected from exposure to elevated CO_2 for relatively short periods (relative to lifespan), none of the experimental treatments caused any significant change to gastropod weight or shell morphometrics over the length of the experiment (**Figure 3** and **Supplementary Tables S1**, **S2**).

Experimental Conditions

The control treatment at 28°C–400 ppm had a measured pH of 8.08 ± 0.02 and calculated CO_2 (μatm) of 329.9 ± 15.7, with similar pCO_2 conditions found in the higher temperature treatment at 31°C–400 ppm, with a pH of 8.08 ± 0.02 and calculated CO_2 (μatm) of 330.0 ± 19.4. In the higher CO_2 treatment at 28°C–700 ppm, there was a lower measured pH of 7.81 ± 0.01 and higher calculated CO_2 (μatm) of 721.8 ± 8.90 compared with the controls. Lastly, with the higher temperature and higher CO_2 treatment at 31°C–700 ppm, there was a lower measured pH of 7.82 ± 0.01 and higher calculated CO_2 (μatm) of 683.9 ± 18.4 compared with the controls (**Table 1**).

DISCUSSION

Whether organisms can withstand altered environmental conditions brought about by global climate change depends on the capacity for their physiological mechanisms to adjust and acclimate to continually changing local conditions. Here, we demonstrate that a key subtidal gastropod, *T. maculatus*, showed the potential for acclimation to higher temperatures, but this effect was diminished by coincident elevated CO_2. When exposed to hotter conditions alone, the temperature at which metabolic rates are the highest (T_{MMR}) increased, but the upper lethal temperature (ULT) was static, which would suggest that when exposed to elevated temperatures alone *T. maculatus* can display metabolic plasticity but that the upper lethal limits are relatively fixed and cannot increase. Deviation from energetic homeostasis as a result of sub-optimal conditions is generally thought to be due to energetic demands exceeding energy gain, which can be compensated for with increased consumption (Leung et al., 2017) or elevated metabolic flux to sustain the ATP demand (Lannig et al., 2010). These strategies are time-limited, meaning that a lack of compensatory feeding to fulfill new higher energy demands and capacity for cellular energy generation results in metabolic depression, an adaptive strategy used across all animal phyla (Guppy and Withers, 1999; Marshall et al., 2011), suggesting lack of energy acquisition may have played an important part in this species' response. This energy mismatch is exacerbated further when the stressors are combined, as it is likely that the energetic stress of the CO_2 exposure drove mortality at lower temperatures. The increased T_{MMR} under future conditions (combined elevated CO_2 and temperature)

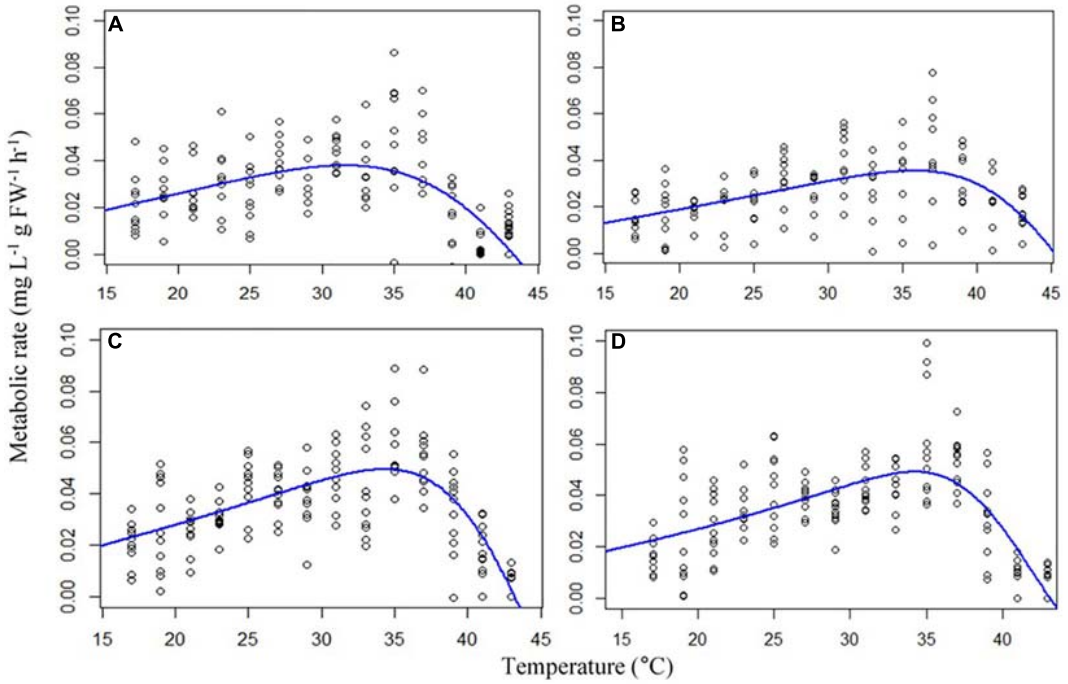

FIGURE 1 | Thermal ramps showing metabolic rates (mg L^{-1} g FW^{-1} h^{-1}) of the gastropod *Trochus maculatus* (n = 10) after 12-weeks exposure to **(A)** control conditions (28°C, 400 ppm) **(B)** high temperature (31°C, 400 ppm) (**C**) high CO_2 (28°C, 700 ppm) and **(D)** a combination of both high temperature and CO_2 (31°C, 700 ppm). Curves are modeled using an Exponentially Modified Gaussian Function.

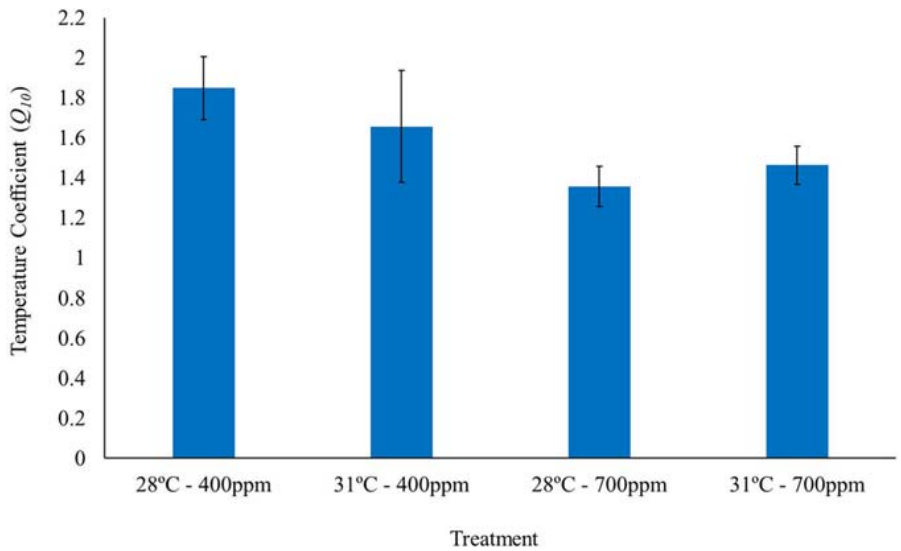

FIGURE 2 | Temperature coefficients (Q_{10}) of gastropods acclimated to different temperatures (28 and 31°C) and CO_2 concentrations (400 and 700 ppm) (n = 15). Temperature coefficient values were calculated for each individual gastropod, as the respiration rate at 10°C below and up to the corresponding T_{MMR} for that treatment. Bars represent mean Q_{10} of all individuals in the given treatment ± standard error.

is therefore likely to be due to the influence of temperature-induced acclimation, meaning that energetic demands at a given temperature would be lower than prior to acclimation (Seebacher et al., 2014; Leung et al., 2021). In contrast, the reduction in ULT under these conditions would not likely pose a major offset to this acclimation in the near future for subtidal organisms as environmental conditions should not reach the reduced ULT (∼39°C when current summer extremes are ∼32°C). For intertidal organisms, however, this benefit would be eliminated by the greater reduction in upper threshold temperatures

TABLE 2 | Temperature at maximum metabolic rate (T_{MMR}) and upper lethal temperature (ULT) as described by an Exponentially Modified Gaussian Function (EMG) model for *Trochus maculatus* after 12-weeks exposure to elevated temperature (31°C) and elevated CO_2 (700 ppm).

		T_{MMR} (°C)	Difference	ULT	Difference	Q_{10}
400 ppm	28°C	31.6	/	47.5	/	1.85
	31°C	35.7	**+4.1**	47.8	**+0.3**	1.65
700 ppm	28°C	34.3	**+2.7**	45.2	**−2.3**	1.36
	31°C	36	**+4.4**	38.8	**−8.7**	1.46

The difference in T_{MMR} and ULT in the elevated compared to the control treatment (400 ppm, 28°C) predicted by the EMG model are also shown (in bold). Mean temperature coefficient (Q_{10}) values for each treatment are shown in the last column.

whenever elevated CO_2 exposure occurs because they are regularly exposed to extreme temperatures (up to 55°C intertidal rock temperature recorded in Hong Kong; Ng et al., 2017).

The effects of CO_2 and temperature on biological functions have been shown to be synergistic across numerous taxa, with the extent of the effects dependent on life-stages and species-specific sensitivities (Dupont et al., 2010; Byrne and Przeslawski, 2013; Hardy et al., 2014). For example, hypercapnia reduces oxygen partial pressure in the haemolymph of crabs (*Cancer pagurus*) during progressive warming (when exposed to 1% CO_2) as well as a 5°C decline in the upper thermal limits of aerobic scope, substantially narrowing the thermal window of this species (Metzger et al., 2007). A similar effect was demonstrated with green abalone (*Haliotis fulgens*) under a combination of hypoxia and hypercapnia, which elicited large changes to metabolic rates, as well as strong accumulation of amino acids, osmolytes and anaerobic end products during moderate temperatures (Tripp-Valdez et al., 2017), indicating the species had reached critical limits and entered a state severe stress (Pörtner, 2010; Tripp-Valdez et al., 2017). In contrast, higher molluscs can regulate acid-base balance by upregulating HCO_3^- to compensate for hypercapnia induced respiratory acidosis, thus avoiding loss of metabolic equilibria or disrupting aerobic capacity (e.g., the cephalopod *Sepia officinalis*; Gutowska et al., 2010). Therefore, the capacity for acid-base regulation is highly variable, particularly among invertebrates, and plays an important role in defense against CO_2-induced physiological stress. Based on the reduction in metabolic function in our species under hypercapnia, we suggest that it is likely that our study species may not have the capacity to regulate acid-base balance to a large degree.

Increased concentrations of CO_2 can directly affect shell-forming invertebrates by erosion of calcium-carbonate containing skeletons or decreasing calcification rates (Feely et al., 2004; Kroeker et al., 2010; Harvey et al., 2013). Some gastropods, including *Trochidae* species, have a nacreous layer in their inner shell structure which is formed by hexagonal platelets of aragonite along with other microstructures of aragonite and calcite which are unique to some gastropods and cephalopods (Chunhabundit et al., 2001; Nudelman et al., 2006). A meta-analysis by Kroeker et al. (2010) of the biological responses to ocean acidification including survival, calcification,

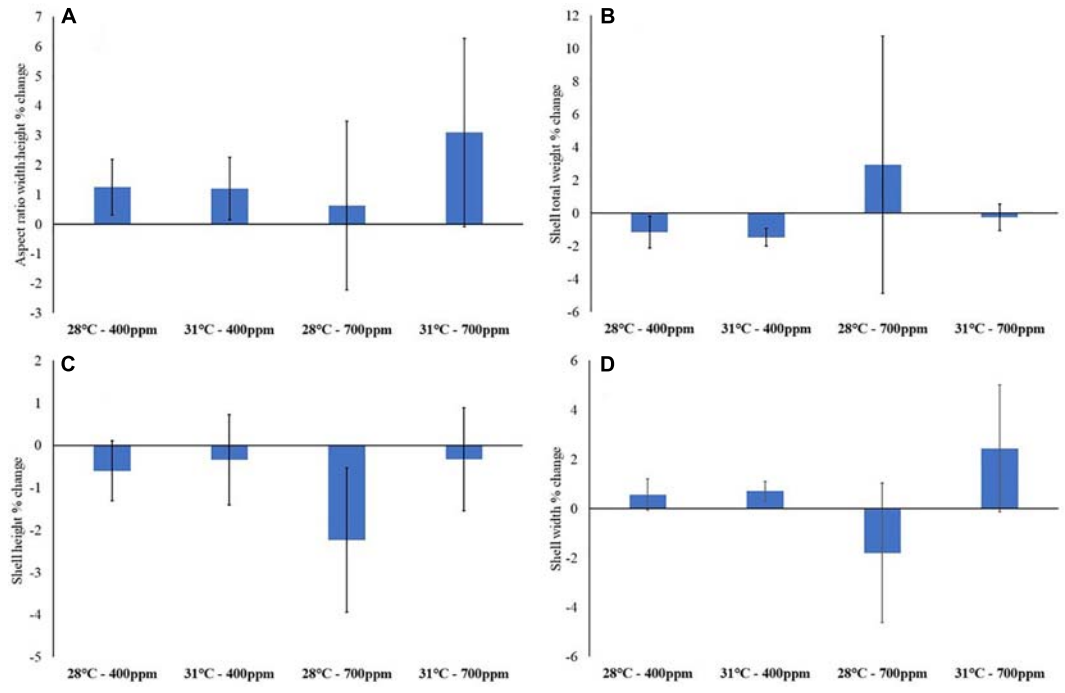

FIGURE 3 | Gastropod biometrics after 12-weeks exposure to control conditions (28°C, 400 ppm), high temperature (31°C, 400 ppm), high CO_2 (28°C, 700 ppm) and a combination of both high temperature and CO_2 (31°C, 700 ppm). **(A)** Aspect ratio (width: height); **(B)** total weight (g); **(C)** shell height; and **(D)** shell width (mm) (n = 15). Values are percentage change from prior to exposure to experimental conditions ± standard error.

growth and reproduction highlighted that organisms which use less soluble, more stable forms of calcium carbonate ($CaCO_3$) (e.g., some sea urchins), such as the trochid gastropod in this study, are more resilient to ocean acidification that those which utilize less stable and less soluble forms. While we did not see any significant shell erosion and this could be interpreted as a more resilient shell chemistry, the experiment here was explicitly designed to test for the physiological effects of the stressors which manifest over shorter exposures. Therefore, whilst the immediate impact of these environmental stressors on key physiological processes will determine the ability of an organism to maintain energetic homeostasis, as well as plasticity and critical limits of thermotolerance, the impact of these stressors on shell formation and degradation should be considered over the longer term.

Although the temperature at which metabolic rate is at its peak appears to be plastic, critical limits are far less flexible in terms of acclimation, but rather more susceptible to reduction under stress. Indeed, with the added effect of CO_2, upper lethal temperatures decreased substantially. This phenomenon has been demonstrated within a unique wild population of European perch fish (*Perca fluviatilis*) which had been warmed 5–10°C over three decades by the thermal discharge of a nearby nuclear power plant. Whilst the chronically heated population displayed thermally compensated resting cardio-respiratory functions, maximum temperature threshold limits exhibited little to no thermal compensation across generations, suggesting that whilst metabolic functions can be flexible, critical limits show much less plasticity (Sandblom et al., 2016). Lack of compensation in lethal limits as oceans gradually warm therefore reduces overall aerobic scope of organisms by narrowing the thermal window between habitat temperature and upper limits, resulting in species operating closer to the bounds of their functional capacity and subsequently leaving them vulnerable to more acute changes in temperature during events such as heatwaves (Pörtner and Farrell, 2008; Hemraj et al., 2020).

The relationship between plasticity and lethal temperatures is largely negative, with strong negative correlations between thermal plasticity and CT_{MAX} (Armstrong et al., 2019). Whilst the shift in T_{MMR} found here may demonstrate plasticity and acclimation to higher temperatures, the inability of this gastropod to substantially shift its lethal limits may not favor this species under continual climate change and especially exposure to heatwaves (Pansch et al., 2018; Leung et al., 2021). Given limited resources and the high maintenance cost of thermal response strategies, a greater acclimation potential but elevated vulnerability to acute exposure due to inability to shift threshold temperatures, highlights the importance of addressing multiple proxies for physiological responses to warming rather than chronic acclimation potential alone (Magozzi and Calosi, 2015; Armstrong et al., 2019)... Nevertheless, even with the impact of CO_2 causing a decrease of ∼9°C the upper lethal temperature to 38.8°C, this still lies well above any temperature experienced in the region (highest summer seawater temperature experienced in Hong Kong in the past 10-years ∼31°C, Environmental Protection Department (EPD) Hong Kong, 2019). Of greater concern are longer-term metabolic effects and potential for energetic deficits which make mortality more likely at temperatures below the lethal limits (Mertens et al., 2015; Leung et al., 2018). Therefore, consideration of the additional effect of other environmental stressors that moderate gastropod biological processes (Marchant et al., 2010; Falkenberg et al., 2014) which may consequently exacerbate sensitivity to temperature should be considered when aiming to determine the long-term survival of populations of marine species.

DATA AVAILABILITY STATEMENT

The original contributions presented in the study are included in the article/**Supplementary Material**, further inquiries can be directed to the corresponding author/s. The full data set for this paper is publically available at: https://datahub.hku.hk/ and DOI: 10.25442/hku.14176961.

AUTHOR CONTRIBUTIONS

CC and BR conceived the ideas and designed methodology. CC collected the data. JM and CC analyzed the data. JM and BR led the writing of the manuscript. All authors contributed critically to the drafts and gave final approval for publication.

FUNDING

This project was funded by a Hong Kong Research Grants Council General Research Fund grant (GRF17122916) to BR.

ACKNOWLEDGMENTS

We thank the staff of the Swire Institute of Marine Science for helping to maintain the experimental systems.

SUPPLEMENTARY MATERIAL

The Supplementary Material for this article can be found online at: https://www.frontiersin.org/articles/10.3389/fmars.2021.643377/full#supplementary-material

REFERENCES

Armstrong, E. J., Tanner, R. L., and Stillman, J. H. (2019). High heat tolerance is negatively correlated with heat tolerance plasticity in nudibranch mollusks. *Physiol. Biochem. Zool.* 92, 430–444. doi: 10.1086/704519

Bates, A. E., Helmuth, B., Burrows, M. T., Duncan, M. I., Garrabou, J., Guy-Haim, T., et al. (2018). Biologists ignore ocean

weather at their peril. *Nature* 560:299. doi: 10.1038/d41586-018-05869-5

Brothers, C. J., Harianto, J., McClintock, J. B., and Byrne, M. (2016). Sea urchins in a high-CO 2 world: the influence of acclimation on the immune response to ocean warming and acidification. *Proc. R. Soc. B Biol. Sci.* 283, 1–7. doi: 10.1098/rspb.2016.1501

Byrne, M. (2011). "Impact of ocean warming and ocean acidification on marine invertebrate life history stages: vulnerabilities and potential for persistence in a changing ocean," in *Oceanography and Marine Biology: An Annual Review*, eds R. N. Gibson, R. J. A. Atkinson and J. D. M. Gordon (Boca Raton, FL: CRC Press), 1–42.

Byrne, M., and Przeslawski, R. (2013). Multistressor impacts of warming and acidification of the ocean on marine invertebrates' life histories. *Integr. Comp. Biol.* 53, 582–596. doi: 10.1093/icb/ict049

Carey, N., Harianto, J., and Byrne, M. (2016). Sea urchins in a high-CO2 world: partitioned effects of body size, ocean warming and acidification on metabolic rate. *J. Exp. Biol.* 219, 1178–1186. doi: 10.1242/jeb.136101

Chunhabundit, S., Chunhabundit, P., Aranyakananda, P., and Moree, N. (2001). Dietary effects on shell microstructures of cultured, maculate top shell (Trochidae: *Trochus maculatus*, Linnaeus, 1758). *SPC Trochus Inf. Bull.* 8, 15–22.

Cox, T. E., and Murray, S. N. (2006). Feeding preferences and the relationships between food choice and assimilation efficiency in the herbivorous marine snail Lithopoma undosum (Turbinidae). *Mar. Biol.* 148, 1295–1306. doi: 10.1007/s00227-005-0166-3

Dickson, A. G., and Millero, F. J. (1987). A comparison of the equilibrium constants for the dissociation of carbonic acid in seawater media. *Deep Sea Res. Part A Oceanogr. Res. Pap.* 34, 1733–1743. doi: 10.1016/0198-0149(87)90021-5

Dupont, S., Ortega-Martínez, O., and Thorndyke, M. (2010). Impact of near-future ocean acidification on echinoderms. *Ecotoxicology* 19, 449–462. doi: 10.1007/s10646-010-0463-6

Environmental Protection Department (EPD) Hong Kong (2019). *Marine Water Quality Data [Data File]*. Available online at: https://cd.epic.epd.gov.hk/EPICRIVER/marine/

Falkenberg, L. J., Connell, S. D., and Russell, B. D. (2014). Herbivory mediates the expansion of an algal habitat under nutrient and CO2 enrichment. *Mar. Ecol. Prog. Ser.* 497, 87–92. doi: 10.3354/meps10557

Feely, R. A., Sabine, C. L., Lee, K., Berelson, W., Kleypas, J., Fabry, V. J., et al. (2004). Impact of anthropogenic CO2 on the CaCO3 system in the oceans. *Science* 305, 362–366. doi: 10.1126/science.1097329

Grigaltchik, V. S., Ward, A. J. W., and Seebacher, F. (2012). Thermal acclimation of interactions: differential responses to temperature change alter predator-prey relationship. *Proc. R. Soc. B Biol. Sci.* 279, 4058–4064. doi: 10.1098/rspb.2012.1277

Gunderson, A. R., Armstrong, E. J., and Stillman, J. H. (2016). Multiple stressors in a changing world: the need for an improved perspective on physiological responses to the dynamic marine environment. *Ann. Rev. Mar. Sci.* 8, 357–378. doi: 10.1146/annurev-marine-122414-033953

Guppy, M., and Withers, P. (1999). Metabolic depression in animals: physiological perspectives and biochemical generalizations. *Biol. Rev. Camb. Philos. Soc.* 74, 1–40. doi: 10.1017/S0006323198005258

Gutowska, M. A., Melzner, F., Langenbuch, M., Bock, C., Claireaux, G., and Pörtner, H. O. (2010). Acid-base regulatory ability of the cephalopod (*Sepia officinalis*) in response to environmental hypercapnia. *J. Comp. Physiol. B.* 180, 323–325. doi: 10.1007/s00360-009-0412-y

Hardy, N. A., Lamare, M., Uthicke, S., Wolfe, K., Doo, S., Dworjanyn, S., et al. (2014). Thermal tolerance of early development in tropical and temperate sea urchins: inferences for the tropicalization of eastern Australia. *Mar. Biol.* 161, 395–409. doi: 10.1007/s00227-013-2344-z

Harley, C. D. G., Connell, S. D., Doubleday, Z. A., Kelaher, B., Russell, B. D., Sarà, G., et al. (2017). Conceptualizing ecosystem tipping points within a physiological framework. *Ecol. Evol.* 7, 6035–6045. doi: 10.1002/ece3.3164

Harvey, B. P., Gwynn-Jones, D., and Moore, P. J. (2013). Meta-analysis reveals complex marine biological responses to the interactive effects of ocean acidification and warming. *Ecol. Evol.* 3, 1016–1030. doi: 10.1002/ece3.516

Hemraj, D. A., Posnett, N. C., Minuti, J. J., Firth, L. B., and Russell, B. D. (2020). Survived but not safe: marine heatwave hinders metabolism in two gastropod survivors. *Mar. Environ. Res.* 162, 105–117. doi: 10.1016/j.marenvres.2020.105117

Hoffmann, A. A., and Sgró, C. M. (2011). Climate change and evolutionary adaptation. *Nature* 470, 479–485. doi: 10.1038/nature09670

Hofmann, G. E., Evans, T. G., Kelly, M. W., Padilla-Gamiño, J. L., Blanchette, C. A., Washburn, L., et al. (2014). Exploring local adaptation and the ocean acidification seascape – studies in the California current large marine ecosystem. *Biogeosciences* 11, 1053–1064. doi: 10.5194/bg-11-1053-2014

Kelly, M. W., and Hofmann, G. E. (2013). Adaptation and the physiology of ocean acidification. *Funct. Ecol.* 27, 980–990. doi: 10.1111/j.1365-2435.2012.02061.x

Kroeker, K. J., Kordas, R. L., Crim, R. N., and Singh, G. G. (2010). Meta-analysis reveals negative yet variable effects of ocean acidification on marine organisms. *Ecol. Lett.* 13, 1419–1434. doi: 10.1111/j.1461-0248.2010.01518.x

Kroeker, K. J., Kordas, R. L., and Harley, C. D. G. (2017). Embracing interactions in ocean acidification research: confronting multiple stressor scenarios and context dependence. *Biol. Lett.* 13:20160802. doi: 10.1098/rsbl.2016.0802

Lannig, G., Eilers, S., Pörtner, H. O., Sokolova, I. M., and Bock, C. (2010). Impact of ocean acidification on energy metabolism of oyster, *Crassostrea gigas*–changes in metabolic pathways and thermal response. *Mar. Drugs* 8, 2318–2339. doi: 10.3390/md8082318

Leung, J. Y. S., Connell, S. D., and Russell, B. D. (2017). Heatwaves diminish the survival of a subtidal gastropod through reduction in energy budget and depletion of energy reserves. *Sci. Rep.* 7:17688. doi: 10.1038/s41598-017-16341-1

Leung, J. Y. S., Nagelkerken, I., Russell, B. D., Ferreira, C. M., and Connell, S. D. (2018). Boosted nutritional quality of food by CO2 enrichment fails to offset energy demand of herbivores under ocean warming, causing energy depletion and mortality. *Sci. Total Environ.* 639, 360–366. doi: 10.1016/j.scitotenv.2018.05.161

Leung, J. Y. S., Russell, B. D., Coleman, M. A., Kelaher, B. P., and Connell, S. D. (2021). Long-term thermal acclimation drives adaptive physiological adjustments of a marine gastropod to reduce sensitivity to climate change. *Sci. Total Environ.* 771, 145–208. doi: 10.1016/j.scitotenv.2021.145208

Lewis, E., and Wallace, D. (1998). *Program Developed for CO2 System Calculations. ORNL/CDIAC-105*. Oak Ridge, TN: Oak Ridge National Laboratory.

Maboloc, E. A., and Mingoa-Licuanan, S. S. (2013). Spawning in *Trochus maculatus*: field observations from Bolinao, Pangasinan (Philippines). *Coral Reefs* 32, 1141. doi: 10.1007/s00338-013-1060-y

Magozzi, S., and Calosi, P. (2015). Integrating metabolic performance, thermal tolerance, and plasticity enables for more accurate predictions on species vulnerability to acute and chronic effects of global warming. *Glob. Chang. Biol.* 21, 181–194. doi: 10.1111/gcb.12695

Manríquez, P. H., González, C. P., Brokordt, K., Pereira, L., Torres, R., Lattuca, M. E., et al. (2019). Ocean warming and acidification pose synergistic limits to the thermal niche of an economically important echinoderm. *Sci. Total Environ.* 693, 133469. doi: 10.1016/j.scitotenv.2019.07.275

Marchant, H. K., Calosi, P., and Spicer, J. I. (2010). Short-term exposure to hypercapnia does not compromise feeding, acid-base balance or respiration of Patella vulgata but surprisingly is accompanied by radula damage. *J. Mar. Biol. Assoc. U.K.* 90, 1379–1384. doi: 10.1017/S0025315410000457

Marshall, D. J., Dong, Y., McQuaid, C. D., and Williams, G. A. (2011). Thermal adaptation in the intertidal snail *Echinolittorina malaccana* contradicts current theory by revealing the crucial roles of resting metabolism. *J. Exp. Biol.* 214, 3649–3657. doi: 10.1242/jeb.059899

Mehrbach, C., Culberson, C. H., Hawley, J. E., and Pytkowicx, R. M. (1973). Measurement of the apparent dissociation constants of carbonic acid in seawater at atmospheric pressure. *Limnol. Oceanogr.* 18, 879–907. doi: 10.4319/lo.1973.18.6.0897

Mertens, N. L., Russell, B. D., and Connell, S. D. (2015). Escaping herbivory: ocean warming as a refuge for primary producers where consumer metabolism and consumption cannot pursue. *Oecologia* 179, 1223–1229. doi: 10.1007/s00442-015-3438-8

Metzger, R., Sartoris, F. J., Langenbuch, M., and Pörtner, H. O. (2007). Influence of elevated CO2 concentrations on thermal tolerance of the edible crab *Cancer pagurus*. *J. Therm. Biol.* 32, 144–151. doi: 10.1016/j.jtherbio.2007.01.010

Ng, T. P. T., Lau, S. L. Y., Seuront, L., Davies, M. S., Stafford, R., Marshall, D. J., et al. (2017). Linking behaviour and climate change in intertidal ectotherms: insights

from littorinid snails. *J. Exp. Mar. Biol. Ecol.* 492, 121–131. doi: 10.1016/j.jembe.2017.01.023

Nguyen, K. D. T., Morley, S. A., Lai, C.-H., Clark, M. S., Tan, K. S., Bates, A. E., et al. (2011). Upper temperature limits of tropical marine ectotherms: global warming implications. *PLoS One* 6:e29340. doi: 10.1371/journal.pone.0029340

Nudelman, F., Gotliv, B. A., Addadi, L., and Weiner, S. (2006). Mollusk shell formation: mapping the distribution of organic matrix components underlying a single aragonitic tablet in nacre. *J. Struct. Biol.* 153, 176–187. doi: 10.1016/j.jsb.2005.09.009

Pansch, C., Scotti, M., Barboza, F. R., Al-Janabi, B., Brakel, J., Briski, E., et al. (2018). Heat waves and their significance for a temperate benthic community: a near-natural experimental approach. *Glob. Chang. Biol.* 24, 4357–4367. doi: 10.1111/gcb.14282

Parmesan, C., and Yohe, G. (2003). A globally coherent fingerprint of climate change impacts across natural systems. *Nature* 421, 37–42. doi: 10.1038/nature01286

Pörtner, H. O. (2008). Ecosystem effects of ocean acidification in times of ocean warming: a physiologist's view. *Mar. Ecol. Prog. Ser.* 373, 203–217. doi: 10.3354/meps07768

Pörtner, H. O. (2010). Oxygen- And capacity-limitation of thermal tolerance: a matrix for integrating climate-related stressor effects in marine ecosystems. *J. Exp. Biol.* 213, 881–893. doi: 10.1242/jeb.037523

Pörtner, H. O., and Farrell, A. P. (2008). Ecology: physiology and climate change. *Science* 322, 690–692. doi: 10.1126/science.1163156

Sandblom, E., Clark, T. D., Gräns, A., Ekström, A., Brijs, J., Sundström, L. F., et al. (2016). Physiological constraints to climate warming in fish follow principles of plastic floors and concrete ceilings. *Nat. Commun.* 7:11447. doi: 10.1038/ncomms11447

Seebacher, F., White, C. R., and Franklin, C. E. (2014). Physiological plasticity increases resilience of ectothermic animals to climate change. *Nat. Clim. Chang.* 5, 61–66. doi: 10.1038/nclimate2457

Sinclair, B. J., Marshall, K. E., Sewell, M. A., Levesque, D. L., Willett, C. S., Slotsbo, S., et al. (2016). Can we predict ectotherm responses to climate change using thermal performance curves and body temperatures? *Ecol. Lett.* 19, 1372–1385. doi: 10.1111/ele.12686

Stillman, J. H., and Somero, G. N. (2000). A comparative analysis of the upper thermal tolerance limits of eastern pacific porcelain crabs, genus *Petrolisthes*: influences of latitude, vertical zonation, acclimation, and phylogeny. *Physiol. Biochem. Zool.* 73, 200–208. doi: 10.1086/316738

Tripp-Valdez, M. A., Bock, C., Lucassen, M., Lluch-Cota, S. E., Sicard, M. T., Lannig, G., et al. (2017). Metabolic response and thermal tolerance of green abalone juveniles (*Haliotis fulgens*: Gastropoda) under acute hypoxia and hypercapnia. *J. Exp. Mar. Bio. Ecol.* 497, 11–18. doi: 10.1016/j.jembe.2017.09.002

Uthicke, S., Liddy, M., Nguyen, H. D., and Byrne, M. (2014). Interactive effects of near-future temperature increase and ocean acidification on physiology and gonad development in adult Pacific sea urchin, *Echinometra* sp. *A. Coral Reefs* 33, 831–845. doi: 10.1007/s00338-014-1165-y

Wang, J., Russell, B., Ding, M. W., and Dong, Y. W. (2018). Ocean acidification increases the sensitivity of and variability in physiological responses of an intertidal limpet to thermal stress. *Biogeosciences* 15, 2803–2817. doi: 10.5194/bg-15-2803-2018

Conflict of Interest: The authors declare that the research was conducted in the absence of any commercial or financial relationships that could be construed as a potential conflict of interest.

frontiers in Marine Science

ORIGINAL RESEARCH
published: 22 April 2021
doi: 10.3389/fmars.2021.644965

Effects of Ocean Acidification on Carbon and Nitrogen Fixation in the Hermatypic Coral *Galaxea fascicularis*

Xinqing Zheng[1,2,3†], Chenying Wang[1,4†], Huaxia Sheng[4], Gaofeng Niu[5], Xu Dong[1,2], Lingling Yuan[6] and Tuo Shi[4,5*]*

[1] Third Institute of Oceanography, Ministry of Natural Resources, Xiamen, China, [2] Fujian Provincial Key Laboratory of Marine Ecological Conservation and Restoration, Xiamen, China, [3] Fujian Provincial Station for Field Observation and Research of Island and Coastal Zone, Zhangzhou, China, [4] State Key Laboratory of Marine Environmental Science, College of Ocean and Earth Sciences, Xiamen University, Xiamen, China, [5] Marine Genomics and Biotechnology Program, Institute of Marine Science and Technology, Shandong University, Qingdao, China, [6] National Center of Ocean Standard and Metrology, Tianjin, China

OPEN ACCESS

Edited by:
Jonathan Y. S. Leung, University of Adelaide, Australia

Reviewed by:
Zhi Zhou, Hainan University, China
Xiangcheng Yuan, South China Sea Institute of Oceanology, Chinese Academy of Sciences, China

***Correspondence:**
Lingling Yuan
yuanoo81@163.com
Tuo Shi
tuoshi@sdu.edu.cn

†These authors share first authorship

Specialty section:
This article was submitted to Global Change and the Future Ocean, a section of the journal Frontiers in Marine Science

Received: *22 December 2020*
Accepted: *30 March 2021*
Published: *22 April 2021*

Citation:
Zheng X, Wang C, Sheng H, Niu G, Dong X, Yuan L and Shi T (2021) Effects of Ocean Acidification on Carbon and Nitrogen Fixation in the Hermatypic Coral Galaxea fascicularis. Front. Mar. Sci. 8:644965. doi: 10.3389/fmars.2021.644965

The supply of metabolites from symbionts to scleractinian corals is crucial to coral health. Members of the Symbiodiniaceae can enhance coral calcification by providing photosynthetically fixed carbon (PFC) and energy, whereas dinitrogen (N_2)-fixing bacteria can provide additional nutrients such as diazotrophically-derived nitrogen (DDN) that sustain coral productivity especially when alternative external nitrogen sources are scarce. How these mutualistic associations benefit corals in the future acidifying ocean is not well understood. In this study, we investigated the possible effects of ocean acidification (OA; pHs 7.7 and 7.4 vs. 8.1) on calcification in the hermatypic coral *Galaxea fascicularis* with respect to PFC and DDN assimilation. Our measurements based on isotopic tracing showed no significant differences in the assimilation of PFC among different pH treatments, but the assimilation of DDN decreased significantly after 28 days of stress at pH 7.4. The decreased DDN assimilation suggests a nitrogenous nutrient deficiency in the coral holotiont, potentially leading to reduced coral calcification and resilience to bleaching and other stressful events. This contrasting impact of OA on carbon and N flux demonstrates the flexibility of *G. fascicularis* in coping with OA, apparently by sustaining a largely undamaged photosystem at the expense of N_2 fixation machinery, which competes with coral calcification for energy from photosynthesis. These findings shed new light on the critically important but more vulnerable N cycling *in hospite*, and on the trade-off between coral hosts and symbionts in response to future climate change.

Keywords: ocean acidification, coral calcification, carbon fixation, nitrogen fixation, symbiosis, photosynthesis

INTRODUCTION

Nutritional interactions are a key reason why scleractinian corals, the main reef builders in the oceans, thrive in the oligotrophic tropical waters where nitrogen (N) sources are particularly scarce (Muscatine and Porter, 1977; Cardini et al., 2014; Peixoto et al., 2017). The obligate relationship between corals and Symbiodiniaceae is the basis of a functioning reef ecosystem. The coral host

provides the endosymbionts with inorganic nutrients for photosynthesis, and in turn acquires photosynthetically fixed carbon (PFC) from the symbionts in the form of glycerol, glucose, amino acids, and other organic compounds that the host cannot synthesize independently (Rowan, 1998). Symbiodiniaceae, hence, play a central role in the trophic foundation of coral reef ecosystems (Silveira et al., 2017) and in the formation of the physical reef structure (Tambutté et al., 2011).

Other microbes are increasingly being recognized as important to the health of the corals and in coral reef biogeochemistry, particularly diazotrophs including dinitrogen (N_2)-fixing bacteria and archaea (Lema et al., 2014; Peixoto et al., 2017). N_2 fixation is one of the main sources of new N in the ocean necessary to sustain marine primary productivity, particularly in coral reef ecosystems where the availability of nitrogenous nutrients can be low (Benavides et al., 2017). Diazotrophs are able to fix N_2 utilizing the nitrogenase enzyme, which cleaves the triple bond of the N_2 molecule to form bioavailable ammonium (NH_4^+; Zehr and Kudela, 2011). In this context, endosymbiotic photosynthesis-dependent diazotrophic cyanobacteria were discovered in the coral tissue of *Montastraea cavernosa* (Lesser et al., 2004), and N_2 fixation activity has been detected in several coral species (Lesser et al., 2007). High throughput sequencing has subsequently identified diverse communities of non-cyanobacterial diazotrophs associated with numerous scleractinian corals from varying geographical regions (Fiore et al., 2010; Olson and Lesser, 2013), exemplifying their importance in meeting nutritional demand of corals (Fiore et al., 2010; Cardini et al., 2014). At the ecosystem level, up to 11% of the N used in coral reef primary production is provided by diazotrophs in supporting the productivity of that ecosystem (Cardini et al., 2014; Lema et al., 2016). The ability of corals to overcome N limitation may determine their success in oligotrophic waters, ultimately influencing the distribution and abundance of coral reefs (Fiore et al., 2010). Additionally, Symbiodiniaceae and associated bacteria form calcifying structures termed symbiolites (Frommlet et al., 2015). This bacterial–algal calcification, induced by Symbiodiniaceae photosynthesis through the assimilation of CO_2 and HCO_3^- and the release of hydroxyl ion from carbon (C) concentrating mechanism, implies that symbiotic bacteria might also facilitate coral calcification (Frommlet et al., 2018).

As a result of anthropogenically-driven increase in the ocean concentration of carbon dioxide (CO_2), tropical coral reefs are highly vulnerable to ocean acidification (OA). This is because the ecosystem structure depends on calcium carbonate-secreting organisms, which are subject to negative impacts of changing ocean carbonate chemistry associated with OA (Byrne et al., 2013; Leung et al., 2017, 2020; Mollica et al., 2018). It has been estimated that coral reefs may transition from net calcium carbonate accretion to net dissolution by the end of this century (Hoegh-Guldberg et al., 2007; Dove et al., 2013; Enochs et al., 2016; Eyre et al., 2018). OA not only inhibits calcification, reduces photosynthesis and species diversity directly, but also indirectly impacts coral-associated microbes, thereby potentially disrupting the normal function of the coral holobiont. This loss of function may in turn impact coral reef ecosystems as a whole (Moya et al., 2012; Kaniewska et al., 2015). However, N_2 fixation activities in the coral holobiont may moderate the host's response to stress (Rädecker et al., 2015). The increased transfer of diazotrophically-derived nitrogen (DDN) to endosymbiotic Symbiodiniaceae occurs particularly under conditions of low availability of external nutrients or during stress (Bednarz et al., 2017, 2019). Moreover, N_2 fixation may be particularly important for providing nutrients to the host under stressful conditions, especially when Symbiodiniaceae are lost from host tissues (Fine and Loya, 2002). Therefore, N_2 fixation may play a key role in regulating coral–Symbiodiniaceae symbiosis.

However, investigations into the coral nutrient were mainly focused on C fixation (Tremblay et al., 2012; Hoadley et al., 2015), and few on N_2 fixation (Bednarz et al., 2017; Lesser et al., 2019). The effects of OA on these processes remain largely unknown and there is simply one study on N_2 fixation response to OA according to the best of our current knowledge (Rädecker et al., 2014). N_2 fixation rates can be detected through the acetylene reduction assay (Capone, 1993) and the $^{15}N_2$-tracer method (Montoya et al., 1996). The former is an indirect method, converting acetylene produced to overall rates of N_2 fixation but usually overestimating the rates. Instead, the latter allows measurement of the net N_2 fixation directly, simply by adding filtered seawater enriched with $^{15}N_2$ gas to the incubation to ensure consistency of $^{15}N_2$ concentrations (White et al., 2020). In this study, we used $H^{13}CO_3^-$ and $^{15}N_2$ as tracers and performed indoor experiments to mimic OA conditions (pHs 7.7 and 7.4) relative to the ambient condition in the field (pH 8.1 as control) to investigate: (i) Whether OA would affect PFC and DDN assimilation in the ecologically important scleractinian coral *G. fascicularis*; (ii) Is there a correlation between the C/N flux and coral calcification and how they interact with each other to cope with OA.

MATERIALS AND METHODS

Experimental Setup

Twelve colonies of healthy, adult *G. fascicularis* with surface areas ranging from 10 to 15 cm^2 were collected from Changjiang (110°65′E, 19°25′N), Hainan, China, at noon in July 2015. The corals were cultivated in an aquarium with approximately 1,000 L of recirculated artificial seawater for up to 3 months of acclimation. The coral genotype was identified as the mt-L1 type of *G. fascicularis* (Lin et al., 2017). A detailed description of the aquarium setup and water quality has been reported elsewhere (Zheng et al., 2018a). Photosynthetically active radiation (PAR) of 150 ± 25 μmol photons m^{-2} s^{-1} was provided on a 12 h/12 h photoperiod using metal halide lamps (Phillips, Amsterdam, Netherlands). The live rock containing denitrifying bacteria was used to stabilize the water quality by removing dissolved inorganic nitrogen (DIN; Li et al., 2017). The DIN and dissolved inorganic phosphorus (DIP) concentrations were all < 0.05 μ M.

Fragments (∼3 cm in diameter) of *G. fascicularis* were grown in the aquarium until coral tissue entirely covered the skeleton. Ninety coral fragments were randomly and equally assigned to three 100-L experimental tanks (30 fragments per tank), each

maintained at a specific pH (8.1, 7.7, and 7.4). The carbonate chemistry was manipulated by bubbling pure CO_2 gas (99% purity) into the artificial seawater in the experimental tanks to maintain the pH (total scale, pH_T) levels (**Supplementary Table 1**) with a pH-stat system (CO2SYS ZB-LS 3.0; Xiamen, China), which monitors and regulates the pH every second with an accuracy of ± 0.02 pH unit (Zheng et al., 2018b). The pH in each tank was recorded every 5 min by the CO2SYS ZB-LS 3.0 (**Supplementary Figure 1**).

The three tanks were maintained at a salinity of approximately 34 ppt and a temperature of 27°C, and irradiated on a 12 h/12 h photoperiod with 150 μmol photons m^{-2} s^{-1} of PAR provided by T5HO lamps (ATI, Hamm, Germany). Submersible pumps (EHEIM, Deizisau, Germany) were used to ensure a high level of seawater circulation and easy dissolution of the CO_2 gas into the seawater. A protein skimmer (Bubble Magus, Jiangmen, China) was used to maintain the inorganic nutrients at low levels (**Supplementary Table 1**).

While parallel, independent replicate tanks were not used per each pH treatment, the water quality was well maintained over the course of experiment and no statistical differences were found among the tanks for all the environmental parameters measured except the pH (**Supplementary Table 1**). Given that the number of replicate coral fragments in each tank was high and comparable to those in previous studies (Rädecker et al., 2014; Kurman et al., 2017), the resulting data should be regarded as reliable as in other OA studies that also adopted a single tank for each pH treatment (Barkley et al., 2017; Comeau et al., 2017; Kurman et al., 2017; Coronado et al., 2019). Additionally, the tanks were rigorously cleaned weekly to eliminate "tank" effects and ensure stable water quality throughout the experiment.

Monitoring of Water Quality and Carbonate Chemistry

A total of 300 mL seawater was sampled weekly for the measurement of inorganic nutrient concentrations (PO_4^{3-}, NO_3^-, NH_4^+, and SiO_3^{2-}) and carbonate chemistry (pH and total alkalinity: TA). Saturated mercuric chloride (7 mg mL^{-1}) was added to preserve the water samples. An aliquot of 100 mL seawater was used for the measurement of inorganic nutrients using a 7,230 Spectrophotometer (Jingmi, Shanghai, China). The pH was measured using a 3,430 portable meter (WTW, Munich, Germany) that was calibrated daily, and TA was measured by potentiometric titration following the standard procedure (Dickson et al., 2007). Changes in seawater carbonate chemistry were calculated from pH_T and TA using the CO_2 Sys Excel Macro (Lewis et al., 1998).

Measurement of Photochemical Efficiency

The photochemical efficiency of the algal symbiont was assessed using an underwater chlorophyll fluorometer (Diving-PAM; Walz, Effeltrich, Germany) that measured the quantum yield of chlorophyll *a* fluorescence. Measurements of the maximum quantum yield (F_v/F_m) and effective quantum yield ($\Delta F/F_m'$) of photosystem II (PSII) were conducted 2 h into the dark and light periods, respectively, in every 14 days ($n = 6$).

Measurement of PFC and DDN Assimilation

The ^{13}C and ^{15}N stable isotopic tracing experiment was carried out to quantify the rates of PFC and DDN assimilation in the coral holobiont. The DDN and PFC assimilation rates were measured using the dissolution method (Großkopf et al., 2012). In summary, $^{15}N_2$ pre-dissolved seawater was made with $^{15}N_2$ gas (98.9 atom%, Cambridge Isotope Laboratories) following the procedure of Shiozaki et al. (2015). Seawater was filtered through 0.2 μm membrane, degassed using Sterapore membrane unit (20 M 1,500 A: Mitsubishi Rayon Co., Ltd., Tokyo, Japan), and filled into 2-L Tedlar bags. Twenty milliliter, of $^{15}N_2$ was injected into each seawater-filled bag, which was tapped slightly until complete dissolution of the gas. The coral fragments were incubated, with one fragment per 1-L polycarbonate bottle (Nalgene, Rochester, NY, United States, the actual volume is ∼1,225 mL) filled with 100 mL of the $^{15}N_2$ pre-dissolved seawater and 1,125 mL seawater from the corresponding experimental tanks (pHs 8.1, 7.7, and 7.4). The ^{13}C-labeled sodium bicarbonate (99 atom% ^{13}C; Cambridge Isotope Laboratories) was added in parallel with $^{15}N_2$ at a final tracer concentration of 70 $\mu mol \cdot L^{-1}$. The incubation lasted 24 h (12 h light/12 h dark; 150 μmol photons $m^{-2} \cdot s^{-1}$). Coral fragments were sampled at the start and end of the isotope tracer experiment to assess the PFC and DDN assimilation rates. Since OA has negligible effect on coral respiration (Comeau et al., 2017; Van der Zande et al., 2020), a 24-h incubation represents the net assimilation of PFC, which has subtracted the respiration of consumed metabolites. The samples collected prior to the incubation were also used to assess the natural isotope ratios $\delta^{13}C$ and $\delta^{15}N$. Samples were immediately snap-frozen in liquid nitrogen followed by storage at −80°C until further processing.

Coral tissue was detached from the skeleton using a WaterPik, filtered onto pre-combusted (450°C, 4 h) 0.3 μm GF-75 filters (Advantec, Taiwan, China) and dried at 60°C overnight. The isotopic values were determined using a Delta V plus isotope ratio mass spectrometer (Thermo Fisher Corporation, Carthage, MO, United States) interfaced with a Flash HT 2000 elemental analyzer (Thermo Fisher Corporation, Carthage, MO, United States). International reference material (USGS40) with a different amount of C/N and certified $\delta^{13}C$ and $\delta^{15}N$ values of −4.5 and −26.2‰, respectively, was inserted every 5 samples to check the drift and to ensure the accuracy of the measurements. The reproducibility for $\delta^{13}C$ and $\delta^{15}N$ measurements were both better than 0.3‰. The PFC and DDN assimilation rates were calculated by using equations proposed by Hama et al. (1983) and Montoya et al. (1996), respectively.

Measurement of Coral Calcification

The coral calcification rates were determined using the buoyant weight method measuring increase in skeletal mass, as reported previously (Davies, 1989). Briefly, the coral fragments were

suspended in seawater beneath an analytical balance that weighs to an accuracy of 0.01 mg. Optimal weighing conditions were reached when the air temperature was stable and close to that of the seawater. A total of eight replicates (n = 8) of coral fragments were measured at two timepoints (day = 14 and 28).

Statistical Analysis

Differences in water quality (pH, TA, pCO_2, and inorganic nutrients) and all parameters among the pH treatments were compared using one-way analysis of variance (ANOVA). The effects of pH and time on the physiological parameters ($\Delta F/F_m'$, F_v/F_m, calcification) were tested using two-way ANOVA. The post-eriori Tukey's test was followed when the differences were significant ($p < 0.05$). Data were checked for normality and homogeneity (Shapiro-Wilk and Levene tests, respectively), and when necessary were transformed to achieve ANOVA assumptions. All data were expressed as an average value ± standard error (SE). Statistical analysis was performed using IBM SPSS Statistics 23 (IBM Corp., Armonk, NY, United States).

RESULTS

Water Quality and Carbonate Chemistry of Seawater

The results of the water quality and carbonate chemistry analyses of seawater are shown in **Supplementary Table 1**. Over the 28-day experimental period, temperature and salinity were kept at 27 ± 0.3°C and 34 ± 0.1 ppt, respectively. No differences in the water temperature and salinity were found among the pH treatments. The inorganic nutrient concentrations were low and comparable to those in the field, with approximate concentrations of 0.03−0.05 μM for phosphate (PO_4^{3+}), 0.45−0.58 μM for nitrite (NO_2^-), < 0.05 for nitrate (NO_3^-), 0.18−0.51 μM for silicate (SiO_3^{2-}), and 0.35−0.84 μM for NH_4^+. Although the average values were higher at pH 7.4, there were no significant differences among the three pH treatments (**Supplementary Table 1**; p = 0.287 for PO_4^{3+}, p = 0.964 for NO_2^-, p = 0.563 for SiO_3^{2-}, and p = 0.665 for NH_4^+).

Data from a total of 8,064 measurements recorded in each tank by the CO2SYS ZB-LS 3.0 system indicated that each treatment pH was very stable during the entire experimental period (**Supplementary Table 1** and **Supplementary Figure 1**). The standard error was ± 0.01 at pHs 7.7 and 8.1, and ± 0.02 at pH 7.4 (**Supplementary Table 1**). The TA was approximately 2,600 μM, and there were no significant differences among treatments (**Supplementary Table 1**; df = 2, F = 1.655, p = 0.244). Because of the relatively high TA (relative to 2,300 μM in the field), the aragonite saturation state (Ω_{arag}) value at pH 7.7 reached 3.29, but rapidly reduced to 1.79 at pH 7.4. The concentration of carbonate (CO_3^{2-}) declined under OA conditions (**Supplementary Table 2**; df = 2, F = 3,337, $p < 0.001$) but other carbonate parameters, including pCO_2, CO_2, and HCO_3^-, increased ($p < 0.001$).

TABLE 1 | Two-way ANOVA for physiological parameters as a function of pH and time.

Dependent variable	Effect	SS	*df*	MS	*F*	*p*
$\Delta F/F_m'$	pH	0.013	2	0.006	3.351	**0.043**
	Time	0.006	2	0.003	1.478	0.238
	pH*time	0.13	4	0.003	1.643	0.178
F_v/F_m	pH	0.003	2	0.001	1.403	0.257
	Time	0.003	2	0.002	1.775	0.182
	pH*time	0.003	4	0.001	0.726	0.579
Calcification	pH	0.443	2	0.221	5.968	**0.005**
	Time	0.096	1	0.096	2.586	0.115
	pH*time	0.032	2	0.016	0.426	0.656

Significant differences ($p < 0.05$) are highlighted in bold. SS, type III sum of squares; df, degree of freedom; MS, mean square; F, F-ratio; p, p-value.

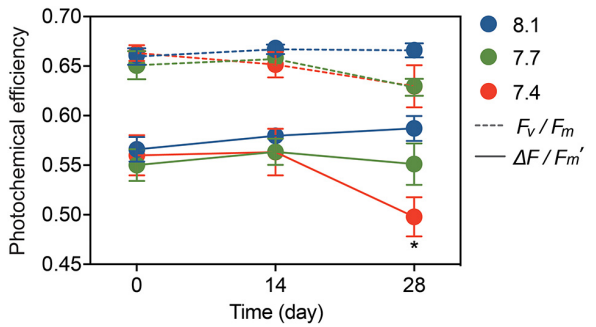

FIGURE 1 | Photochemical efficiency of *G. fascicularis* over the course of the experiment: the maximum quantum yield (F_v/F_m) and effective quantum yield ($\Delta F/F_m'$) of PSII. Values are expressed as mean ± SE from six determinations (n = 6). The asterisk (*) represents significant difference in the $\Delta F/F_m'$ between pH 7.4 and other pH treatments ($p < 0.05$).

Photochemical Efficiency of the Algal Symbiont

Statistical analysis showed no significant pH × time interactions for F_v/F_m (**Table 1**; df = 4, F = 0.726, p = 0.579), and no significant differences among the pH treatments (**Table 1**; df = 2, F = 1.403, p = 0.257) or times (**Table 1**; df = 2, F = 1.775, p = 0.182). The trend for $\Delta F/F_m'$ was similar to that for F_v/F_m, but the values of $\Delta F/F_m'$ declined significantly from 0.58 ± 0.01 at pH 8.1 to 0.49 ± 0.02 at pH 7.4 after 28-day stress (**Figure 1**, **Table 1**, and **Supplementary Table 3**; df = 2, F = 3.351, p = 0.043).

PFC and DDN Assimilation Rates

Galaxea fascicularis exhibited detectable gross PFC and DDN assimilation under control and OA conditions (**Figure 2**). At day 0, the assimilation of PFC and DDN were similar among all treatments (6.55–6.80 nmol C_{tracer} μmol C_{tissue}^{-1} d^{-1} for PFC assimilation, and 0.16–0.17 nmol N_{tracer} μmol N_{tissue}^{-1} d^{-1} for DDN assimilation; **Supplementary Table 3** and **Figure 2**). The OA treatments did not affect PFC assimilation rates (**Figure 2A** and **Table 2**; F = 0.884, p = 0.461), but the DDN assimilation rates decreased at pH 7.4 (0.03 ± 0.02 nmol N_{tracer} μmol N_{tissue}^{-1} d^{-1}) compared with those at pH 8.1 after 28-day stress (**Figure 2B**

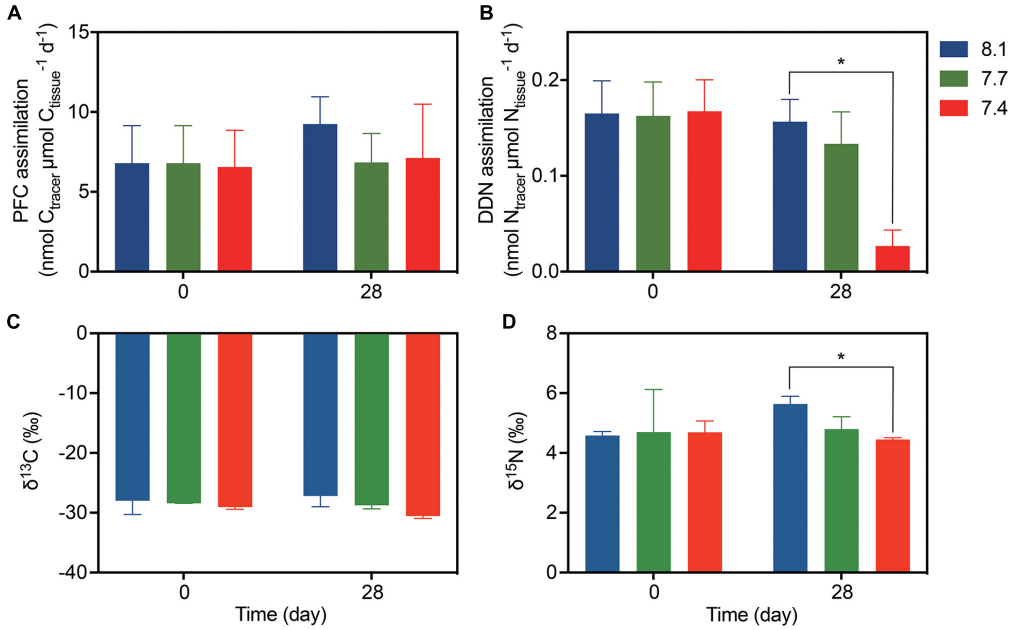

FIGURE 2 | The assimilation rates and isotope values of *G. fascicularis* (mean ± SE) over the course of the experiment. **(A)** The PFC and **(B)** DDN assimilation rates at the start and end of the different pH treatments. **(C)** Carbon and **(D)** nitrogen stable isotope values for the coral holobiont at the start and end of the different pH treatments. Values are expressed as mean ± SE of three determinations (n = 3). The asterisk (*) represent significant difference between pH 7.4 and pH 8.1 ($p < 0.05$).

and **Table 2**; F = 7.454, p = 0.024). For natural isotope ratio, no significant effect was found for $\delta^{13}C$ values (**Figure 2C** and **Table 2**; F = 2.053, p = 0.223), but the $\delta^{15}N$ values decreased significantly at pH 7.4 compared with those at pH 8.1 after 28-day stress (**Figure 2C** and **Table 2**; F = 7.313, p = 0.033).

TABLE 2 | One-way ANOVA for physiological parameters as a function of time.

Dependent variable		SS	*df*	MS	*F*	*p*
$\Delta F/F_m'$	0 day	0.001	2	0.000	0.215	0.809
	14 day	0.001	2	0.001	0.402	0.674
	28 day	0.022	2	0.011	4.697	**0.025**
F_v/F_m	0 day	0.000	2	0.000	0.384	0.689
	14 day	0.000	2	0.000	0.929	0.430
	28 day	0.007	2	0.004	2.336	0.121
PFC assimilation	0 day	0.343	2	0.171	0.032	0.969
	28 day	10.4	2	5.2	0.884	0.461
DDN assimilation	0 day	0.000	2	0.000	0.005	0.995
	28 day	0.029	2	0.014	7.454	**0.024**
$\delta^{13}C$ (‰)	0 day	1.799	2	0.899	0.162	0.854
	28 day	17.146	2	8.573	2.053	0.223
$\delta^{15}N$ (‰)	0 day	0.019	2	0.010	0.009	0.991
	28 day	2.216	2	1.108	7.313	**0.033**
Calcification	14 day	0.179	2	0.09	6.392	**0.008**
	28 day	0.414	2	0.207	3.747	**0.041**

Significant differences ($p < 0.05$) are highlighted in bold. SS, type III sum of squares; df, degrees of freedom; MS, mean square; F, F-ratio; p, p-value.

Calcification Rate

There were no significant pH × time interactions for coral calcification (**Table 1**; df = 2, F = 0.426, p = 0.656), and no significant differences among times (**Table 2**; df = 2, F = 2.586, p = 0.115), but significant differences among pH treatments were found (**Table 1**; df = 2, F = 5.968, p = 0.005). At pH 8.1, *G. fascicularis* maintained stable calcification rates, averaging 0.22 ± 0.05% $week^{-1}$ and 0.18 ± 0.05% $week^{-1}$ during the first and the second 14 days of growth, respectively (**Supplementary Table 3** and **Figure 3A**). The calcification rates at pH 8.1 were significantly higher than those at pH 7.4 during the first (−0.01 ± 0.03% $week^{-1}$) and the second 14 days (−0.14 ± 0.13% $week^{-1}$), and significant carbonate dissolution was found at pH 7.4 (**Figure 3A**). The coral calcification rate decreased at pH 7.7, but was not significantly different from that at pH 8.1 (**Figure 3A**). Generalized linear models showed a significant positive relationship between the calcification rate and Ω_{arag} over the experimental period (**Figure 3B**).

DISCUSSION

Our measurements revealed that the effective quantum yield of the algal symbiont in *G. fascicularis* decreased significantly at pH 7.4 after 28 days of OA stress, but the algal maximum quantum yield and the coral assimilation of PFC did not appear to be affected by OA (**Figures 1**, **2A**). Conflicting results of OA impact on algal photosynthesis have been reported, ranging from decreased photochemical efficiency in *Acropora millepora*

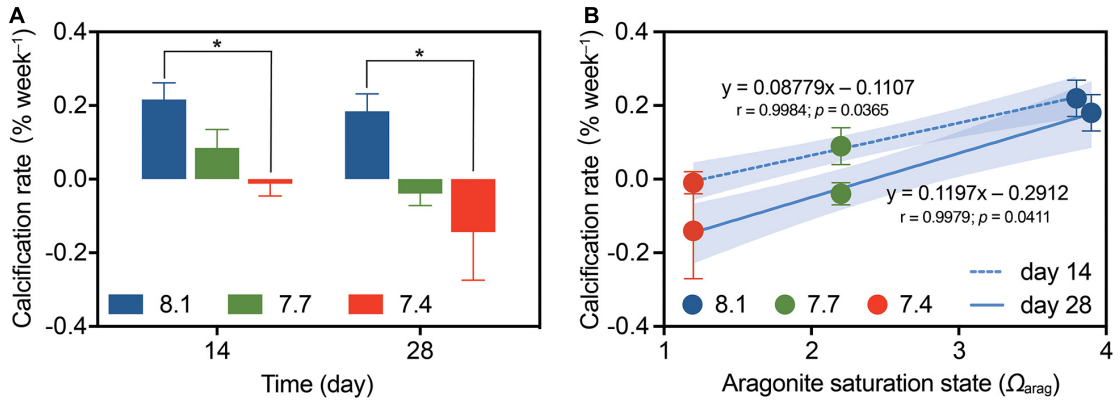

FIGURE 3 | The calcification rates of *G. fascicularis* (mean ± SE) over the course of the experiment. **(A)** Values are expressed as mean ± SE from eight determinations (n = 8); The asterisk (*) represent significant difference between pH 7.4 and pH 8.1 ($p < 0.05$). **(B)** Relationship between coral calcification rate and the aragonite saturation state (Ω_{arag}) based on the measurements after 14 days (dotted) or 28 days (solid) of different pH treatments. The p-values associated with each generalized linear model are shown. Shades surrounding the trend lines indicate 95% confidence level.

at pH 7.6−7.7 and pH 7.8−7.9 (Kaniewska et al., 2012) and negative effects of long-term OA on coral productivity (Anthony et al., 2008), unaffected photosynthesis in *A. digitifera* at pH 7.56 (Takahashi and Kurihara, 2013), to enhanced net photosynthesis in *Porites* spp., *A. millepora*, and *Pocillopora damicornis* around volcanic CO_2 seeps (pH 7.8) (Strahl et al., 2015). For many plants, acidification has a "fertilizing effect" on photosynthesis, as high pCO_2 alleviates C limitation in the Calvin cycle, and facilitates greater rates of photosynthesis compared with those under ambient conditions (Vogel et al., 2015). The absence of the "fertilizing effect" of OA on photosynthesis in *G. fascicularis* suggests that this phenomena might be species-specific and maximum carbon fixation in the coral may have already attained under normal ambient pH condition. This could also be due to the fact that Symbiodiniaceae are located within the gastroderm of the coral host (i.e., not in direct contact with seawater) and thereby cannot efficiently sequester CO_2 in acidified seawater. As a result, host respiration probably provides some CO_2 that is easier to accesses than the external dissolved inorganic carbon to Symbiodiniaceae for photosynthesis (Furla et al., 2000). Moreover, the virtually unaffected assimilation of PFC in corals could be tied to the stable Symbiodiniaceae community. Symbiodiniaceae have been shown to be able to thrive in low pH and a stable Symbiodiniaceae community under OA may be expected to provide PFC to the coral holobiont (Noonan et al., 2013). This was further confirmed by the results of $\delta^{13}C$ values showing no difference among different pH treatments (**Figure 2C**). The natural C isotope abundance has been used to understand the balance of autotrophy and heterotrophy in hermatypic corals (Wall et al., 2020), with the $\delta^{13}C$ values positively relating to the photosynthate or autotrophic input (Tremblay et al., 2015; Allgeier et al., 2020). Therefore, the similar $\delta^{13}C$ values among different pH treatments suggest stable PFC assimilation.

Microbes involved in N cycling may be fundamental to coral resilience to climate change (Rädecker et al., 2014, 2015). Rapid and significant decrease in DDN assimilation rates under OA (pH 7.71 with pCO_2 1,080 μatm) has been reported in *Seriatopora hystrix* based on the acetylene reduction assay (Rädecker et al., 2014). In this study, the rates of DDN assimilation were differentially affected depending on the severity of the OA stress, with a non-significant decrease at pH 7.7 and a significant sharp decline at pH 7.4 (**Figure 2B**). The unaffected DDN assimilation at pH 7.7 may be attributed to the homeostasis of microbial, particularly diazotrophic community, whereas the marked decrease of DDN assimilation at pH 7.4 may be related to the disordered symbiosis with diazotrophs. Evidences that corals maintain high bacterial compositional stability under mild OA conditions (pH 7.9) have been reported in *A. millepora* and *S. hystrix* (Webster et al., 2016; Glasl et al., 2019). In contrast, a break in the coral–bacterial symbiosis and marked changes in bacterial abundance and diversity were found under severe OA (Morrow et al., 2015; Zaneveld et al., 2017). The abundance of cyanobacterial symbionts and *Endozoicomonas* sp., which were proposed to contribute to N cycling, was significantly reduced in the coral microbiome at a CO_2 seep (Morrow et al., 2015). These findings imply that OA may disrupt the community structure of microbes involved in N cycling, which poses a threat to coral growth and calcification. The significant decrease in coral calcification rates under OA in the present study (**Figure 3A**) may also be attributed to the disordered processes associated with calcifying bacteria, such as the recently discovered photosynthesis-induced, bacterial—algal calcification (Frommlet et al., 2015, 2018), or changes in the community structure of some symbiotic cyanobacteria that promote calcium carbonate formation (Durak et al., 2019; Nitschke et al., 2020).

The $\delta^{15}N$ values is positively correlated with the availability of N nutrient or heterotrophic input in coral holobiont (Donovan et al., 2020), therefore, the declined $\delta^{15}N$ values at lowed pH in the present study (**Figure 2D**) suggest reduced N utilization and heterotrophy in *G. fascicularis* under OA conditions. In N-replete corals, acquisition and translocation of PFC were significantly higher and thus resulted in enhanced host calcification (Langdon and Atkinson, 2005; Béraud et al., 2013). Conversely, N-deficient

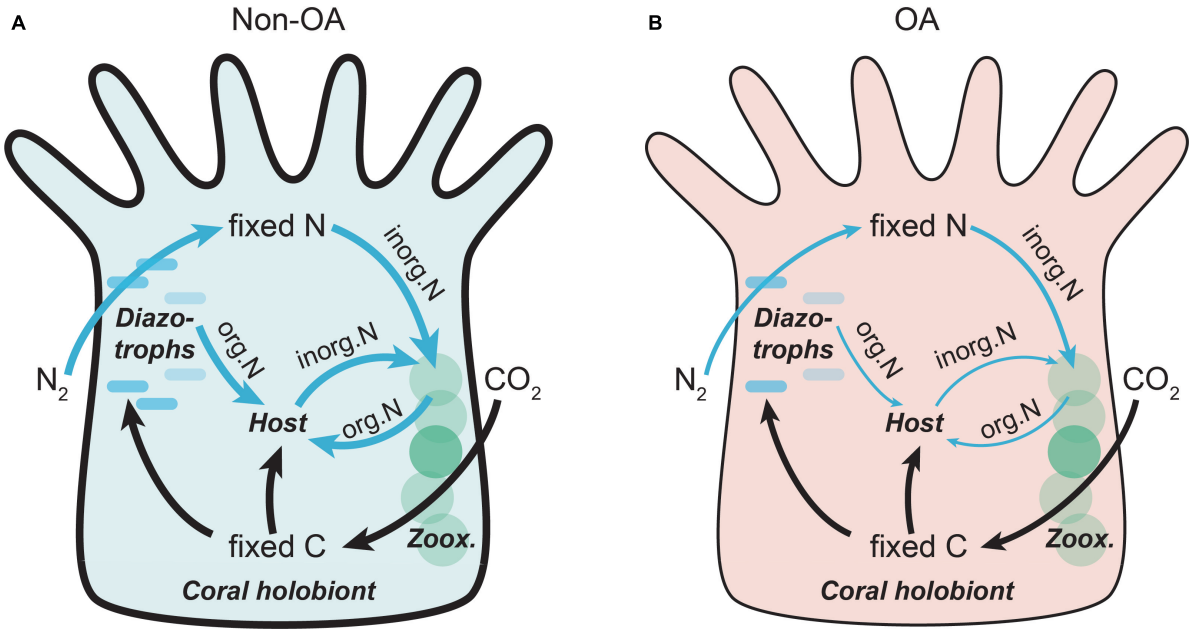

FIGURE 4 | Schematic diagram illustrating the effects of OA on translocation and flux of fixed carbon and nitrogen in the coral holobiont. Shown are conceptual models under **(A)** Non-OA and **(B)** OA conditions. The diazotrophs provide fixed inorganic nitrogen to the Symbiodiniaceae, whereas direct ingestion and digestion of diazotrophic cells is a primary pathway of organic nitrogen to the coral host. The fluxes of carbon (black) and nitrogen (blue) are represented as arrows, the width of which corresponds to the levels of the flux. The thickness of coral epidermis corresponds to the resulting coral calcification rates at different conditions. Zoox., zooxanthellae; inorg.N, inorganic nitrogen; org.N, organic nitrogen.

corals showed reduced metabolism and nutrient limitation, leading to reduced calcification rates and decreased symbiont growth and density (Wiedenmann et al., 2013; Ezzat et al., 2015). The combined reduction of DDN assimilation rates and $\delta^{15}N$ natural isotope abundance under OA in *G. fascicularis* (**Figure 2**) potentially may have compromised the coral calcification, although interpreting this in symbiotic corals is difficult because calcification is affected by various processes (Karcher et al., 2020).

Corals have the capacity to maintain elevated pH levels in calcifying fluids despite decreased seawater pH (Mcculloch et al., 2012). However, the upregulation of calcifying fluid pH is believed to be an energy-requiring process that involves removal of protons from the calcifying fluid by Ca^{2+} ATPases (Tambutté et al., 2011). In this study, the coral calcification rates decreased linearly with prolonged acidification and were negatively correlated with the corresponding Ω_{arag} of the seawater. Hence, a lowering of the Ω_{arag} makes the calcification process more energy consuming (Hohn and Merico, 2012). Furthermore, the N cycle is driven by complex and unique microbial transformations that are energetically expensive. For example, N_2 fixation requires at least 16 ATPs to reduce N_2 to NH_3 (Benavides et al., 2017). It has been found in corals that N_2 fixation was inhibited when photosynthesis was blocked, but could be recovered if glucose was added (Shashar et al., 1994), suggesting that N_2 fixation strongly depends on photosynthesis to meet its energetic demands (Garcia et al., 2013). As calcification and N_2 fixation are both energy-intensive processes, they probably compete for energy within the coral holobiont. Because PFC assimilation was not increased under OA condition, the increased energy demand to cope with OA stress must create an energy deficit and result in decreased rates of DDN assimilation and calcification.

Based on our measurements and published modeling data (Benavides et al., 2017), we propose a conceptual model of C and N fluxes in the coral holobiont under non-OA vs. OA conditions (**Figure 4**). Under non-OA control condition, fixed inorganic nitrogen, mostly in the form of $NH4^+$, is primarily available to the Symbiodiniaceae, whereas the ingestion and digestion of diazotrophic cells provides organic nitrogen (e.g., in the form of amino acids) to the coral host. The release of organic carbon and energetic substrates from Symbiodiniaceae thus enhances diazotrophic growth and subsequent DDN assimilation, actively promoting coral calcification. On the contrary, OA triggers decreases in the overall assimilation of DDN, leading to insufficient organic nutrient supply to the growth and metabolism of the coral host, further exacerbating the coral calcification. To cope with this limited nutrient availability and imbalance between organic and inorganic nutrients, the coral appears to have evolved a trade-off mechanism to conserve and recycle the remaining fixed inorganic nitrogen to temporarily satisfy the demand of Symbiodiniaceae for barely unaffected assimilation of PFC and energy supply to the holobiont. The contrasting impacts of OA on PFC and DDN assimilation strongly suggests the flexibility of corals to sustain a largely undamaged photosystem and coral–algal symbiosis at the expense of N_2 fixation machinery and/or change

in the coral–bacterial symbiosis. While this strategic trade-off might work temporarily, it should be noted that long-term loss of bioavailable N would limit Symbiodiniaceae growth and photosynthesis, ultimately suppressing coral resilience to OA (Anthony et al., 2008). Taken together, the findings and proof-of-concept model presented in our study highlight the importance of N cycling and nutrient dynamics for calcifying organisms such as corals to adapt and acclimatize to future acidifying oceans (Thomsen et al., 2013; Leung et al., 2019). In this light, we emphasize the need for research focusing on other essential elements, such as N, which have important roles in addition to C in shaping marine symbioses.

DATA AVAILABILITY STATEMENT

The original contributions presented in the study are included in the article/**Supplementary Material**, further inquiries can be directed to the corresponding author/s.

ETHICS STATEMENT

Corals were collected under permit number 2014003 for the Domestication and Breeding of Aquatic Wild Animals, issued by Department of Ocean and Fisheries of Hainan Province of the People's Republic of China.

AUTHOR CONTRIBUTIONS

XZ, TS, and LY conceived and designed the study. CW performed the experiments, with the help from HS for isotopic measurements, XD for water quality assessment, and GN for statistical analysis. XZ, CW, and TS interpreted the data and wrote the manuscript. All authors read and approved the final version of the manuscript.

FUNDING

This work was supported by the National Key Research and Development Program of China (Grant Nos. 2016YFA0601203 and 2020YFA0607602), the National Natural Science Foundation of China (Grant Nos. 41876119 and 41976127), the Scientific Research Foundation from the Fujian Provincial Station for Field Observation and Research of Island and Coastal Zone, administered by the Third Institute of Oceanography, Ministry of Natural Resources of China (Grant No. TIO 2019017).

ACKNOWLEDGMENTS

We are grateful to Yuanchao Li and Shiquan Chen from Hainan Academy of Ocean and Fisheries Sciences for assistance in coral sampling, and Yan Li and Wencong Huang for help with aquaria maintenance.

SUPPLEMENTARY MATERIAL

The Supplementary Material for this article can be found online at: https://www.frontiersin.org/articles/10.3389/fmars.2021.644965/full#supplementary-material

REFERENCES

Allgeier, J. E., Andskog, M. A., Hensel, E., Appaldo, R., Layman, C., and Kemp, D. W. (2020). Rewiring coral: anthropogenic nutrients shift diverse coral-symbiont nutrient and carbon interactions toward symbiotic algal dominance. *Glob. Chang. Biol.* 26, 5588–5601. doi: 10.1111/gcb.15230

Anthony, K. R. N., Kline, D. I., Diazpulido, G., Dove, S., and Hoeghguldberg, O. (2008). Ocean acidification causes bleaching and productivity loss in coral reef builders. *Proc. Natl. Acad. Sci. U.S.A* 105, 17442–17446. doi: 10.1073/pnas.0804478105

Barkley, H. C., Cohen, A. L., McCorkle, D. C., and Golbuu, Y. (2017). Mechanisms and thresholds for pH tolerance in Palau corals. *J. Exp. Mar. Biol. Ecol.* 489, 7–14. doi: 10.1016/j.jembe.2017.01.003

Bednarz, V. N., Grover, R., Maguer, J. F., Fine, M., and Ferrier-Pagès, C. (2017). The assimilation of diazotroph-derived nitrogen by Scleractinian corals depends on their metabolic status. *MBio* 8:e02058–16. doi: 10.1128/mBio.02058-16

Bednarz, V. N., van de Water, J. A., Rabouille, S., Maguer, J. F., Grover, R., and Ferrier-Pagès, C. (2019). Diazotrophic community and associated dinitrogen fixation within the temperate coral *Oculina patagonica*. *Environ. Microbiol.* 21, 480–495. doi: 10.1111/1462-2920.14480

Benavides, M., Bednarz, V. N., and Ferrier-Pagès, C. (2017). Diazotrophs: overlooked key players within the coral symbiosis and tropical reef ecosystems? *Front. Mar. Sci.* 4:10. doi: 10.3389/fmars.2017.00010

Béraud, E., Gevaert, F., Rottier, C., and Ferrier-Pagès, C. (2013). The response of the scleractinian coral *Turbinaria reniformis* to thermal stress depends on the nitrogen status of the coral holobiont. *J. Exp. Biol.* 216, 2665–2674. doi: 10.1242/jeb.085183

Byrne, M., Lamare, M., Winter, D., Dworjanyn, S. A., and Uthicke, S. (2013). The stunting effect of a high CO_2 ocean on calcification and development in sea urchin larvae, a synthesis from the tropics to the poles. *Philos. Trans. R Soc. Lond. B Biol. Sci.* 368:20120439. doi: 10.1098/rstb.2012.0439

Capone, D. G. (1993). "Determination of nitrogenase activity in aquatic samples using the acetylene reduction procedure," in *Handbook of Methods in Aquatic Microbial Ecology*, eds P. F. Kemp, J. J. Cole, B. F. Sherr, and E. B. Sherr (London: CRC Press), 621–631. doi: 10.1201/9780203752746-74

Cardini, U., Bednarz, V. N., Foster, R. A., and Wild, C. (2014). Benthic N_2 fixation in coral reefs and the potential effects of human-induced environmental change. *Ecol. Evol.* 4, 1706–1727. doi: 10.1002/ece3.1050

Comeau, S., Carpenter, R. C., and Edmunds, P. J. (2017). Effects of pCO_2 on photosynthesis and respiration of tropical scleractinian corals and calcified algae. *ICES J. Mar. Sci.* 74, 1092–1102. doi: 10.1093/icesjms/fsv267

Coronado, I., Fine, M., Bosellini, F. R., and Stolarski, J. (2019). Impact of ocean acidification on crystallographic vital effect of the coral skeleton. *Nat. commun.* 10, 1–9. doi: 10.1038/s41467-019-10833-6

Davies, P. S. (1989). Short-term growth measurements of corals using an accurate buoyant weighing technique. *Mar. Biol.* 101, 389–395. doi: 10.1007/BF00428135

Dickson, A. G., Sabine, C. L., and Christian, J. R. (2007). *Guide to Best Practices for Ocean CO_2 Measurements*. Sidney, BC: North Pacific Marine Science Organization.

Donovan, M. K., Adam, T. C., Shantz, A. A., Speare, K. E., Munsterman, K. S., Rice, M. M., et al. (2020). Nitrogen pollution interacts with heat stress to increase

coral bleaching across the seascape. *Proc. Natl. Acad. Sci. U.S.A.* 117, 5351–5357. doi: 10.1073/pnas.1915395117

Dove, S. G., Kline, D. I., Pantos, O., Angly, F. E., Tyson, G. W., and Hoeghguldberg, O. (2013). Future reef decalcification under a business-as-usual CO_2 emission scenario. *Proc. Natl. Acad. Sci. U.S.A.* 110, 15342–15347. doi: 10.1073/pnas.1302701110

Durak, G. M., Laumann, M., Wolf, S. L. P., Pawar, A., Gebauer, D., and Böttcher, T. (2019). Pseudo-biomineralization: complex mineral structures shaped by microbes. *ACS Biomater. Sci. Eng.* 5, 5088–5096. doi: 10.1021/acsbiomaterials.9b00387

Enochs, I. C., Manzello, D. P., Kolodziej, G., Noonan, S. H., Valentino, L., and Fabricius, K. E. (2016). Enhanced macroboring and depressed calcification drive net dissolution at high-CO_2 coral reefs. *Proc. R. Soc. B Biol. Sci.* 283:20161742. doi: 10.1098/rspb.2016.1742

Eyre, B. D., Cyronak, T., Drupp, P., De Carlo, E. H., Sachs, J. P., and Andersson, A. J. (2018). Coral reefs will transition to net dissolving before end of century. *Science* 359, 908–911. doi: 10.1126/science.aao1118

Ezzat, L., Maguer, J. F., Grover, R., and Ferrier-Pages, C. (2015). New insights into carbon acquisition and exchanges within the coral-dinoflagellate symbiosis under NH_4^+ and NO_3^- supply. *Proc. Biol. Sci.* 282, 20150610. doi: 10.1098/rspb.2015.0610

Fine, M., and Loya, Y. (2002). Endolithic algae: an alternative source of photoassimilates during coral bleaching. *Proc. Biol. Sci.* 269, 1205–1210. doi: 10.1098/rspb.2002.1983

Fiore, C. L., Jarett, J. K., Olson, N. D., and Lesser, M. P. (2010). Nitrogen fixation and nitrogen transformations in marine symbioses. *Trends Microbiol.* 18, 455–463. doi: 10.1016/j.tim.2010.07.001

Frommlet, J. C., Sousa, M. L., Alves, A., Vieira, S. I., Suggett, D. J., and Serôdio, J. (2015). Coral symbiotic algae calcify ex hospite in partnership with bacteria. *Proc. Natl. Acad. Sci. U.S.A.* 112, 6158–6163. doi: 10.1073/pnas.1420991112

Frommlet, J. C., Wangpraseurt, D., Sousa, M. L., Guimaraes, B., Medeiros da Silva, M., Kuhl, M., et al. (2018). Symbiodinium-induced formation of microbialites: mechanistic insights from in vitro experiments and the prospect of its occurrence in nature. *Front. Microbiol.* 9:998. doi: 10.3389/fmicb.2018.00998

Furla, P., Galgani, I., Durand, I., and Allemand, D. (2000). Sources and mechanisms of inorganic carbon transport for coral calcification and photosynthesis. *J. Exp. Biol.* 203, 3445–3457.

Garcia, N. S., Fu, F.-X., and Hutchins, D. A. (2013). Colimitation of the unicellular photosynthetic diazotroph *Crocosphaera watsonii* by phosphorus, light, and carbon dioxide. *Limnol. Oceanogr.* 58, 1501–1512. doi: 10.4319/lo.2013.58.4.1501

Glasl, B., Smith, C. E., Bourne, D. G., and Webster, N. S. (2019). Disentangling the effect of host-genotype and environment on the microbiome of the coral *Acropora tenuis*. *PeerJ* 7:e6377. doi: 10.7717/peerj.6377

Großkopf, T., Mohr, W., Baustian, T., Schunck, H., Gill, D., Kuypers, M. M., et al. (2012). Doubling of marine dinitrogen-fixation rates based on direct measurements. *Nature* 488, 361–364. doi: 10.1038/nature11338

Hama, T., Miyazaki, T., Ogawa, Y., Iwakuma, T., Takahashi, M., Otsuki, A., et al. (1983). Measurement of photosynthetic production of a marine phytoplankton population using a stable ^{13}C isotope. *Mar. Biol.* 73, 31–36. doi: 10.1007/BF00396282

Hoadley, K. D., Rollison, D., Pettay, D. T., and Warner, M. E. (2015). Differential carbon utilization and asexual reproduction under elevated pCO_2 conditions in the model anemone, *Exaiptasia pallida*, hosting different symbionts. *Limnol. Oceanogr.* 60, 2108–2120. doi: 10.1002/lno.10160

Hoegh-Guldberg, O., Mumby, P. J., Hooten, A. J., Steneck, R. S., Greenfield, P., Gomez, E., et al. (2007). Coral reefs under rapid climate change and ocean acidification. *Science* 318, 1737–1742. doi: 10.1126/science.1152509

Hohn, S., and Merico, A. (2012). Effects of seawater pCO_2 changes on the calcifying fluid of scleractinian corals. *Biogeosci. Discuss.* 9, 2655–2689. doi: 10.5194/bgd-9-2655-2012

Kaniewska, P., Campbell, P. R., Kline, D. I., Rodriguezlanetty, M., Miller, D. J., Dove, S., et al. (2012). Major cellular and physiological impacts of ocean acidification on a reef building coral. *PLos One* 7:e34659. doi: 10.1371/journal.pone.0034659

Kaniewska, P., Chan, C. K. K., Kline, D., Ling, E. Y. S., Rosic, N., Edwards, D., et al. (2015). Transcriptomic changes in coral holobionts provide insights into physiological challenges of future climate and ocean change. *PLos One* 10:e0139223. doi: 10.1371/journal.pone.0139223

Karcher, D. B., Roth, F., Carvalho, S., El-Khaled, Y. C., Tilstra, A., Kurten, B., et al. (2020). Nitrogen eutrophication particularly promotes turf algae in coral reefs of the central Red Sea. *PeerJ* 8:e8737. doi: 10.7717/peerj.8737

Kurman, M. D., Gomez, C. E., Georgian, S. E., Lunden, J. J., and Cordes, E. E. (2017). Intra-specific variation reveals potential for adaptation to ocean acidification in a cold-water coral from the Gulf of Mexico. *Front. Mar. Sci.* 4:111. doi: 10.3389/fmars.2017.00111

Langdon, C., and Atkinson, M. J. (2005). Effect of elevated pCO_2 on photosynthesis and calcification of corals and interactions with seasonal change in temperature/irradiance and nutrient enrichment. *J. Geophys. Res. Oceans* 110:C09S07. doi: 10.1029/2004JC002576

Lema, K. A., Clode, P. L., Kilburn, M. R., Thornton, R., Willis, B. L., and Bourne, D. G. (2016). Imaging the uptake of nitrogen-fixing bacteria into larvae of the coral *Acropora millepora*. *ISME J.* 10:1804. doi: 10.1038/ismej.2015.229

Lema, K. A., Willis, B. L., and Bourne, D. G. (2014). Amplicon pyrosequencing reveals spatial and temporal consistency in diazotroph assemblages of the *Acropora millepora* microbiome. *Environ. Microbiol.* 16, 3345–3359. doi: 10.1111/1462-2920.12366

Lesser, M. P., Falcón, L. I., Rodríguez-Román, A., Enríquez, S., Hoegh-Guldberg, O., and Iglesias-Prieto, R. (2007). Nitrogen fixation by symbiotic cyanobacteria provides a source of nitrogen for the scleractinian coral Montastraea cavernosa. *Mar. Ecol. Prog. Ser.* 346, 143–152. doi: 10.3354/meps07008

Lesser, M. P., Mazel, C. H., Gorbunov, M. Y., and Falkowski, P. G. (2004). Discovery of symbiotic nitrogen-fixing cyanobacteria in corals. *Science* 305, 997–1000. doi: 10.1126/science.1099128

Lesser, M. P., Morrow, K. M., and Pankey, M. S. (2019). N_2 fixation, and the relative contribution of fixed N, in corals from Curaçao and Hawaii. *Coral Reefs* 38, 1145–1158. doi: 10.1007/s00338-019-01863-z

Leung, J. Y. S., Chen, Y., Nagelkerken, I., Zhang, S., Xie, Z., and Connell, S. D. (2020). Calcifiers can adjust shell building at the nanoscale to resist ocean acidification. *Small* 16:e2003186. doi: 10.1002/smll.202003186

Leung, J. Y. S., Connell, S. D., Nagelkerken, I., and Russell, B. D. (2017). Impacts of near-future ocean acidification and warming on the shell mechanical and geochemical properties of gastropods from intertidal to subtidal zones. *Environ. Sci. Technol.* 51, 12097–12103. doi: 10.1021/acs.est.7b02359

Leung, J. Y. S., Doubleday, Z. A., Nagelkerken, I., Chen, Y., Xie, Z., and Connell, S. D. (2019). How calorie-rich food could help marine calcifiers in a CO_2-rich future. *Proc. Biol. Sci.* 286:20190757. doi: 10.1098/rspb.2019.0757

Lewis, E., Wallace, D., and Allison, L. J. (1998). *Program Developed for CO_2 System Calculations*. Upton, NY: Brookhaven National Lab.

Li, Y., Zheng, X., Yang, X., Ou, D., Lin, R., and Liu, X. (2017). Effects of live rock on removal of dissolved inorganic nitrogen in coral aquaria. *Acta Oceanologica Sin.* 36, 87–94. doi: 10.1007/s13131-017-1092-1

Lin, Z., Chen, M., Dong, X., Zheng, X., Huang, H., Xu, X., et al. (2017). Transcriptome profiling of *Galaxea fascicularis* and its endosymbiont Symbiodinium reveals chronic eutrophication tolerance pathways and metabolic mutualism between partners. *Sci. Rep.* 7:42100. doi: 10.1038/srep42100

Mcculloch, M., Trotter, J., Montagna, P., Falter, J., Dunbar, R., Freiwald, A., et al. (2012). Resilience of cold-water scleractinian corals to ocean acidification: boron isotopic systematics of pH and saturation state up-regulation. *Geochim. Cosmochim. Acta* 87, 21–34. doi: 10.1016/j.gca.2012.03.027

Mollica, N. R., Guo, W., Cohen, A. L., Huang, K.-F., Foster, G. L., Donald, H. K., et al. (2018). Ocean acidification affects coral growth by reducing skeletal density. *Proc. Natl. Acad. Sci. U.S.A.* 115, 1754–1759. doi: 10.1073/pnas.1712806115

Montoya, J. P., Voss, M., Kahler, P., and Capone, D. G. (1996). A simple, high-precision, high-sensitivity tracer assay for N_2 fixation. *Appl. Environ. Microbiol.* 62, 986–993. doi: 10.3389/fmars.2017.00010

Morrow, K. M., Bourne, D. G., Humphrey, C., Botte, E. S., Laffy, P., Zaneveld, J., et al. (2015). Natural volcanic CO_2 seeps reveal future trajectories for host-microbial associations in corals and sponges. *ISME J.* 9, 894–908. doi: 10.1038/ismej.2014.188

Moya, A., Huisman, L., Ball, E., Hayward, D., Grasso, L., Chua, C., et al. (2012). Whole transcriptome analysis of the coral *Acropora millepora* reveals complex

responses to CO_2-driven acidification during the initiation of calcification. *Mol. Ecol.* 21, 2440–2454. doi: 10.1111/j.1365-294X.2012.05554.x

Muscatine, L., and Porter, J. W. (1977). Reef corals: mutualistic symbioses adapted to nutrient-poor environments. *Bioscience* 27, 454–460. doi: 10.2307/1297526

Nitschke, M. R., Fidalgo, C., Simoes, J., Brandao, C., Alves, A., Serodio, J., et al. (2020). Symbiolite formation: a powerful in vitro model to untangle the role of bacterial communities in the photosynthesis-induced formation of microbialites. *ISME J.* 14, 1533–1546. doi: 10.1038/s41396-020-0629-z

Noonan, S. H. C., Fabricius, K. E., and Humphrey, C. (2013). Symbiodinium community composition in Scleractinian corals is not affected by life-long exposure to elevated carbon dioxide. *PLos One* 8:e63985. doi: 10.1371/journal.pone.0063985

Olson, N. D., and Lesser, M. P. (2013). Diazotrophic diversity in the Caribbean coral, *Montastraea cavernosa*. *Arch. Microbiol.* 195, 853–859. doi: 10.1007/s00203-013-0937-z

Peixoto, R. S., Rosado, P. M., Leite, D. C. D. A., Rosado, A. S., and Bourne, D. G. (2017). Beneficial microorganisms for corals (BMC): proposed mechanisms for coral health and resilience. *Front. Microbiol.* 8:341. doi: 10.3389/fmicb.2017.00341

Rädecker, N., Meyer, F. W., Bednarz, V. N., Cardini, U., and Wild, C. (2014). Ocean acidification rapidly reduces dinitrogen fixation associated with the hermatypic coral *Seriatopora hystrix*. *Mar. Ecol. Prog. Ser.* 511, 297–302. doi: 10.3354/meps10912

Rädecker, N., Pogoreutz, C., Voolstra, C. R., Wiedenmann, J., and Wild, C. (2015). Nitrogen cycling in corals: the key to understanding holobiont functioning? *Trends Microbiol.* 23, 490–497. doi: 10.1016/j.tim.2015.03.008

Rowan, R. (1998). Diversity and ecology of zooxanthellae on coral reefs. *J. Phycol.* 34, 407–417. doi: 10.1046/j.1529-8817.1998.340407.x

Shashar, N., Cohen, Y., Loya, Y., and Sar, N. (1994). Nitrogen fixation (acetylene reduction) in stony corals: evidence for coral-bacteria interactions. *Mar. Ecol. Prog. Ser.* 111, 259–264. doi: 10.3354/meps111259

Shiozaki, T., Nagata, T., Ijichi, M., and Furuya, K. (2015). Nitrogen fixation and the diazotroph community in the temperate coastal region of the northwestern North Pacific. *Biogeosciences* 12, 4751–4764. doi: 10.5194/bg-12-4751-2015

Silveira, C. B., Cavalcanti, G. S., Walter, J. M., Silva-Lima, A. W., Dinsdale, E. A., Bourne, D. G., et al. (2017). Microbial processes driving coral reef organic carbon flow. *FEMS Microbiol. Rev.* 41, 575–595. doi: 10.1093/femsre/fux018

Strahl, J., Stolz, I., Uthicke, S., Vogel, N., Noonan, S., and Fabricius, K. (2015). Physiological and ecological performance differs in four coral taxa at a volcanic carbon dioxide seep. *Comp. Biochem. Physiol. A Mol. Integr. Physiol.* 184, 179–186. doi: 10.1016/j.cbpa.2015.02.018

Takahashi, A., and Kurihara, H. (2013). Ocean acidification does not affect the physiology of the tropical coral *Acropora digitifera* during a 5-week experiment. *Coral Reefs* 32, 305–314. doi: 10.1007/s00338-012-0979-8

Tambutté, S., Holcomb, M., Ferrier-Pagès, C., Reynaud, S., Tambutté, É, Zoccola, D., et al. (2011). Coral biomineralization: from the gene to the environment. *J. Exp. Mar. Biol. Ecol.* 408, 58–78. doi: 10.1016/j.jembe.2011.07.026

Thomsen, J., Casties, I., Pansch, C., Kortzinger, A., and Melzner, F. (2013). Food availability outweighs ocean acidification effects in juvenile *Mytilus edulis*: laboratory and field experiments. *Glob. Chang. Biol.* 19, 1017–1027. doi: 10.1111/gcb.12109

Tremblay, P., Grover, R., Maguer, J. F., Legendre, L., and Ferrier-Pagès, C. (2012). Autotrophic carbon budget in coral tissue: a new ^{13}C-based model of photosynthate translocation. *J. Exp. Biol.* 215, 1384–1393. doi: 10.1242/jeb.065201

Tremblay, P., Maguer, J. F., Grover, R., and Ferrier-Pagès, C. (2015). Trophic dynamics of scleractinian corals: stable isotope evidence. *J. Exp. Biol.* 218, 1223–1234. doi: 10.1242/jeb.115303

Van der Zande, R. M., Achlatis, M., Bender-Champ, D., Kubicek, A., Dove, S., and Hoegh-Guldberg, O. (2020). Paradise lost: end-of-century warming and acidification under business-as-usual emissions have severe consequences for symbiotic corals. *Glob. Chang. Biol.* 26, 2203–2219. doi: 10.1111/gcb.14998

Vogel, N., Fabricius, K. E., Strahl, J., Noonan, S. H. C., Wild, C., and Uthicke, S. (2015). Calcareous green alga Halimeda tolerates ocean acidification conditions at tropical carbon dioxide seeps. *Limnol. Oceanogr.* 60, 263–275. doi: 10.1002/lno.10021

Wall, C. B., Kaluhiokalani, M., Popp, B. N., Donahue, M. J., and Gates, R. D. (2020). Divergent symbiont communities determine the physiology and nutrition of a reef coral across a light-availability gradient. *ISME J.* 14, 945–958. doi: 10.1038/s41396-019-0570-1

Webster, N., Negri, A., Botté, E., Laffy, P., Flores, F., Noonan, S., et al. (2016). Host-associated coral reef microbes respond to the cumulative pressures of ocean warming and ocean acidification. *Sci. Rep.* 6:19324. doi: 10.1038/srep19324

White, A. E., Granger, J., Selden, C., Gradoville, M. R., Potts, L., Bourbonnais, A., et al. (2020). A critical review of the $^{15}N_2$ tracer method to measure diazotrophic production in pelagic ecosystems. *Limnol. Oceanogr. Methods* 18, 129–147. doi: 10.1002/lom3.10353

Wiedenmann, J., D'Angelo, C., Smith, E. G., Hunt, A. N., Legiret, F., Postle, A. D., et al. (2013). Nutrient enrichment can increase the susceptibility of reef corals to bleaching. *Nat. Clim. Chang.* 3, 160–164. doi: 10.1038/NCLIMATE1661

Zaneveld, J. R., McMinds, R., and Thurber, R. V. (2017). Stress and stability: applying the Anna Karenina principle to animal microbiomes. *Nat. Microbiol.* 2:17121.

Zehr, J. P., and Kudela, R. M. (2011). Nitrogen cycle of the open ocean: from genes to ecosystems. *Annu. Rev. Mar. Sci.* 3, 197–225. doi: 10.1146/annurev-marine-120709-142819

Zheng, X., Li, Y., Chen, S., and Lin, R. (2018a). Effects of calcium ion concentration on calcification rates of six stony corals: a mesocosm study. *Aquaculture* 497, 246–252. doi: 10.1016/j.aquaculture.2018.07.041

Zheng, X., Wang, C., Hadi, T. A., Ye, Y., and Pan, K. (2018b). An ocean acidification-simulated system and its application in coral physiological studies. *Acta Oceanologica Sin.* 37, 55–62. doi: 10.1007/s13131-018-1223-3

Conflict of Interest: The authors declare that the research was conducted in the absence of any commercial or financial relationships that could be construed as a potential conflict of interest.

frontiers in Marine Science

ORIGINAL RESEARCH
published: 28 April 2021
doi: 10.3389/fmars.2021.645660

Morphological Properties of Gastropod Shells in a Warmer and More Acidic Future Ocean Using 3D Micro-Computed Tomography

Eva Chatzinikolaou[1], Kleoniki Keklikoglou[1,2] and Panos Grigoriou[3]*

[1] Hellenic Centre for Marine Research (HCMR), Institute of Marine Biology, Biotechnology and Aquaculture (IMBBC), Heraklion, Crete, Greece, [2] Biology Department, University of Crete, Heraklion, Crete, Greece, [3] Hellenic Centre for Marine Research (HCMR), CretAquarium, Heraklion, Crete, Greece

The increased absorption of atmospheric CO_2 by the ocean reduces pH and affects the carbonate chemistry of seawater, thus interfering with the shell formation processes of marine calcifiers. The present study aims to examine the effects of ocean acidification and warming on the shell morphological properties of two intertidal gastropod species, *Nassarius nitidus* and *Columbella rustica*. The experimental treatments lasted for 3 months and combined a temperature increase of 3°C and a pH reduction of 0.3 units. The selected treatments reflected the high emissions (RCP 8.5) "business as usual" scenario of the Intergovernmental Panel on Climate Change models for eastern Mediterranean. The morphological and architectural properties of the shell, such as density, thickness and porosity were examined using 3D micro-computed tomography, which is a technique giving the advantage of calculating values for the total shell (not only at specific points) and at the same time leaving the shells intact. *Nassarius nitidus* had a lower shell density and thickness and a higher porosity when the pH was reduced at ambient temperature, but the combination of reduced pH and increased temperature did not have a noticeable effect in comparison to the control. The shell of *Columbella rustica* was less dense, thinner and more porous under acidic and warm conditions, but when the temperature was increased under ambient pH the shells were thicker and denser than the control. Under low pH and ambient temperature, shells showed no differences compared to the control. The vulnerability of calcareous shells to ocean acidification and warming appears to be variable among species. Plasticity of shell building organisms as an acclimation action toward a continuously changing marine environment needs to be further investigated focusing on species or shell region specific adaptation mechanisms.

Keywords: climate change, ocean acidification, shell density, shell thickness, shell porosity, gastropod, micro-CT

OPEN ACCESS

Edited by:
Jonathan Y. S. Leung, University of Adelaide, Australia

Reviewed by:
Fiorella Prada, University of Bologna, Italy
Kristina Barclay, University of Calgary, Canada

****Correspondence:***
Eva Chatzinikolaou
evachatz@hcmr.gr

Specialty section:
This article was submitted to Global Change and the Future Ocean, a section of the journal Frontiers in Marine Science

Received: *23 December 2020*
Accepted: *30 March 2021*
Published: *28 April 2021*

Citation:
Chatzinikolaou E, Keklikoglou K and Grigoriou P (2021) Morphological Properties of Gastropod Shells in a Warmer and More Acidic Future Ocean Using 3D Micro-Computed Tomography. Front. Mar. Sci. 8:645660. doi: 10.3389/fmars.2021.645660

INTRODUCTION

The last three decades were the warmest period of the last 1,400 years in the Northern Hemisphere of the planet (IPCC, 2014). The upper 75 m of the sea surface have been experiencing strongest warming (0.11°C per decade) over the period 1971 to 2010 (IPCC, 2014). According to the IPCC (2014) high GHG emissions scenario (RCP8.5) the global mean surface temperature will

be 1.4 - 2.6°C higher during the next 25-44 years. At the same time, the oceans have absorbed approximately 25% of all the CO_2 released into the atmosphere by humans since the start of the Industrial Revolution, which has resulted in a reduction of the ocean surface pH by 0.1 units (Orr et al., 2005; IPCC, 2014). The carbonates dissolved in seawater include biogenic magnesium calcites from coralline algae, aragonite from corals and pteropods, and calcite from coccolithophorids and foraminifera (Feely et al., 2004). As the oceans become enriched in anthropogenic CO_2, the chemistry of the ocean is changing because the calcium carbonate saturation state is decreased especially in cooler mid-high latitude environments (Kleypas et al., 2006). A reduction of 20-30% of mean carbonated ions has been observed in surface seawaters (Feely et al., 2004). The dissolution of particulate organic carbon in the ocean affects the calcification rates of organisms, which are predicted to decrease by 40% until 2100 if anthropogenic CO_2 emissions are not reduced (Andersson et al., 2006). Biogenic calcification rates are predicted to fall below the $CaCO_3$ dissolution rate, meaning that $CaCO_3$ would be dissolving faster than it is being produced (Andersson et al., 2006). The impacts of ocean acidification may be first witnessed in coastal ecosystems which express higher variability in carbonate chemistry and are more unstable environments compared to the deep sea (Feely et al., 2004; Andersson et al., 2006; Harris et al., 2013).

Shell calcification processes in marine organisms can be affected by ocean acidification as has been documented for a number of molluscan taxa (Gaylord et al., 2011; Coleman et al., 2014; Queirós et al., 2015; Marshall et al., 2019; Doney et al., 2020). The scientific literature on the effects of ocean acidification on molluscs has expanded rapidly indicating a general trend of shell growth reduction under low pH conditions. For example, *Nucella lamellosa* in Canada inhibited its shell growth when exposed for a very short period (6 days) to a pH treatment that was 0.2-0.4 units lower than ambient (Nienhuis et al., 2010). Ries et al. (2009) indicated that shell calcification of *Littorina littorea* and *Urosalpinx cinerea* was reduced after exposure to low pH (0.1–0.2 units) for a period of 60 days. *Strombus luhuanus* suffered a significant reduction of growth even after a very moderate pH decrease (0.04 units) over a 6-month period (Shirayama and Thornton, 2005). However, shell growth of some other species such as *Nassarius festivus* in Hong Kong was not significantly affected by reduced pH (950 and 1250 μatm for 31 days) (Zhang et al., 2016), thus indicating that sensitivity to ocean acidification is species-specific and needs to be explored in fine detail (Doney et al., 2020). Similarly, shell growth of *Nucella ostrina* was not affected when pH was reduced by 0.5 units for a period of 6 months, although its shell became 10% weaker under predation cues (Barclay et al., 2019). Temperature as a factor alone has been also proven to affect the formation of mollusc shells, such as in *Chamelea gallina* that formed lighter, thinner and more porous shells at higher temperatures resulting in reduced shell fracture load (Gizzi et al., 2016). Furthermore, the combined effect of low pH (7.8) and increased temperature (28°C) in the pearl oyster *Pinctada fucata* significantly reduced the net calcification rate, as well as the calcium and carbon shell contents (Li et al., 2016).

The gastropod shell is enlarged by deposition of minerals from the outer edge of the mantle to the aperture lips and consists of four layers, the outer periostracum that is composed of conchin and three more $CaCO_3$ layers (Ruppert and Barnes, 1996). Three different polymorphs of biogenic $CaCO_3$ structures have been found in marine shells (aragonite, calcite and vaterite) that represent complex composites of one or more mineral phases and organic molecules (Nehrke et al., 2012). Calcifiers can adjust their shell strength and properties, which depend on the thickness and packing (i.e., porosity) of calcium carbonate crystals, in order to build more durable shells under ocean acidification conditions (Leung et al., 2020). Ocean acidification might be causing a shift to a more disorganized crystallographic structure in shells, thus reducing their structural integrity and the ability of marine calcifiers to biomineralise (Fitzer et al., 2015).

Some marine calcifiers will still be able to maintain synthesis of their shells even when external seawater parameters are thermodynamically unfavorable for the formation of $CaCO_3$ because they can increase fluid pH and carbonate ion concentration at the very local site of crystal nucleation (DeCarlo et al., 2018). Shells that are composed by the less soluble form of $CaCO_3$ (low-Mg calcite) will be less affected than others (Leung et al., 2017b). According to Ries et al. (2009), species exhibiting increased skeletal or shell dissolution under acidified conditions are mainly composed of the more soluble aragonite and high-Mg calcite $CaCO_3$ polymorphs. Shell thickness of *Subninella undulata* was found to be more resilient to ocean acidification, which might be the result of the more robust periostracum layer that reduces the rate of shell dissolution (Coleman et al., 2014). On the contrary, the Japanese tritons *Charonia lampas* suffered increased dissolution and significant corrosive effects under acidification conditions especially in the older parts of their shell, which resulted in smoother, thinner and less dense shells (Harvey et al., 2018). *Tegula funebralis* showed signs of dissolution on the exterior of their shells when exposed to 0.5 pH units lower than ambient for 6 months, which was attributed to the increased presence of crystal edges and faces on their outer fibrous calcite layer potentially increasing the surface area on which dissolution can occur (Barclay et al., 2020). Thicker and architecturally more diverse shells are a fitness advantage for molluscs as an adaptation to predators (Fisher et al., 2009). Ocean acidification may not only lead to increased fragility of shells but may also elevate energetic costs for shell formation or repairing (Leung et al., 2020). The capacity of molluscs to maintain their shell calcification mechanisms under altered environmental conditions will regulate their successful adaptation and persistence in the future. Shell growth measured traditionally as shell length may continue to develop normally, even under acidified and adverse climatic conditions; however, the newly produced shells might be thinner and more fragile (Byrne and Fitzer, 2019).

In the present study, the individual and combined effects of low pH and high temperature were tested on two gastropod species, *Nassarius nitidus* and *Columbella rustica* (superfamily Buccinoidea). *N. nitidus* is a scavenger able to withstand a great range of salinity and temperature ranges commonly found to low sublittoral and intertidal areas (up to 15 m depth)

(Eriksson and Tallmark, 1974). *C. rustica* is a herbivore (Taylor, 1987) and a scavenger or occasional carnivor (Starmühlner, 1969) living between rocks and in silt patches of the midlittoral zone (Delamotte and Vardala-Theodorou, 2007). Both species are abundant in the Mediterranean and are well adjusted to temperature and pH alterations since they inhabit coastal systems such as rock pools and lagoons where such fluctuations of environmental conditions are common (Wahl et al., 2016). Both species have shells consisting of the more soluble aragonite material (Bouillon, 1958; Cespuglio et al., 1999; Foster and Cravo, 2003), while in other gastropod species a more resistant mixture of low magnesium calcite and aragonite can be found (Ries et al., 2009). The morphological properties of the shell of the abovementioned two species, and more specifically their shell density, thickness and closed porosity, were examined using an advanced 3D imaging and analytical technique (3D micro-computed tomography). This method offers an additional insight in the internal shell micro-structure of the selected gastropods since it allows measurements of specific architectural parameters of the full intact shell. The selected treatments were based on the high emissions RCP 8.5 scenario of the Intergovernmental Panel on Climate Change models for the eastern Mediterranean until the year 2100 (IPCC, 2014), which is commonly referred to as the "business as usual" scenario, suggesting that this is a likely outcome if the society does not make any concerted efforts to cut greenhouse gas emissions.

MATERIALS AND METHODS

Specimen Selection and Experimental Setup

Nassarius nitidus specimens (n = 48; size range 17.7-20.8 mm; mean shell length 19.5 ± 0.8 mm) were collected from subtidal lagoons (1 m depth) in Amvrakikos Bay (Western Greece) (39°3′41″N, 20°48′14.3″E) and *Columbella rustica* (n = 36; size range 10.1-12.3 mm; mean shell length 11.1 ± 0.7 mm) were collected from the coast of Gournes (Heraklion, North Crete) (35°20'06.0"N, 25°16'43.9"E). Acclimatization of gastropods lasted about one month (rate: 0.05 units/10 days for pH; 0.7°C/10 days for temperature). Organisms were maintained following standard aquarist practices and were fed *ad libitum*. The mean ambient temperature in the natural environment was 20°C and in the warm treatments it was 23°C (future RCP 8.5 scenario prediction - increase of 3°C). The ambient pH was 8 and the low pH treatment was 7.7 (future RCP 8.5 scenario prediction - decrease of 0.3 units). The gastropods were equally divided per experimental treatment (i.e., 12 *N. nitidus* and 9 *C. rustica* per treatment), placed in individual tanks (2-4 l) and maintained under the following four experimental treatments for a total period of three months (88 days): a) one control with ambient temperature (20°C) and pH (pH = 8) (code tank 8A), b) one with ambient temperature (20°C) and low pH (pH = 7.7) (code tank 7A), c) one with warmer temperature (23°C) and ambient pH (pH = 8) (code tank 8W) and d) one with warmer temperature (23°C) and low pH conditions (pH = 7.7) (code tank 7W).

A semi-closed experimental system was used to ensure controlled experimental conditions (for details see Chatzinikolaou et al., 2017). Submerged aquarium heaters (RESUN) were used to rise temperature to the desired level in the warm treatments. A bubbling CO_2 system attached to the CO_2 bottles through a manometer (Gloor model 5100/10) and connected to a pH controller system (Tunze 7070/2) was used to adjust the low pH treatments. The pH electrodes were calibrated twice every month with 5.00, 7.00 and 10.00 WTW NBS buffers. Temperature and pH (on the National Bureau of Standards scale -pH_{NBS}) were additionally measured daily (3420 WTW multi-meter), while salinity (salinometer) and oxygen (OxyGuard) were checked every two days. A submerged pump (Boyo WM-15) with additional airstones was used to ensure sufficient water circulation. In addition, 50% of the water in the experimental tanks was renewed twice a week thus maintaining a high water quality within the system (NO_2 < 0.1 mg/l, NO_3 < 0.5 mg/l, NH_3/NH_4 < 0.2 mg/l). Nitrogenous waste products were also assessed twice a week by using photometric test kits (Tetra kit). Total alkalinity (TA) was measured every two weeks according to the Standard Operating Procedure (SOP 3b) described in Dickson et al. (2007) using an open-cell titration (Metrohm Dosimat 765; 0.1 mol/kg in HCl). Measured parameters (pH and TA) were used to calculate the additional parameters of the seawater carbonate system (**Supplementary Material - Table I**) using CO2SYS program with the dissociation constants of Mehrbach et al. (1973) as refitted by Dickson and Millero (1987).

Three individuals of each species were randomly collected from each treatment at the end of the experiment (3 months). Specimens were anesthetized using a rising concentration of $MgCl_2$ starting at 1.5% and gradually reaching 3.5% according to the European Directive 2010/63 EU on the protection of animals used for scientific purposes. The samples were stored at −20°C until scanning was performed.

Scanning and Reconstruction of Images

All scans were performed with a SkyScan 1172 micro-tomograph (Bruker, Kontich, Belgium) at the Hellenic Center for Marine Research (HCMR). The scanner uses a tungsten source and is equipped with an 11 PM CCD camera (4,000 × 2,672 pixels), which can reach a maximal resolution of <0.8 μm/pixel. Specimens were scanned at a voltage of 70 kV and a flux of 142 μA with an aluminum filter of 0.5 mm and images were acquired at a pixel size of 6.51 μm with a camera binning of 1 × 1. Exposure time was 6,455 msec for *N. nitidus* and 7,005 msec for *C. rustica* specimens. Scans were performed for a half rotation of 180° to minimize scanning duration, since initial tests had shown there was no significant loss of information or increase of artifacts compared to a full rotation. All scans were performed over a short period of time without recalibrating the instrument's settings and using the exact same scanning parameters in order to ensure full comparability of the results.

Projection images were reconstructed into cross sections using SkyScan's NRecon software (Bruker, Kontich, Belgium) which employs a modified Feldkamp's back-projection algorithm.

The scans of the same species were reconstructed using the same range of attenuation coefficients (*N. nitidus*: 0.04 - 0.16, *C. rustica*: 0.00 - 0.21) in order to obtain comparable results. The reconstructed images were stored as 8-bit PNG images due to storage limitations, since initial comparisons had shown no significant differences ($p > 0.05$) in the analyses results in comparison to 16-bit TIFF images.

Image Analysis

Cross section images were loaded into the software CT Analyzer v.1.14.4.1 (CTAn, Bruker, Kontich, Belgium) and the mean gray scale values of the total shell were calculated using the binary threshold module as a proxy for relative shell density. For the present analyses, no absolute density values (e.g., Hounsfield units) were required, but only comparability between the scans (relative densities). In the present study, density refers to micro-density (i.e., density of the shell material including $CaCO_3$ and intraskeletal organic matrix) and not to bulk density which includes porosity. The range of the gray scale histogram was the same for specimens of the same species (*N. nitidus*: 1-255, *C. rustica* 40-255).

The 3D analysis was performed in each micro-CT scan using the custom processing plug-in of CTAn software, in order to calculate the closed porosity of the shell, which is the total volume of enclosed pores of each specimen, defined as a% percentage of the total shell volume. Porosity can be connected to the outer surface of the shell (open porosity) or not (closed porosity). A 3D model of the closed pores for each gastropod species was generated by the creation of a surface mesh of the closed pores using CTAn software, which was then visualized using the CTVol software (Bruker, Kontich, Belgium).

The structure thickness of each specimen was calculated using 3D analysis in CTAn software through the application of the "sphere-fitting" measurement (i.e., estimation of the mean of the diameters of the largest spheres which can be fitted in each point of the selected shell structure) (Hildebrand and Rüegsegger, 1997). Finally, a color-coded dataset was created for structure thickness in CTAn software in order to visualize the structure thickness distribution throughout each specimen. The 3D model of the structure thickness distribution was visualized through the CTVox software (Bruker, Kontich, Belgium).

Statistical Analyses

Statistical analyses were conducted using the software Minitab (version 13.2). Prior to analyses, all data were checked for normality distribution (Anderson-Darling test; normal for $p > 0.05$) and homogeneity of variances (Bartlett's test; equal variances for $p > 0.05$). Since all data were normal and had equal variances, one-way ANOVA tests were used to test differences between treatments in density, porosity and structure thickness for both species. When necessary, *post hoc* analysis (Tukey's tests) was performed to determine the significance of the factors interaction. Significant differences were considered at a threshold of $\alpha = 0.05$. Confidence intervals for the Tukey's tests are considered significant when they are not including the zero value.

RESULTS

Mean density, structure thickness and% of closed porosity for the four treatments are presented in **Figure 1** for *Nassarius nitidus* and in **Figure 2** for *Columbella rustica*. Results for statistical comparisons are presented in **Tables 1**, **2**, while Tukey's *post hoc* tests are presented in **Supplementary Material - Table II**. None of the comparisons performed for the morphological parameters of the *N. nitidus* full shell indicated statistically significant differences between the four treatments (**Table 1**, $p > 0.05$). The increased variability observed between individuals and the relatively low number of specimens due to the logistical constraints of performing a micro-CT analysis could possibly be the reason for this limited statistical significance; however, the observed trends can still offer a useful insight in shell architecture of *N. nitidus* and therefore the respective data presented in **Figure 1** are being further described. *Nassarius nitidus* had a lower mean shell density and a lower mean structure thickness in the 7A treatment (low pH, ambient temperature) in comparison to all other treatments; however these differences were not statistically significant ($p > 0.05$). The 8A control treatment (ambient pH and temperature) had the highest mean density and thickness (**Figures 1A,B** and **Table 1**). The combination of low pH and warm temperature (7W) was not detrimental for *N. nitidus* since the respective values were more similar to the control (8A). Mean porosity of the *N. nitidus* shell appears to be increased in all treatments in comparison to the control (**Figure 1C**), although again here the increased variability between individuals eliminated the statistical significance of these differences. The 3D models used for the visualization of *N. nitidus* closed porosity for all treatments are presented in **Figure 3**. Increased porosity in both low pH treatments (7A and 7W, **Figures 3A,C**, respectively) is seen around the shell lip, while in both warm treatments porosity is increased closer to the shell apex (7W and 8W, **Figures 3C,D**, respectively).

Columbella rustica indicated lower variability between individuals in comparison to *N. nitidus* (**Tables 1**, **2**). The shell density of *C. rustica* in acidified and warmer conditions (7W) was significantly lower in comparison to all other treatments ($p < 0.001$, see Table II in **Supplementary Material** for all *post hoc* comparisons). On the contrary, when the temperature was increased but the pH remained at ambient values (8W), shell density was significantly higher than all other treatments ($p < 0.001$), including the control (**Figure 2A**). The exact same pattern was observed for structure thickness of the total shell in *C. rustica* (**Figure 2B**). Shells under acidified and warmer conditions (7W) were significantly thinner, while shells in warmer but ambient pH conditions (8W) were significantly thicker ($p < 0.001$). In addition, the% of closed porosity was significantly higher (more than double) in the acidified and warmer conditions (7W) in comparison to all other treatments (**Figure 2C** and **Table 2**, $p = 0.015$). The 3D models used for the visualization of *C. rustica* closed porosity for all treatments are presented in **Figure 4**, where increased porosity can be seen in the acidified and warm treatment (7W, **Figure 4C**).

The distribution of structure thickness as% percentage of the shell volume for all the four treatments and for both species is

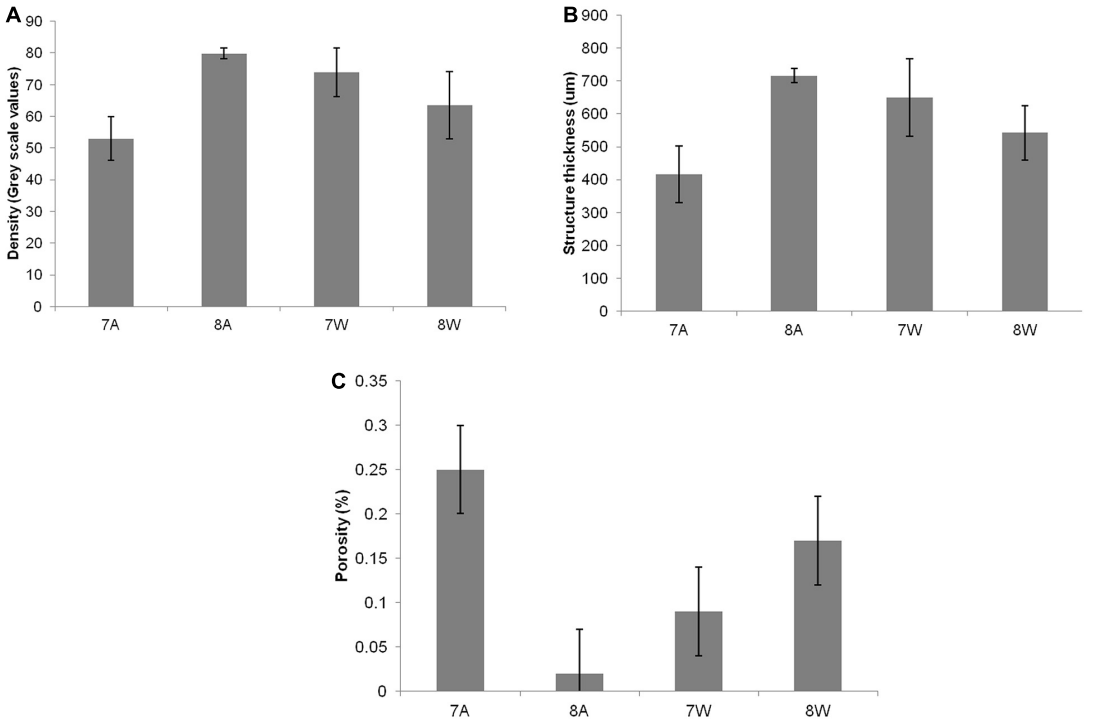

FIGURE 1 | (A) Mean density (grey scale values) of total shell. **(B)** Mean structure thickness of total shell. **(C)** Shell closed porosity (%) for *Nassarius nitidus*. The horizontal axis presents the four different experimental treatments as coded in the text (8A: 20°C and pH = 8; 7A: 20°C and pH = 7.7; 8W: 23°C and pH = 8; 7W: 23°C and pH = 7.7). Error bars represent ± SE (i.e., variation among individuals). N = 12 *N. nitidus* per treatment.

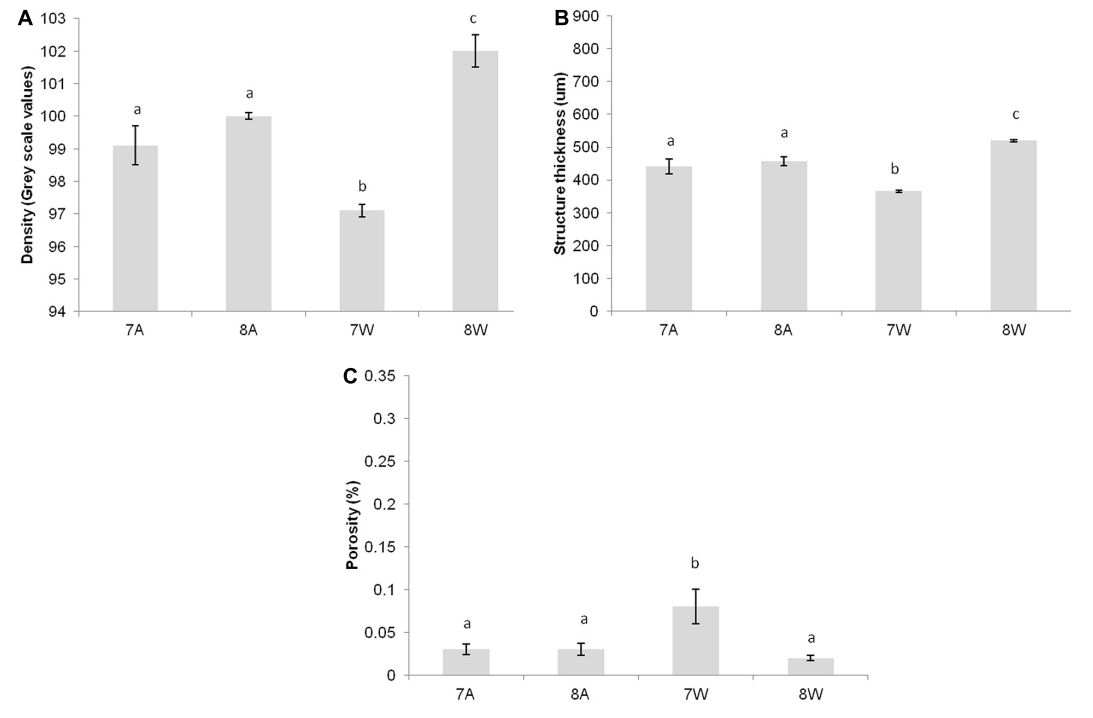

FIGURE 2 | (A) Mean density (gray scale values) of total shell. **(B)** Mean structure thickness of total shell. **(C)** Shell closed porosity (%) for *Collumbela rustica*. The horizontal axis presents the four different experimental treatments as coded in the text (8A: 20°C and pH = 8; 7A: 20°C and pH = 7.7; 8W: 23°C and pH = 8; 7W: 23°C and pH = 7.7). Error bars represent ± SE (i.e., variation among individuals). *N* = 9 *C. rustica* per treatment.

TABLE 1 | Mean density (gray scale values) of the total shell, structure thickness (um) and porosity% (± SE) for *Nassarius nitidus* in the four experimental treatments A (7A), B (8A), C (7W), and D (8W) as coded in the text (8A: 20°C and pH = 8; 7A: 20°C and pH = 7.7; 8W: 23°C and pH = 8; 7W: 23°C and pH = 7.7).

Nassarius nitidus			
Treatment	**Density (gray scale)**	**Structure thickness (um)**	**Porosity%**
7A	52.9 (± 6.9)	416.4 (± 86.8)	0.25 (± 0.10)
8A	79.8 (± 1.7)	716.1 (± 21.8)	0.02 (± 0.01)
7W	73.9 (± 7.6)	650.2 (± 118)	0.09 (± 0.07)
8W	63.4 (± 10.6)	542.1 (± 81.9)	0.17 (± 0.07)
ANOVA	F = 2.56, p = 0.128	F = 2.40, p = 0.143	F = 1.87, p = 0.212

Results of statistical tests (ANOVA or Kruskal Wallis) and significance (*) are indicated. N = 12 N. nitidus per treatment.

TABLE 2 | Mean density (gray scale values) of the total shell, structure thickness (um) and porosity% (± SE) for *Columbella rustica* in the four experimental treatments A (7A), B (8A), C (7W), and D (8W) as coded in the text (8A: 20°C and pH = 8; 7A: 20°C and pH = 7.7; 8W: 23°C and pH = 8; 7W: 23°C and pH = 7.7).

Columbella rustica			
Treatment	**Density (gray scale)**	**Structure thickness (um)**	**Porosity%**
7A	99.1 (± 0.6)	440.8 (± 22.2)	0.03 (± 0.006)
8A	100.0 (± 0.1)	457.1 (± 13.9)	0.03 (± 0.007)
7W	97.1 (± 0.2)	365.3 (± 3.8)	0.08 (± 0.020)
8W	102.0 (± 0.5)	519.7 (± 3.2)	0.02 (± 0.003)
ANOVA	F = 24.97, p < 0.001*	F = 22.66, p < 0.001*	F = 6.58, p = 0.015*

Results of statistical tests (ANOVA or Kruskal-Wallis) and significance (*) are indicated. N = 9 C. rustica per treatment.

presented in **Figures 5A,B**. The CTAn 3D analysis indicated a maximum total number of 132 classes with a range of 13 um each for *N. nitidus*, which were grouped as 17 classes with a range of about 100 um for each class to facilitate graphical presentation. Similarly, a maximum total number of 92 classes with a range of 13 um each was estimated for *C. rustica*, which were grouped as 12 classes with a range of about 100 um for each class.

The thickness of the *N. nitidus* shell under normal conditions (8A) ranges up to a maximum of 1608.7 um and the highest percentage of values (peak of the distribution) is found within the range of 605.7 – 709.9 um (**Figure 5A**). Gastropods under acidified conditions (7A) present a shift of their thickness distribution toward lower values and in this case the highest percentage is found within the range of 110.7 – 501.5 um (74.8%). The shell thickness distribution of *N. nitidus* which have been maintained under a combination of increased temperature and low pH (7W) is more similar to the control one (also peaks at 605.7 - 709.9 um), but again in this case a higher percentage is found within the region of lower (i.e., less dense) values (< 306.1 um). Gastropods under normal pH but warmer temperature (8W) have a peak distribution at 501.5-605.7 um and again present higher percentages at lower thickness values (< 397.3 um) in comparison to the control. A statistical comparison (ANOVA) of each thickness class separately between the four treatments confirms the above suggestions and indicates significant differences between the classes 201.9 − < 306.1 (F = 4.65, p = 0.036), 306.1 − < 397.3 (F = 5.53, p = 0.024), 397.3− < 501.5 (F = 4.66, p = 0.036), 605.7 − < 709.9 (F = 4.27, p = 0.045) and 709.9− < 801.1 (F = 3.77, p = 0.050).

The shell thickness of *C. rustica* under normal conditions (8A) ranges up to a maximum of 1009.5 um and the peak of the distribution is found within the range of 397.3-501.5 um (**Figure 5B**). Gastropods under acidified and ambient temperature conditions (7A) present a similar distribution pattern with 8A with the same maximum thickness value and the same peak for the highest percentage. When the temperature is higher, the distribution peak remains within the same range as the control, but low pH treatment (7W) results in more values toward the thinner ranges (78.4% of the shell volume with thickness <501.5 um), while normal pH (8W) results in more values toward the thicker ranges (73% of the shell volume with thickness >397.3 um). Also *C. rustica* under higher temperature with normal pH (8W) develop shells that reach greater maximum thickness values (up to 1204.9 um) than all the other treatments. A statistical comparison (ANOVA) of each thickness class separately between the four treatments confirms the above suggestions and indicates significant differences between the classes <110.7 um (F = 10.29, p = 0.006), 110.7-201.9 um (F = 22.33, p = 0.001), 201.9 − <306.1 (F = 7.65, p = 0.013), 605.7 − < 709.9 (F = 8.13, p = 0.011) and 709.9 − < 801.1 (F = 5.11, p = 0.035), as well as for classes >1009.5 (F = 12.58, p = 0.003) where only samples of 8W were found.

Although the statistical analysis of the full shell thickness did not indicate significant differences between the experimental treatments in *N. nitidus* (p > 0.05, **Table 1**) due to the increased variability between samples, the 3D color coded images constructed by the micro-CT analysis (CTVox) (**Figure 6**) and the subsequent comparisons between separate thickness classes (**Figure 5A**) revealed a clear degree of differentiation. Gastropods in low pH and ambient temperature (7A) had a very thin shell throughout its total structure (**Figure 6A**), obviously different from all other treatments. The control treatment shell (8A) is the one that visually presented the thickest areas (**Figure 6B**). The sample from the combined low pH - high temperature (7W) treatment had also a similar thickness pattern with the control (**Figure 6C**) with thicker areas located along the shell ribs and lip. The warm but ambient pH treatment (**Figures 6D**, 8W) was not as severely thin as the 7A was, but revealed some distinct areas close to the siphon canal and the shell lip which appeared thinner in comparison to the control.

The 3D color coded images for *C. rustica* thickness (**Figure 7**) and the subsequent comparisons between separate thickness classes (**Figure 5B**) indicated a clear visual pattern of the impact of low pH and increased temperature in the shell structure of this species. Specimens treated under low pH and increased temperature (7W, **Figure 7C**) appeared thinner especially around the opening of the shell, which was also obvious for specimens treated under low pH and ambient temperature (7A, **Figure 7A**). The control shell (8A, **Figure 7B**) is clearly thicker and the

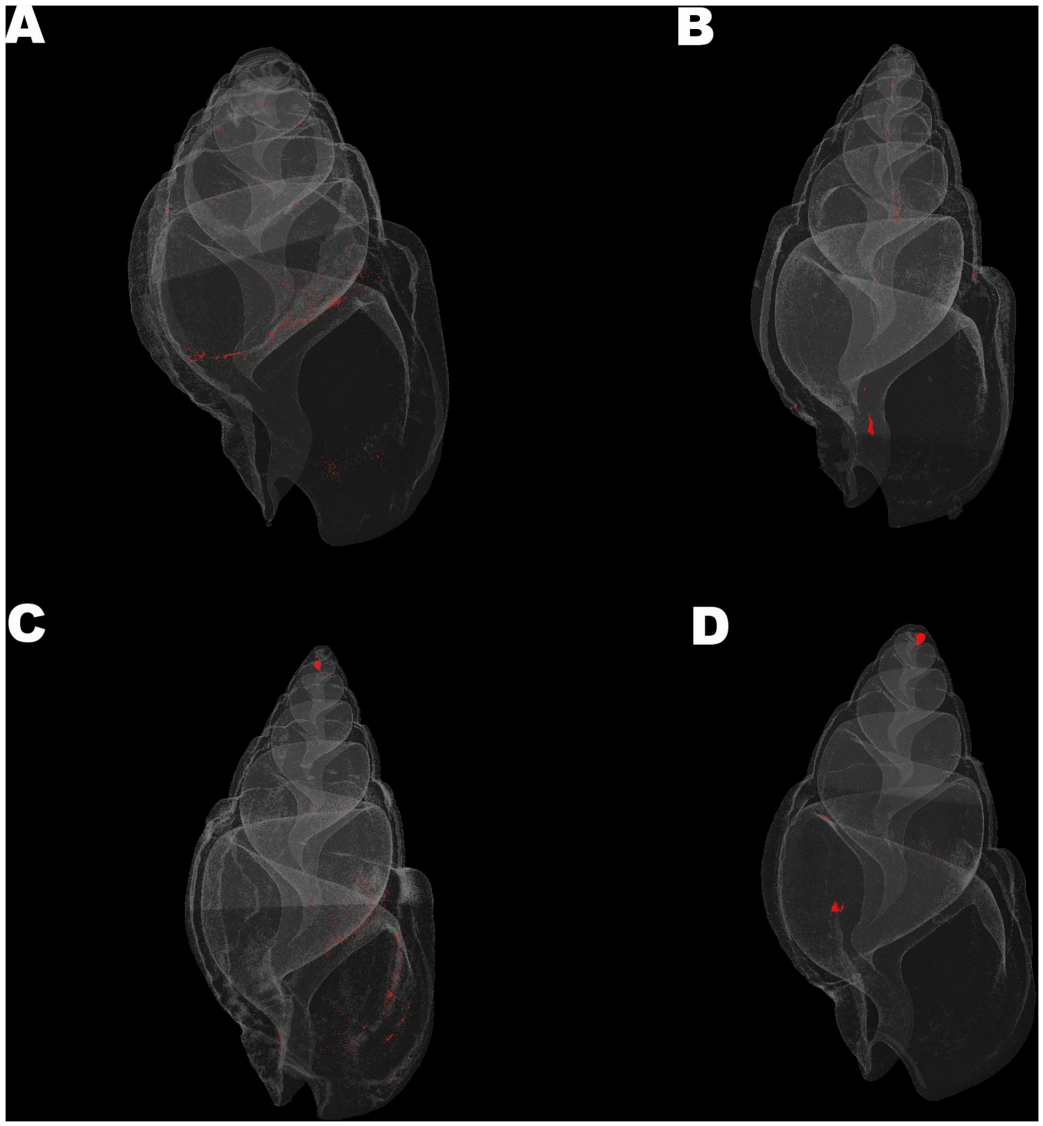

FIGURE 3 | Visualization of shell closed porosity for *Nassarius nitidus* in the four experimental treatments **(A)** (7A), **(B)** (8A), **(C)** (7W), and **(D)** (8W) as coded in the text (8A: 20°C and pH = 8; 7A: 20°C and pH = 7.7; 8W: 23°C and pH = 8; 7W: 23°C and pH = 7.7).

shell surface appears also smoother in comparison to shells of acidic conditions. The gastropods shells maintained under higher temperature but normal pH (8W, **Figure 7D**) were also thickened around the opening and lip, as was also confirmed by the average shell values of the 3D analysis (**Table 2**, $p < 0.001$, Tukey's *post hoc* tests in Table II, **Supplementary Material**).

DISCUSSION

The shell degradation of gastropods as a result of ocean acidification (low pH) has been documented in previous studies for several species (Bibby et al., 2007; Gazeau et al., 2013; Melatunan et al., 2013; Queirós et al., 2015; Chatzinikolaou et al., 2017; Harvey et al., 2018; Barclay et al., 2020). The capacity of marine organisms to construct calcium carbonate ($CaCO_3$) shells and skeletons can be impaired by reduced pH (Doney et al., 2009). It is evident that such impacts are very much species specific and for some species the effects are more detrimental than others (Byrne and Fitzer, 2019; Barclay et al., 2020). Building and maintaining marine biomaterials under ocean acidification depends on the balance between calcification and dissolution, while ocean warming has the potential to ameliorate or highlight some of the negative effects on shell strength and elasticity (e.g., weaker shells with less dense biominerals and increased porosity) (Byrne and Fitzer, 2019). Therefore, it is interesting to compare the shell morphological characters of different species which are living in different micro-habitats or are characterized by different modes of life, in order to define what might be the factors of increased susceptibility for some specific species

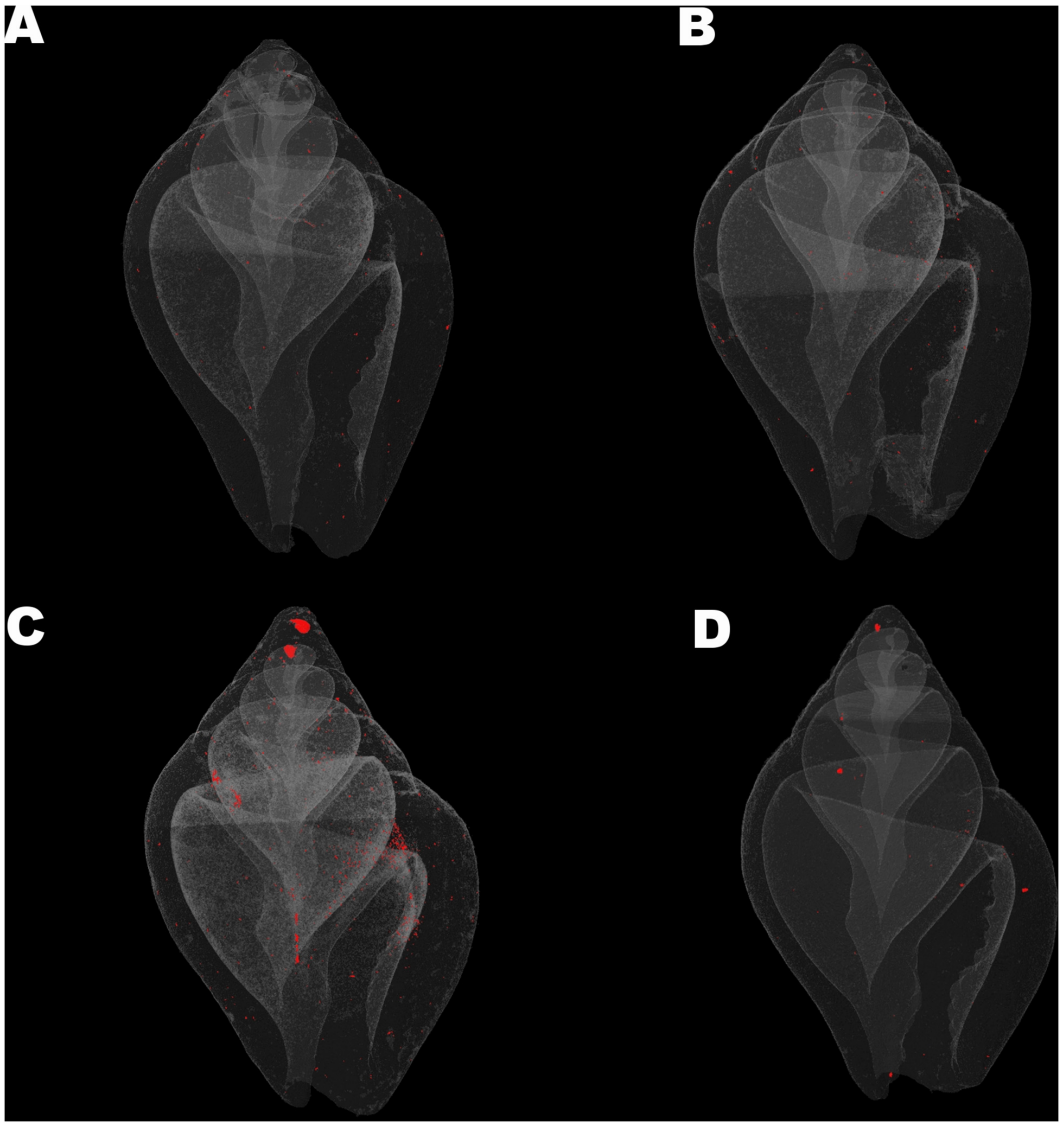

FIGURE 4 | Visualization of shell closed porosity for *Collumbela rustica* in the four experimental treatments **(A)** (7A), **(B)** (8A), **(C)** (7W), and **(D)** (8W) as coded in the text (8A: 20°C and pH = 8; 7A: 20°C and pH = 7.7; 8W: 23°C and pH = 8; 7W: 23°C and pH = 7.7).

in comparison to others. Different species are characterized by different vulnerability and tolerance responses regarding ocean acidification and warming, and this variability may affect their ecological interactions and the respective marine habitat biodiversity (Chatzinikolaou et al., 2017). The effects of ocean acidification on the growth and shell production by juvenile and adult shelled molluscs are variable among species and even within the same species, precluding the drawing of a general picture (Gazeau et al., 2013). Conventional metrics previously used to quantify shell growth need to be enriched with methods for evaluating changes to biomineral structure and mechanical integrity caused by ocean acidification (Byrne and Fitzer, 2019).

The authors of the present study have previously investigated the effects of acidic conditions on the density of specific shell regions of *Nassarius nitidus* and they have reported a reduction of 38.1% in the shell lip, 51.4% in the lip distal (newest regions) and 47.7% in the apex (oldest region) (Chatzinikolaou et al., 2017). In the present study, a more thorough examination for the same species was performed during which the full shell was examined instead of isolated shell regions. In addition, while the previous study investigated only differences in shell density, the present study also investigated additional morphological characters of the shell, such as enclosed porosity and thickness. Although the results of the present study did not indicate statistically significant differences between treatments for *N. nitidus*, they can still be considered as a valuable informative insight into the architectural shell properties of this species using an innovative 3D imaging analysis technique. As observed in the present study, low pH affected (although not significantly) the average density and structure thickness of the total shell in *N. nitidus* when

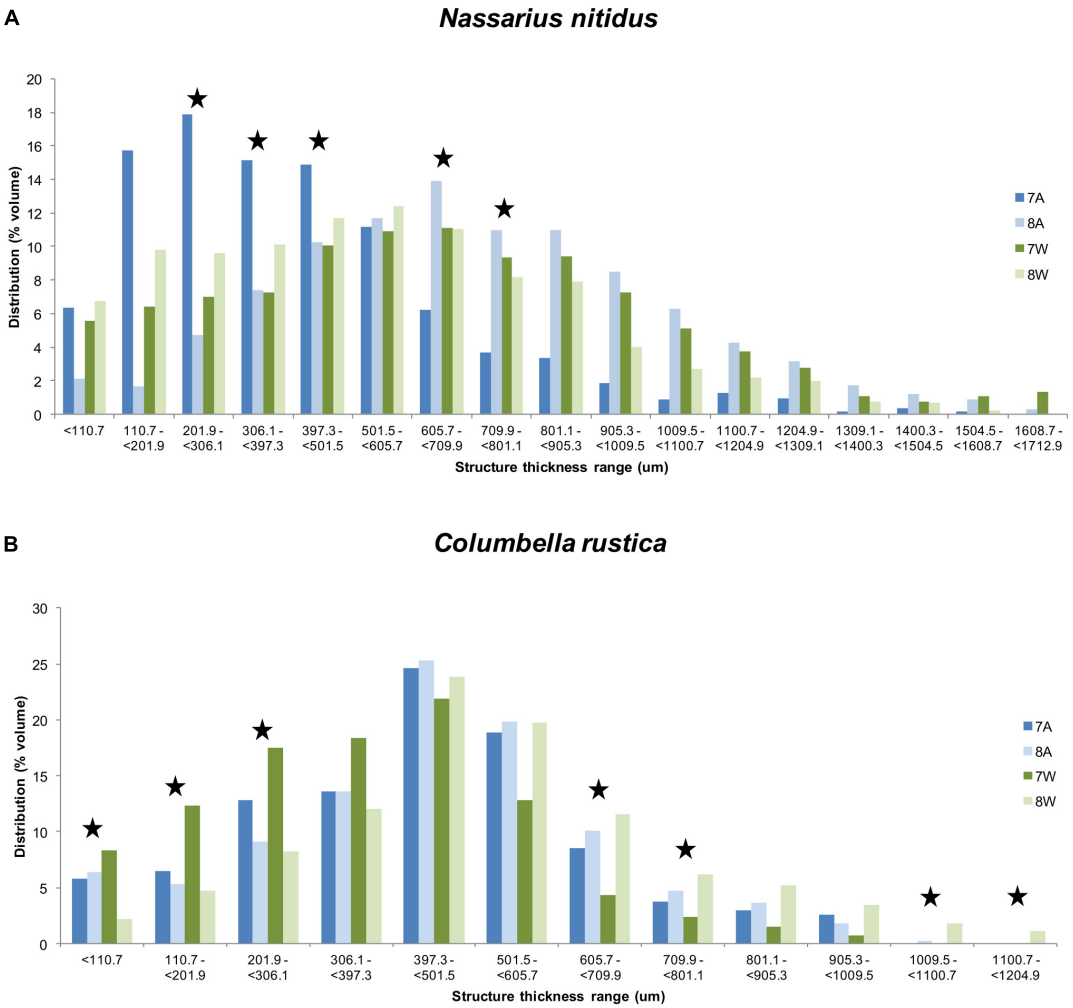

FIGURE 5 | Distribution (% average shell volume) of structure thickness classes (about 100 um per class) for *Nassarius nitidus* **(A)** and *Columbella rustica* **(B)** for the four experimental treatments as coded in the text (8A: 20°C and pH = 8; 7A: 20°C and pH = 7.7; 8W: 23°C and pH = 8; 7W: 23°C and pH = 7.7). Stars indicate thickness ranges with statistically significant differences ($p < 0.05$).

temperature was at ambient levels. Furthermore, when thickness classes were separately examined, *N. nitidus* shell had a significant shift toward thinner values at lower pH, and this was especially evident in ambient temperatures. The significant differences revealed when thickness classes were examined separately maybe the result of increased variability observed between individuals. The 3D visual analysis of structure thickness also confirmed that the whole shell has suffered extensive damages and erosion. However, when the temperature was increased *N.nitidus* somehow compensated for the shell loss caused by the acidic conditions (7W), presumably by accelerating shell production processes. The effect of elevated seawater temperature has been previously correlated with an increase in the growth of this genus, such as in *N. reticulatus* (Barroso et al., 2005; Chatzinikolaou and Richardson, 2008) and *N. festivus* (Morton and Chan, 2004). Also *Columbella rustica* in the present study formed significantly denser and thicker shells, especially around the lip, when the temperature was higher (8W) thus indicating an acceleration of shell growth and calcification processes which has been commonly observed in several gastropod species, even seasonally under ambient conditions (Morton and Chan, 2004; Barroso et al., 2005; Chatzinikolaou and Richardson, 2008). The amount of energy available for growth is determined by the ingestion and the respiration rate of an organism, which are indeed functions related to temperature (Hughes, 1986).

The combined impact of low pH and increased temperature was clearly disadvantageous for *C. rustica*, indicating that a negative future scenario of climate change as suggested by IPCC could be detrimental. The average shell density and thickness of *C. rustica* in acidified and warmer conditions were significantly reduced in comparison to all other treatments, while% porosity (i.e., the number of enclosed pores in reference to the total shell volume) was significantly higher. The number of pores in *C. rustica* shell under such stressful conditions was more than double in comparison to gastropods maintained under ambient conditions. Porosity is an important indicator of mechanical

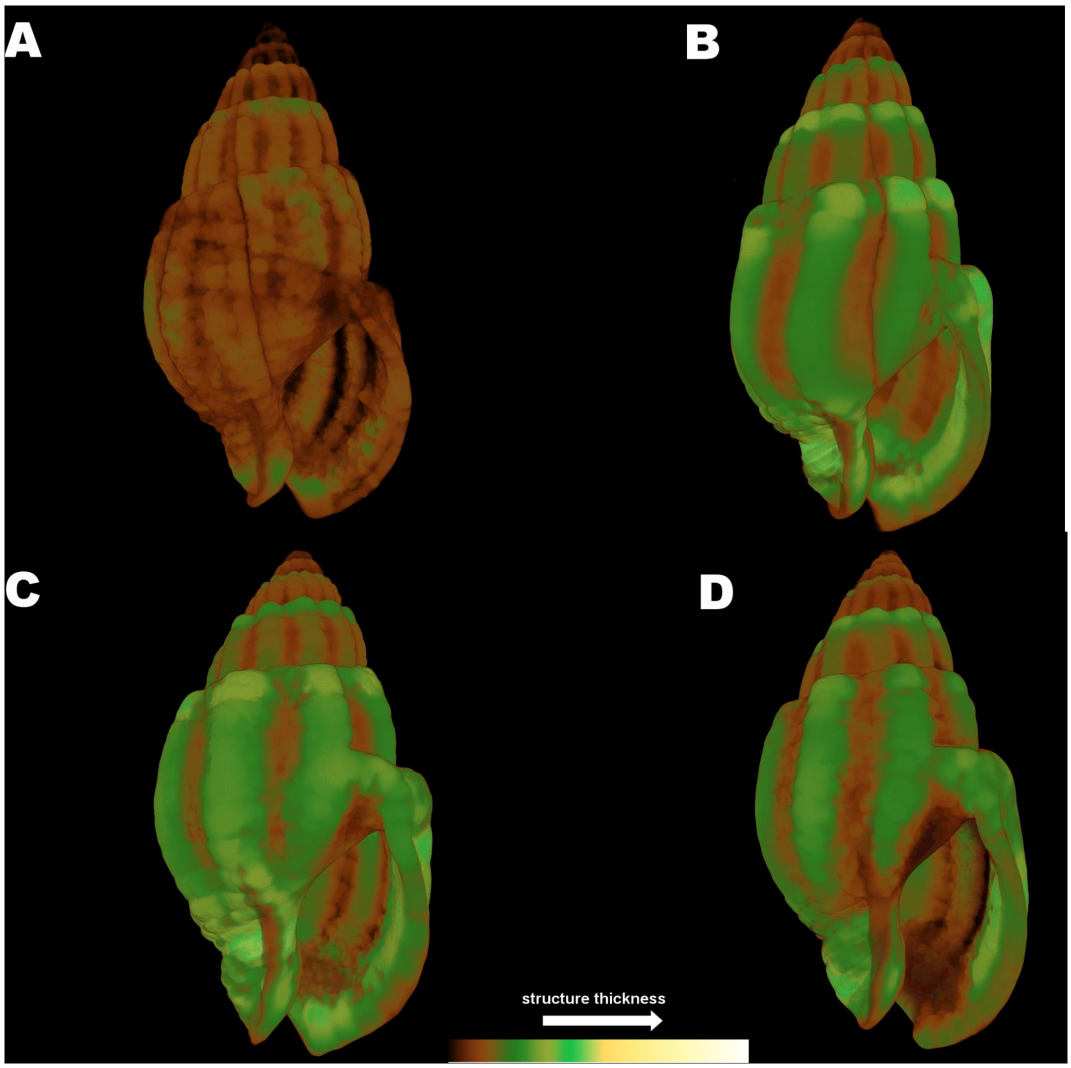

FIGURE 6 | Color coded visualization of shell structure thickness for *Nassarius reticulatus* in the four experimental treatments **(A)** (7A), **(B)** (8A), **(C)** (7W), and **(D)** (8W) as coded in the text (8A: 20°C and pH = 8; 7A: 20°C and pH = 7.7; 8W: 23°C and pH = 8; 7W: 23°C and pH = 7.7). The bar on the bottom of the image indicates thickness scaling (cooler colors indicate thicker structures, warmer colors indicate thinner structures).

strength, where shells with a greater number of pores are more fragile (Leung et al., 2020). Shell pores usually penetrate all shell layers except the outermost organic layer (periostracum) and their interior is filled with organic compounds which are used for the periostracum repair (Reindl and Haszprunar, 1994). The increased% of porosity observed in *C. rustica* may be the result of an accelerated shell repair process, since the contents of the enclosed pores are important for shell secretion (Reindl and Haszprunar, 1994). Increased porosity has been also associated with a lower organic matter content of the shell, indicating less plasticity, reduced calcium carbonate nucleation and minimized crystal growth (Leung et al., 2020). Some calcifiers might adjust the packing of carbonate crystals (e.g., porosity) under ocean acidification in order to build more durable shells that will be able to absorb physical stress effectively, however this requires a costly energy budget (Leung et al., 2020).

C. rustica shells under acidic conditions in the present study were thinner especially around the shell lip and the apex. A previous study also indicated that the maximum reduction (8%) estimated in the shell density of this species was in the apex, which is the oldest shell part and might often be eroded (Chatzinikolaou et al., 2017). Similarly in *Nucella lapillus* low pH caused apex dissolution and a 20–30% reduction in shell lip density (Queirós et al., 2015). *Mytilus edulis* shells grown under ocean acidification conditions displayed significant reductions in shell aragonite thickness, shell thickness index and changes to shell shape, making them more vulnerable to fracture (Fitzer et al., 2015). *Mytilus californianus* larvae had thinner and weaker shells than individuals raised under present-day pH conditions indicating an aggravated vulnerability of new settlers to crushing and drilling attacks by predators (Gaylord et al., 2011). Similarly, treatment of the brachiopod *Liothyrella*

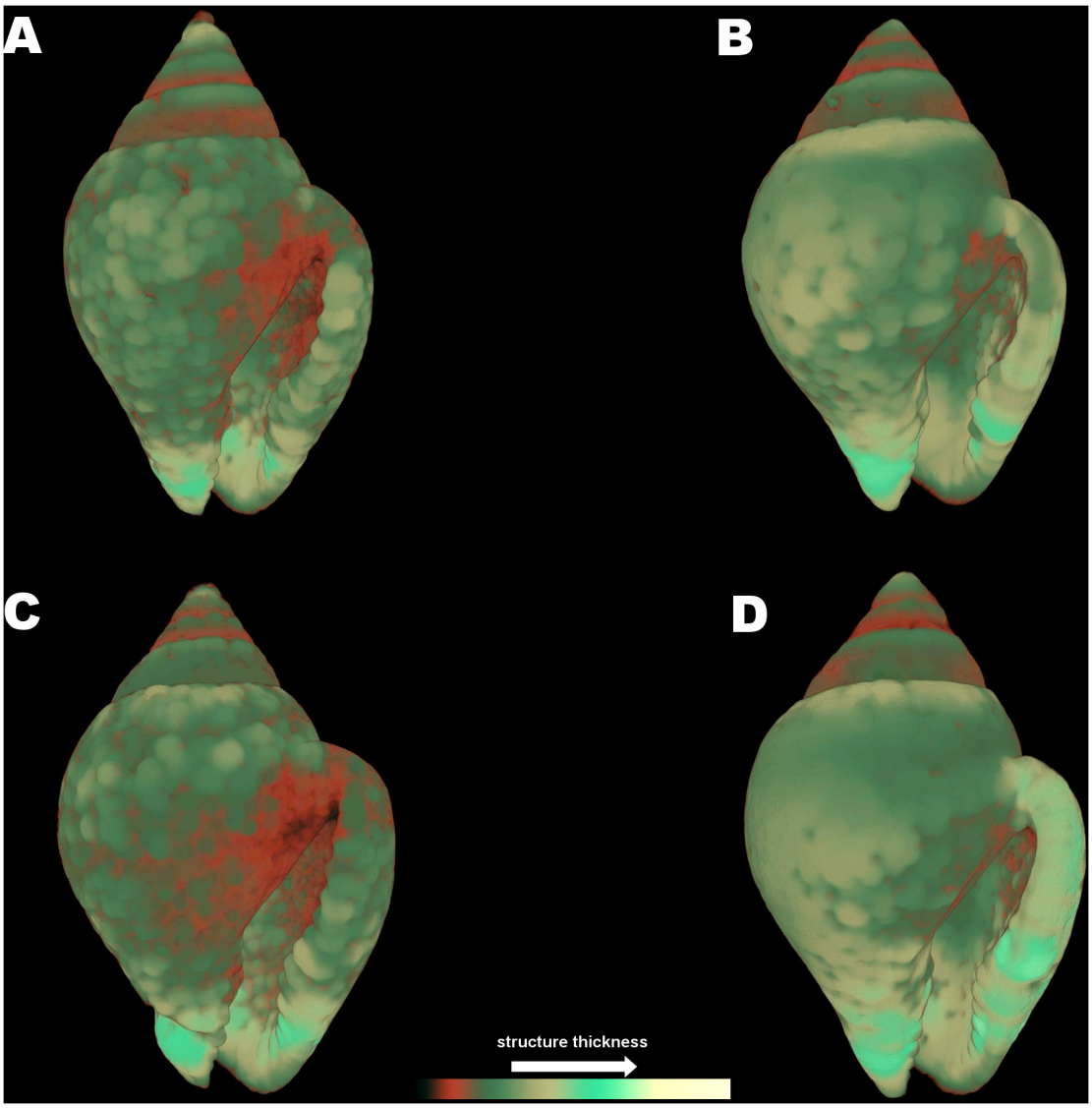

FIGURE 7 | Color coded visualization of shell structure thickness for *Columbella rustica* in the four experimental treatments **(A)** (7A), **(B)** (8A), **(C)** (7W), and **(D)** (8W) as coded in the text (8A: 20°C and pH = 8; 7A: 20°C and pH = 7.7; 8W: 23°C and pH = 8; 7W: 23°C and pH = 7.7). The bar on the bottom of the image indicates thickness scaling (cooler colors indicate thicker structures, warmer colors indicate thinner structures).

uva under decreased pH resulted in substantial shell dissolution after 7 months and decreased outer primary layer thickness, while increasing temperature alone did not affect shell thickness (Cross et al., 2019). The monomineralic aragonite-producing gastropods were not able to alter the carbonate polymorph in their shells in order to produce calcite under low pH conditions and minimize shell dissolution (Leung et al., 2017a). However, the effect of ocean acidification in shell thickness is also species specific and there are indications that some species are enhancing their shell production to compete shell dissolution under unfavorable conditions. Specimens of the limpet *Patella caerulea* that were collected from a low pH CO_2 vent site, displayed increased thickness and a twofold increase in aragonite area fraction indicating an enhanced shell production under acidified conditions thus managing to counteract dissolution (Langer et al., 2014). Shell thickening in the limpet *P. caerulea* was enhanced at the apex area and reduced along the flank area, also indicating region specific shell production (Langer et al., 2014).

Shell porosity is a shell architectural and morphological character that has not been yet thoroughly studied since it is not possible to estimate these values without using a non-destructive method such as the micro-CT tomography. Similarly, the estimation of shell thickness as an average value for the total shell, as well as the identification of the% percentages per thickness class is also a unique feature of this study estimated using this innovative imaging technique. The micro-computed tomography (micro-CT) allows the creation of interactive, quantitative, three-dimensional X-ray images at submicron resolution which can

be used to measure morphological characters of the calcified shell without interfering with its integrity. Previous studies have determined thickness of the gastropod shell by measuring only selected points on photographs of cross sections (Coleman et al., 2014), while the present method allows for the estimation of the average value of thickness of the full intact shell and of the% distribution of these values in different size classes, thus offering a more representative depiction of the shell structure. Even if shell growth is not directly affected by acidification conditions this does not ensure that shell functionality and efficiency also remains unaltered. For example, *Nucella ostrina* is able to maintain calcification and shell growth under acidified conditions, but the loss of carbonate material due to dissolution weakens the shells as indicated by biomechanical tests (Barclay et al., 2020). Gaylord et al. (2011) indicated that the functional decline in shell integrity and strength of *M. californianus* under low pH, might not be the result of reductions in calcification and shell thickness but could be provoked by changes in shell architecture or material properties.

Ocean warming and acidification have been proven to affect physiological responses in marine molluscs (e.g., depression of metabolic rate, Bibby et al., 2007; alterations of immune responses and enzyme production, Matozzo et al., 2013), as well as behavioral responses related to predator avoidance (Bibby et al., 2007), reduction of feeding efficiency (Vargas et al., 2013) and movement restriction (Ellis et al., 2009). *Hexaplex trunculus* was less successful in reaching their food source under low pH (Chatzinikolaou et al., 2019). If such physiological and behavioral restrictions already deteriorate the ability of organisms to successfully cope with predation pressure, a thinner shell will certainly make the situation less favorable. The normally occurring shell thickening of *Littorina littorea* in the presence of predatory crabs was prohibited under low pH conditions, therefore limiting the morphological defense mechanisms in this species and threatening its survival (Bibby et al., 2007). *Austrocochlea porcata* exhibited depressed shell repair rate and compromised shell integrity under lower than ambient pH (pH = 7.7), both representing critical attributes for survival and protection against predators (Coleman et al., 2014). Molluscs under ocean acidification may display complex patterns of energy allocation toward predatory defense, as well as alterations in chemoreception, cue detection and predator avoidance behavior that may influence predator-prey interactions (Kroeker et al., 2014). If atmospheric CO_2 levels continue to rise and ocean pH to subsequently drops, less resistant species may face increased predation pressure and competition in comparison to more successful taxa within the same community, thus altering the balance within intertidal communities (Coleman et al., 2014). Nevertheless, the effects of ocean acidification in the natural environment are subject to ecological and evolutionary processes, since marine calcifiers have demonstrated a remarkable degree of adaptation in a future high-CO_2 world being able to adapt and produce durable shells (Leung et al., 2020). Further investigation of species or shell region specific adaptation mechanisms could enlighten the potential plasticity of shell building organisms to acclimate to a continuously changing marine environment.

DATA AVAILABILITY STATEMENT

The raw data supporting the conclusions of this article will be made available by the authors, without undue reservation.

AUTHOR CONTRIBUTIONS

EC designed the research, participated in the experiment, scanned the samples, analyzed the images, performed the statistical analysis and wrote the manuscript. KK participated in the experiment, scanned the samples, analyzed the images. PG participated in the experiment, participated in the statistical analysis. All authors contributed to the article and approved the submitted version.

FUNDING

The study was funded under the projects ECCO (HFRI, Hellenic Foundation for Research and Innovation for the support of Post-doctoral Researchers, project ID 343) and MOUNT – Modern unifying trends in marine biology (NSRF - MIS 5002470).

ACKNOWLEDGMENTS

The authors would like to thank CretAquarium for providing the experimental tanks and the project BIOIMAGING-GR (NSFR - MIS 5002755) for offering expertise on scanning protocols and workflows.

SUPPLEMENTARY MATERIAL

The Supplementary Material for this article can be found online at: https://www.frontiersin.org/articles/10.3389/fmars.2021.645660/full#supplementary-material

REFERENCES

Andersson, A. J., Mackenzie, F. T., and Lerman, A. (2006). Coastal ocean CO_2—carbonic acid—carbonate sediment system of the Anthropocene. *Glob. Biogeochem. Cycles* 20:GB1S92.

Barclay, K. M., Gaylord, B., Jellison, B. M., Shukla, P., Sanford, E., and Leighton, L. R. (2019). Variation in the effects of ocean acidification on shell growth and strength in two intertidal gastropods. *Mar. Ecol. Prog. Ser.* 626, 109–121. doi: 10.3354/meps13056

Barclay, K. M., Gingras, M. K., Packer, S. T., and Leighton, L. R. (2020). The role of gastropod shell composition and microstructure in resisting dissolution caused by ocean acidification. *Mar. Environ. Res.* 162:105105. doi: 10.1016/j.marenvres.2020.105105

Barroso, C. M., Moreira, M. H., and Richardson, C. A. (2005). Age and growth of *Nassarius reticulatus* in the ria de aveiro, north-west Portugal. *J. Mar. Biol. Assoc. U. K.* 85, 151–156. doi: 10.1017/s0025315405010970h

Bibby, R., Cleall-Harding, P., Rundle, S., Widdicombe, S., and Spicer, J. (2007). Ocean acidification disrupts induced defences in the intertidal

gastropod *Littorina littorea*. *Biol. Lett.* 3, 699–701. doi: 10.1098/rsbl.2007.0457

Bouillon, J. (1958). Quelques observations sur la nature de la coquille chez les mollusques. *Ann. Soc. R. Zool. Malacol. Belg.* 89, 229–237.

Byrne, M., and Fitzer, S. (2019). The impact of environmental acidification on the microstructure and mechanical integrity of marine invertebrate skeletons. *Conserv. Physiol.* 7:coz062.

Cespuglio, G., Piccinetti, C., and Longinelli, A. (1999). Oxygen and carbon isotope profiles from *Nassa mutabilis* shells (*Gastropoda*): accretion rates and biological behaviour. *Mar. Biol.* 135, 627–634. doi: 10.1007/s002270050663

Chatzinikolaou, E., Grigoriou, P., Keklikoglou, K., Faulwetter, S., and Papageorgiou, N. (2017). The combined effects of reduced pH and elevated temperature on the shell density of two gastropod species measured using micro-CT imaging. *ICES J. Mar. Sci.* 74, 1135–1149. doi: 10.1093/icesjms/fsw219

Chatzinikolaou, E., Grigoriou, P., Martini, E., and Sterioti, A. (2019). Impact of ocean acidification and warming on the feeding behaviour of two gastropod species. *Mediterr. Mar. Sci.* 20, 669–679. doi: 10.12681/mms.19187

Chatzinikolaou, E., and Richardson, C. A. (2008). Population dynamics and growth of *Nassarius reticulatus* (*Gastropoda*: *Nassariidae*) in Rhosneigr (Anglesey, UK). *Mar. Biol.* 153, 605–619. doi: 10.1007/s00227-007-0835-5

Coleman, D. W., Byrne, M., and Davis, A. R. (2014). Molluscs on acid: gastropod shell repair and strength in acidifying oceans. *Mar. Ecol. Prog. Ser.* 509, 203–211. doi: 10.3354/meps10887

Cross, E., Harper, E. M., and Peck, L. S. (2019). Thicker shells compensate extensive dissolution in brachiopods under future ocean acidification. *Environ. Sci. Technol.* 53, 5016–5026. doi: 10.1021/acs.est.9b00714

DeCarlo, T. M., Comeau, S., Cornwall, C. E., and McCulloch, M. T. (2018). Coral resistance to ocean acidification linked to increased calcium at the site of calcification. *Proc. R. Soc. B.* 285:20180564. doi: 10.1098/rspb.2018.0564

Delamotte, M., and Vardala-Theodorou, E. (2007). *Shells from the Greek Seas*. Athens: Goulandri Natural History Museum, 330.

Dickson, A. G., and Millero, F. J. (1987). A comparison of the equilibrium constants for the dissociation of carbonic acid in seawater media. *Deep Sea Res. A* 34, 1733–1743. doi: 10.1016/0198-0149(87)90021-5

Dickson, A. G., Sabine, C. L., and Christian, J. R. (2007). Guide to best practices for ocean CO_2 measurements. *PICES Special Publication* 3, 1–191.

Doney, S. C., Busch, D. S., Cooley, S. R., and Kroeker, K. J. (2020). The impacts of ocean acidification on marine ecosystems and reliant human communities. *Annu. Rev. Environ. Resour.* 45, 11.1–11.30.

Doney, S. C., Fabry, V. J., Feely, R. A., and Kleypas, J. A. (2009). Ocean acidification: the other CO_2 problem. *Annu. Revis. Mar. Sci.* 1, 169–192.

Ellis, R. P., Bersey, J., Rundle, S. D., Hall-Spencer, J. M., and Spicer, J. I. (2009). Subtle but significant effects of CO_2 acidified seawater on embryos of the intertidal snail, *Littorina obtusata*. *Aquat. Biol.* 5, 41–48. doi: 10.3354/ab00118

Eriksson, S., and Tallmark, B. (1974). The influence of environmental factors on the diurnal rhythm of the prosobranch gastropod *Nassarius reticulatus* (L.) from a non-tidal area. *Zoon* 2, 135–142.

Feely, R. A., Sabine, C. L., Lee, K., Berelson, W., Kleypas, J., Fabry, J., et al. (2004). Impact of anthropogenic CO_2 on the $CaCO_3$ system in the oceans. *Science.* 305, 362–366. doi: 10.1126/science.1097329

Fisher, J. A. D., Rhile, E. C., Liu, H., and Petraitis, P. S. (2009). An intertidal snail shows a dramatic size increase over the past century. *Proc. Natl. Acad. Sci U.S.A.* 106, 5209–5212. doi: 10.1073/pnas.0812137106

Fitzer, S. C., Vittert, L., Bowman, A., Kamenos, N. A., Phoenix, V. R., and Cusack, M. (2015). Ocean acidification and temperature increase impact mussel shell shape and thickness: problematic for protection? *Ecol. Evol.* 5, 4875–4884. doi: 10.1002/ece3.1756

Foster, P., and Cravo, A. (2003). Minor elements and trace metals in the shell of marine gastropods from a shore in tropical East Africa. *Water Air Soil Pollut.* 145, 53–65.

Gaylord, B., Hill, T. M., Sanford, E., Lenz, E. A., Jacobs, L. A., Sato, K. N., et al. (2011). Functional impacts of ocean acidification in an ecologically critical foundation species. *J. Exp. Biol.* 214, 2586–2594. doi: 10.1242/jeb.055939

Gazeau, F., Parker, L. M., Comeau, S., Gattuso, J. P., O'Connor, W. A., Martin, S., et al. (2013). Impacts of ocean acidification on marine shelled molluscs. *Mar. Biol.* 160, 2207–2245. doi: 10.1007/s00227-013-2219-3

Gizzi, F., Caccia, M. G., Simoncini, G. A., Mancuso, A., Reggi, M., Fermani, S., et al. (2016). Shell properties of commercial clam *Chamelea gallina* are influenced by temperature and solar radiation along a wide latitudinal gradient. *Sci. Rep.* 6:36420.

Harris, K. E., DeGrandpre, M. D., and Hales, B. (2013). Aragonite saturation state dynamics in a coastal upwelling zone. Geophys. *Res. Lett.* 40, 2720–2725. doi: 10.1002/grl.50460

Harvey, B. P., Agostini, S., Wada, S., Inaba, K., and Hall-Spencer, J. M. (2018). Dissolution: the achilles' heel of the triton shell in an acidifying Ocean. *Front. Mar. Sci.* 5:371. doi: 10.3389/fmars.2018.00371

Hildebrand, T., and Rüegsegger, P. (1997). A new method for the model-independent assessment of thickness in three-dimensional images. *J. Microsc.* 185, 67–75. doi: 10.1046/j.1365-2818.1997.1340694.x

Hughes, R. N. (1986). *A Functional Biology of Marine Gastropods*. London: Croom Helm Ltd, 245.

IPCC (2014). "Climate change 2014: synthesis report," in *Contribution of Working Groups I, II and III to the 5th Assessment Report of the Intergovernmental Panel on Climate Change*, eds R. K. Pachauri and L. A. Meyer (Geneva: IPCC), 151.

Kleypas, J. A., Feely, R. A., Fabry, V. J., Langdon, C., and Sabine, C. L. (2006). *Impacts of Ocean Acidification on Coral Reefs and Other Marine Calcifiers: A Guide to Future Research*. Report of a workshop held 18-20 April 2005, St. Petersburg, FL, sponsored by NSF, NOAA, and the US Geological Survey. Contribution No. 2897. Seattle, WA: NOAA.

Kroeker, K. J., Sanford, E., Jellison, B. M., and Gaylord, B. (2014). Predicting the effects of ocean acidification on predator-prey interactions: a conceptual framework based on coastal molluscs. *Biol. Bull.* 226, 211–222. doi: 10.1086/bblv226n3p211

Langer, G., Nehrke, G., Baggini, C., Rodolfo-Metalpa, R., Hall-Spencer, J. M., and Bijma, J. (2014). Limpets counteract ocean acidification induced shell corrosion by thickening of aragonitic shell layers. *Biogeosciences* 11, 7363–7368. doi: 10.5194/bg-11-7363-2014

Leung, J. Y. S., Chen, Y., Nagelkerken, I., Zhang, S., Xie, Z., and Connell, S. D. (2020). Calcifiers can adjust shell building at the nanoscale to resist ocean acidification. *Small* 16:2003186. doi: 10.1002/smll.202003186

Leung, J. Y. S., Connell, S. D., Nagelkerken, I., and Russell, B. D. (2017a). Impacts of near-future ocean acidification and warming on the shell mechanical and geochemical properties of gastropods from intertidal to subtidal zones. *Environ. Sci. Technol.* 51, 12097–12103. doi: 10.1021/acs.est.7b02359

Leung, J. Y. S., Russell, B. D., and Connell, S. D. (2017b). Mineralogical plasticity acts as a compensatory mechanism to the impacts of ocean acidification. *Environ. Sci. Technol.* 51, 2652–2659. doi: 10.1021/acs.est.6b04709

Li, S., Huang, J., Liu, C., Liu, Y., Zheng, G., Xie, L., et al. (2016). Interactive effects of seawater acidification and elevated temperature on the transcriptome and biomineralization in the pearl oyster *Pinctada fucata*. *Environ. Sci. Technol.* 50, 1157–1165. doi: 10.1021/acs.est.5b05107

Marshall, D. J., Abdelhady, A. A., Wah, D. T. T., Mustapha, N., Gödeke, S. H., De Silva, L. C., et al. (2019). Biomonitoring acidification using marine gastropods. *Sci. Total Environ.* 692, 833–843. doi: 10.1016/j.scitotenv.2019.07.041

Matozzo, V., Chinellato, A., Munari, M., Bressan, M., and Marin, M. G. (2013). Can the combination of decreased pH and increased temperature values induce oxidative stress in the clam *Chamelea gallina* and the mussel *Mytilus galloprovincialis*? *Mar. Pollut. Bull.* 72, 34–40. doi: 10.1016/j.marpolbul.2013.05.004

Mehrbach, C., Culberson, C. H., Hawley, J. E., and Pytkowicz, R. M. (1973). Measurement of the apparent dissociation constants of carbonic acid in seawater at atmospheric pressure. *Limnol. Oceanogr.* 18, 897–907. doi: 10.4319/lo.1973.18.6.0897

Melatunan, S., Calosi, P., Rundle, S. D., Widdicombe, S., and Moody, A. J. (2013). Effects of ocean acidification and elevated temperature on shell plasticity and its energetic basis in an intertidal gastropod. *Mar. Ecol. Prog. Ser.* 472, 155–168. doi: 10.3354/meps10046

Morton, B., and Chan, K. (2004). The population dynamics of *Nassarius festivus* (*Gastropoda*: *Nassariidae*) on three environmentally different beaches in Hong Kong. *J. Mollusc. Stud.* 70, 329–339. doi: 10.1093/mollus/70.4.329

Nehrke, G., Poigner, H., Wilhelms-Dick, D., Brey, T., and Abele, D. (2012). Coexistence of three calcium carbonate polymorphs in the shell of the Antarctic clam *Laternula elliptica*. *Geochem. Geophys. Geosyst.* 13:Q05014.

Nienhuis, S., Palmer, A. R., and Harley, C. D. G. (2010). Elevated CO_2 affects shell dissolution rate but not calcification rate in a marine snail. *Proc. R. Soc. B Biol. Sci.* 277, 2553–2558. doi: 10.1098/rspb.2010.0206

Orr, J. C., Fabry, V. J., Aumont, O., Bopp, L., Doney, S. C., Feely, R. A., et al. (2005). Anthropogenic ocean acidification over the twenty-first century and its impact on calcifying organisms. *Nature* 437, 681–686. doi: 10.1038/nature04095

Queirós, A. M., Fernandes, J. A., Faulwetter, S., Nunes, J., Rastrick, S. P. S., Mieszkowska, N., et al. (2015). Scaling up experimental ocean acidification and warming research: from individuals to the ecosystem. *Glob. Change Biol.* 21, 130–143. doi: 10.1111/gcb.12675

Reindl, S., and Haszprunar, G. (1994). Light and electron microscopical investigations on shell pores (caeca) of fissurellid limpets (*Mollusca*: *Archaeogastropoda*). *J. Zool.* 233, 385–404. doi: 10.1111/j.1469-7998.1994.tb05272.x

Ries, J. B., Cohen, A. L., and McCorkle, D. C. (2009). Marine calcifiers exhibit mixed responses to CO_2-induced ocean acidification. *Geology.* 37, 1131–1134. doi: 10.1130/g30210a.1

Ruppert, E. E., and Barnes, R. D. (1996). *Invertebrate Zoology*. Philadelphia, PA: Saunders College Publishing, 1055.

Shirayama, Y., and Thornton, H. (2005). Effect of increased atmospheric CO_2 on shallow water marine benthos. *J. Geophys. Res.* 110:C09S08.

Starmühlner, F. (1969). Zur molluskenfauna des felslitorals bei rovinj (Istrien). *Malacologia* 9, 217–242.

Taylor, J. D. (1987). Feeding ecology of some common intertidal neogastropods at Djerba, Tunisia. *Vie Milieu* 37, 13–20.

Vargas, C. A., de la Hoz, M., Aguilera, V., San Martin, V., Manríquez, P. H., Navarro, J. M., et al. (2013). CO_2-driven ocean acidification reduces larval feeding efficiency and changes the food selectivity in the mollusk Concholepas concholepas. *J. Plankton Res.* 35, 1059–1068. doi: 10.1093/plankt/fbt045

Wahl, M., Saderne, V., and Sawall, Y. (2016). How good are we at assessing the impact of ocean acidification in coastal systems? Limitations, omissions and strengths of commonly used experimental approaches with special emphasis on the neglected role of fluctuations. *Mar. Freshw. Res.* 67, 25–36. doi: 10.1071/mf14154

Zhang, H., Shin, P. K. S., and Cheung, S. G. (2016). Physiological responses and scope for growth in a marine scavenging gastropod, *Nassarius festivus* (Powys, 1835), are affected by salinity and temperature but not by ocean acidification. *ICES J. Mar. Sci.* 73, 814–824. doi: 10.1093/icesjms/fsv208

Conflict of Interest: The authors declare that the research was conducted in the absence of any commercial or financial relationships that could be construed as a potential conflict of interest.

Advantages of publishing in Frontiers

OPEN ACCESS
Articles are free to read for greatest visibility and readership

FAST PUBLICATION
Around 90 days from submission to decision

HIGH QUALITY PEER-REVIEW
Rigorous, collaborative, and constructive peer-review

TRANSPARENT PEER-REVIEW
Editors and reviewers acknowledged by name on published articles

Frontiers
Avenue du Tribunal-Fédéral 34
1005 Lausanne | Switzerland

Visit us: www.frontiersin.org
Contact us: frontiersin.org/about/contact

REPRODUCIBILITY OF RESEARCH
Support open data and methods to enhance research reproducibility

DIGITAL PUBLISHING
Articles designed for optimal readership across devices

FOLLOW US
@frontiersin

IMPACT METRICS
Advanced article metrics track visibility across digital media

EXTENSIVE PROMOTION
Marketing and promotion of impactful research

LOOP RESEARCH NETWORK
Our network increases your article's readership